UNCLASSIFIED

AD NUMBER

AD-B003 260

CLASSIFICATION CHANGES

TO	**UNCLASSIFIED**
FROM	**N/A**

AUTHORITY

N/A

AD NUMBER

AD-B003 260

NEW LIMITATION CHANGE

TO

DISTRIBUTION STATEMENT - A

Approved for public release;
distribution is unlimited.

LIMITATION CODE: 1

FROM

DISTRIBUTION STATEMENT - B

LIMITATION CODE: 3

AUTHORITY

AFATL (DLMH)
Eglin AFB, FL 32542

AD B003260

HIGH ALT!TUDE SUPERSONIC TARGET (HAST)
PHASE II

BEECH AIRCRAFT CORPORATION

TECHNICAL REPORT AFATL-TR-74-129

DDC

RECEIVED
APR 22 1975

B

AUGUST 1974

AIR FORCE ARMAMENT LABORATORY

AIR FORCE SYSTEMS COMMAND ● UNITED STATES AIR FORCE

EGLIN AIR FORCE BASE, FLORIDA

High Altitude Supersonic Target (HAST)
Phase II
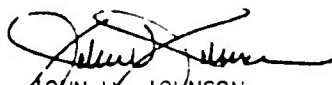
John A. Engelland
William M. Byrne

FOREWORD

This technical report covers Phase II of a multiphased development program to provide the High Altitude Supersonic Target (HAST) for tri-service use. The program is under the sponsorship of the Air Force Armament Laboratory, Eglin Air Force Base, Florida. Colonel Kenneth E. Stout (DLMH) is the Program Manager.

The HAST vehicle development program and the target payload integration function are being carried out by the Beech Aircraft Corporation of Wichita, Kansas under Contract F08635-70-C-0100. Radar augmentation and vector miss distance scoring are being developed by the Government Electronic Division of Motorola, Scottsdale, Arizona, and infrared augmentation devices by Ordnance Research, Inc. of Fort Walton Beach, Florida. These development programs for target payloads are under other contracts with the Air Force and are not covered by this technical report.

Beech Aircraft has subcontracted work on the propulsion system and on the recovery system. The United Technology Center developed the controlled thrust assembly and The Marquardt Company, the ducted power unit. Deceleration devices have been developed by Irvin Industries, Incorporated. Within the Beech Aircraft Corporation, Mr. John A. Engelland is Program Manager and Dr. William M. Byrne is Project Engineer. Mr. B. D. Hunter directed the development effort for the United Technology Center, Mr. E. W. Wecker for The Marquardt Company and Mr. P. R. Delurgio for Irvin Industries. Data and inputs from these subcontracts have been incorporated into the report.

A three and one half year program from January 1971 through June 1974 covering final design, ground test, and fabrication of flight test vehicles is covered in this phase of the program and by this technical report. This is a follow-on to Phase I which covered preliminary design of the flight vehicle and initial development of propulsion and recovery system and which was reported in AFATL-TR-71-25. A flight test program utilizing target vehicles and payloads developed under current contracts is being conducted but not reported in this technical report. This report is identified as 1070E411 MER within the Beech Aircraft Corporation.

This technical report has been reviewed and is approved for publication.

JOHN W. JOHNSON
Deputy Chief, Guided Weapons Division

ABSTRACT

A High Altitude Supersonic Target (HAST) is under development by the Air Force Armament Laboratory to provide a high performance, air launched, advanced aerial target system for tri-service use. This technical report covers the second phase of the multiphased development program. Final design of the target vehicle and supporting equipment was completed and flight test vehicles and supporting equipment were fabricated in this phase. Ground test programs were conducted on subsystems and components. Acceptance tests were conducted on components and the complete vehicle. Analyses confirmed that the canard-clipped delta wing configuration could meet required maneuvers. Materials for the airframe were selected which provide a fair compromise of both manufacturing costs and efficient and reliable thermo-structural performance capability. A hybrid rocket propulsion system was specified and test firings have confirmed the ignition and boost thrust capability and that a variable thrust can be obtained by use of an oxidizer throttle valve. To meet maneuvering requirements a free siphon device has been developed to provide positive expulsion of the oxidizer under all vehicle flight conditions. Maneuvers can be preprogrammed or initiated by radio command and hardware computer tie-in simulations have confirmed the effectiveness of the automatic flight control system to control the vehicle throughout the required flight regime.

TABLE OF CONTENTS

TABLE OF CONTENTS (Continued)

TABLE OF CONTENTS (Concluded)

LIST OF FIGURES

LIST OF FIGURES (Continued)

LIST OF FIGURES (Concluded)

LIST OF TABLES

LIST OF TABLES (Concluded)

LIST OF ABBREVIATIONS AND SYMBOLS

A.C. Aerodynamic Center, $\bar{x}/\ell$

AFCS Automatic Flight Control System

AGE Aerospace Ground Equipment

ALPO$_4$ Aluminum Phosphate

C_A Axial Force/qS

$C_{A_{FRIC}}$ Skin Friction Coefficient

$C_{A_{INLET}}$ Incremental axial force coefficient due to ram air turbine - includes internal drag and momentum losses and additive drag due to external flow variation with ram air requirements.

$C_{A_{PWR}}$ Base pressure relief in axial force coefficient when power is on

C_{RAT} Power required for pumping oxidizer converted to coefficient form

C_{D_A} Additive drag coefficient associated with air management characteristics of turbine speed control

C_{D_B} Base Drag Coefficient

C/MOS Complementary Metal Oxide Semiconductor

C_N Normal force/qS

CTA Controlled Thrust Assembly

CORR Correction factor to additive drag - accounts for effect of inlet lip suction

C_Y Side Force/qS

C_{Y_p} $\partial(C_Y)/\partial(\frac{p\ell}{2v})$

C_{Y_r} $\partial(C_Y)/\partial(\frac{r\ell}{2v})$

C_m Pitching Moment/qS ℓ

C_{m_q} $\partial(C_m)/\partial(\frac{q\ell}{2v})$

C_{m_α} $\partial(C_m)/\partial(\frac{\alpha\ell}{2v})$

C_n Yawing Moment/qS ℓ

C_{n_p} $\partial(C_n)/\partial(\frac{p\ell}{2v})$

C_{n_r} $\partial(C_n)/\partial(\frac{r\ell}{2v})$

C_ℓ Rolling Moment/qS ℓ

C_{ℓ_p} $\partial(C_\ell)/\partial(\frac{p\ell}{2v})$

C_{ℓ_r} $\partial(C_\ell)/\partial(\frac{r\ell}{2v})$

LIST OF ABBREVIATIONS AND SYMBOLS (Continued)

DCAS	Defense Contract Administration Service
DPU	Ducted Power Unit (Consisting of RAT, Alternator and Oxidizer Pump)
EMI	Electromagnetic Interference
FCDC	Flexible Contained Detonating Cords
FET	Field Effect Transistor
F.S.	Fuselage Station - Distance from Zero Reference Point
G.E.D.	Government Electronics Division of Motorola
GFE	Government Furnished Equipment
HAST	High Altitude Supersonic Target
IRFNA	Inhibited Red Fuming Nitric Acid
ITCS	Integrated Target Control System
K	Multiplier by 1000
M_N	Mach number, V/a
MOPS	Multiple Output Power Supply
MTBF	Mean Time Between Failure
M_c	Cruise Mach Number
M_L	Launch Mach Number
M_i	Instantaneous Mach Number
N_x	Axial Load Factor, g
N_z	Normal Load Factor, g
N_2	Nitrogen Gas
OMA	Oxidizer Management Assembly
OTV	Oxidizer Throttle Valve
Op Amp	Operational Amplifier
Q	Pitch Rate, Deg/Sec (Flight Dynamics Section)
RAS	Radar Augmentation System
RAT	Ram Air Turbine
RF	Radar and Scoring Systems Fixed Payload

LIST OF ABBREVIATIONS AND SYMBOLS (Continued)

S	Reference Area (0.922 ft^2) (Flight Dynamics Section)
S	LaPlace Operator (Flight Control Section)
S & A	Safe and Arm Device
TCA	Thrust Chamber Assembly
TIG	Tungsten Inert Gas
V	Total Vehicle Velocity, ft/sec
VDC	Volts Direct Current
VMDI	Vector Miss Distance Indication
VSWR	Variable Standing Wave Ratio
a	Speed of Sound, ft/sec
g	Acceleration Due to Gravity, ft/sec^2
h	Altitude, feet
h_c	Cruise Altitude
h_i	Instantaneous Altitude
h_L	Launch Altitude
n.m.	Nautical Miles
ℓ	Reference Length (200 in)
p	Roll Rate, Deg/Sec
psig	Gage Pressure Square Inch
psia	Ambient Pressure Square Inch
psid	Pressure Difference Square Inch
q	Dynamic Pressure, $1/2 \rho v^2$, lb/ft^2 (Flight Dynamics Section)
q	Body Axis Pitch Rate (Flight Control Section)
qc	Impact Pressure (Flight Control Section)
r	Yaw Rate, deg/sec
t_o	Time Zero (from target launch)
$\bar{x}$	Distance from Nose to Aerodynamic Center, in.
α	Angle of Attack, Deg
β	Side Slip Angle, Deg

LIST OF ABBREVIATIONS AND SYMBOLS (Concluded)

γ	Flight Path Angle, Deg
Δ	Altitude Error
Δh^*	Altitude Error from Climb Programmer
$\dot{\Delta h}$	Altitude Error Time Rate (Differentiated)
ΔN_z	Normal Load Factor Command
$\dot{\psi}$	Yaw Error
$\Delta \psi_D$	Derived Heading Change
$\Delta \psi_I$	1st Heading Change Command
$\Delta \psi_{II}$	2nd Heading Change Command
δ_A	Aileron Deflection, Deg (Positive - Right aileron down)
δ_C	Canard Deflection, Deg (Positive - Leading edge up)
θ	Pitch Angle, Deg.
ρ	Air Density, Slugs/Ft^3
ϕ	Roll Error
$\dot{\phi}$	Roll Error Time Rate (Differentiated)
ϕ_I	1st Roll Command
ϕ_{II}	2nd Roll Command

Subscripts (Used in Flight Dynamics Section)

α	Derivative with Respect to Angle of Attack
δ_c	Derivative with Respect to Canard Deflection
β	Derivative with Respect to Side Slip Angle
α^2	Derivative with Respect to Angle of Attack Squared
δ_c^2	Derivative with Respect to Canard Deflection Squared
δ_A	Derivative with Respect to Aileron Deflection
o	Value of Coefficient at Zero Degrees Angle of Attack and Canard Deflection

SECTION I

INTRODUCTION

The High Altitude Supersonic Target (HAST) is under development by the U.S. Air Force to provide a high altitude, advanced, supersonic target for tri-service use. The program is sponsored by the Air Force Armament Laboratory of the Armament Development and Test Center. The target system has as design objectives the consolidated requirements for high altitude supersonic targets of the U. S. Army, Navy and Air Force. A sequential multiphased program with the Beech Aircraft Corporation has been undertaken to develop the target vehicle and support equipment and to integrate augmentation and scoring systems. Results of the second phase of this program are covered in this report.

During the first phase a preliminary design was formulated. In that phase design trade-off studies were conducted to select the most effective subsystems and components. Structural and aeroheating studies were made to determine airframe and material requirements. Electrical and flight control requirements were analyzed and the system required to perform all maneuvers and control requirements was formulated. Preliminary drawings were prepared and from the preliminary design initial vehicle performance was computed. This first phase culminated in a preliminary design review in which the proposed design was presented for approval and recommendations by the sponsoring agency.

Authority to proceed with the final design was granted to the contractor after the formal review of the program was completed. Technical and program progress of the contractor was reviewed and monitored very closely by the Air Force Program Office as the final design was being completed and at a Final Design Review authority was given to proceed with the procurement of components and the fabrication of ground test assemblies and flight test vehicles. In addition to other more informal reviews held to assess the progress of the program, a First Development Article Configuration Inspection was held prior to the start of the flight test program. The conclusion of the second phase is a prototype vehicle design and twelve flight test vehicles which will be used to verify the design and to test components in a flight test environment.

Beech Aircraft Corporation has designated the HAST target vehicle as Model 1070. References to Model 1070 throughout the report is synonymous with the HAST target vehicle. Augmentation and scoring systems are being developed under programs separate from the target vehicle system and results of these development programs are reported under other technical reports. The contractor for the target vehicle was given the responsibility for the interface and integration of these systems and the results of that effort are covered in Section VIII of this report.

Assistance to the program has been provided by other Air Force organizations. The Air Force Rocket Propulsion Laboratory has continued to support the technical monitoring of the hybrid propulsion system development program and the series of Preflight Readiness Tests was conducted at that facility. The Flight Dynamics Laboratory and the 4950 VNA Hybrid Computer Group at Wright-Patterson AFB provided facilities and participated in the flight simulation of the flight control system hardware. Technical memorandums generated by this group are listed in the references. The Armament Development and Test Center provided range services and launch and recovery aircraft for the recovery flight program conducted during this phase.

The HAST has the mission of accurately simulating high performance threat aircraft of current capabilities and that postulated in the next decades. The performance simulation covers altitude, speed, and maneuvering capabilities. In addition to its capability to duplicate the performance of aircraft, the HAST will look like threat aircraft to the missile systems using the HAST as a target. Active radar return will duplicate the signature of threat aircraft with a realistic bi-static response. The radar return will also provide the characteristic pattern of jet engine turbine blades or jet engine modulation. An infrared source will be carried to simulate the IR signature of threat aircraft.

1

A vector miss distance indicator system will be installed to score the success of a mission against the HAST. With this system an instantaneous readout at a ground station will be available in digital format. The readout will show the closest approach, the vector from the HAST, and the fuzing point of a missile launched against the HAST. This scoring system is a self-contained, noncooperative system, which needs no modification of the ordnance fired at it in order to function.

With the HAST system a target will be provided to evaluate the most advanced air defense weapon systems in a realistic environment and to train combat crews with an accurate simulation of high performance aircraft.

The HAST extends the Mach-Altitude flight envelope from the present requirement of Mach 2 at 70,000 feet to Mach 4 at 100,000 feet. It also provides a maneuverable and recoverable rocket powered target system carrying state-of-the-art augmentation and scoring systems. Meeting these design requirements for the target vehicle has required advancement in hybrid rocket propulsion, in control and guidance, and in structures and use of materials. The report contained herein describes how these advancements have been attained.

The report updates much of the preliminary design which was presented in an earlier report covering the first phase of the program; however, this report is written so reference to the previous work is not essential to understanding. Subsequent phases of this development program will provide for flight test of prototype vehicles, production engineering and qualification, and operational evaluation of the qualified system.

SECTION II

DESIGN REQUIREMENTS

R&D Statement-of-Work DLIV 71-65 of 7 December 1970, defined for the contractor the second phase of a program initiated for the development of a high performance, air-launched, advanced aerial target system. Initial development efforts sponsored by the AF Armament Laboratory (AFATL), AF Rocket Propulsion Laboratory (AFRPL), and AF Flight Dynamics Laboratory (AFFDL), had previously established the feasibility of a high performance target concept utilizing a hybrid rocket propulsion system. The major tasks of this phase of the program were configuration design and analysis, propulsion system development, manufacture of test hardware, and engineering design tests. Recovery system development was conducted under the previous phase of the contract.

Design requirements provided direction concerning physical characteristics, performance, launch method and launch envelope, destruct systems, maneuverability, reliability, interchangeability, interior arrangements, sectionalization, readiness, operating life, storage life, environment, materials and standard parts, maintainability and accessibility, aerodynamic, structural design criteria, propulsion system, electrical system, electronics and avionics, radar and infrared augmentation, scoring, flare/chaff dispenser, command control functions, ITCS, ordnance, recovery, safety, workmanship, and quality assurance. The purpose for such detailed requirements was to assure that the government would receive a satisfactory end product for the next phase of the program. Not all of the design requirements have been met because it became necessary to make appropriate relaxations as development progressed. Relaxations suggested by the contractor were approved and controlled through a series of formal design reviews as well as numerous informal reviews. Adequacy of the design was controlled by review of specifications, test plans, acceptance test procedures, and test results.

Physical characteristic requirements were defined to limit the vehicle to a reasonable useful size. The length was restricted so that no single section could exceed 180 inches to assure carrier elevator compatibility. The total length of the final vehicle design is 200 inches. The basic fuselage outside diameter was restricted to 13 inches. Vehicle gross weight was specified to be commensurate with mission requirements and structural constraints due to launch and free flight conditions. The gross weight of the final design is a nominal 1,200 pounds. The vehicle was required to provide space for installation of 2,500 cubic inches of ancillary payload equipment with a maximum weight of 85 pounds of modular design.

Vehicle flight performance was specified based on immediate and future weapon system evaluation and on training needs. The vehicle was to be capable of automatic climb from a launch altitude of 35,000 feet to all preset altitudes within the flight performance envelope of Figure 1. Preset cruise altitudes had to be available in 5,000-foot increments between 35,000 feet and 60,000 feet and in 10,000-foot increments above 60,000 feet. The vehicle was required to be capable of flying straight and level at all preset altitudes and speeds within the flight envelope. Endurance was to be five minutes of powered flight at 90,000 feet/Mach 4.0 when launched at 40,000 feet/Mach 0.9 and not less than ten minutes of powered flight at 80,000 feet/Mach 3.0 when launched at 50,000 feet/Mach 1.5. Additionally, the vehicle had to be capable of the following specific missions.

TABLE I. SPECIFIC MISSIONS

Mach No.	Altitude (Ft)	Cruise Range (NM)
2.6 to 2.8	35,000	30
2.6 to 2.8	100,000	100
3.2 to 3.5	60,000	50
3.2 to 3.5	100,000	100

Because of unavoidable compromises, the final vehicle design does not have the capability to meet all of these flight performance requirements. Determination of just how well these requirements will be met is one of the primary objectives of the next program phase.

The vehicle was required to be capable of air launch from the A-4 A-7, F-4 F-8 F-101, F-106, F-14 and F-15 aircraft. The primary launch aircraft for the next program phase is the F-4 A parallel program to provide launch capability from the F-101B has been conducted. The vehicle had to be capable of safe, effective air launch within an altitude/Mach number envelope derived from the minimum design launch condition presented in Figure 1.
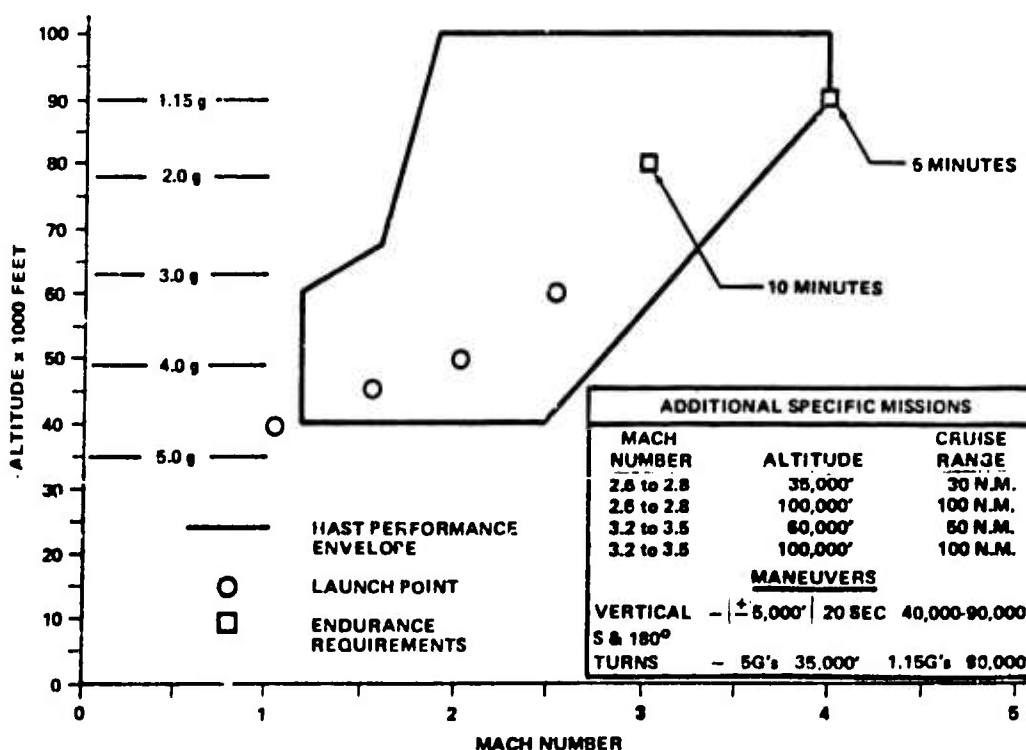
Figure 1. HAST Flight Envelope

A destruct system was required to render the vehicle aerodynamically unstable either by radio command or automatically under several conditions indicative of unsatisfactory flight. A self-contained maneuvering system was required to provide target realism. The vehicle was required to be capable of constant altitude "S" turns and 180-degree turns between the range of 5 g's at 35,000 feet and 1.15 g's at 90,000 feet. Vertical maneuvers up or down of 5 g's at 35,000 feet and 2 g's at 60,000 feet and 20-second maximum 5,000-foot altitude changes between 40,000 feet and 90,000 feet were also required.

The time required to checkout the vehicle and prepare it for flight was limited to 30 minutes and average checkout time limited to 10 minutes. Preflight servicing and launcher installation time was limited to three men working for 20 minutes while the effectiveness of this servicing was to be valid for 8 hours. Warmup time was restricted to 10 minutes and with power applied, the vehicle

4

was to be able to maintain this warmed up condition for a minimum of one hour. These requirements were taken as goals to be met by a production vehicle and no attempt has been made to demonstrate achievement of these goals during this development phase. The present vehicle acceptance test procedure can be completed in approximately six hours. This procedure, however, is designed to probe the vehicle to a depth consistent with development hardware checkout and will not be routinely used on production type vehicles for checkout. It is anticipated that data generated relative to reliability during the flight test phase of the program will allow a less comprehensive preflight checkout without undue risk concerning vehicle readiness. It is possible that automatic checkout equipment may be required to meet the above mentioned 10-minute checkout requirement.

An operating life requirement of 50 hours from acceptance to removal for bench servicing was established for all components while a storage life of 5 years was required. Evidence of operating life has been obtained from extensive testing on the first flight test article while compliance with the storage requirement is yet to be demonstrated.

Environmental requirements of a production vehicle specified that it would be capable of guaranteed performance during or after encountering probable surface extremes based on "Operations, ground worldwide", and "Operations, shipboard worldwide" conditions in accordance with MIL-STD-210. Internal pressurization of vehicle sections was not allowed. Vehicles were to be designed in accordance with MIL-STD-470 to insure maximum ease for maintenance or removal and replacement of all components and parts. Because of the high packaging density employed and efforts to minimize structural weight and complexity, no access panels were used, and it was necessary in some instances to trade-off accessibility. Flight test operations will determine whether these trade-off decisions were made properly.

The basic vehicle was required to possess adequate aerodynamic damping such that steady, stable, level flight could be achieved throughout the flight envelope. In straight and level flight the stabilized vehicle was required to maintain its original line of flight with 4 miles per 100 miles neglecting the effect of winds while not deviating more than 10 percent in initial cruise altitude. Structural design criteria called for the vehicle to be capable of withstanding all captive flight, launching, free-flight, and handling loads. As it turned out, captive flight loads were generally responsible for the structural design. These loads were generated in accordance with MIL-STD-8591. Additional structural requirements were that failure should not occur at the design ultimate loads and that yield and ultimate factors of safety must be at least 1.15 and 1.50, respectively. The structural design of the vehicle was adequate to meet these requirements as evidenced by static testing.

The propulsion system was required to be a hybrid rocket engine capable of meeting the desired performance requirements above. The engine was required to develop a maximum boost thrust of variable duration followed by transfer to any one of several selectable thrust levels during sustain. The design exceeds these requirements in that the sustain thrust level is controlled by the autopilot via an analog voltage which gives infinitely variable sustain thrust level control. The oxidizer was specified to be mixed oxides of nitrogen (MON-25) in accordance with MIL-P-26539 or inhibited red fuming nitric acid (IRFNA) conforming to MIL-P-7254, Type IIIB. IRFNA was chosen because of its slightly higher density-impulse and because the contractor had greater storage experience with it. Minimum proof and burst pressures for both the oxidizer tank and the pressurant tank (if required) were defined as a function of the working pressure. Testing has proven these requirements to be met. Igniter firing and electromagnetic radiation hazard requirements were also defined and met.

Two electrical power sources were required to provide vehicle power and supply 28 VDC for payloads. The primary power source was to provide all power during normal operation while an auxiliary power source was required to provide power for recovery system deployment, destruct, and operation of a locator beacon and command receiver in the event of the failure of the primary system. The alternator of the ducted power unit will provide 45 amps at 28 volts continuously. It has proven its ability to initiate vehicle ordnance devices and their necessary transient loads without

damage to the equipment or excessive spiking on the primary bus. The alternator which is designed to operate at a constant nominal speed of 30,000 rpm has been operated successfully from 17,000 to 40,000 rpm. The auxiliary power source is a diode isolated nickle-cadmium battery pack located in the boattail area. It has been confirmed that this source will deliver the electrical power as specified.

The necessary antennas for the vehicle were required to be designed to minimize drag while providing acceptable antenna patterns consistent with operational requirements of the various essential systems. All basic vehicle antennas have proven to provide proper patterns of acceptable strength while minimizing drag by making use of antennas whose radomes are flush with the surface with the exception of the transponder antennas which extend beyond the basic vehicle nose contour by less than 5/16 of an inch.

SECTION III

SUMMARY

The preliminary design of a target vehicle to meet these Design Requirements was established in Phase 1 of the HAST Development Program. Further analysis and design refinements were continued in Phase II and a Final Design Review was conducted by the Air Force with participation by the Army and Navy. As a result of this review, authority was given the contractor to proceed with the fabrication and assembly of twelve flight test vehicles and three sets of spares for support of a flight test program.

The approved design is an air-launched wing-canard vehicle 200 inches in length with a 40-inch wing span, a 26-inch high vertical stabilizer and a 13-inch diameter fuselage. A three-view drawing of the vehicle showing the size, shape and essential features of the profile is contained in Figure 2. It weighs approximately 1200 pounds at launch, depending on the payload carried and the amount of oxidizer loaded.

Control is provided in two axes with canards for pitch control and wing trailing edge ailerons for lateral control. With this configuration and control scheme a rudder control is not required. The canards are of triangular planform with double wedge section. The wings have a clipped delta planform of modified double wedge section with vertical stabilizers attached to the tips to increase the effective wing span and to provide yaw stability. Canards, wings and vertical stabilizers are interchangeable from either side.

The fuselage has a constant diameter of thirteen inches with a 3.5-caliber von Karman nose and a tapered boattail. The forward 35 inches of the nose cone is the radome. A tunnel or raceway is provided on the lower centerline for electrical and nitrogen lines. An inlet and exhaust system is attached to the lower body centerline to provide air to a ram air turbine. Location for an optional infrared augmentation system is provided on the lower centerline aft of the inlet and exhaust system. Launch fittings and an umbilical connection are located on the upper body surface for aircraft carry and launch. A forward mounted pitot/static tube provides vehicle air data for the automatic flight control system.

The major internal components and their location in the target vehicle are shown in Figure 3. A nose volume of 1800 inches is reserved for the radar augmentation and scoring payload. Immediately behind the payload volume is the integrated target control system and the air data sensors. The canard actuators are also located here. A torodial tank is provided for nitrogen to force the oxidizer from the oxidizer tankage and to provide aeration in the thrust chamber assembly during low flow rates. The oxidizer is stored in a tankage arrangement which provides center of gravity control as the oxidizer and the fuel in the thrust chamber assembly are consumed. The rear tank is equipped with a free siphon device to ensure an uninterrupted supply of oxidizer during all vehicle maneuvers. The HAST carries approximately 496 pounds of oxidizer, 156 pounds of fuel, with the nitrogen gas and the igniter accounting for another 4 pounds of consumables.

A parachute recovery module is fitted between the oxidizer tanks and the thrust chamber assembly. A ducted power unit is located beneath the recovery module. The ducted power unit is a dual purpose machine which uses a ram air turbine to power an alternator for electric power and an oxidizer pump to boost the oxidizer to the high pressure required by the thrust chamber assembly. Clustered in the remaining space in this mid-section are the vehicle control logic electronics and the autopilot. Also, in this area is the oxidizer throttle valve which regulates the flow of oxidizer into the thrust chamber assembly.

The solid fuel of the propulsion system is contained in the thrust chamber assembly. The case of this assembly carries structural loads. At the rear of this assembly is the nozzle and fitted around the nozzle is the aileron actuator and the emergency/recovery battery.

7
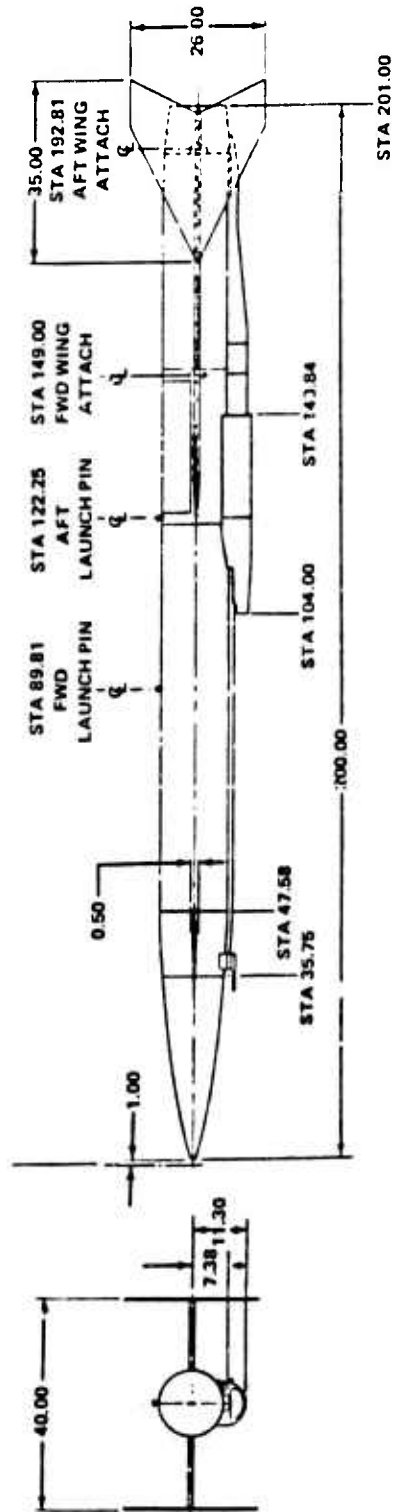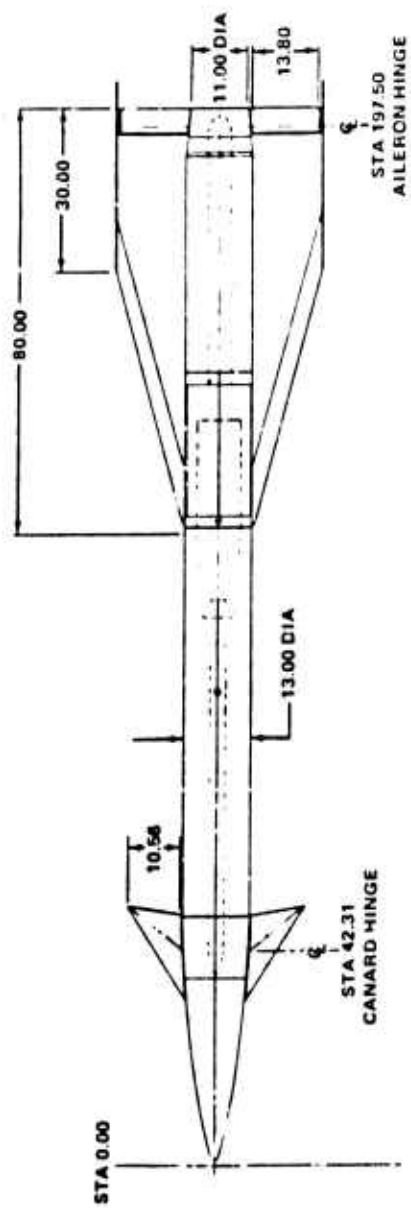
Figure 2. HAST Vehicle Three-View
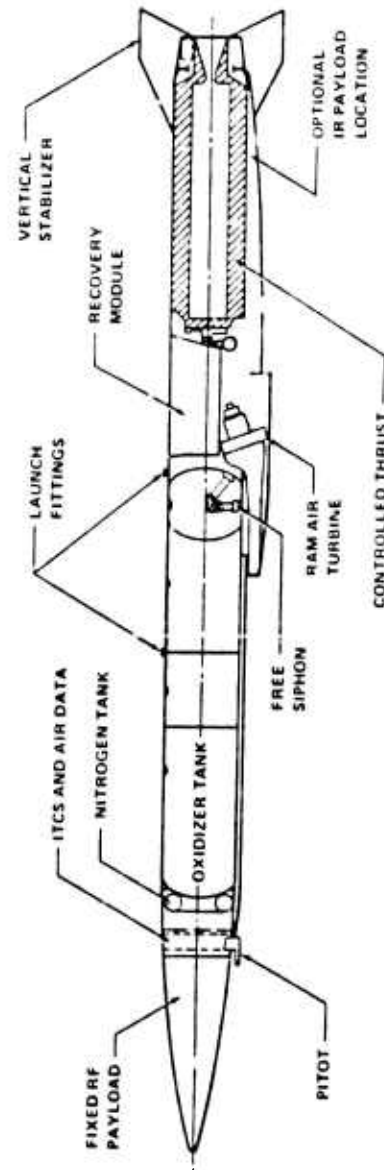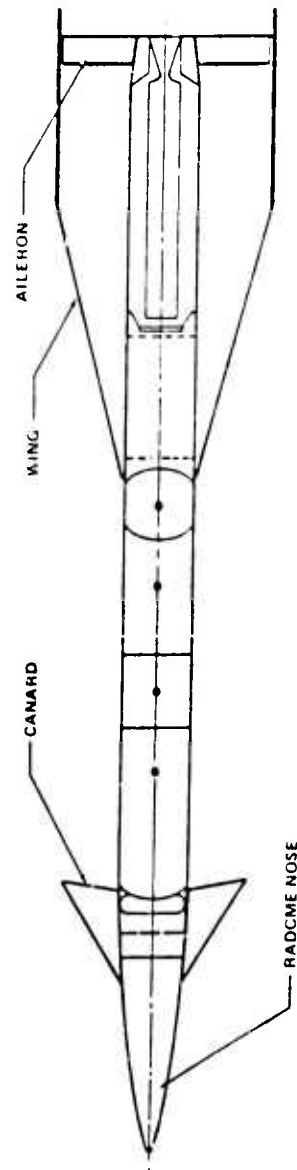
Figure 3. HAST Inboard Profile

Labels (upper diagram):
AILERON
WING
CANARD
RADOME NOSE

Labels (lower diagram):
VERTICAL STABILIZER
RECOVERY MODULE
LAUNCH FITTINGS
ITCS AND AIR DATA
NITROGEN TANK
OXIDIZER TANK
FIXED RF PAYLOAD
PITOT
FREE SIPHON
RAM AIR TURBINE
CONTROLLED THRUST
OPTIONAL IR PAYLOAD LOCATION

9

1. FLIGHT DYNAMICS

The basic aerodynamic data for the HAST vehicle was developed during the previous phase. Trade-offs were made and the theoretical analysis was confirmed by a series of wind tunnel tests. These data were refined as additional studies were made and the system design developed. Results of test data, particularly the propulsion system tests, were incorporated into the performance model.

During this phase, several flight missions which have been selected for use during the flight test phase were simulated through the use of a three-degrees-of-freedom digital trajectory analysis program. This program includes the autopilot control parameters, a throttling control method and the hybrid rocket engine characteristics. Two of the missions presented in this report were to run to demonstrate the range and endurance and one to determine the maneuvering characteristics. An extensive analysis of the basic aerodynamic characteristics was made since these data directly determine the preformance of the vehicle.

The analysis shows that the specified Mach number and altitudes are easily achieved but that the endurance at altitude by these development test vehicles is not attained.

2. STRUCTURES AND MATERIALS

The objective in structures and materials was to design, substantiate the structural integrity, and fabricate the major airframe subsystem

A design criteria was used in which the structural design environment and strength and rigidity requirements are defined. The loads encountered during ground handling, captive flight, launch, free flight and recovery were investigated to determine the maximum load environment experienced during the life cycle of the HAST 1070 vehicle. Finite element models of the aero surfaces were developed and analysis of the structure has been conducted to determine the margins of safety. Fuselage substructure was analyzed for critical conditions which result during application of ejection and captive flight loads. An aeroelastic analysis was conducted to show that the vehicle was flutter-free throughout both the captive flight and free flight regimes. Static tests of structural subsystems and a free-free vibration test of a complete missile of flight configuration were accomplished to substantiate analysis.

Materials for the structural subsystem were selected on the basis of cost, minimum weight, process familiarity, availability, strength and stiffness at temperature, and compatibility with inhibited red fuming nitric acid.

3. AUTOMATIC FLIGHT CONTROL SYSTEM

Extensive analyses were performed on the flight control system during the phase. As hardware components became available, these were acceptance tested against specifications and procedures prepared during the phase. The analysis and hardware test programs culminated in a hardware-computer tie-in for a complete flight control simulation.

A linear analysis of the airframe and control system was performed to assure that a single gain stability augmentation system was feasible over the entire performance envelope and the gains selected could perform satisfactorily. A total of 25 flight conditions over the HAST performance envelope were studies.

The known nonlinearities and hardware characteristics were modeled with the decoupled equations of motion into a point stability analog computer simulation of the stability augmentation portion of the flight control system. The objectives of this simulation were to investigate the effects of actuator rates, gyroscope characteristics, and nonlinearities on stability using previously selected gain values. For the most part, the results of linear analysis was reinforced.

The hybrid computer facility at Wright-Patterson Air Force Base was used for a complete flight control system simulation. The objectives were to reinvestigate stability after inclusion of cross-axis coupling, to finalize the throttle control design and to determine the effects of re-defined hardware characteristics. Several inadequacies in the overall design were detected and corrected. The simulation results indicated that the proposed flight control system would provide stability in climb, cruise, and maneuvering flight. Turning, climbing and altitude hold capabilities appeared to far exceed the system requirements.

4. ELECTRICAL AND ELECTRONIC SYSTEM

The HAST electronics and electrical subsystems comprise a considerable part of the target components. Electronic cases and assemblies have been designed to use the available space around other major target assemblies to provide the greatest possible volume for the propulsion and payload systems.

From launch aircraft takeoff until the vehicle is recovered the electrical and electronic systems control target functions are vital to the success of the mission. Prior to launch a self-test is made by electronics of 22 flight critical items within the vehicle. If these items are normal a READY lamp will illuminate and a launch can be made; otherwise, a FAULT lamp will illuminate and the launcher will not function. After launch, timing logic is provided for propulsion system sequencing, pitch control enabling, and destruct and recovery system arming.

Power is provided from three different sources. Each portion of a flight requires varying amounts of power from one or two sources. Sources of power are the launch aircraft, the ducted power unit, and the command/recovery battery. Aircraft power is provided for electrical system prelaunch warmup and checks of telemetry. During the prelaunch self-test and during flight prior to recovery, power from the ducted power unit (DPU) is applied. The output of the alternator of the DPU is rectified to supply a nominal 28 VDC at 47 amperes full load which is greater than the maximum power requirements for target vehicle operation and for payload power requirements. The battery supplies power for the command receiver, C-band transponder, and the locater beacon; and, also, for recovery or destruct initiation.

Target performance during a mission can be preprogrammed prior to flight. The flight program may be modified during a mission by radio command uplink. Radio commands, in some cases, will exclude preprogrammed events. The flight path of the target is preprogrammed by the settings of 19 ten-position and one five-position switches. Among the functions which may be preselected are cruise Mach number and altitude, maneuver, and change of Mach number and altitude.

The autopilot module provides a point of interfacing for the target flight control sensors and the altitude control actuators. The autopilot module receives attitude and rate information from the gyros, altitude and speed information from the air data module, and programming from the digital logic board. Calculations and scaling operations are performed on the input to drive the canard and aileron actuators. The autopilot module consists of five multilayered printed circuit boards which plug into a double sided mother board. Interconnections are made through two high density connectors at two of the end multilayer boards.

The purpose of the destruct system is to render the vehicle aerodynamically unstable should unacceptable deviations from the desired flight path occur. Destruct system circuits are contained on the digital logic board which collects information from various destruct sources and sends the destruct command to the destruct electro explosive device relay. Destruct can be initiated by radio command or by several internal and external conditions.

A transponder and a command receiver/decoder are installed to provide communication with the target. The transponder increases the tracking capability of the radar. The command receiver receives and processes control commands for destruct, heading update, recovery and flight programming. A locater beacon is also installed to assist the helicopter crew in the recovery operation.

11

The HAST telemetry system samples, encodes and transmits to a receiving station, information relevant to the performance of the test vehicle. It will also accept the transmit scoring information from the vector miss distance indicator scoring system. The HAST system is in two basic configurations. One for those vehicles whose primary purpose is flight dynamics and vehicle performance and the other for the vehicles which contain a scoring system. The first configuration is a modularized package which permits changing or deletion of test parameters depending on the flight schedule or program progress and has a capability of up to 186 channels. The second configuration is greatly reduced due to space limitations imposed by the addition of the scoring system.

5. PROPULSION SYSTEM

A hybrid rocket engine was specified by the Air Force as the propulsion system for the HAST. The designation of hybrid is derived from the use of a liquid oxidizer and a solid fuel. The combination of oxidizer and fuel chosen is non-hypergolic and requires an igniter to be fired in the proper sequence to initiate combustion. By use of an oxidizer throttle valve the oxidizer flow rate can be controlled, which in turn, determines the thrust level of the engine. A throttling ratio as high as 10:1 can be attained. The thrust level is controlled by the automatic flight control system.

Components and subassemblies which supply oxidizer to the throttle valve at the desired pressure and flow capability are referred to as the oxidizer management assembly. Included are a gaseous nitrogen subsystem, oxidizer tankage, an oxidizer start valve, a free siphon, and a ducted power unit. Components and subassemblies which combine the oxidizer with fuel to produce thrust at the desired level are referred to as the controlled thrust assembly. Included are an oxidizer throttle valve, a manifold assembly, a case assembly, fuel grain billets and a nozzle.

Since the propulsion system was one of the longest lead time items of the HAST, some development work was undertaken in the first phase, as well as theoretical analysis. This work included the investigation of positive expulsion schemes and of heavywall thrust chamber assembly tests. As a result, a free siphon design was selected and fuel grain composition shape and burn patterns were investigated. Throttle valve design and nozzle designs were evaluated. Tradeoff studies were conducted on a variety of pressurization candidates.

An extensive test program was conducted during Phase II on the subsystems of the propulsion system and proof and preflight readiness tests were conducted with the complete system. Components were tested under environmental extremes.

With the completion of the preflight readiness tests and with modification incorporated during the propulsion system test program, the system is considered acceptable for the flight test program.

SECTION IV

FLIGHT DYNAMICS

This section presents both the aerodynamic analysis and the aerodynamic heating analysis of the HAST missile. The configuration analyzed represents a HAST missile with the RF payload onboard. For this analysis, the gross weight was 1201 pounds with 480.2 pounds of usable oxidizer and 144 pounds of usable fuel. Three flight missions were simulated through the use of a three-degrees-of-freedom digital trajectory analysis program. Performance and maneuvering characteristics were analyzed. Time history data for these missions are shown and the missile's range and endurance are discussed. The basic aerodynamic data used in the digital simulation program was based on analysis of wind tunnel data contained in References 1 and 2.

The aerodynamic heating analysis, the thermal data associated with aerodynamic heating during the hottest HAST mission, and thermal data obtained during testing required for analysis verification are presented. Also included are the insulation requirements for thermal protection of the electronic, recovery and payload components of the vehicle.

1. PERFORMANCE AND MANEUVERABILITY

The performance of the HAST missile was determined using a three-degrees-of-freedom digital trajectory analysis program. This program includes the autopilot control parameters, a throttling control method and the hybrid rocket engine characteristics. The basic aerodynamic data used in this simulation are contained in paragraph 2 of this section.

In general, a typical mission involves the following sequence of events. The missile is launched from the carrier aircraft. There is a two-second delay before longitudinal autopilot activation and engine ignition in order to allow the missile to clear the carrier aircraft. However, the lateral-directional autopilot is operational during this time to maintain heading. The desired cruise Mach number and altitude are translated by the control system into the required thrust and control settings to reach cruise conditions. The engine is throttled back and the control reset after the missile reaches cruise conditions. The missile flies at constant Mach number and altitude until burnout occurs. The missile then continues to hold cruise altitude while the airspeed bleeds off. When the canard required for trim reaches maximum deflection (20 degrees), the missile begins its descent. The parachute system is deployed when the impact pressure decreases to 150 psf, and the missile reaches an altitude of 50,000 feet or less. The missile descends on the main parachute until it reaches 10,000 feet, then a mid-air recovery is accomplished.

Two missions were run to demonstrate the missile's range and endurance at selected flight conditions throughout the flight envelope.

Mission 1 consisted of a launch at Mach 1.5, 50,000 feet and cruise at Mach 4.0, 90,000 feet. A time history of the flight trajectory and associated aerodynamic parameters is shown in Figures 4 and 5. The missile reached the cruise condition 112 seconds after launch at 41 nautical miles downrange. Burnout occurred 215 seconds after launch at a distance of 108 nautical miles. The parachute was deployed 614 seconds after launch at 50,000 feet. The missile was recovered 1784 seconds after launch and 226 nautical miles downrange.

Mission 2 was a launch at Mach 1.5, 45,000 feet and cruise at Mach 3.5, 100,000 feet. Time history data for this mission are shown in Figure 6 and 7. Cruise was reached at 111 seconds and 37 nautical miles after launch. Burnout occurred at 247 seconds and 115 nautical miles after launch. The missile was recovered 1771 seconds and 214.7 nautical miles after launch.

The maneuvering characteristics of the HAST missile were also determined using the three-degrees-of-freedom digital trajectory analysis program. The three-degree program is used for maneuvers involving only longitudinal motion.

13
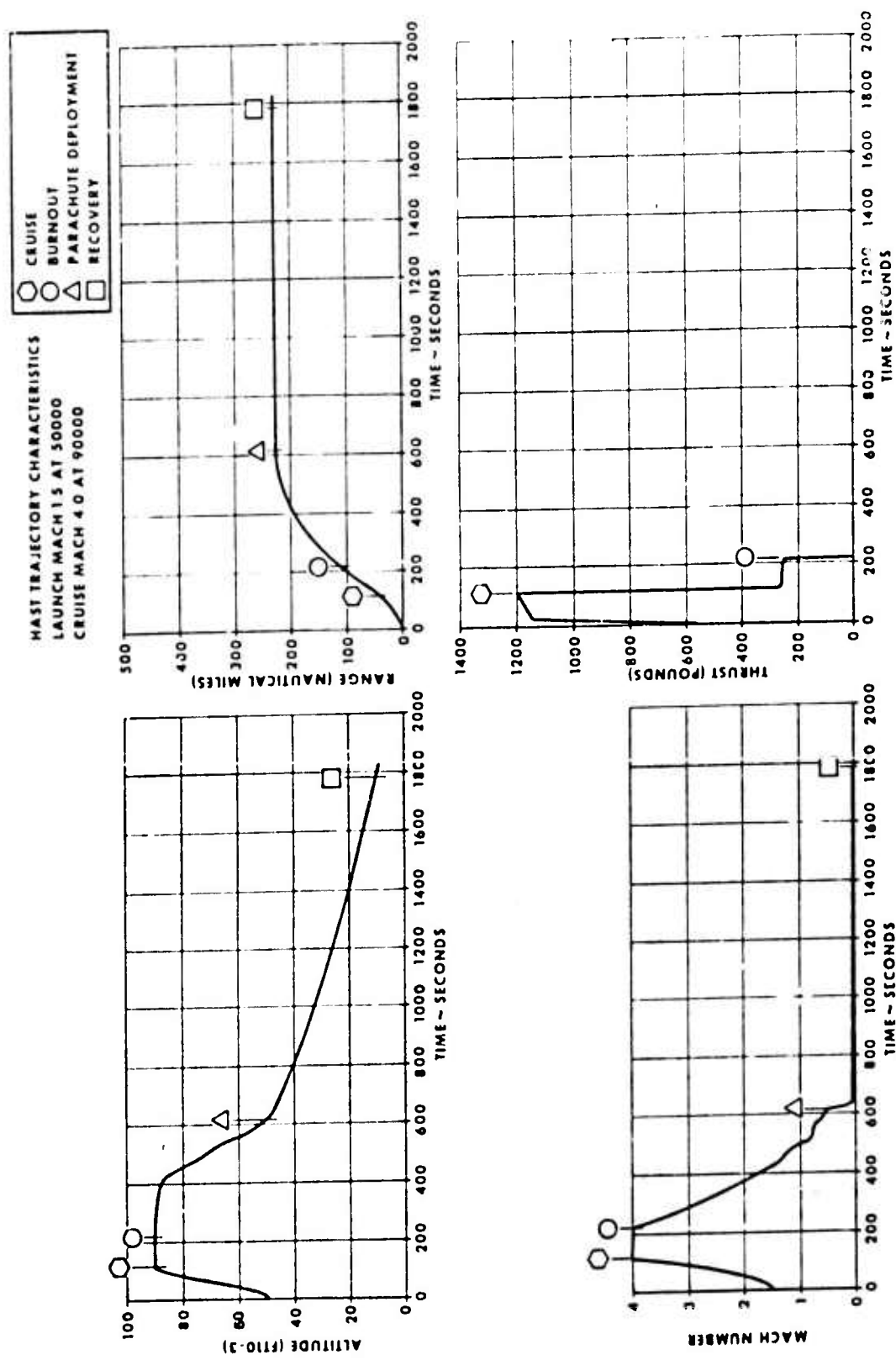
Figure 4. Mission 1 Flight Trajectory

14
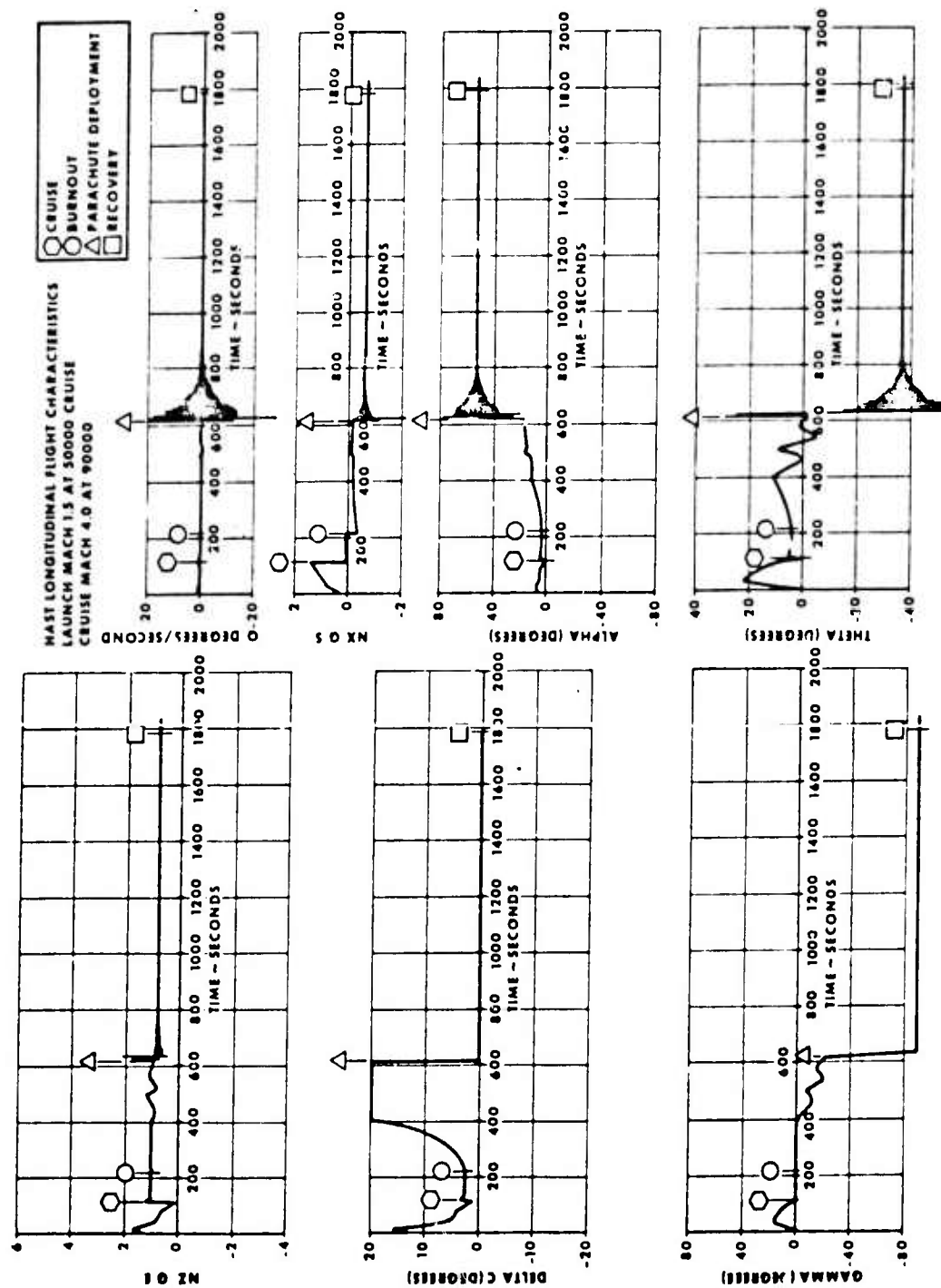
Figure 5. Mission 1 Aerodynamic Parameters

15
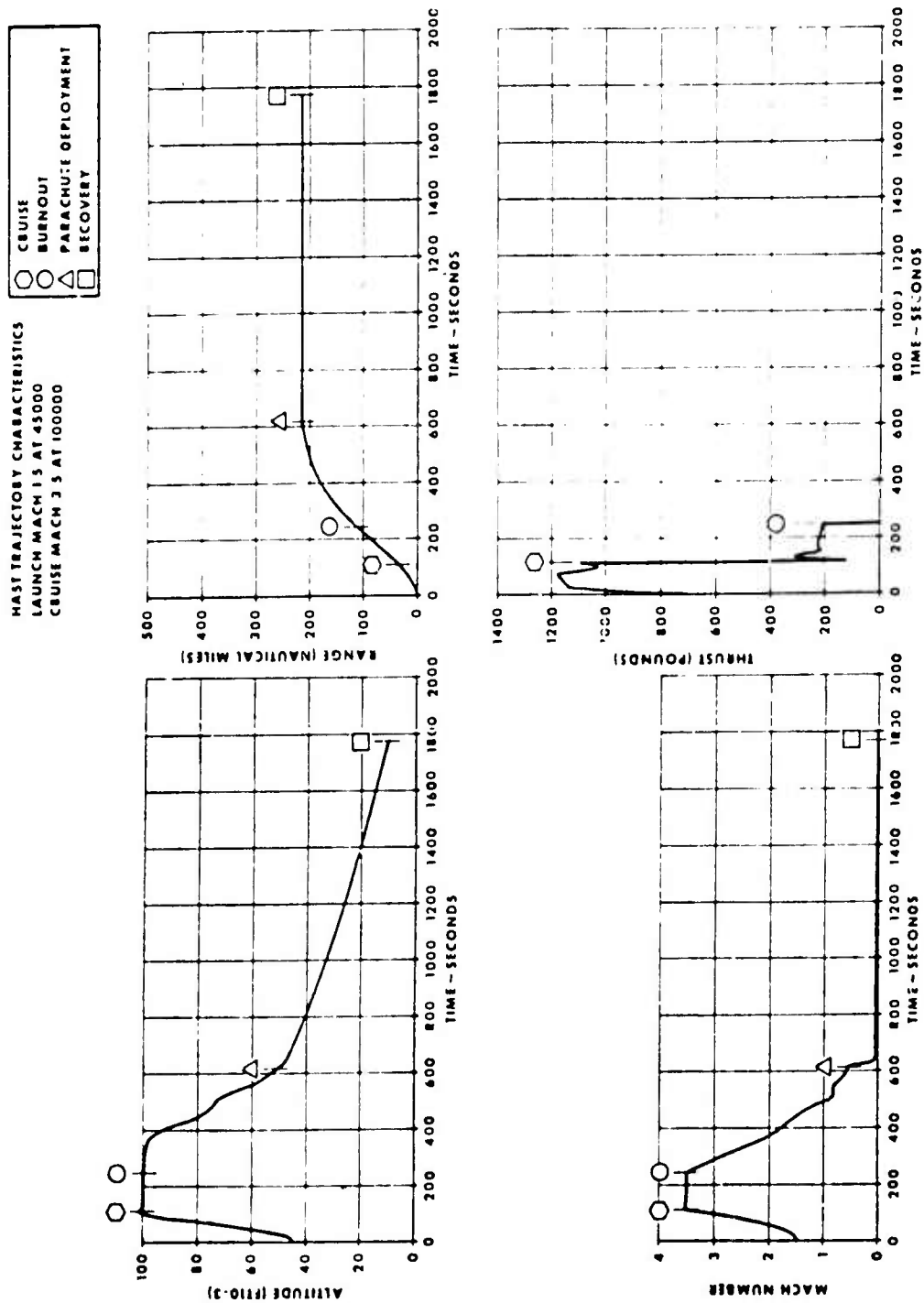
Figure 6. Mission 2 Flight Trajectory
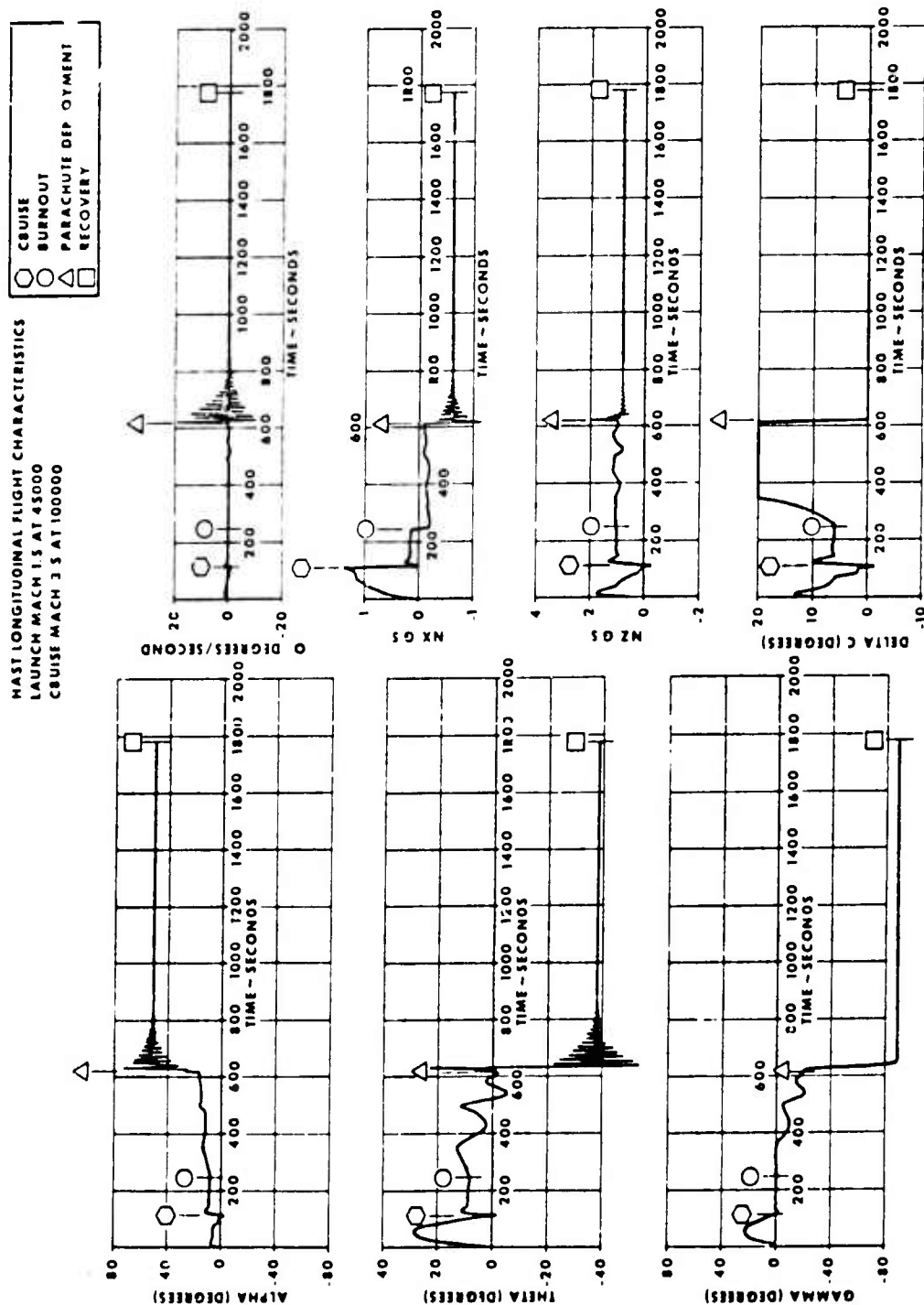
Figure 7. Aerodynamic Parameters

17

Mission 3 represents a 5,000-foot altitude change maneuver. The missile was launched at Mach 1.2, 40,000 feet and cruised at Mach 1.5, 40,000 feet. Cruise was reached 28 seconds after launch. Fifty seconds after launch the command was given to increase the altitude 5,000 feet. The maneuver was terminated 70 seconds after launch when an altitude of 45,000 feet was reached. Time history data for this mission are shown in Figures 8 and 9.

2. BASIC AERODYNAMIC DATA

The basic aerodynamic data of this section were used in digital computer programs to simulate the HAST flight trajectories. An extensive analysis of the basic aerodynamic characteristics was made since these data directly determine the performance of the vehicle.

The static stability derivatives were determined from analysis of data from two HAST wind tunnel tests (References 1 and 2). The basic rotary derivatives for the HAST were based on theoretical methods which related them directly to the static derivatives and the missile geometry.

All the coefficients contained in this section are based on a reference area (S) of 0.922 ft^2 and a reference length (ℓ) of 200 inches and are in the body axis system. Moment coefficients are referenced to fuselage Station 115.

a. Longitudinal Stability Derivatives. The total axial force, normal force and pitching moment coefficients can be expressed:

$$C_A = C_{A_0} + C_{A_\alpha 2}\, \alpha^2 + C_{A_{\delta_c 2}}\, \delta_c^2 + C_{A_{\alpha\delta_c}}\, \alpha\delta_c \tag{1}$$

$$+ C_{A_{PWR}} + C_{A_{FRIC}} + C_{A_{INLET}}$$

$$C_N = C_{N_0} + C_{N_\alpha}\, \alpha + C_{N_\alpha 2}\, |\alpha|\, \alpha \tag{2}$$

$$C_M = C_{M_0} + C_{M_\alpha}\, \alpha + C_{M_\alpha 2}\, \alpha\, |\alpha| + C_{M_{\delta_c}}\, \delta_c \tag{3}$$

$$+ C_{M_\alpha 2\delta_c}\, \alpha\, |\alpha|\, |\delta_c| + (C_{M_q}\, q + C_{M_{\dot\alpha}}\, \dot\alpha)\ \frac{\ell}{2V}$$

The stability derivatives contained in these equations are presented as a function of Mach number in Figures 10 through 13. Also shown is the aerodynamic center variation.

The terms $C_{A_{FRIC}}$ and $C_{A_{INLET}}$ represent the increment in axial force coefficient due to skin friction at altitudes other than 40,000 feet, and the drag due to the ram air turbine, respectively. Both of these terms are computed within the digital simulation programs.

The friction coefficient is determined by the following set of relations:

For $0 < h < 40,000$ ft,

$$C_{A_{FRIC}} = 0.0125 \left(\frac{h - 40,000}{10,000}\right) \tag{4}$$

For $40,000$ ft $< h < 70,000$ ft,

$$C_{A_{FRIC}} = 2.5 \times 10^{-6} h + (0.0136 - 0.337 \times 10^{-6}\, h)\, M_N - 0.10 \tag{5}$$

For $h > 70,000$ ft,

$$C_{A_{FRIC}} = 3.63 \times 10^{-6} h + (0.020 - 0.433 \times 10^{-6} h)\, M_N - 0.179 \tag{6}$$

18
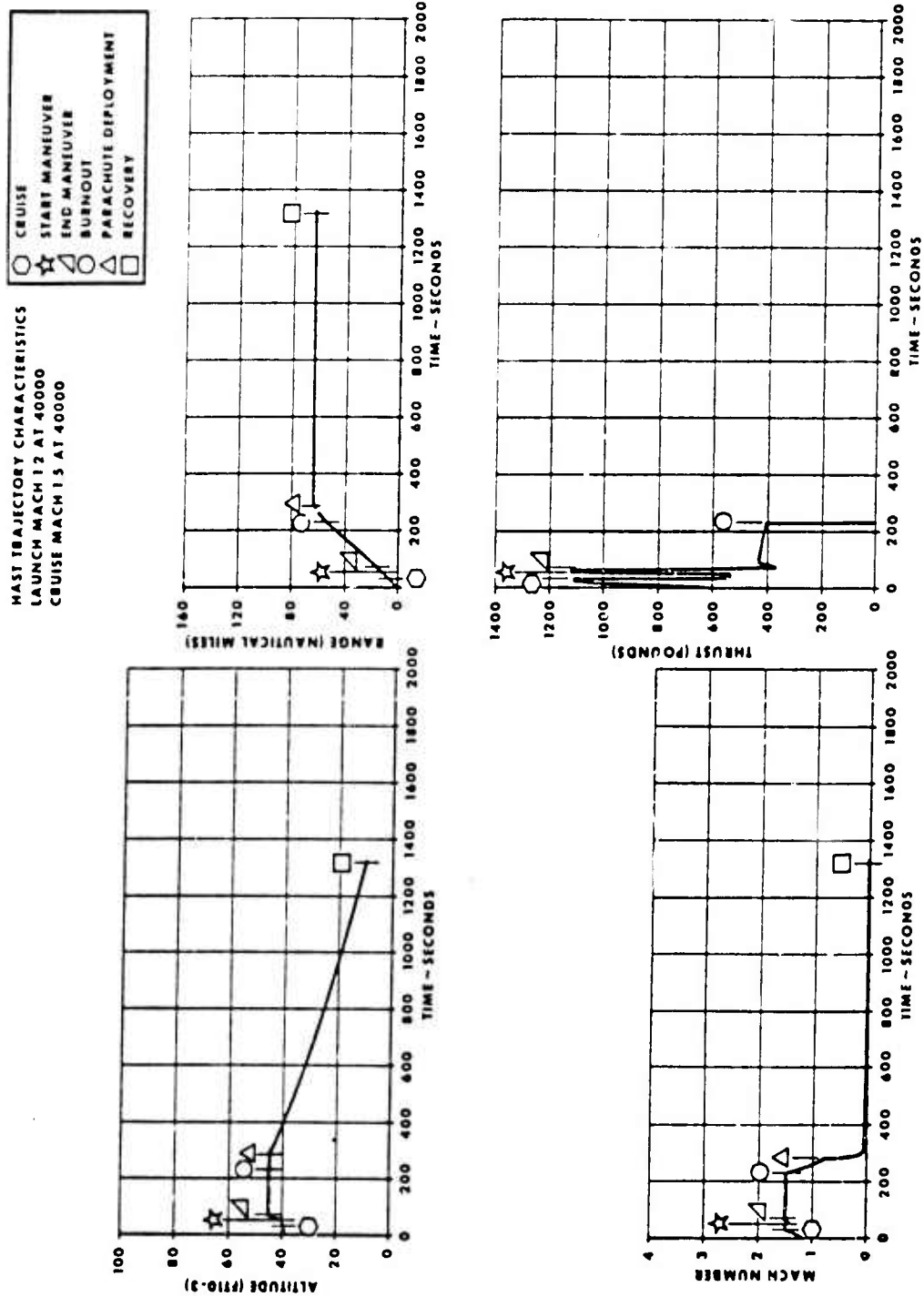
Figure 8. Mission 3 Flight Trajectory

19
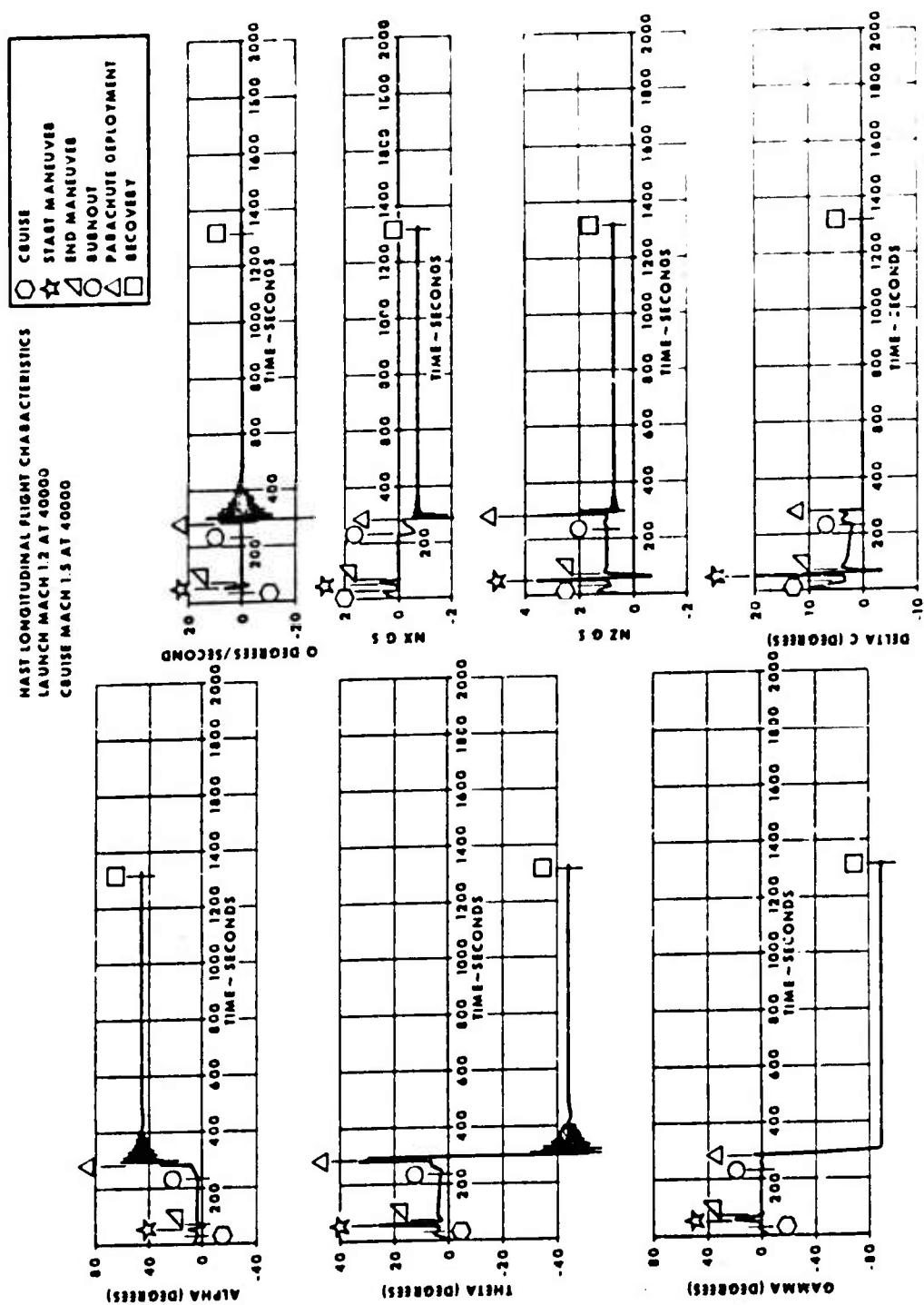
Figure 9. Mission 3 Aerodynamic Parameters
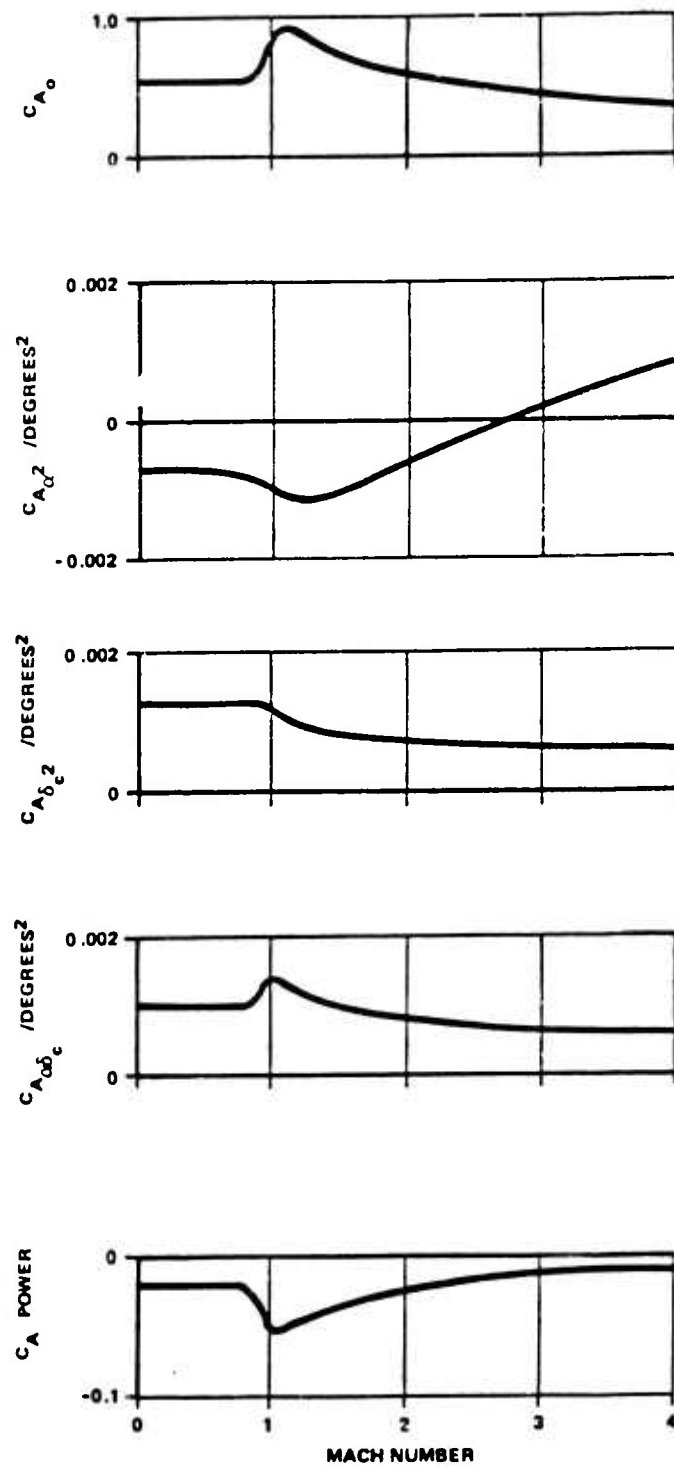
Figure 10. HAST Axial Force Coefficient
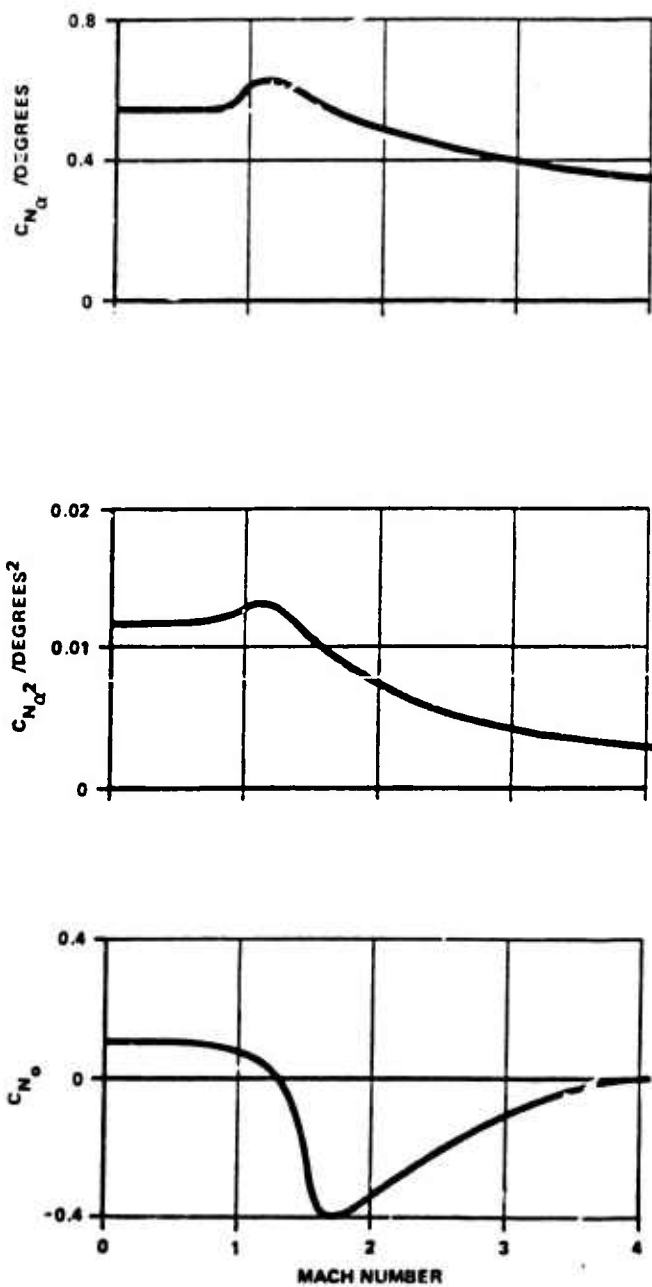
Figure 11. HAST Normal Force Coefficient

22
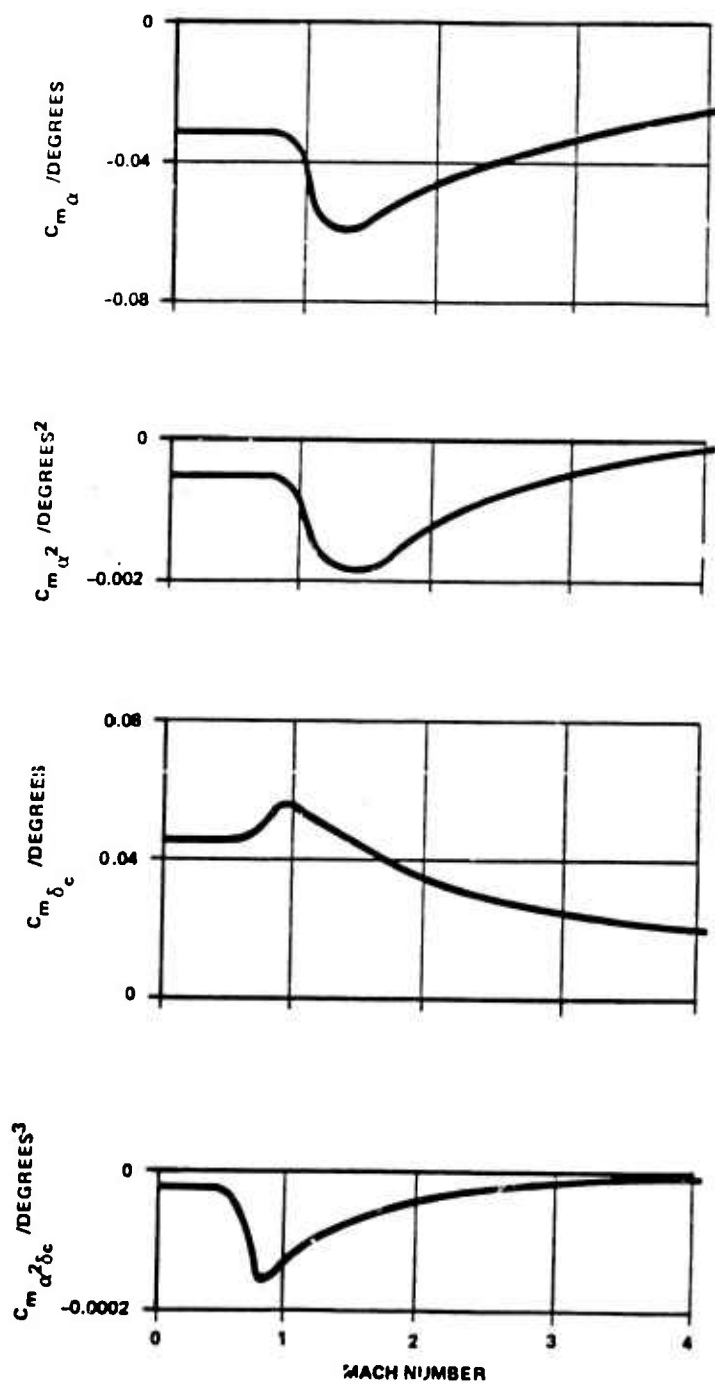
Figure 12. HAST Pitching Moment Coefficient
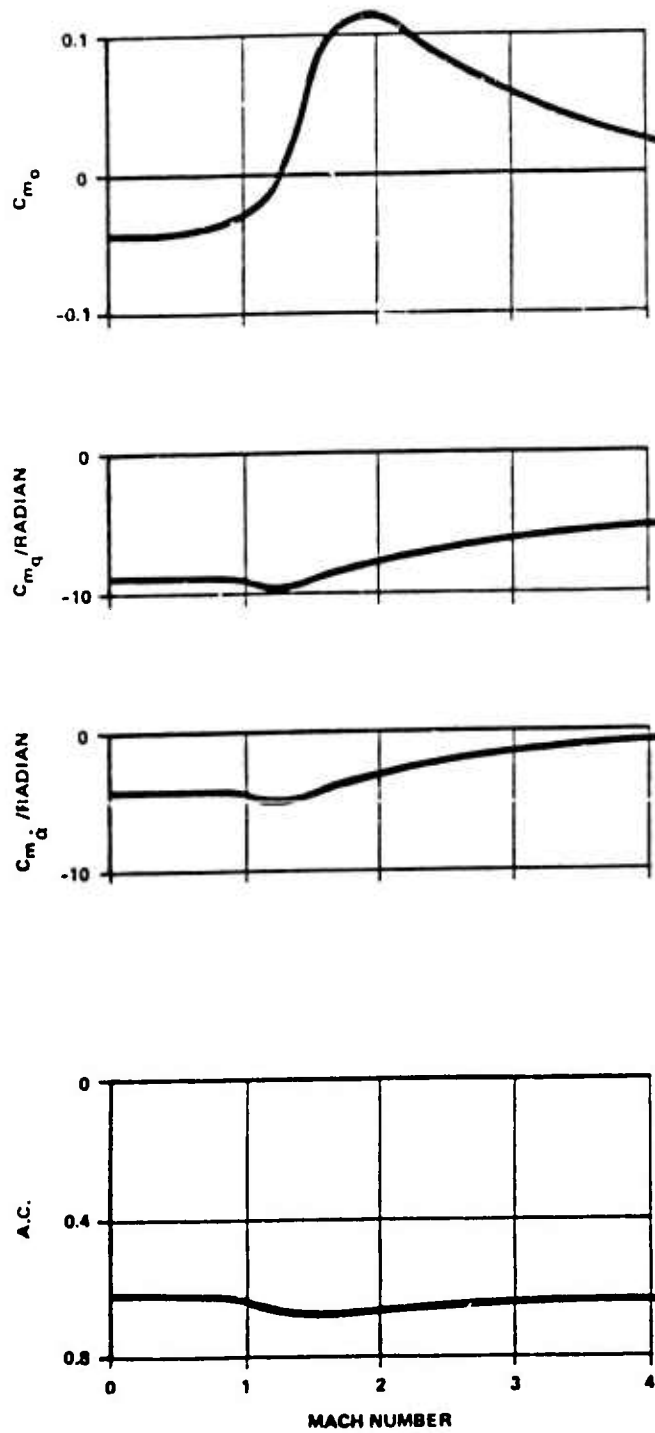
Figure 13. HAST Pitching Moment Coefficient
and Aerodynamic Center

24

The axial force coefficient due to the ram air turbine is determined by the following relations:

For Power on,

$$C_{A_{INLET}} = C_{A_{RAT}} \cdot (1 - CORR)C_{D_A} \qquad (7)$$

For Power Off,

$$C_{A_{INLET}} = (CORR)C_{D_A} \cdot 0.188 \, C_{D_B} \qquad (8)$$

b. Lateral Stability Derivatives. The total side force, yawing moment and rolling moment coefficients can be expressed:

$$C_Y = C_{Y_\beta} \beta + (C_{Y_p} p + C_{Y_r} r) \; \frac{\ell}{2V} \qquad (9)$$

$$C_n = C_{n_\beta} \beta + C_{n_{\delta_a}} \delta a + (C_{n_p} p + C_{n_r} r) \; \frac{\ell}{2V} \qquad (10)$$

$$C_\ell = C_{\ell_\beta} \beta + C_{\ell_{\delta_a}} \delta a + (C_{\ell_p} p + C_{\ell_r} r) \; \frac{\ell}{2V} \qquad (11)$$

The stability derivatives contained in these equations are presented as a function of Mach number and angle of attack in Figures 14 through 16.

3. AERODYNAMIC HEATING

Since the HAST flight envelope lies above 37,000 feet altitude, the aeroheating is primarily a function of Mach number. The maximum heat-rate due to aerodynamic heating will occur at a flight condition of Mach 4.0 at 90,000 feet altitude.

A computer program was used to predict the aerodynamic heating for HAST. This program was used to analyze stagnation flow, side-wall flow, wedge flow and conical flow for both subsonic and supersonic velocities. Confidence in the computer results was obtained by comparing predicted results with flight data for the X-15 airplane at similar Mach numbers. Very good agreement was obtained.

Unless otherwise stated the predicted results are based on zero angle-of-attack operation of the vehicle. Data was obtained for the HAST wing for Mission 1 with angle-of-attack included. A comparison of surface temperatures 2.0 inches aft of the leading edge was obtained for the upper and lower surfaces. The angle-of-attack varied from 0.2° to 11.6°. The flow for the top and bottom surfaces went through shock angles which were created by the effective angle-of-attack (a function of wedge angle, 2.7° and angle of attack). A maximum temperature differential between top and bottom surfaces of 100°F was observed. The maximum variation from the zero angle-of-attack flat plate configuration was 70°F. These variations would not affect the structural integrity of the vehicle significantly.

The local aerodynamic heating rates may be altered when the flow field or boundary layer is modified in regions where flow interference is created due to wing-body intersections or shock wave boundary layer interaction. Corrections to the program are made through application of an interference coefficient.
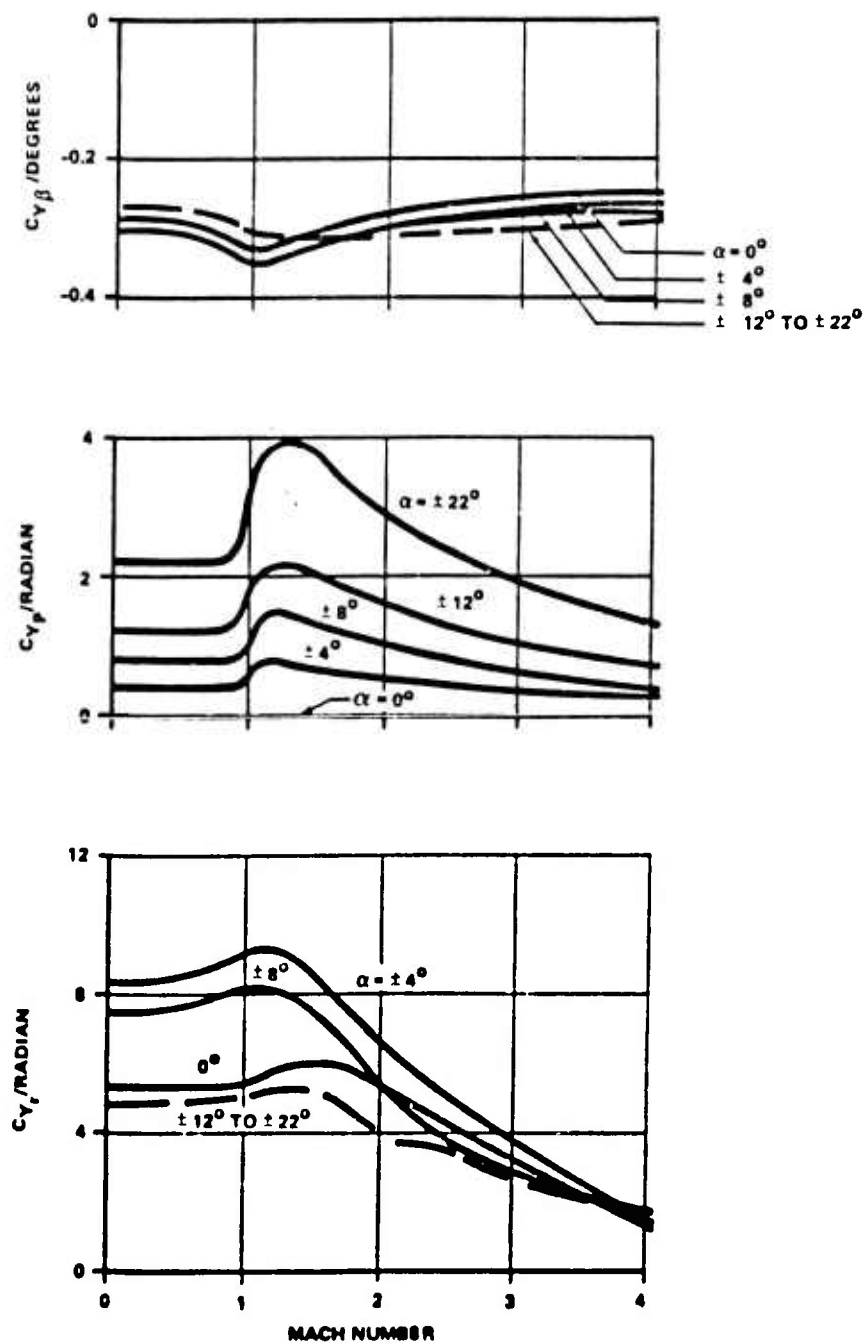
Figure 14. HAST Side Force Coefficient

26
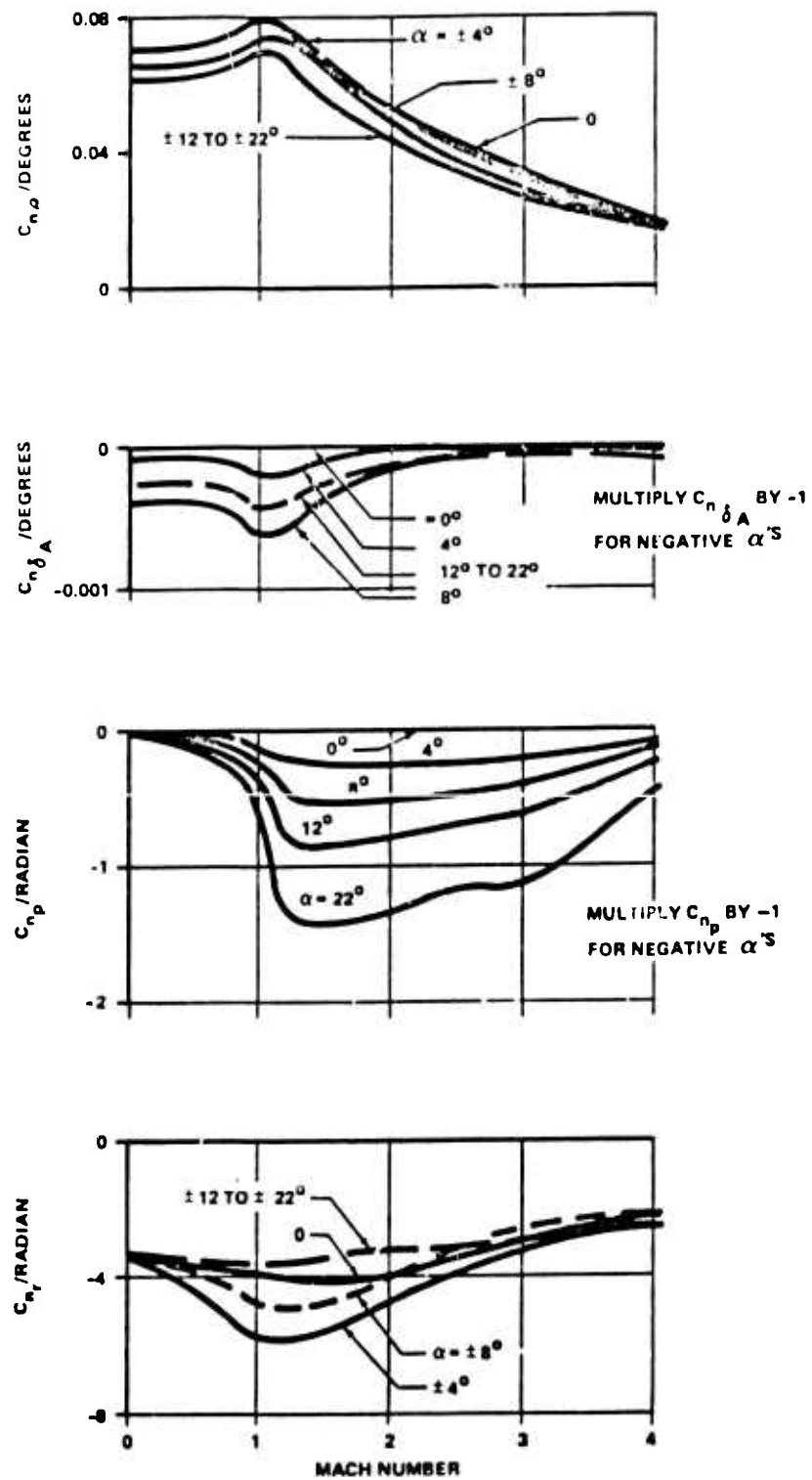
Figure 15. HAST Yawing Moment Coefficient
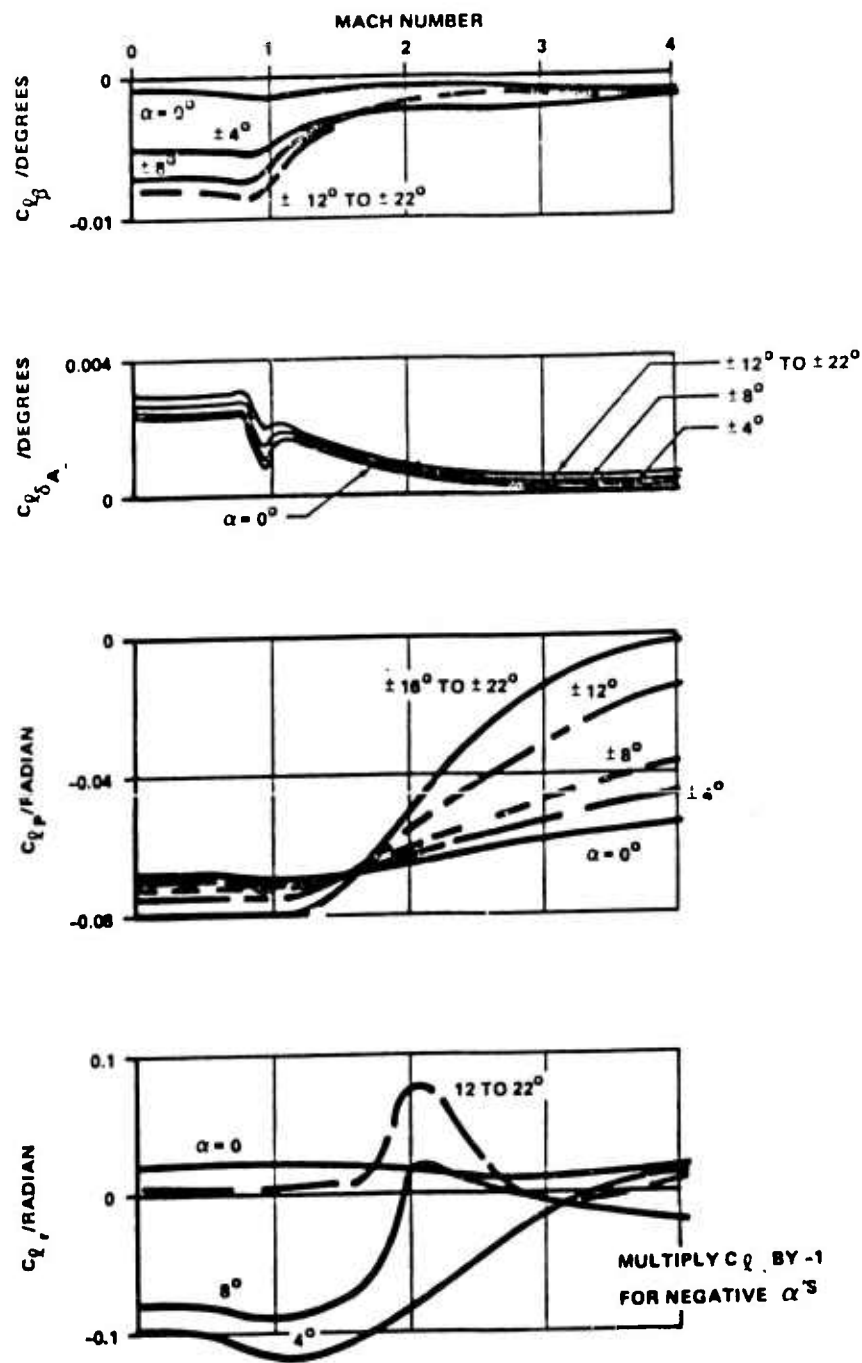
Figure 16. HAST Rolling Moment Coefficient

a. Predicted Temperature Surveys of HAST Components. Temperature surveys are presented for Flight Mission No. 1 described in Figure 4. The emissivity of the surfaces was 0.80. The results include interference effects where applicable and are representative of the maximum temperature at which the vehicle will be expected to operate. Figure 2 shows the location of canards, stabilizers, and wings where interference effects occur.

(1) Stabilizer. The first component to be discussed is the stabilizer. The shaded area of Figure 17, where the maximum increase in heating due to interference occurs is also shown on an expanded scale in Figure 17. The lines parallel to the leading edge represent lines of constant temperature, where no interference heating occurred.

The leading edge, outboard of the shaded area, is shown to be a constant temperature of $1124°F$. The point noted by $898°F$, the shaded area of Figure 17, is where maximum increase of heat transfer coefficient on the surface occurs.

The nose of the stabilizer was calculated as being the stagnation point on a sphere. The other leading edge temperatures were obtained for a cylinder swept $63°$ degrees.

(2) Wing. The previous discussion showed the effect of the wing on the stabilizer heat transfer. In this section, the effect of stabilizer interference on the wing is shown. The results for the surface are shown in Figure 18. Based on this information, the interference heating on the wing is negligible.

(3) Canard. As on the wing, the fuselage interference has a negligible effect on the heat transfer to the surface of the canard. The temperature of the canard leading edge near the fuselage will be increased. This increase is similar to that shown for the wing.

The data for the canard are shown plotted in Figure 19. As on previous plots the lines parallel to the leading edge represent lines of constant temperature.

(4) Fuselage. A Longitudinal temperature profile for the fuselage is shown in Figure 20. The material and its thickness is shown for each of the components.

(5) Forward Tunnel. The heat transfer coefficients are approximately 115 percent higher than those obtained on a flat plate with no disturbance. This would cause an increase in surface temperatures of approximately $130°F$ on the HAST vehicle operating at the flight condition assumed for this analysis.

b. Insulation Requirements. The insulation requirements have been established for controlling the temperature of the internal components of the HAST vehicle. The design criterion for this study was obtained using Flight Mission No. 1. The results of this analysis indicate necessary protection is provided by 3/16 inch of Fiberfrax® insulation in the moderately high temperature areas, and 1/4 inch of Min-k® insulation in the high temperature areas. Added protection is obtained by aluminizing or foil covering the insulation materials to decrease the emissivity. These insulation requirements for the various sections of the vehicle are detailed in Figure 21.

The temperatures denoted in Figure 21 represent the maximum at which the components are expected to operate. All heating is created by aerodynamic heating except the top side of the aft tunnel and the nozzle. These two areas are heated significantly by the thrust chamber assembly.

c. Aerodynamic Heating Tests. Wind tunnel tests were conducted at Tunnel A of Arnold Engineering Development Center simulating the flight condition expected during Mission No. 1. These tests were conducted at a Mach number of 4.03. Thermographic phosphorus paint on a low thermal conductivity material was used to obtain the heating rates on two HAST models; (1/2 scale, 1/2 length model, and 1/4 scale full length model). The main objective of these tests was to investigate "hot spots" created by interference heating.
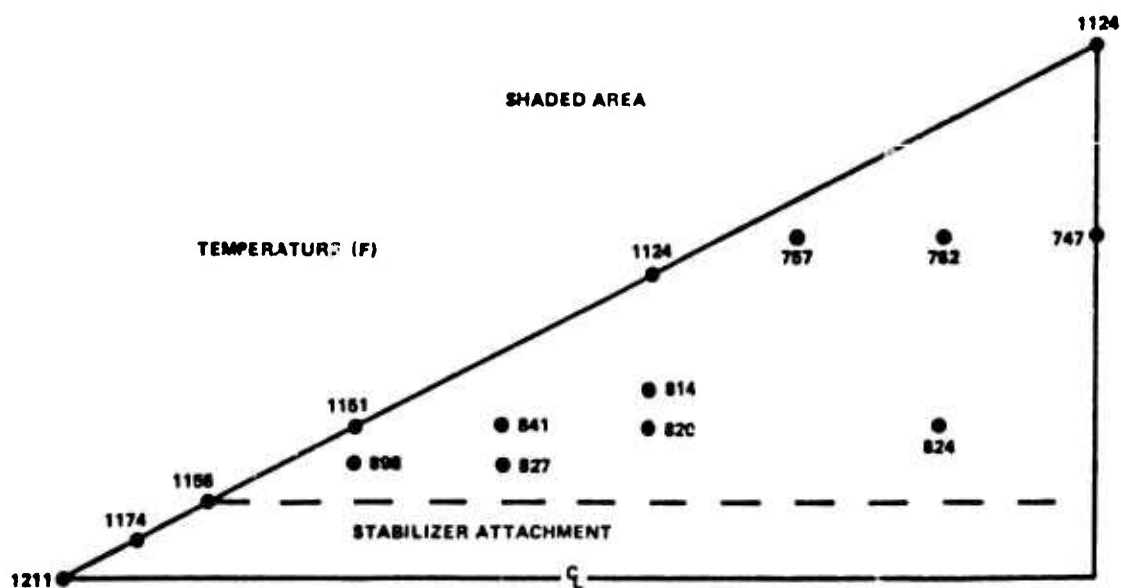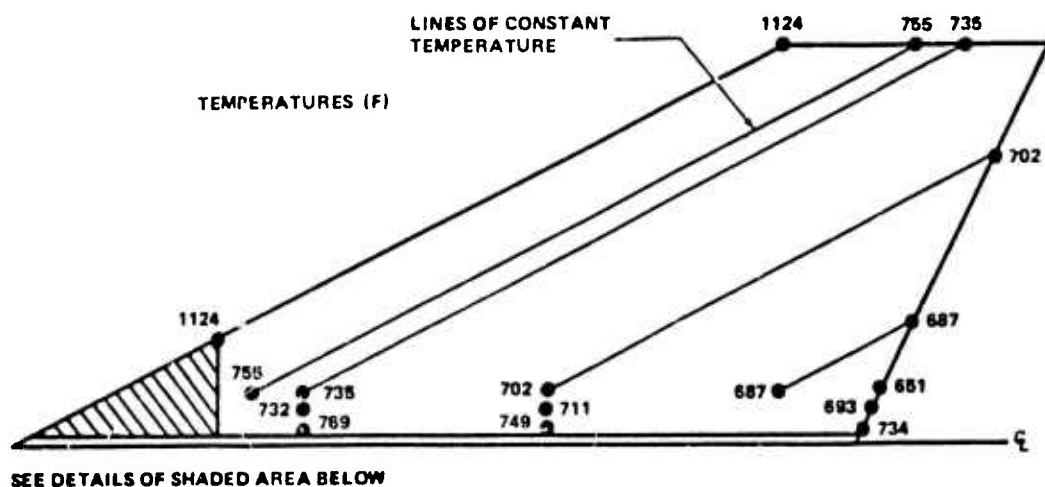
Figure 17. Predicted Temperatures on Stabilizer

TEMPERATURES (F)

1043 692 671   650   637   629   618   607   600

LINES OF CONSTANT
TEMPERATURE

847

SEE DETAILS OF SHADED AREA BELOW

847   692   691   687
                                691   677

SHADED AREA   698   688
                                694   684
                               718 715 715 703   693

847
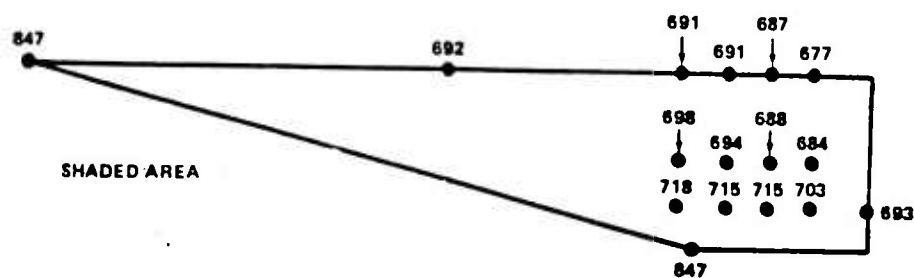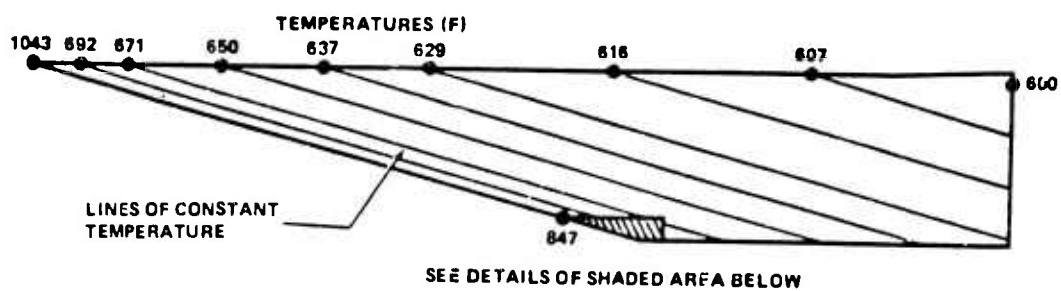
Figure 18. Predicted Temperatures on Wing

LINES OF CONSTANT
TEMPERATURE

1130   596   560   520   485
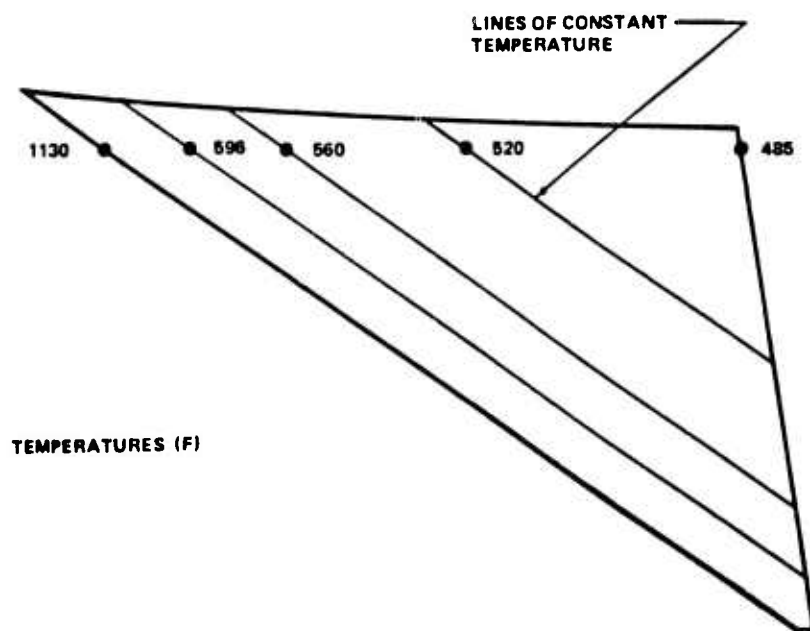
TEMPERATURES (F)

Figure 19. Predicted Temperatures on Canard

31
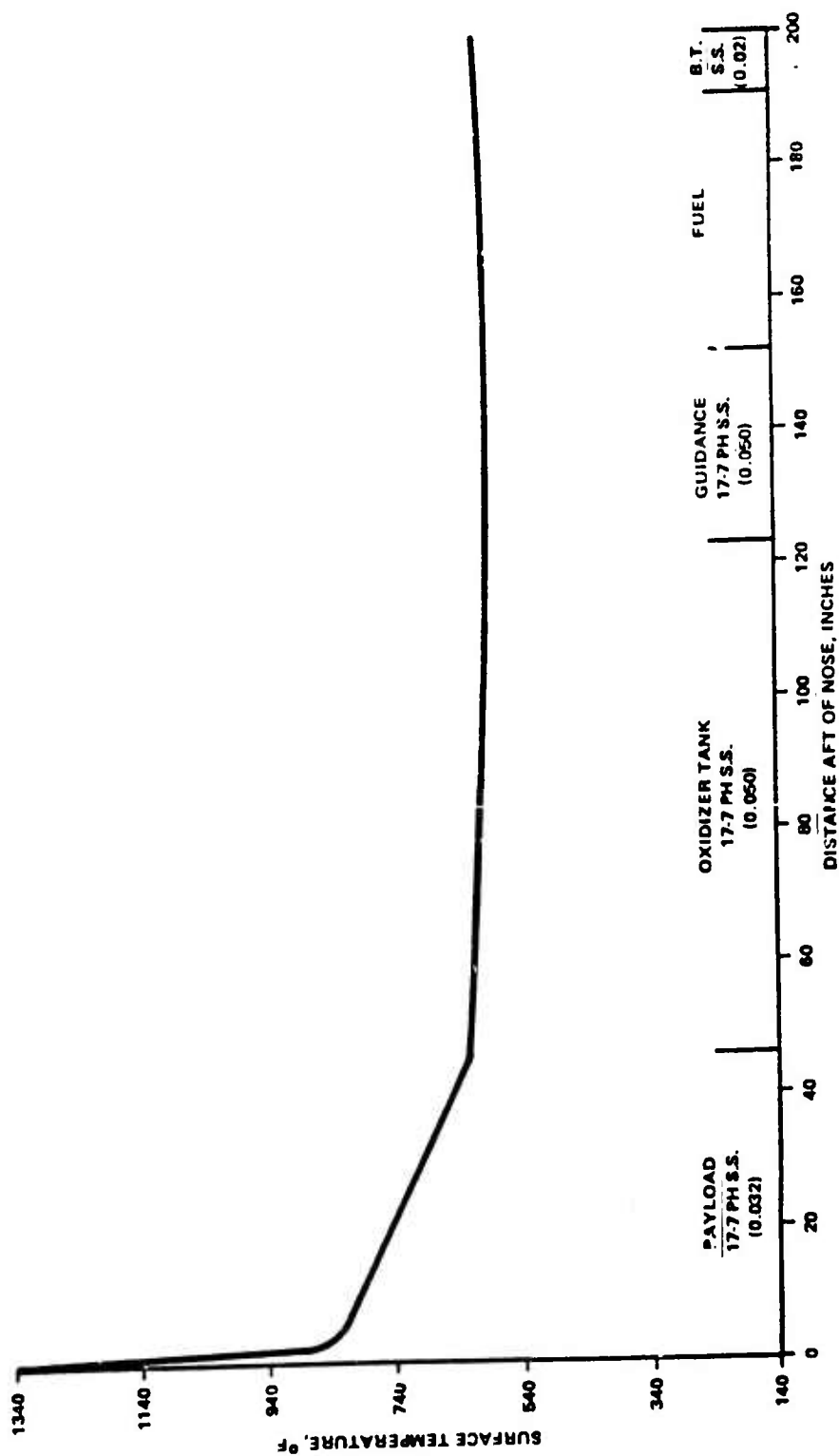
Figure 20. Longitudinal Temperature Profile of Fuselage
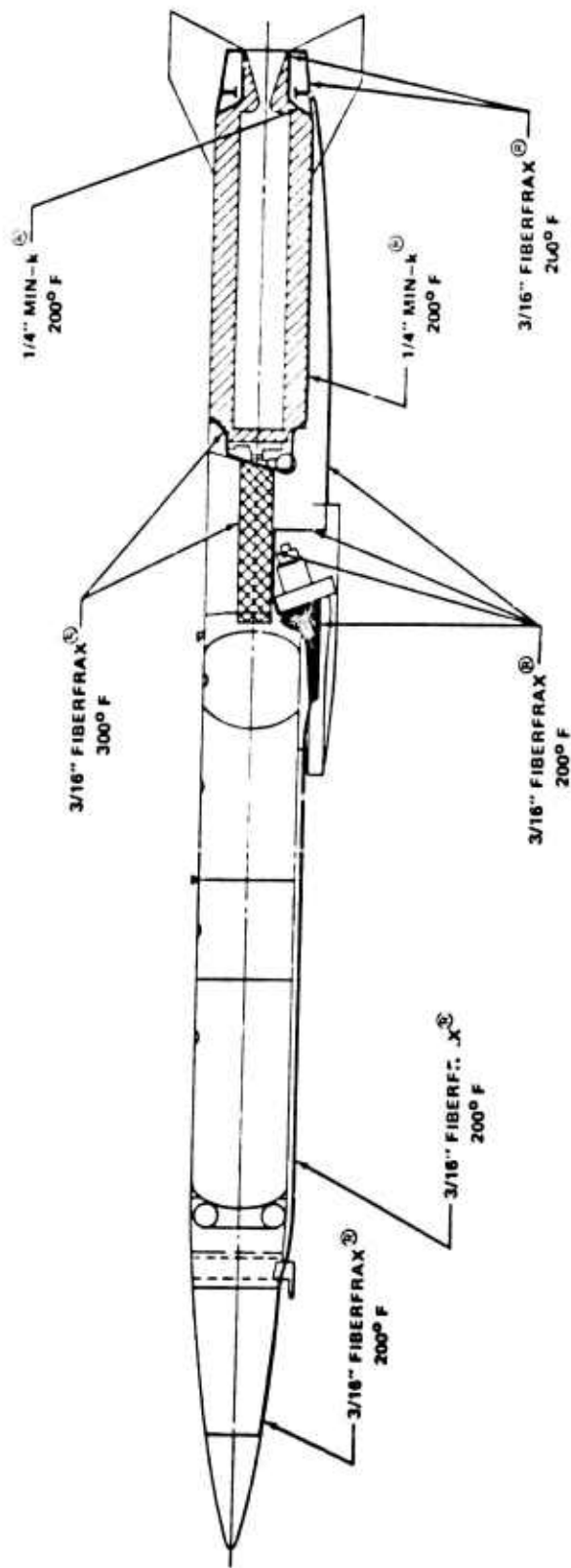
Figure 21. HAST Insulation Requirements

3/16" FIBERFRAX® 200° F

3/16" FIBERF:. X® 200° F

3/16" FIBERFRAX© 300° F

3/16" FIBERFRAX® 200° F

1/4" MIN–k 200° F

1/4" MIN–k 200° F

3/16" FIBERFRAX® 200° F

The data from this test is shown in Figure 22. Two sets of temperatures are shown for each of the "hot spot" locations, angles-of-attack of 0° and 12°. The hottest area on the vehicle other than nose or leading edges of the aerodynamic surfaces was in the region surrounded by the pitot tube, tne canard, and the antennas. Shocks off of these three components interact causing a temperature of 915°F for angle-of-attack of 0° and 985°F at 12° angle-of-attack. Since there are no structural members in this area and these temperatures are well below the melting point of stainless steel no problems are anticipated.
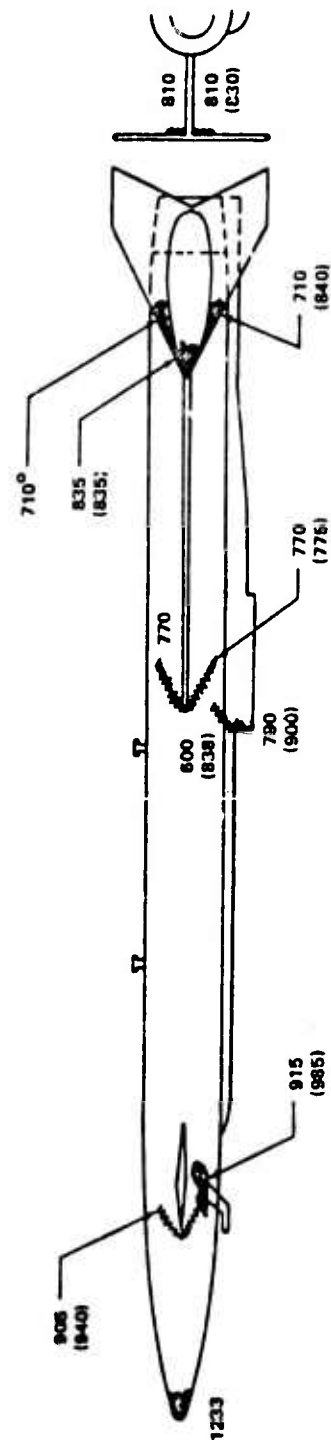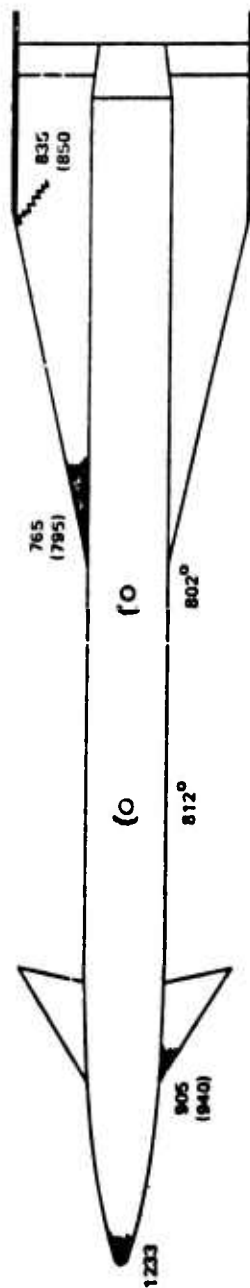
Figure 22. Data from Aeroheating Tests

SECTION V

STRUCTURES AND MATERIALS

The objective in structures and materials was to design, substantiate the structural integrity, and fabricate the HAST (Beech Model 1070) major airframe subsystem.

A design criteria was used in which the structural design environment and strength and rigidity requirements are defined. The loads encountered during ground handling, captive flight, launch, free flight and recovery were investigated to determine the maximum load environment experienced during the life cycle of the HAST 1070 vehicle. Finite element models of the aero surfaces were developed and analysis of the structure has been conducted to determine the margins of safety. Fuselage substructure was analyzed for critical conditions which result during application of ejection and captive flight loads. An aeroelastic analysis was conducted to show that the vehicle was flutter-free throughout both the captive flight and free-flight regimes. Static tests of structural subsystems and a free-free vibration test of a complete missile of flight configuration were accomplished to substantiate analyses.

Materials for the structural subsystem were selected on the basis of cost, minimum weight, process familiarity, availability, strength and stiffness at temperature, and compatibility with inhibited red fuming nitric acid.

1. STRUCTURAL CONFIGURATION

Major sections of the target vehicle are described in the following pages and are illustrated in Figure 23.

a. **Nose Section.** The 3.5-caliber von Karman nose is tangent to the basic 13-inch diameter body at Station 45.5. The forward 35 inches of nose is the radome. The radome material is composed of aluminum phosphate matrix reinforced with glass fabric for radar transparency and temperature consideration. A steel frame is used at the production joint at F.S. 35.75. This frame provides a transition for the radome material and the forward fuselage section.

The total radome volume of 1800 inch^3 is reserved for payload. Payload is defined as that equipment not required for vehicle launch and controlled flight. Aluminum bracketry is used internally for payload installation and assembly.

The air data portion of the guidance electronics, canard torque tube and attach fittings and the electro-mechanical canard control actuator are installed in a 12.58-inch section aft of the radome. The leading edge of the external raceway is attached to this section The basic material for this section is 17-7 PH stainless steel which is fabricated by forming, welding and chem milling. The bracketry for equipment installation is attached with screws to welded in place structural clips. Insulation is used as required for temperature control.

b. **Tankage Section.** The oxidizer tankage is 13 inches in diameter from Station 50.749 where the forward end welds with the tank cylindrical section, to Station 118.331 where the aft end welds with the tank cylindrical section. Tankage ends are elliptical (dome) shape with minor axis of 6.438 inches. The tankage section has a forward tank and an aft tank. The oxidizer flow is from the forward tank through a capillary screen into an aft tank. The forward tank section is divided at Station 89.810 to provide structure for the forward launch lug. A bulkhead assembly at this location consists of a lug support, a cap and a web welded together. A baffle is located at Station 76.620. At Station 109.150 an intermediate dome end is located so that the aft tank section is formed with aft dome end. The forward dome end is located at Station 46 830 the intermediate dome end at Station 109.500 and the aft dome end at Station 122.250 of the tank.

Provisions for attachment of the multifunction valve and tankage pressurization are welded into the forward dome end of the forward tank. The aft tank is pressurized from the forward tank

1070-890000 PARACHUTE MODULE ASSEMBLY

1070-440001 AFT FUSELAGE SECTION

1070-130000 AILERON

1070-640000 VERTICAL STABILIZER

1070-100011 WING

1070-430026 AFT RACEWAY ELECTRICAL EQUIPMENT COVER INSTALLATION

1070-430027 RAM AIR TURBINE INLET FARING

1070-430024 FORWARD RACEWAY

1070-430011 MID SECTION ASSEMBLY

1070-430010 OXIDIZER TANK SECTION

1070-420000 FORWARD FUSELAGE SECTION

1070-670010 CANARD

1070-410000 NOSE ASSEMBLY OR RADOME

Figure 23. Major Sections of HAST Airframe

37

pressure. Provisions for an oxidizer start valve are incorporated into the aft dome end of the aft tank. Angles are bonded to the bottom of the tankage 'or recaway attachment. All tankage material is 17-7 PH stainless steel.

c. Midsection. The basic midsection structure is steel longerons welded to the aft launch lug frame structure at Station 112.25 and to the forward wing attach frame structure at Station 149.

The upper half of this section is enclosed with a steel cover assembly which is part of the parachute module assembly and is formed to make the basic 13-inch diameter body in this area. This structural cover is attached to the longerons and frames with flush structural screws.

The lower half of this section is enclosed with a steel shell which is the cover for the ram air turbine compartment at the forward end and the guidance electronic compartment at the aft end. This shell is formed to provide body contour required for the ram air turbine, turbine exhaust, air inlet duct and guidance electronic compartment. The shell is welded to the longerons and frames. All midsection material is 17-4 PH stainless steel.

Modular electronic equipment assemblies are mounted to the basic midsection structure with access for installation and service through the parachute module assembly opening.

d. Thrust Chamber. The thrust chamber assembly (TCA) is the basic 13-inch body diameter between the forward and aft wing attachment frames at Station 149.00 and Station 194.5 and is attached to these frames with flush structural screws. A nozzle housing tapering from 6- to 7-inch diameter extends from Station 194.5 to 201.0. The TCA incorporates attachments for the aft equipment fairing and is fabricated from 4130 alloy steel heat treated to 180,000 psi.

e. Boattail. The boattail tapers the last 8.19 inches of body to an 11-inch diameter. The taper starts at Station 192.81 and interfaces with the aft wing attachment frame assembly. This frame assembly is a 17-4 PH stainless steel investment casting which provides the aft wing attachment at Station 194.50 and also includes the aileron hinge support at Station 197.50. The frame assembly is attached to the motor case with flush structural screws. A 304 stainless steel boattail cover attaches to the aft end of frame assembly and completes the body (reference Station 201.00).

f. Aileron Control Linkage. The aileron control linkage consists of a 17-4 PH stainless steel bellcrank assembly that is driven directly from a geared electro-mechanical aileron actuator mounted to the aft wing attach frame assembly. Push rods from this bellcrank actuate the aileron to produce ± 10 degrees of aileron travel.

An emergency destruct system is incorporated in the bellcrank assembly. This system is operated with a squib powered pin puller which separates the bellcrank from the aileron actuator and drives the bellcrank to a hard-over aileron position with a compression spring.

g. Canard Control Linkage. The canard control linkage consists of an aluminum bellcrank that is driven directly from a geared electromechanical actuator which is mounted to the forward structure assembly. A steel push rod from this bellcrank actuates a steel canard torque tube to produce ± 20 degrees canard travel. Anti-friction bearings installed in fittings at the outer skin are used to support the canard torque tube. The canards are attached directly to each end of the torque tube with structural screws.

h. Raceway. An external raceway for routing a nitrogen aeration line and electrical wiring from the nose section to the midsection is required to bypass the oxidizer tankage. This raceway is located on the lower centerline of the body and is rectangular in shape, 3.5 inches wide by 0.83 inch in depth. The leading edge of the raceway is located on the forward nose electronic module near Station 36 and the aft end of the raceway enters the air inlet fairing fillet near Station 107.

All raceway-housed equipment is secured to raceway supports with screws. The raceway supports are adhesively bonded to the body skin with high temperature adhesive. All raceway material is 17-7 PH stainless steel.

38

i.   Canard. The canards are attached directly to both ends of the canard torque tube which is located in the aft nose section at Station 42.31 with canard captive structural screws. The canard is solid cast 17-4 PH stainless steel.

j.   Aileron. The ailerons are constant chord full span with the hinge centerline at Station 197.50. The aileron installs on the wing assembly with the outboard hinge bearing located in the wing structure. The inboard end of the aileron plugs into the aileron actuating bellcrank that is installed in the body aft wing attachment frame.

Fabrication of the aileron assembly is accomplished with a one piece skin that forms the leading edge and is welded at the trailing edge. A 3/4 inch diameter tube is used as a spar and welds to the skin top and bottom at the aileron hinge station. A square ended fitting is welded to the tube and closure rib at the inboard end of the aileron and mates with the aileron bellcrank. An outboard hinge bearing fitting is welded to the tube and outboard closure rib. All material is 17-7 PH stainless steel.

k.   Vertical Stabilizer. The vertical stabilizers are attached to the wing tips on the horizontal centerline of the wing with stabilizer captive flush structural screws.

The stabilizers are fabricated from resistance welded PH 15-7 M. stainless steel honeycomb panel. This panel is 1/4 inch thick with 0.012 face sheets and a honeycomb structure of 0.002 gage. 5/16 inch square cells.

The leading and trailing edge taper is accomplished by crushing the panel and welding the face sheets together. Stainless steel inserts are welded in for attachment to the wing structure.

l.   Wing. The wings are a clipped delta planform with a sweep of 75 degrees and a constant thickness of one inch except for the leading edge taper. Flush attachment of the wing to the body is at Station 149.00 and Station 194.50 and is accomplished with structural screws that are captive in the wing fittings. The wing fittings mount flush to the body by incorporating recesses in body frames. A plug-in wing shear pin is located in the wing at Station 127.00.

The wing is fabricated from resistance welded PH 15-7 M. stainless steel honeycomb panel. This panel is one inch thick with 0.012 face sheets and a honeycomb structure of 0.002 gage 5/16 inch square cells. The leading edge taper is accomplished by crushing the panel and welding the face sheets together. The attachment fittings, edge member closures and doublers are installed flush with the basic one-inch thick wing by forming the honeycomb panel and welding the external fitting flanges on both sides. High temperature sealant is used at the wing-body interface.

m.   Ram Air Turbine Inlet Fairing. The inlet fairing provides an aerodynamic cover and a boundary layer diverter for the ram air turbine inlet duct. The leading edge of the air inlet is at Station 104.00 and the aft end matches the constant midsection shape that houses the ram air turbine. The inlet fairing assembly consists of a cast 17-4 PH stainless steel leading edge fitting that provides for attachment of the aft end of raceway and leading edge of the boundry layer diverter. The 17-4 PH stainless steel sheet is formed to contour and welded to the leading edge fitting. A formed 17-7 PH stainless steel flange is bonded to the aft tank section for attachment of the inlet fairing assembly with flush structural screws.

n.   Aft Fairing. An external fairing for routing electrical wiring from the midsection to the boattail section is required to bypass the thrust chamber. This fairing is located on the lower side of thrust chamber at the vertical centerline and matches the contour of the aft end of the lower midsection skin. The forward portion of this fairing is used for installation of electronic equipment. The fairing sections are made from stainless steel. A steel flange is attached to the thrust chamber for attachment of the fairing sections with flush structural screws.

2. MATERIAL SELECTION

Materials were selected which provide a fair compromise of both manufacturing cost and efficient and reliable thermostructural performance capability.

The trajectories producing critical environments indicated that either a thermally protected structure or a structure composed of material capable of maintaining mechanical stability at high temperatures be selected. An early study indicated that the latter proved to be the most economical. Materials which have been considered for acceptable mechanical properties at high temperatures are listed in Table II. Generally the age hardenable stainless steels are selected in meeting the structural requirements of the HAST.

These steels are heat treatable to attain maximum strength which allows forming in the annealed condition, and strengthening after welding. The materials are readily available, working methods are known and they offer the best compatibility to inhibited red fuming nitric acid.

3. STRUCTURAL DESIGN CRITERIA

This section establishes the strength and rigidity requirements for the HAST vehicle. It is divided into the following sections: General Criteria, Design Life, Atmospheric Environment, Thermodynamic Environment, Environmental Loads and Load Factors.

a. **General Criteria.** The cumulative effects of elastic, permanent or thermal deformations, acting singly or together, which result from application of design limit loads and temperatures shall not:

(1) Inhibit or degrade the mechanical operation of the missile or of the carriage or launching vehicle or device.

(2) Adversely affect the missile's aerodynamic characteristics or the aerodynamic characteristics of the carriage, launching vehicle or device.

(3) The target structure will be designed to meet the following operational load environments: free flight, captive flight, launching, handling, hoisting, and shipping conditions. A summary of the factors of safety are presented in Table III.

b. **Design Life.** This section of the design criteria will define storage and operational life for the target system. The design life will consist of storage life, operational life, and readiness.

(1) **Storage Life.** The target shall have a minimum storage capability of five years after packaging and acceptance and shall, after storage under conditions normally encountered in service, be capable of the specified performance.

(2) **Operational Life.** The target shall have a reliable operating life in accordance with MIL-HDBK 217. The minimum reliable operating life shall be fifty hours from time of acceptance to removal for bench servicing. The reliable operating life of fifty hours shall include normal captive and free flight, preflight checkout, and system tests.

(3) **Readiness.** The target shall be designed to require the least possible test or checkout after delivery.

c. **Atmospheric Environment.** The target shall be capable of guaranteed performance during or after encountering the probable surface extremes based on "Operations,Ground,Worldwide" and "Operations, Shipboard, Worldwide" conditions in accordance with MIL-STD-210A.

TABLE II. MATERIAL FOR EVALUATION

Material Type	Designation	Density lb/cu in
Iron-Base Super Alloys (CR-NI) Wrought	B-979	0.295
AGE Hardenable Stainless Steel Wrought	17-4 PH	0.280
	17-7PH	0.276
	PH 15-7 M	0.277
	PH 14-8 M	0.278
AGE Hardenable Stainless Steel Cast	AM-355	0.282
Ultra High Strength Steel Wrought	H-11	...
	D-6A	0.283
	4340	0.283
	18 Ni	0.290
Nickel Base Super Alloys Cast, Wrought	Inconel X-718	0.296
	Rene-41, R-41	0.298
Titanium	Ti-6AL-4V	0.160
	Ti-1AL-8V-5FE	0.168
	Ti-3AL-13V-11CR	0.176
Aluminum	2219-T62	0.103

TABLE III. FACTORS OF SAFETY

Yield	1.15 Limit Load
Ultimate	1.50 Limit Load
Proof Pressure	150% Working Pressure
Burst Pressure	133% Proof Pressure
Casting Factor	1.33

d. **Thermodynamic Environment.** The target system will be exposed to many types of heating and cooling from many different sources during the design life of the system. The extreme temperature environments will be combined with critical loads environments, where applicable, to determine the critical structural environments. The effect of thermal environments (MIL-STD-210A) aerodynamic heating, internal electronic equipment and thrust chamber and flare will be considered.

e. **Environmental Loads and Load Factors.** This section of the structural design criteria specifies the load factors where applicable for the complete system structural environment. The system environment is divided into the following basic categories: ground handling, transportation, captive flight, ejection, free flight, and recovery.

(1) **Ground Handling.** The ground handling environment will consist of hoisting, jacking, cradling, and handling. The target weight for this category will range from maximum to minimum.

(a) **Hoisting.** The limit load factor for hoisting will be 4.0 acting through the center of gravity within the limits of a 20-degree cone.

(b) **Jacking.** The limit load factor for the jacking condition will be 2.0 vertical, 0.50 fore, aft, and lateral.

(c) **Cradling.** The limit load factor for the cradle condition will be 2.5 in all directions.

(d) **Handling.** The limit load factor for the handling condition will be 2.5 in all directions.

(2) **Transportation.** The transportation load factor environment will consist of the railroad shipment, truck shipment and aircraft shipment. The target weight variation for this category will range from maximum to minimum.

(a) **Railroad Shipment.** The limit load factor for rail shipment will be a maximum fore and aft load factor of ± 7.0, the maximum lateral load factor will be ± 3.5, acting singly or in combination.

(b) **Truck Shipment.** The limit load factor for truck shipment will be a maximum fore and aft load factor of ± 7.0, the maximum lateral load factor of ± 3.5, acting singly or in combination.

(c) **Aircraft Shipment.** The limit load factors which can be considered to be imposed upon the cargo during normal flight or in emergencies is as follows: forward - 8.0 g's, sideward - 1.5 g's, vertical (up) - 2.0 g's, aft - 1.5 g's.

(3) **Captive Flight.** The target will comply with MIL-A-8591C wing carriage. The captive flight conditions will be investigated for the entire launch envelope for the respective carrier aircraft. From the launch envelope, shown in Figure 24, the maximum and minimum aerodynamic loads will be generated in accordance with MIL-A-8591C. The captive flight aerodynamics will be produced from free flight aerodynamics by using appropriate wind tunnel tests.

(4) **Ejection.** The target shall be capable of being launched from any point within the launch envelope.

(5) **Free Flight.** The target missile shall be designed to withstand all loads produced in the free flight regime under the criteria established in this section. This section will be divided into aerodynamic loads, maneuvering loads, and boost loads.
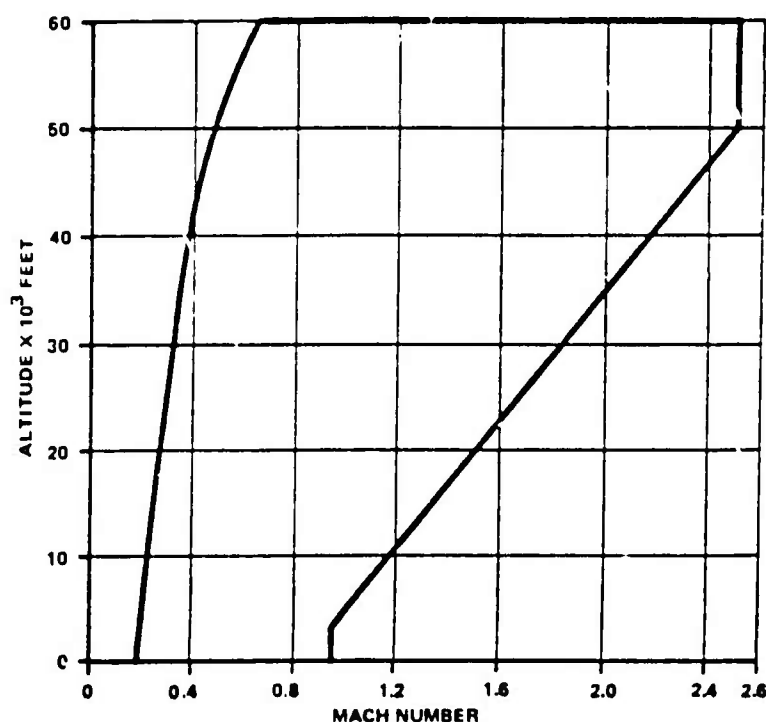
Figure 24. Captive Flight and Launch Envelope

(a) Aerodynamic Loads. Free flight aerodynamic characteristics will be derived from Technical Report AEDC-TR-71-178, Static Stability and Inlet Characteristics of the HAST Missile at Transonic Mach Numbers, September 1971, for the range of Mach numbers from 0.8 to 1.35 and Technical Report AEDC-TR-72-6, Aerodynamic Characteristics of the HAST Missile at Mach Numbers 2.25, 3 and 4, January 1972, (References 1 and 2).

The free flight envelope and other missions will be investigated completely to determine the maximum aerodynamic forces and moments. The maximum aerodynamic loads will be superimposed with other applicable loads and conditions, such as thermal stresses, temperature environments, gust loads, and maneuvering loads. The critical loading conditions will be determined by considering all phases of the environment.

(b) Maneuvering. The maximum limit load factor for maneuvering will be ± 5.0 g's. The maneuvering capability of the HAST vehicle is given in the following set of maneuvers:

43

TABLE IV. MANEUVERING CAPABILITY

"S" turn @ 35K Mach 2.6 - 2.8	5.0 g's
"S" turn @ 90K Mach 1.8 - 4.0	1.15 g's
180° turn @ 35K Mach 2.6 - 2.8	5.0 g's
180° turn @ 90K Mach 1.8 - 4.0	1.15 g's
Vertical (up-down) @ 35K Mach 2.6 - 2.8	5.0 g's
Vertical (up-down) @ 60K Mach 1.2 - 3.5	2.0 g's
Change in altitude of ± 5K, between 40K and 90K, in 20 seconds, Mach 1.2 - 4.0.	

The maneuvering loads will be combined with gust loads in a manner which will model the probability of gust during maneuvers.

4. STRUCTURAL DESIGN LOADS

This section presents the loads used in the stress analysis and static testing of the HAST vehicle. The loads presented are the design loads determined to be the most severe loads experienced based on the structural Design Criteria described above.

a. **Body Limit Loads.** Body limit shear and bending moment diagrams are presented in Tables V through IX. Tables V through VIII are determined from captive flight conditions and Table IX was determined from ejection loads.
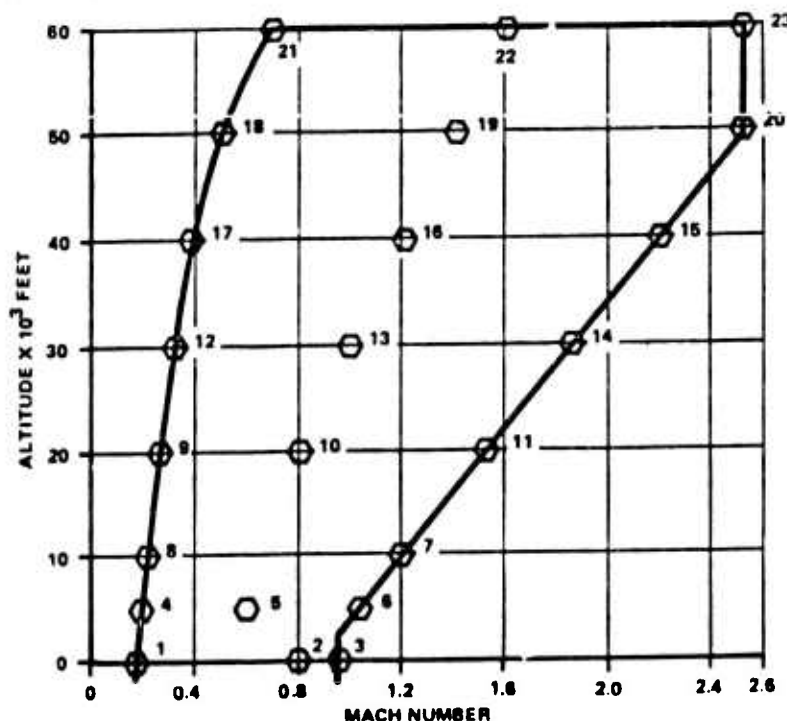
Figure 25. Aerodynamic Loading Conditions

44

TABLE V. STATIC TEST LOADING, CONDITION CP6PP7PN

| Missile Station | Vertical | | | Associated Lateral | | |
	Load	Resultant Shear	Resultant Moment	Load	Resultant Shear	Resultant Moment
14.0	-305	-305	--	-260	-260	
42.31	-1369	-1674	-8,635	-1090	-1350	-7,361
76.62	442	-1232	-66,070	-1140	-2490	-53,679
89.81	(Reaction) -4708	-5940	-82,333 -73,510	(Reaction) -1753.5	-4243.5	-86,522
112.64	276	-5664	-209,120	-1500	-5743.5	-183,401
122.25	(Reaction) 10,497	4833	-263,551	(Reaction) 10,869.5	5126	-238,596
130.65	+56	4889	-222,954	-500	4626	-195,538
149.00	-1847	3042	-133,241	-2100	2526	-110,651
192.81	-3042	0	+29	-2526	0	+13

LOADING CONDITION CODING

CF   i   P   N   7   N   P

Airload Yawing Moment - P - Positive / N - Negative

Airload Side Force - P - Positive / N - Negative

Aerodynamic Loading Condition (Figure 25)

Yawing Acceleration - P - Positive / N - Negative

Pitching Acceleration - P - Positive / N - Negative

Pt. No. on Load Factor Envelope

Type of Loading Condition

CF - Captive Flight

CA - Catapulting

AL - Arrested Landing

45
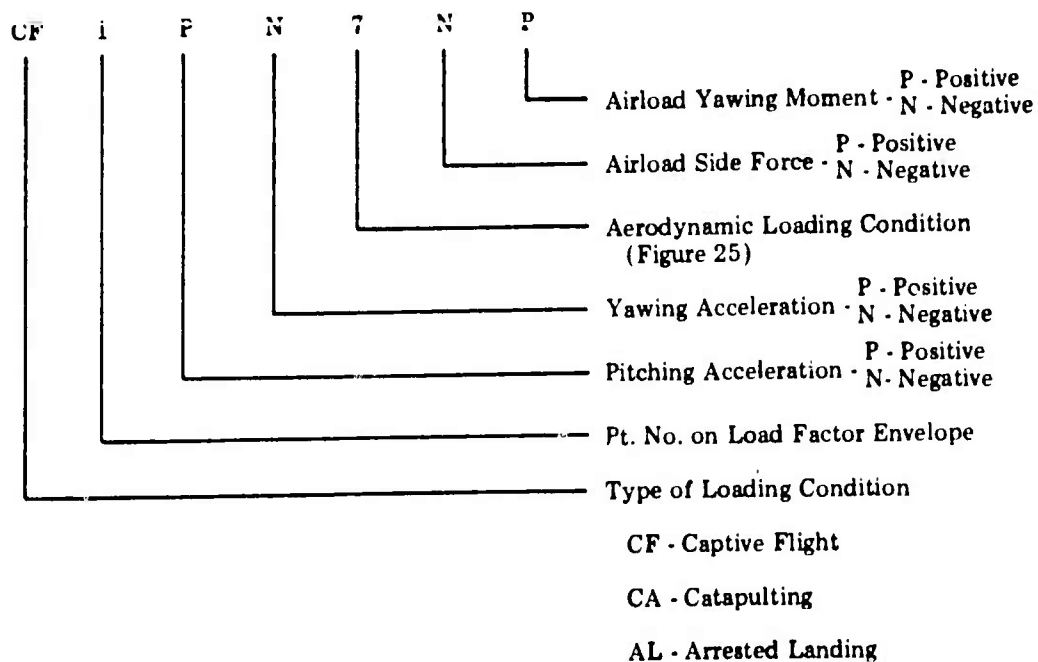
TABLE VI. WING NET LOADS DISTRIBUTION, (W/O AILERON)

Captive Flight (MIL-A-8591C) - Condition 19 of Figure 25

$N_z = -6.0$ (down); $\theta = 6.0$ (nose up)

Buttock Line	[1] Load	S	Y	V_z	M_x [2]	[3]M_y
19.583	472.578	193.323	19.583	472.58	0	-204.33
18.26	17.923	171.772	18.763	490.50	634.24	174.19
16.79	77.732	182.349	17.860	568.24	1438.46	993.63
15.32	15.464	149.177	16.140	583.70	2286.36	1669.63
13.85	220.493	186.585	14.763	804.19	3345.68	3060.05
12.38	60.178	180.472	13.187	864.37	4576.39	3807.40
10.91	222.692	184.954	11.635	1087.06	6008.54	5574.90
9.44	184.273	160.498	9.997	1271.34	7709.24	11544.14
7.97	280.222	177.474	8.339	1551.56	9681.61	15864.27
6.50	-9.777	173.890	6.761	1541.78	11959.85	15678.50

1        $L_{(Ail)} = 176.39$ (not included); $X_{(Ail)} = 198.556$; $Y_{(Ail)} = 12.959$

2        $M_{x(fin)} = 2166.67$ in-lb (not included)

Total load = 1718.17; $X_{cp} = 183.184$; $Y_{cp} = 15.385$ (included M_{XF} and the aileron load)

Load (w/o aileron) = 1541.78; $X_{cp} = 182.722$; $Y_{cp} = 14.257$

3   Ref Axis = 192.891

TABLE VII. WING NET LOADS DISTRIBUTION, (W/O AILERON)

Captive Flight (MIL-A-8591C) · Condition 20 of Figure 25

Most forward center of pressure · Maximum Mx_F

N_z = 6.0 (down); θ = 6.0 (nose up); See Condition 19 of Figure 25 for inertia loads.

Buttock Line	[1] Load	X	Y	V_Z	[2] M_x	[3] M_y
19.583	270.45	189.393	19.583	270.45	0	946.16
18.26	48.34	171.739	18.764	318.77	382.15	1968.64
16.79	126.68	176.757	17.776	445.47	975.73	4012.52
15.32	53.79	157.597	16.160	499.27	1675.75	5910.96
13.85	71.91	158.178	14.683	571.18	2469.58	8407.20
12.38	70.79	143.419	13.053	641.97	3356.89	11909.34
10.91	77.78	150.825	11.512	719.75	4347.40	15181.26
9.44	401.02	146.519	9.983	1120.77	5623.03	33777.45
7.97	254.65	137.908	8.603	1375.43	7431.71	47778.97
6.50	15.22	192.699	6.560	1360.21	9452.68	47776.051

1    $L_{(a)}$ = -3.33 lbs @ (197.844, 12.476); (not included)

2   Mx_F = 2672.65 in-lbs (not included)

3   Reference Axis = 192.891

Total Load · 1356.88 lbs.; (X = 157.669, Y = 15.4215) (W/fin and aileron loads)

Load (w/o aileron) = 1360.21 lbs.; (X = 157.767, Y = 15.414)

L_U = 307.1 lbs. @ (186.634, 105.37) L_L = 804.8 lbs. @ (186.634, 94.63)

Water Line	Load	X	Z	V_y	[1] M_x	[2] M_z
113				0	0	0
	38.33	198.598	111.320			
110.5				38.33	-31.42	-15.40
	22.13	191.448	108.942			
108				60.46	-148.08	-182.52
	63.55	188.182	106.731			
105.5				124.01	-377.45	-870.04
	100.26	186.594	104.236			
103				224.27	-811.41	-2113.98
	82.83	178.674	101.992			
100.5				307.10	-1495.68	-3797.60
100				307.10 804.80	-1649.23 4322.05	-3797.60 -9952.16
99.5				804.80	3919.65	-9952.16
	217.07	178.674	98.008			
97				587.73	2126.43	-5539.99
	262.76	186.594	95.764			
94.5				324.97	989.16	-2280.07
	169.55	188.182	93.269			
92				158.42	388.06	-478.32
	57.99	191.448	91.058			
89.5				100.43	82.33	-40.37
	100.43	198.598	88.680			
87				0	0	0

1   Reference Axis = Water Line 100.0

2   Reference Axis = Missile Station 199.0

48

TABLE IX. HAST STATIC TEST LOADING CONDITION EJECTION

Vertical				Vertical		
Missile Station	Load	Resultant Shear	Resultant Moment	Load	Resultant Shear	Resultant Moment
14.0	1486	1486	--	-1477	-1477	--
42.31	1251	2737	42,069	-1089	-2566	-41,814
76.62	1825	4562	135,975	21	-2545	-129,853
89.81	(Reaction) -2475	2087	196,148	(Reaction) 1582	-963	-163,422
112.64	265	2352	243,794	1864	901	-185.410
122.25	(Reaction) -6338	-3986	266.397	(Reaction) -107	794	-176,751
130.65	-639	-4625	232,915	1251	2045	-170,081
149.00	1245	-3380	148,046	981	3026	-132 555
192.81	3380	0	-32	-3026	0	14

b. Wing and Canard Free Flight Limit Loads. Critical free flight wing and canard limit loads are presented in Table X. Aero surface loads were calculated as total loads and distributed as point loads on each surface for use in a digital computer program.

TABLE X. CRITICAL FREE FLIGHT PLUS GUST LOADS

Condition	Total	Canard	Wing	Nose	Body
F35H2.8+G	5216	599	3455	413	749
F40H0.2+G	4982	1753	1287	336	1606
F90V4.0+G	2155	196	1517	206	236

Example Conditional Designation

F - Free Flight

35 - 35,000 ft altitude

H - Horizontal Maneuver

2.8 - Mach Number

G - Gust Load Increment

Wing and Stabilizer Captive Flight Loads. Critical wing and stabilizer captive flight net maximum loads are presented in Tables VI through VIII. These loads were derived using the angles of attack and sideslip as prescribed in MIL-A-8591C for wing carriage of stores.

c. Airload Data. HAST airloads are based on the aerodynamic data as discussed in the previous section. Component airloads were calculated for ten free flight maneuver conditions and twenty-three captive flight conditions.

d. Inertia Loads. Free flight loads are based on varying weights determined from performance data. The weight of the missile at a given altitude-velocity combination during a specified mission was used.

5. FREE FLIGHT LOADS

Free flight loads were calculated for several points along the high speed, high load factor boundary of Figure 25, and at 40,000 feet and Mach 1.2 gust increments were directly added to these conditions. The total loads were divided into component loads using a computer program based on NASA Report 1307, Lift and Center of Pressure of Wing, Body, and Tail Combinations at Subsonic, Transonic and Supersonic Speeds (Reference 3).

Examination of Figure 1 indicated that the following conditions produce loads that should be investigated. Component loads for these conditions are presented in Table XI.

TABLE XI. FREE FLIGHT LOADS

Mach Number = 2.8	Altitude = 35,000 ft	Weight = 719 lbs
Maneuver Load Factor = 5.0	Gust Increment = 2.254	
Mach Number = 1.2	Altitude = 40,000 ft	Weight = 895 lbs
Maneuver Load Factor = 4.65	Gust Increment = 0.917	
Mach Number = 4.0	Altitude = 90,000 ft	Weight = 806 lbs
Maneuver Load Factor = 2.5	Gust Increment = 0.173	

6. LOAD DISTRIBUTION

Airload distributions were accomplished by using equations derived from the potential flow theory as presented in NACA TN 1662, Aerodynamic Properties of Slender Wing Body combination at Subsonic, Transonic and Supersonic Speeds, Ames Aeronautical Laboratory, July 1948 (Reference 4). Potential flow theory was determined to be applicable since the HAST airframe is a slender body (L/D = 15.4) with a low aspect ratio wing (AR = 0.593). In addition the body is near the center of the Mach cone. Other analysis methods investigated were the Ackeret and Buseman linear theories and Newtonian theory. The airload distribution on the body in the presence of the wing was predicted by using the equation noted on the following page.

$$\frac{d(L/q)}{dx} = 4 \alpha S \left\{ \left[\frac{ds}{dx} \left(1 - \frac{a^4}{S^4} \right) + \frac{dc}{dx} \left(1 - \frac{a^2}{S^2} \right) + \ldots \right. \right. \tag{12}$$

$$\left. \left. \ldots + \left[\frac{da}{dx} \left(1 + \frac{a^2}{S^2} \right) \left(\frac{a}{2s} - \frac{s}{2a} \left(1 + \frac{a^2}{S^2} \right) \right) \right] \sin^{-1} \left(\frac{2a/s}{1 + a^2/S^2} \right) \right.$$

Where   L = Lift

                q = Free-stream dynamic pressure

                a = Radius of body

                S = Local Semispan

Similarly, the airload distributions on the canard and wing were determined by using the following equation:

$$\frac{\Delta p}{q_w} = \frac{4 \alpha \left[\frac{ds}{dx} \left(1 - \frac{a^4}{S^4} \right) + \frac{da}{dx} \left[2 \frac{a}{S} \left(\frac{a^2}{S^2} - \frac{a^2}{r^2} \right) \right] \right]}{\sqrt{ \left(1 + \frac{a^4}{S^4} \right) \cdot \left(\frac{r^2}{S^2} \right) \left(1 + \frac{a^4}{r^4} \right) }} \tag{13}$$

Where   P = Static pressure

                q = Free stream dynamic pressure

                S = Local semispan

                a = Radius of body

                r = Spanwise coordinate variable

Strength analysis of the aerodynamic surfaces was accomplished by using the distributed airloads in a finite element digital computer program.

7. CAPTIVE FLIGHT LOADS

Captive flight loads were calculated using the method outlined in MIL-A-8591C for twenty-three captive flight, catapult and arrested landing conditions. The inertia load factors for wing mounted stores were used. The twenty-three captive flight analysis conditions are shown in Figure 25.

The maximum lug and sway brace loads determined from this analysis are shown in Table XII. These loads were used to substantiate the strength of the airframe substructure.

TABLE XII. CRITICAL CAPTIVE FLIGHT LOADS

Lug and Sway Brace Limit Loads		
	Load Type	Load (lbs)
Forward Lug	Tensile	14303.0
	Shear	10972.0
Aft Lug	Tensile	29025.0
	Shear	10972.0
Left Forward Sway Brace	Compressive	8985.0
Right Forward Sway Brace	Compressive	8985.0
Left Aft Sway Brace	Compressive	21651.0
Right Aft Sway Brace	Compressive	21651.0

The maximum body shear and moment loads occur during captive flight and ejection and were presented in Tables V through IX. These loads were used to structurally substantiate major sections of the body.

8. STRENGTH SUBSTANTIATION

The structural integrity of HAST structure was substantiated by both analysis and testing. Selected segments are presented.

a. **Body Analysis.** The primary mode of failure for the payload section and the forward body guidance section were determined to be from buckling. The primary mode of failure of the oxidizer tankage was attributed to tensile failure due to the combination of body bending and internal pressurization. Conventional methods of stress analysis were used for the structural substantiation of the body. Margins of safety are presented in Table XIII.

b. **Aerodynamic Surfaces.** A structural analysis of the wing using a finite element digital computer program was accomplished. Distributed airloads for the critical flight conditions were applied to a representative structural model. Analysis indicated that the wing was capable of sustaining the static loads imposed. The canard was analyzed in a similar manner as the wing and determined to be structurally adequate.

Since the finite element and analysis method is used extensively in the structural substantiation of major components of the HAST airframe, a brief explanation of the theory involved follows.

TABLE XIII. STRUCTURAL MARGINS OF SAFETY

	Material	Thickness	Design Load Condition	Margin of Safety
Nose Cone	17-7 PH	0.025	Ejection	0.60
Forward Body	17-7 PH	0.040	Ejection	1.19
Nitrogen Torus Tank	17-7 PH	N.A.	Burst	0.00
Fwd Oxidizer Tank	17-7 PH	0.032	Captive Flight	0.09
Fwd Launch Pin Frame	17-7 PH	N.A.	Free Flight	0.41
Aft Oxidizer Tank	17-7 PH	0.063	Captive Flight	0.17
Aft Launch Pin Frame	17-4 PH	N.A.	Captive Flight	0.00
Mid-Body	17-4 PH	0.06	Captive Flight	0.15
Canard	17-4 PH	N.A.	Free Flight	0.27
Fwd Wing Attach Frame	17-4 PH	N.A.	Captive Flight	Large
Wing	PH 15-7M	N.A.	Captive Flight	0.06
Aft Wing Attach Frame	17-7 PH	N.A.	Captive Flight	0.40
Stabilizer	PH 15-7M	N.A.	Captive Flight	0.10

(N.A. - Not Applicable)

The structure is modeled in a series of discrete structural elements joined to form a series of nodes. The model used for this structure is discussed in the following section. Once the model has been designed, a stiffness matrix can be generated for each element. An element stiffness matrix relates the forces and displacements of the element, i.e. -

$$p = K_p \quad v \tag{14}$$

where

p = column of element nodal forces

v = column of element absolute displacements, and

K_p = element stiffness matrix

The stresses on the element boundaries must be replaced with force resultants at the nodes.

From a consideration of the compatibility of the element displacements at each node and the equilibrium of the internal and external forces at each node, the element stiffness matrices can be combined to form a stiffness matrix for the structure. The resulting force-displacement relation is

53

$$f = K_f \, d \tag{15}$$

where

      f = column of external forces (loads) at the nodes of the structure

      d = column of displacements at the nodes of the structure, and

      K_f = structure stiffness matrix

The preceding equation can be solved for the displacements when the loads and the constraints on the structure are specified. Alternately, an element stress-displacement relation of the form

$$\sigma = S \, v \tag{16}$$

where

      σ = column of element stresses

      v = column of element absolute displacements, and

      S = element stress matrix

can be used to calculate selected stresses in the elements.

The calculations described above are performed automatically by the computer program once the structure nodal coordinates, elements, loads and constraints have been specified.

    c.   **Structural Static Test.** A structurally complete Model 1070 HAST missile was subjected to static loads to determine structural adequacy for flight conditions found to be critical. Dummy actuators were installed to lock the canards and the ailerons and transfer the hinge moments resultant from the loading into the basic structure. The test article was mounted in an inverted horizontal position on a reinforced 10-inch wide flange steel I-beam, using steel brackets to simulate launcher attachments at launch pins and sway brace points. The I-beam was supported at missile stations 61 and 155 so that the test article centerline was approximately 75 inches above the laboratory floor. The entire test article was assembled and mounted during the vertical stabilizer test. Load was applied to the stabilizer through compression pads.

A dummy stabilizer was substituted during wing and aileron tests to simplify application of stabilizer moments to the wing. Distributed loads were applied to the wing through compression pads, tension patches cemented to the ailerons, and the dummy stabilizer. Compression pads were cemented to the canards for distributed load application and location. Vertical and horizontal loads for body tests were applied through canard and wing attachments, and load bands located at missile stations 14.0, 76.62, 112.64, and 130.65. The wings were removed and stub fittings installed at the wing attachment points. Drag loads were applied through wing attach fittings and/or the canard hinge. Load was supplied with hydraulic cylinders which were anchored to the laboratory floor or to a structural steel framework; two small loads were supplied by using weights. Whiffletrees were used to combine the applied loads to minimize the number of hydraulic cylinders necessary for load distribution. Pressures were metered to the cylinders by a Model 10 M Hydraulic Load Maintainer, manufactured by John S. Edison, Inc.

Strain gages were installed on the test article. The gages were connected to a B and F Instruments, Inc., Multichannel Digital Strain Indicator, Model SY161-50-V-P3, Serial 381, which provided a printed readout of strain at each increment of loading. Graduated scales were suspended from the test article. The scales were read during test with a surveyor's transit. Each hydraulic

cylinder was connected to the test article through a BLH Electronics load cell. Each load cell, cylinder and load maintainer combination was calibrated in the Baldwin pull test machine prior to test. The load cells were monitored during test to assure proper loading.

d. **Method of Test.** The calibrated stabilizer load system was set up and a set of deflection scale and strain gage readings was taken. Load was applied to 20, 40, 60, 80, 100, and 115 percent of limit load. Load cell, strain gage, and deflection scale readings were taken at each increment.

The calibrated wing load system for Condition 19 was set up and a set of deflection scale and strain gage readings was taken. Load was applied to 20, 40, 60, 80, 100 and 115 percent of limit load values for Condition 19. Load cell, strain gage and deflection scale indications were recorded at each increment. This procedure was repeated using Condition 20 setup and loads.

The calibrated body load system was set up for Negative Ejection Condition and a set of strain gage and deflection scale readings was recorded. Load was applied in increments to 20, 40, 60, 80, 100 and 115 percent of limit load. A set of load cell, deflection scale and strain gage readings were recorded at each increment. This procedure was repeated for Conditions Positive Ejection and CF6PP7NP (See Table V).

Figures 26 through 34 present deflection curves resulting from loads application to major structural subsystems. After applying 115 percent of limit loads in each test condition, the applied loads were removed. No evidence of permanent set or deformation was observed.

Application of ultimate loads were not attempted since the static test vehicle was required as an antenna alignment and RF payload vehicle.

9. AEROELASTIC ANALYSIS

To assure a flutter-free vehicle throughout its flight regime the following maximum dynamic pressure configurations have been investigated for both subsonic and supersonic flight:

TABLE XIV. DYNAMIC PRESSURE CONFIGURATIONS

		Mach No.	Altitude (Ft)	Configuration Designation	
				Symmetric	Anti-Symmetric
Full Gross Weight	Launch	0.9	40,000	100C	101C
Most Forward CG	Launch	2.0	50,000	100C	101C
	Cruise	2.6	35,000	102F	103F
Forward Oxidizer Empty					
Most Aft CG	Cruise	2.6	35,000	102F	103F
Forward Oxidizer Empty					
Most Aft CG	Cruise	4.0	90,000	104F	105F
High Temperature					
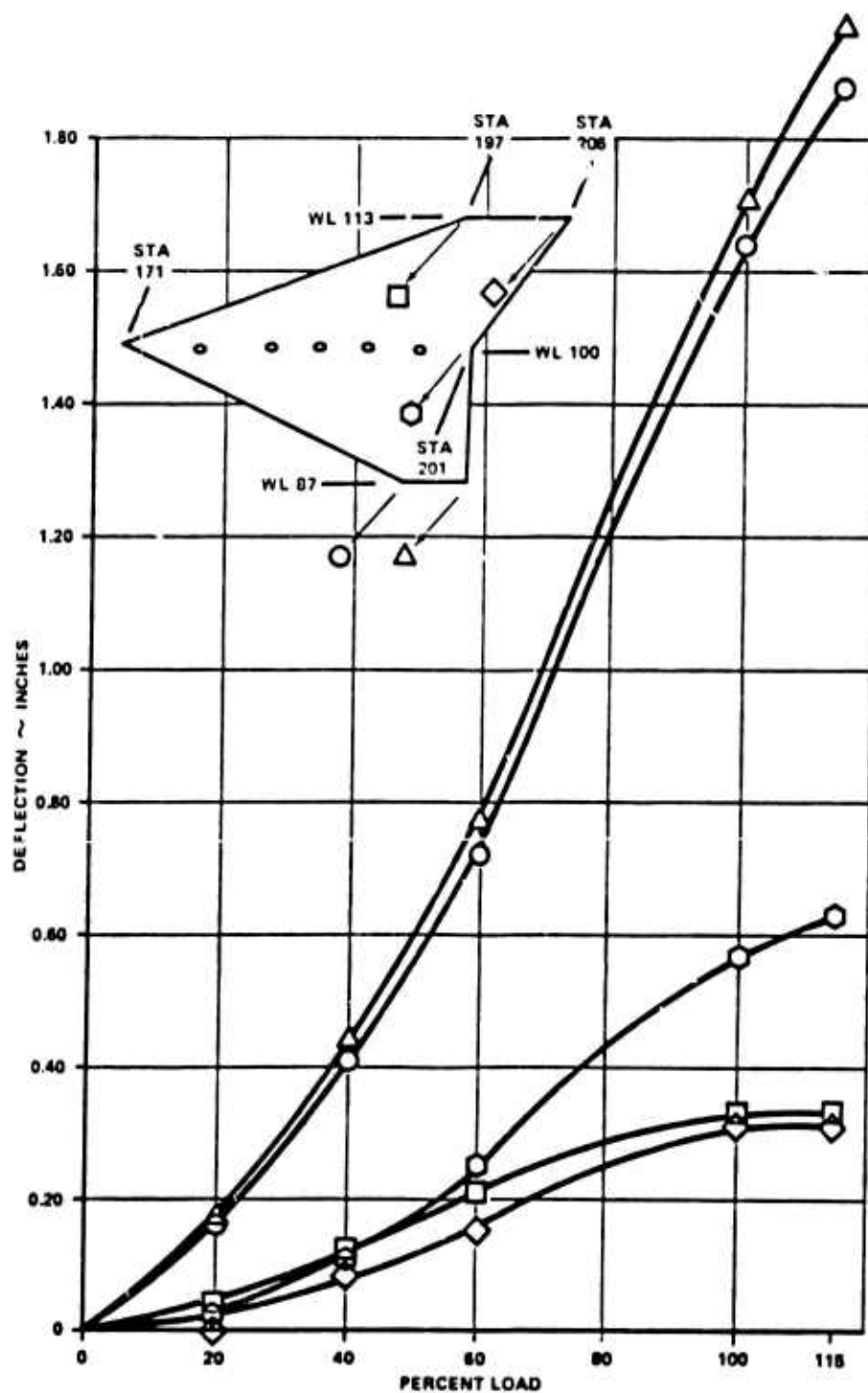
Figure 26. Vertical Stabilizer Deflections, Condition 20
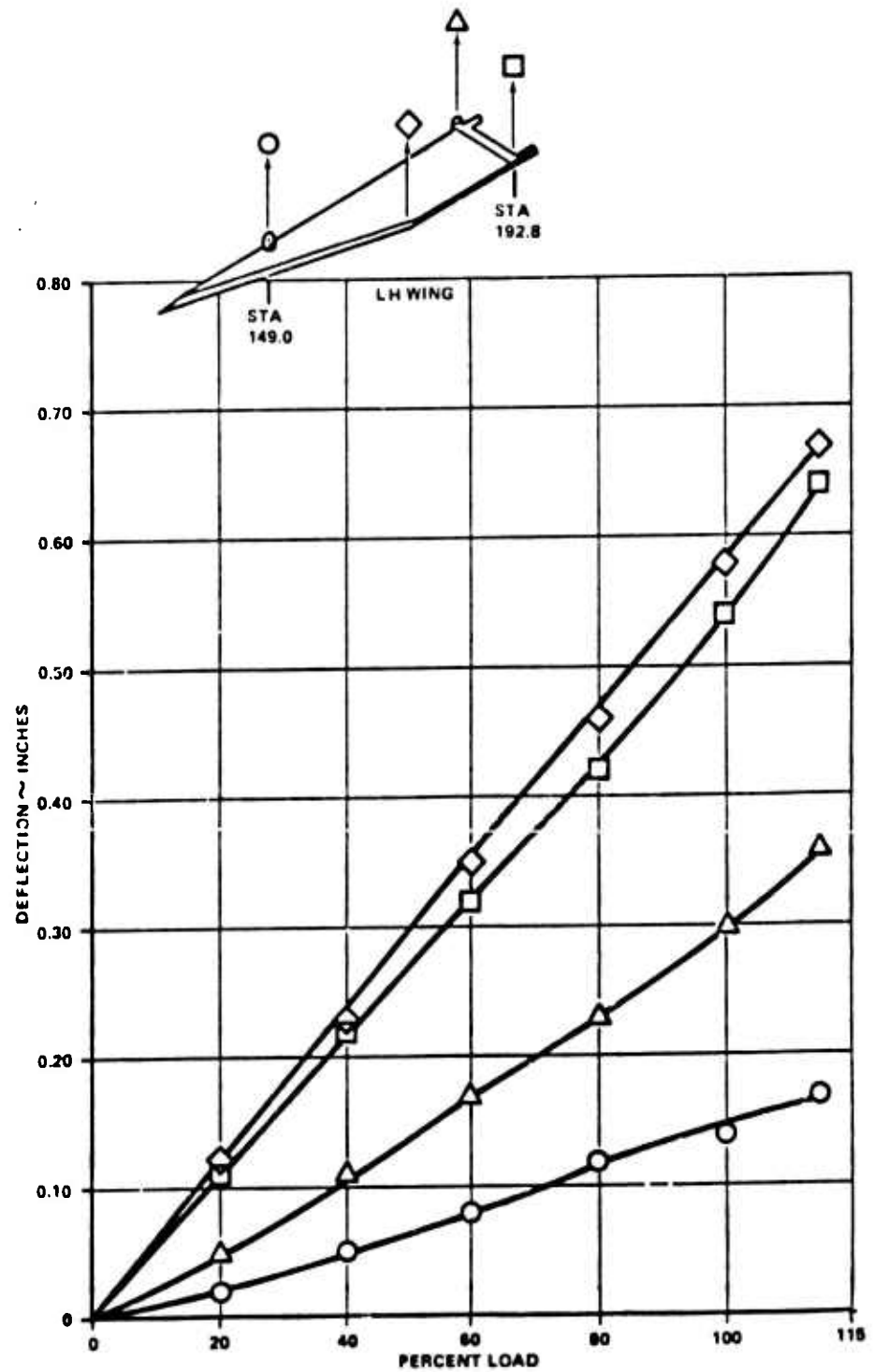
Figure 27. Wing Deflections, Condition 19

57
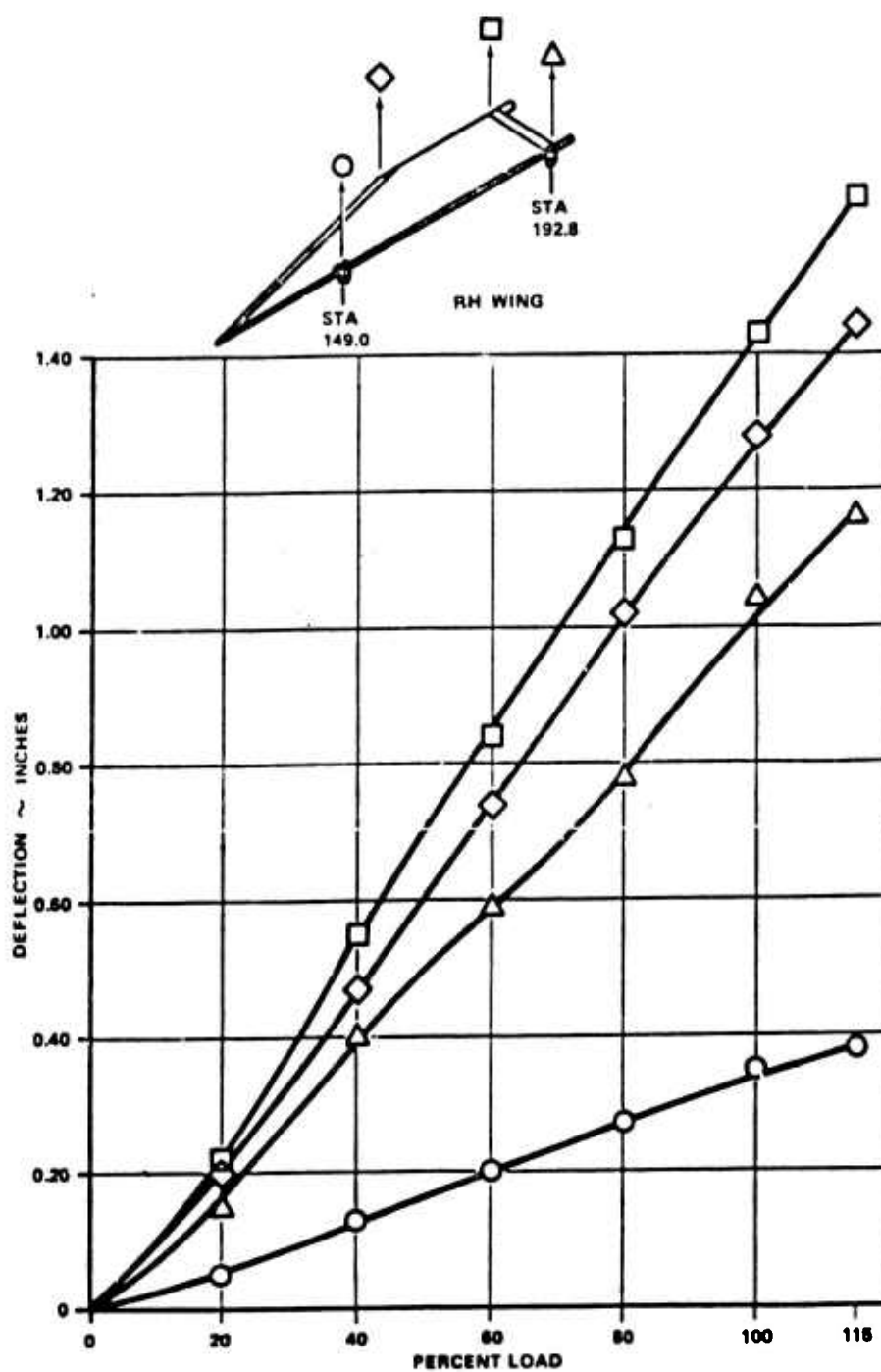
Figure 28. Wing Deflections, Condition 20
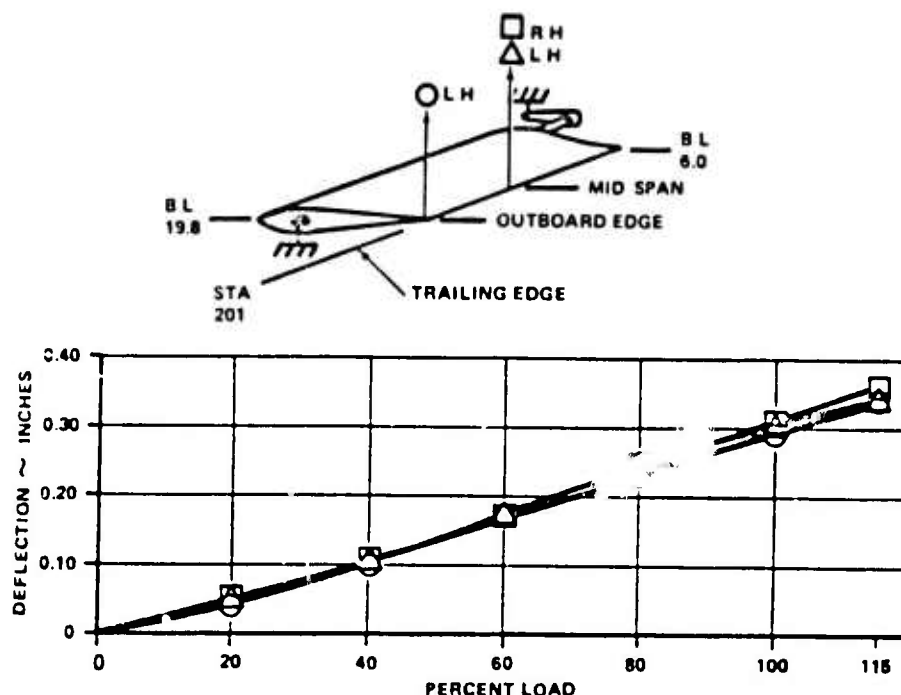
Figure 29. Aileron Deflections, Maximum Load Condition

a.   Analysis. The technique used in the structural dynamics representation of the missile is that of a finite element model employing plates and beams in a component substructure coupling vibration analysis.

In the symmetric analysis of the launch configuration the vehicle was constrained in vertical translation at its launch lug attach points (reference Body Stations 89.81 and 122.25). The first six symmetric vibration modes for configurations 100C, 100F, and 102F are presented in Tables XIV and XV. The effects of heating on structural stiffness at a Mach number of 4.0 were investigated in Configuration 104F. The high temperature mode shapes (Configuration 104F) are nearly the same as the low temperature mode shapes (Configuration 102F) although a consistent decrease in frequency was realized as was expected.

In the anti-symmetric analysis the missile required a full six-degrees-of-freedom at all modes except those along the body which were constrained in longitudinal translation vertical translation and pitch. Due to the large number of required degrees-of-freedom and the nature of the launch constraints the missile was analyzed as three substructure components.

A least squares curve fitting routine minimizing the error in bending slopes as well as deflections was used to generate coefficients for a surface polynomial representation of the vibration mode shapes. These polynomial representations were used as input into the subsonic and supersonic unsteady aerodynamic programs.

The subsonic unsteady aerodynamic program is based on the Doublet Lattice method of representation and has the capability of modeling a coplanar canard-wing and control surface configuration. Supersonic unsteady aerodynamics were generated using the Mach Box technique.

59
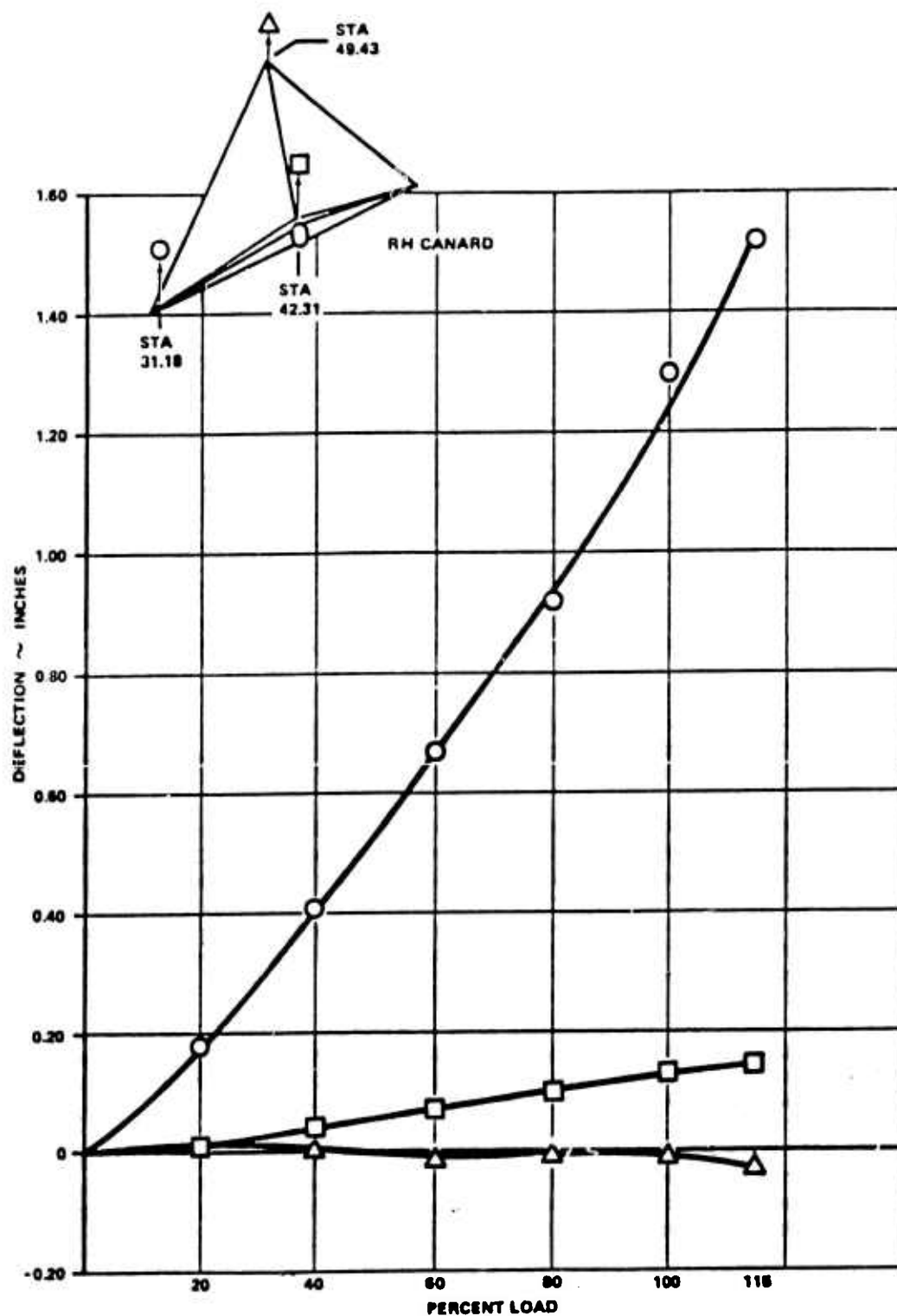
Figure 30. Canard Deflection, Maximum Load Condition

60
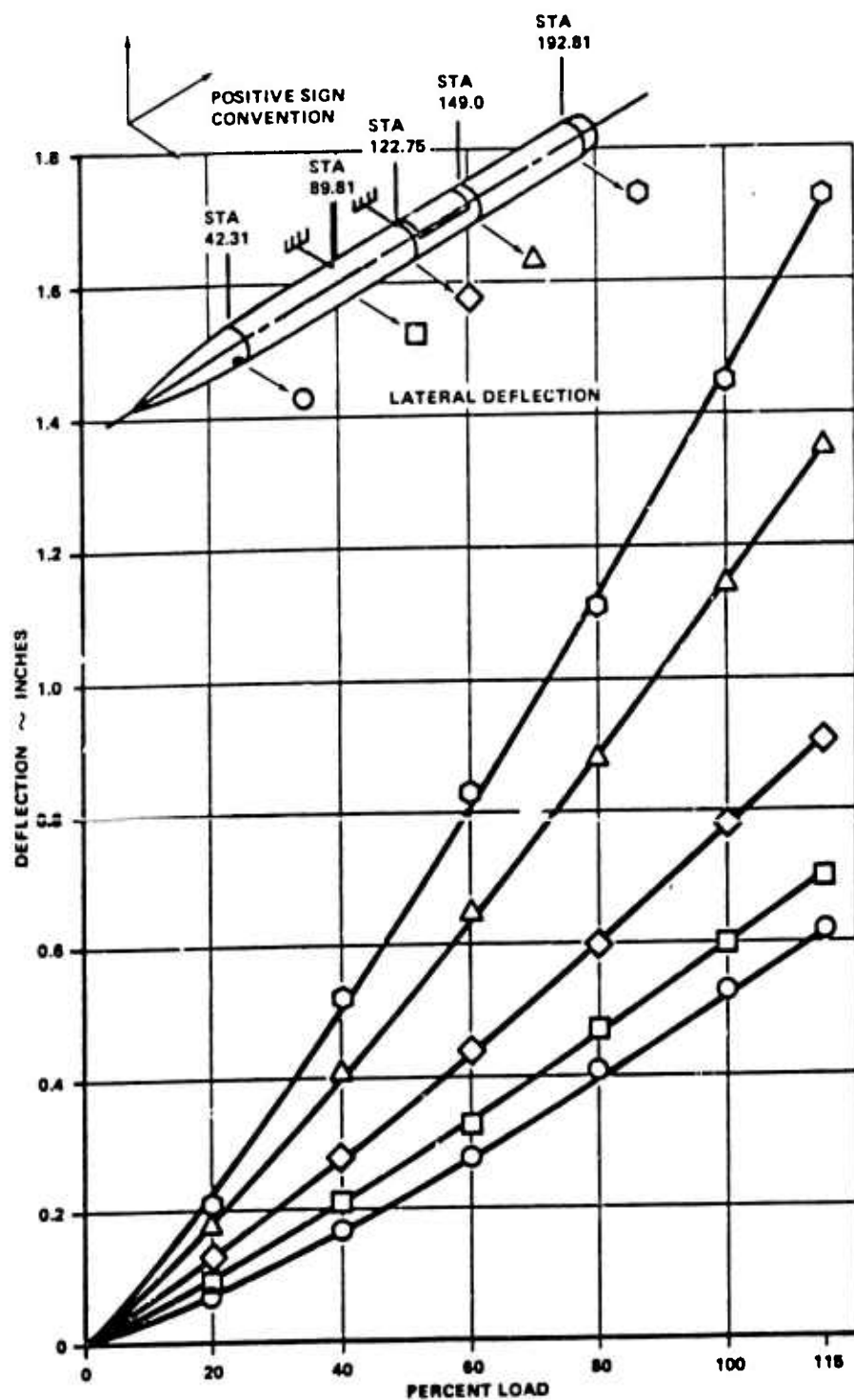
Figure 31. Body Deflections, Lateral Conditions

61
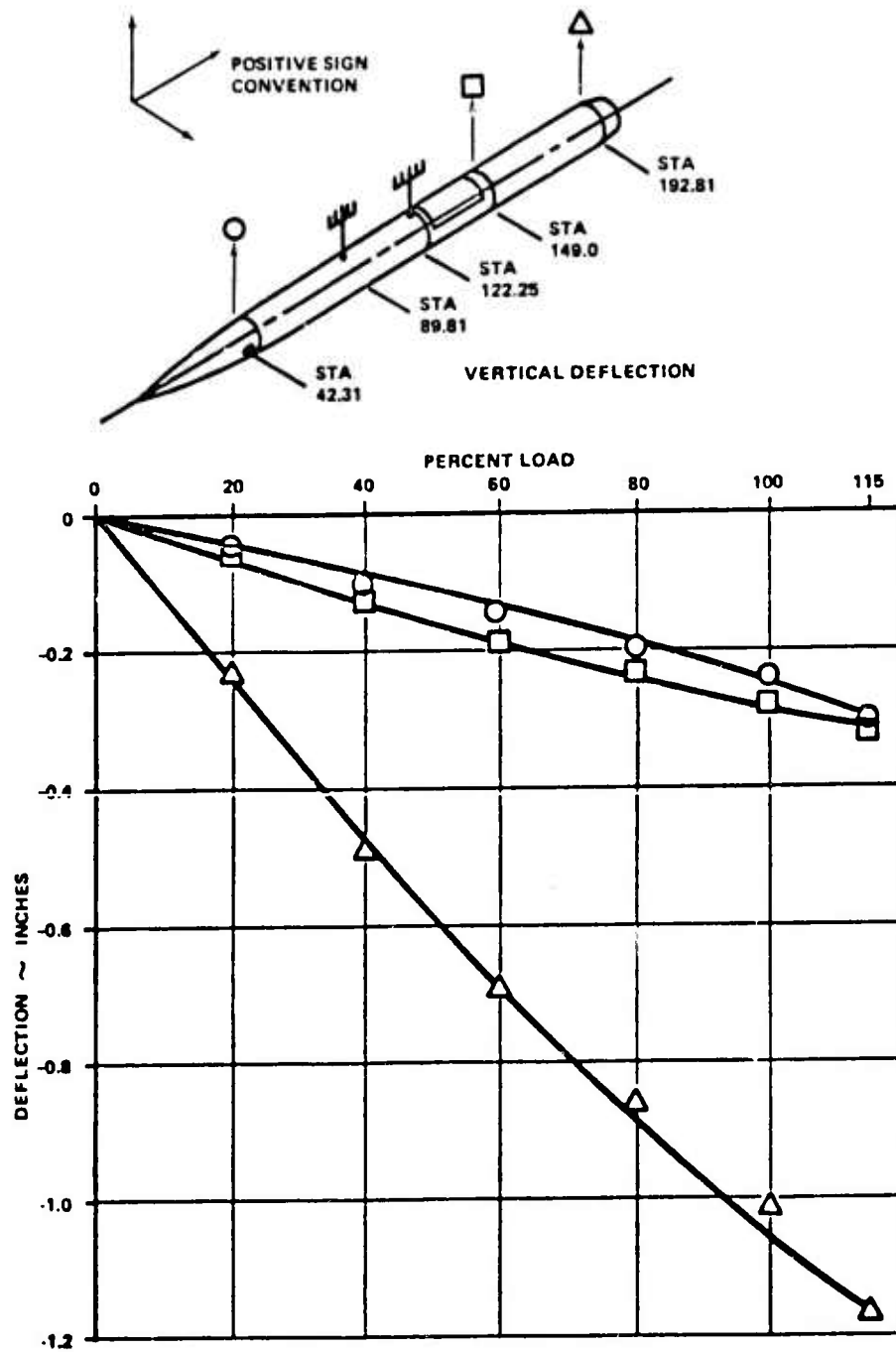
Figure 32. Body Deflections, Vertical
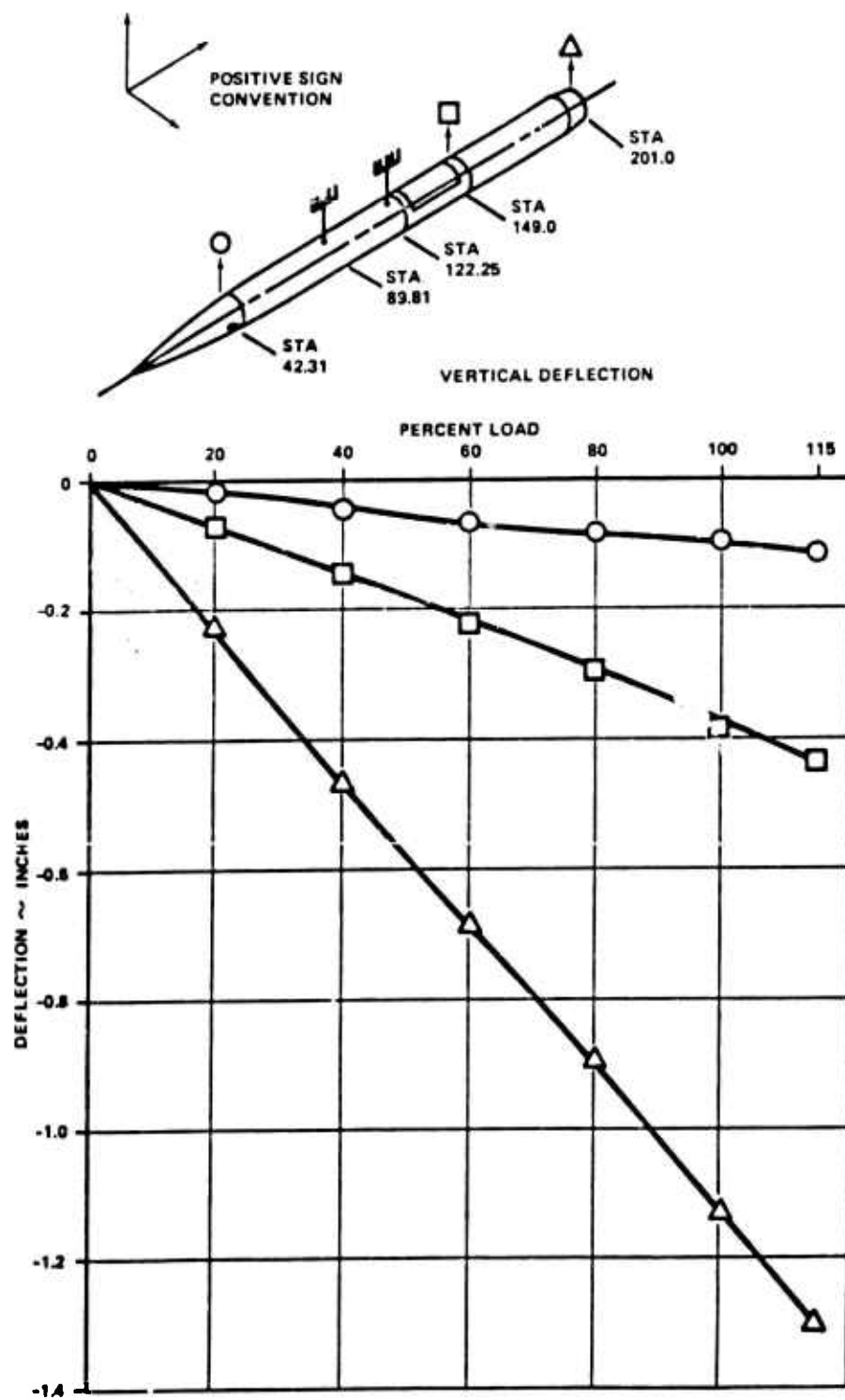
Figure 33. Body Deflections, Negative Ejection Conditions

63
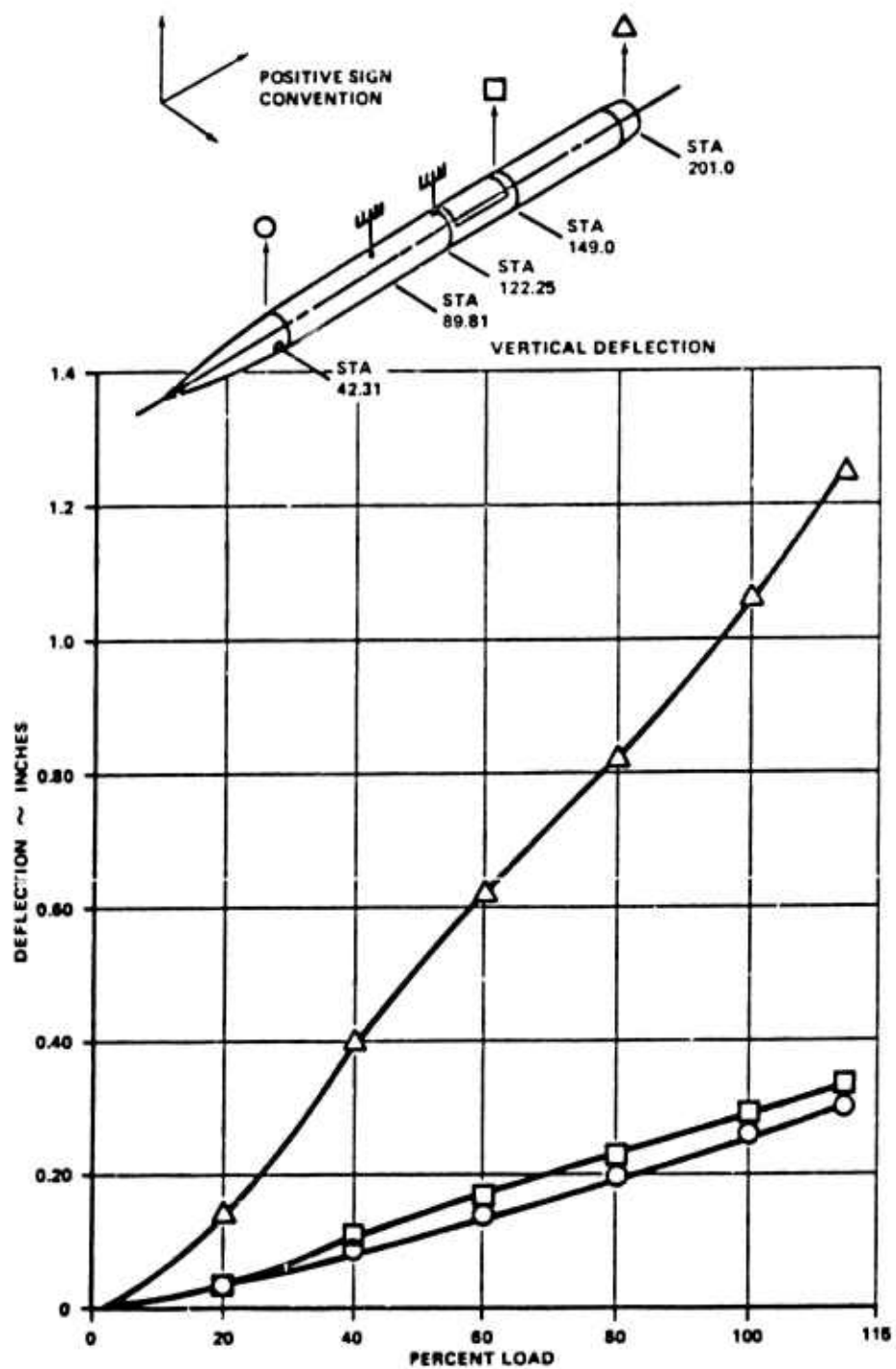
Figure 34. Body Deflections, Positive Ejection Conditions

The anti-symmetric aerodynamic representation of the vehicle is the same as that of the symmetric representation with the addition of the vertical stabilizer which contributes mainly to the aft body side bending degree-of-freedom.

The flutter program is capable of handling a constrained and/or free-free analysis. The eigenvalue-eigenvector routine employes the QR method (Reference 5).

Due to the similarity of the 102F and 104F structural mode shapes, the generalized aerodynamics of the 102F configuration at a Mach number of 2.6 was applied to the high temperature 104F configuration to determine stability trends due to heating. Overall, the symmetric flutter analysis verifies that the basic vehicle (controls locked) to be stable throughout its flight regime.

Due to the similarity of the 103C and 105C structural mode shapes the generalized aerodynamics of the 103F configuration at a Mach number of 2.6 was also applied to the high temperature 105F configuration to investigate stability trends due to heating. The anti-symmetric flutter analysis verifies that the basic vehicle (controls locked) to be stable throughout its flight regime.

In the symmetric analysis the canard was represented as an active control surface in the cruise configurations and inactive during captive flight analysis.

The aileron was considered primarily as an anti-symmetric device although high frequency symmetric motion against the actuator stiffness (usually referred to as free-play) could occur and was, therefore, investigated.

TABLE XV. MODAL FREQUENCY - C.P.S.

SYMMETRIC CONDITION				
Mode Number	100C	Configuration 100F	102F	104F
1	23.88	34.28	36.2	33.48
2	30.53	76.95	79.42	74.29
3	79.41	88.17	104.90	97.93
4	122.20	141.81	153.6	146.84
5	159.70	195.69	197.5	184.81
6	200.40	213.78	258.50	243.91

TABLE XVI. MODAL FREQUENCY

Mode Number	Configuration		
	101C	103F	105F
1	45.3	48.2	43.76
2	79.7	82.9	77.56
3	91.0	110.5	99.22
4	164.1	177.91	167.42
5	173.31	178.83	172.79
6	193.37	195.77	186.18

ANTI-SYMMETRIC CONDITION

b. Free-Free Vibration Test. A flight configuration vehicle designated KJ-1 was suspended at the launch lugs with springs. The natural frequencies of the suspension system were determined to be low and would not influence the test results. Shakers were placed at missile stations 35.75 and 200.0. The test was conducted to locate response frequencies by taking frequency sweeps and then taking modal readings at resonant frequencies. Comparison of analysis and test frequencies are presented in Table XVII.

TABLE XVII. MODAL FREQUENCY C.P.S.

FREE-FREE CONDITION

Mode Number	Analysis	Test
	100 F	
1	34.28	32.3
2	76.95	78.9
3	88.17	110.1
4	141.81	--
5	195.69	--
6	213.28	--

Comparison of analytical and test results indicate that the analytical modes do represent the actual vehicle. The analytical flutter analysis, therefore, does have an acceptable level of confidence.

10. MISSILE WEIGHT

The HAST airframe consists of cast stainless steel frames, bulkheads and fittings. Heavy framing members enclose the wings. The HAST subsystems include positive expulsion system, ram air turbine, recovery system and a full complement of payload. The basic vehicle with RF payload

weights 1210.0 pounds. The complete vehicle with both RF and IR payloads weighs 1256.5 pounds. Weight distributions for both basic vehicle with RF and basic vehicle with RF + IR payload are presented in Table XVIII.

TABLE XVIII. WEIGHT DISTRIBUTION

ITEM	WEIGHT
AFCS	37.0
Fuselage	161.4
Canards	13.3
Electrical	12.1
Propulsion	186.3
ITCS	15.1
Recovery	40.8
Stabilizers	9.2
Wings	31.9
Payload	75.4
Usable Fuel	144.0
Usable Oxidizer	480.2
Usable Nitrogen	3.3
Basic Launch - with RF	1210.0
IR System	46.5
Basic Launch - with RF + IR	1256.5

SECTION VI

FLIGHT CONTROL SYSTEM

This section presents a chronological summary of the engineering activity during the development of the HAST flight control system. Figure 35 illustrates the significant milestones of this effort. Each milestone will be discussed in view of its context and contribution to the overall system development.

1. LINEAR ANALYSIS

Linear analysis of the airframe and the control system was performed to assure that a single gain stability augmentation system was feasible over the entire performance envelope and that gains selected could perform satisfactorily.

Because cross-axis coupling is minimal the airframe equations were treated by classical separation of longitudinal and lateral-directional equations. Further, by utilizing the throttling concept, speed effects around various specific flight conditions were neglected and independent modes of motion were treated separately. A total of 25 flight conditions, representing the proposed HAST performance envelope, was studied.

A complete set of control system gains was chosen by linear analysis techniques to be used in further analyses. The longitudinal axis gains which govern canard position were chosen to be:

K_q · Pitch rate gain = 0.6 rad/rad/sec

$K_{\Delta h}$ · Altitude error gain = 0.12 rad/1000 ft

$K_{\Delta \dot{h}}$ · Altitude error rate gain = 0.77 rad/1000 ft/sec

In general terms, these gains provide underdamped longitudinal characteristics at low dynamic pressures and overdamped characteristics for high dynamic pressures. The lateral-directional axis gains which govern aileron position (fixed vertical stabilizers are used) were chosen to be:

$K_{\Delta \psi}$ · Yaw error gain = 1.0 rad/rad

$K_{\Delta \theta}$ · Roll error gain = 5.0 rad/rad

K_p · Roll rate gain = 4.0 rad/rad/sec

with lead-lag compensation in roll and roll rate terms of $\frac{S+8}{S+50}$. The results reemphasized the fact that heading control with ailerons only cannot be affected for negative lift. In the HAST configuration this condition exists when the canard surfaces are leading edge down. Consequently, heading control must be removed during these canard excursions or at any time a negative normal load is present.

2. THREE-DEGREES-OF-FREEDOM SIMULATION

The known nonlinearities and hardware characteristics were modeled with the decoupled equations of motion into a point stability analog computer simulation of the stability augmentation portions of the flight control system. The objectives of this simulation were to investigate the effects of actuator rates, gyroscope characteristics, and nonlinearities on stability using previously selected gain values. In addition, gain margin and system response for totally closed loop operation were determined.
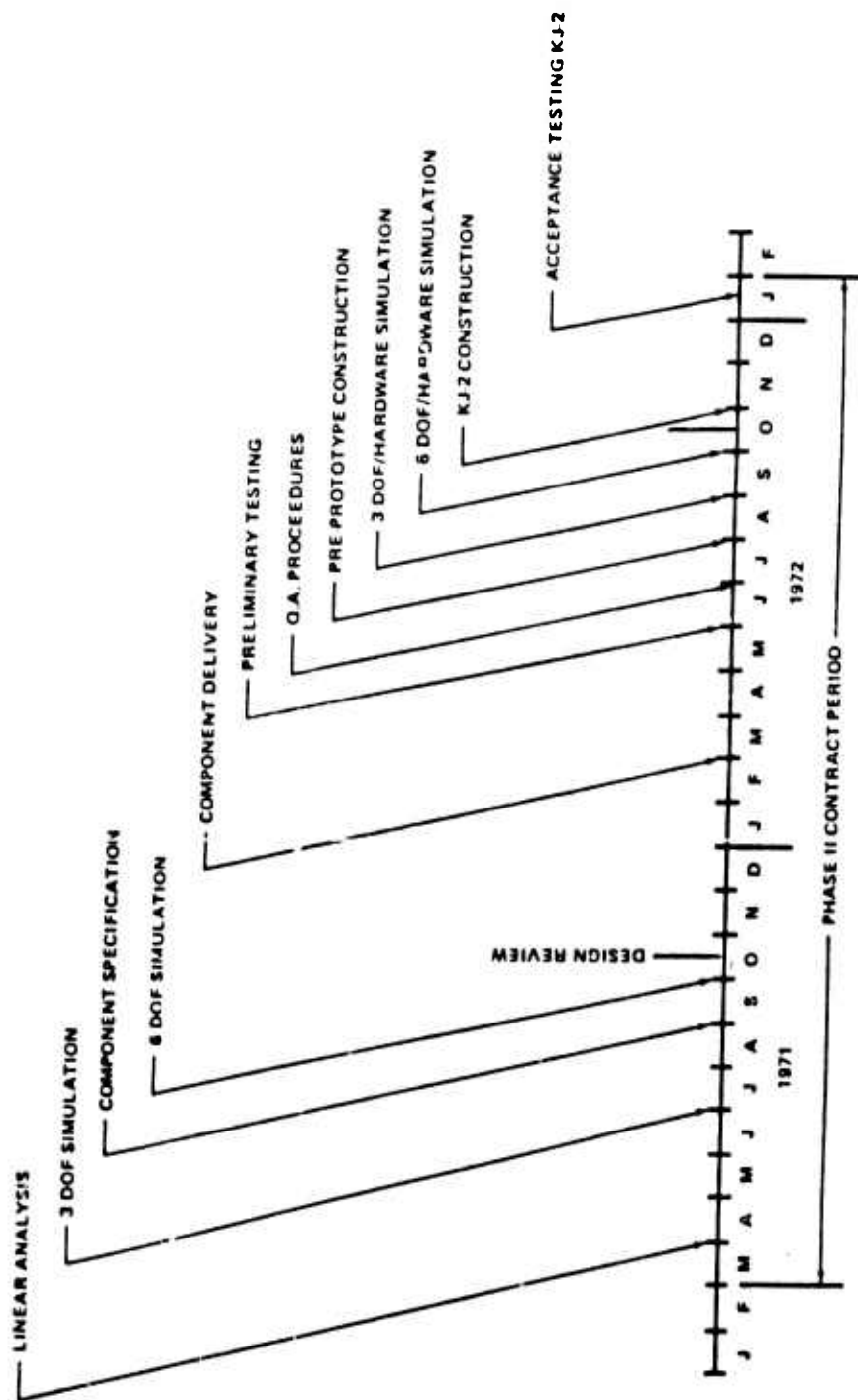
Figure 35. HAST AFCS Phase II Chronology

For the most part the results of linear analysis were reinforced. The longitudinal gain set was found to be satisfactory over the entire flight envelope. Even better response could be obtained by increasing both altitude rate and pitch rate gains at low dynamic pressure and decreasing these gains for high dynamic pressures. This complexity was not added to the system but can be, if desired, at some later time. The lateral-directional gain set provided satisfactory but the ratio of yaw to roll and roll rate gains was altered in order to decrease the permissible steady state yaw error. This was accomplished by reducing roll and roll rate gains by a factor of ten. Appropriate actuator rates, gyro characteristics and ranges were also determined.

3. COMPONENT SPECIFICATIONS

At this stage of the development it became mandatory to complete purchase specifications and negotiations for flight test hardware. These items included the canard and aileron servoamplifiers and actuators, angular rate gyroscopes, the air data system including the pitot-static tube accelerometer and heading reference gyroscope. Even though the maneuvering and throttle valve designs had not been proven by simulation, it was also necessary to commit the circuit design integrating the entire system. This was made feasible by the contractor retaining the design and manufacture of these circuits and absorbing changes necessitated by further analyses and purchased hardware performance. In many cases it became evident that some requirements would need to be compromised by schedule and cost considerations. These compromises were fully analyzed in later studies.

4. SIX-DEGREES-OF-FREEDOM SIMULATION

A hybrid computing facility at Wright-Patterson Air Force Base was used for a complete flight control system simulation. The objectives of the simulation were:

- Reinvestigate stability after inclusion of cross-axis coupling and in-flight maneuvering

- Finalize the throttle valve control design

- Determine the effects of redefined hardware characteristics.

A wide range of flight centers of gravity and weight conditions were simulated.

Simulation results indicated that the proposed flight control system would provide vehicle stability in climb, cruise and maneuvering flight. Required maneuvers could be accomplished within the limits of airframe loading and could be initiated by command or on board timing. Turning, climbing and altitude hold capabilities appeared to far exceed the system requirements.

Several alternations to the control scheme were investigated which could simplify the design. The throttle control concept using energy altitude was abandoned when a design using only Mach number error exhibited equal performance with greatly simplified electronics. Another design simplification would be to remove the roll rate gyroscope and replace it with a filtered differentiation circuit. Electronic circuit noise, at present, has prevented removal of the rate gyro.

Several inadequacies in the overall design were detected and corrected. The necessity of increasing roll and roll rate gains for flight conditions where aileron effectiveness is low (above 90,000 feet) became apparent. An increase by a factor of ten was incorporated for extremely high altitude flight and greatly improved lateral-directional characteristics in that regime. Entrance and exit from turning maneuvers exhibited high loading and poor response until command shaping was incorporated. Command shaping allowed the vehicle to respond more smoothly, eliminated large transient loads and the resulting motions. High g level turns at relatively low speeds dictated increasing torquing rate for the heading reference gyroscope inner gimbal (azimuth). Increased rate allows the inner gimbal to track the vehicle in any turn the airframe is capable of making within the

present performance envelope. An inner gimbal torquing rate of 10 degrees per second (increased from 3 degrees per second) was required to minimize heading reference loss during turn maneuvers. Revision of the pushover/pullup maneuver circuitry was incorporated to reduce load and motion transients during onset and recovery of these maneuvers. These design refinements were successfully incorporated prior to the Design Review and were presented at that time.

5. COMPONENT DELIVERY

The first set of purchased components was scheduled to be delivered in late November 1971. Since nearly all of this equipment was being developed solely for the HAST project, early delivery dates could not be met. Delayed delivery forced abandonment of planned system integration testing using breadboarded circuits. Since multilayer circuit boards require long lead time the flight control circuitry was committed without these tests. A single set of purchased components was finally accumulated by the end of February 1972.

6. PRELIMINARY TESTING

Engineering tests were made on the flight control hardware as it arrived. These tests had several objectives. In addition to establishing the actual performance characteristics of each component, it was also necessary to lay the groundwork for future quality assurance test techniques and test equipment. During the course of development testing many deficiencies were discovered both by vendor and Beech testing programs. The following paragraphs summarize the general test results and the action taken to remedy performance inadequacy

Servo-amplifiers and actuators proved to be exemplary in many respects. Positioning accuracy under load reflects high stall torque and stiffness with minimal backlash. The actuators are small, light and exhibit good overall efficiency. Several deficiencies were also indicated. Response and null stability of the aileron actuator dictated an improved servo-amplifier design using an active lead circuit to provide greater stability. At the same time, the quality of electronic components in the amplifier was improved to lessen temperature effects and extend operating reliability margins. All aileron and canard servo-amplifiers have been replaced with this improved type. While the service life requirements were easily met, extended operations indicate a fairly predictable actuator failure at about 130 hours of hot and cold environment operation under nominal flight loads. Additionally, the aileron actuator would not meet EMI emission requirements. These shortcomings have been verified by the manufacturer. The manufacturer has recommended a higher quality motor to increase MTBF and an internal wiring change to decrease EMI to acceptable levels. Several actuators have been returned for new motors and EMI correction. Neither fault is expected to in any way compromise the flight test program.

The angular rate gyroscope developed for the HAST flight control system is a standard production gyroscope with temperature compensation electronics added. Gyroscopes of this size and type generally exhibit a large variance in output characteristics with temperature. Since the HAST environment includes both extreme hot and cold, temperature compensation was not only necessary but has proven to be successful. The gyroscope retained excellent sensitivity, response and accurancy. Because the AC output is demodulated to DC voltage level, the gyroscope output is sensitive to input power waveform and magnitude. This characteristic became evident as an uneven regulation was encountered in the missile power supply. At present regulation levels, a 10 to 15 percent output error can occur. This level of error is acceptable because the system gain tolerance for dampening in pitch and roll (the primary uses of these signal outputs) is not crucial.

Early testing of the heading reference gyroscope proved the feasibilty of torque control of the inner gimbal position control for high turning rates. Analysis and testing of a prototype gyroscope led to control circuit redesign which improved both caging accuracy and stability of the inner gimbal position control. Both aspects were crucial to the success of later models with nine-degrees-per-second torquing rates. Early technical risk areas of this concept, internal heating, torquer scaling and hot and cold environment, were successfully eliminated. A problem of performance under vibration was identified. A resonance centered at about 120 Hz drives the inner

gimbal at between three and five degrees per second at only a five g level. The severity of the drive-out is caused by the large anti-symmetric masses of the torquer motors attached to the gimbal suspension system. Several attempts to alleviate the drive-out were stymied by other problem restraints. Bearing tolerances which alter and reduce the resonance cause increases in static drift. Isolation mounting requires a much larger mount and increased volume allocation for unrestricted sway space. After the vehicle free-free vibration testing indicated there would be very small forcing in the frequency domain around the 120 Hz gyro resonance at its location, it was decided that some deviations in the specified performance would be acceptable until the vibration environment could be defined by flight test data.

Because of the extreme pressure resolution required to make accurate pressure altitude and Mach number indications above 80,000 feet, the testing of air data modules dictated the use of a relatively new and sophisticated pressure control and measurement instrument. The air data test set utilizes servo-controlled valves and quartz Bourdon tube manometers to control and measure both static and impact pressures used as inputs to the air data module. Use of this instrument has allowed an unprecedented ease in testing, repeatability and accuracy in the evaluation of the air data module at both the contractor and vendor facilities.

Testing done by the vendor revealed a manufacturing problem in obtaining a static pressure diaphragm seal. The diaphragm seal is a difficult problem for several reasons. First, the accuracy requirements at very low pressures (high altitude) dictate a thin, flexible diaphragm; this causes the deflections of the diaphragm to be large at pressure altitudes below the range of the transducer, sea level to 30,000 feet. The flexibility over the required temperature extremes limit the arrangement and materials suitable for this critical seal. A technique using epoxy bonding has apparently proven successful, but development of this technique delayed deliveries.

The configuration of the pitot-static tube has been based solely on analysis of wind tunnel testing which defined the flow field characteristics of the HAST vehicle in flight. The success of the contour compensation being used must be determined by flight test.

7. QUALITY ASSURANCE

The information gained by engineering evaluation tests was utilized to prepare a receiving, inspection, and ac tance test for each major component used in the flight control system. These tests follow a v inspection which assures physical conformance to specification and the absence of shipping damage. Acceptance tests were designed to cover all operation and performance requirements of the component specification and are witnessed by DCAS personnel. Failure to meet the acceptance test criteria causes the component to be returned to the vendor for corrective action.

8. PREPROTOTYPE CONSTRUCTION

All components of the flight control system were integrated into a preprototype system excepting the gyroscopes and accelerometer. This rather elaborate breadboard was constructed for use with real time computer simulation of the HAST vehicle in flight. It included actuator loaders, a modified air data module, an oxidizer throttling valve, a cartridge relay board, a ground control and launch panel simulation. The actuator loaders were capable of generating torque as a function of flight condition, aerodynamic coefficient and position. The modified air data module accepted electrical rather than pressure input to compute its output. The cartridge relay board was used to initiate "onboard" programming in conjunction with the launch panel and lanyard switch. The normal complement of radio commands for maneuvers and destruct could be initiated by control panel simulation.

The preprototype system was a useful tool. Many integration problems such as surface directional sense, wiring errors, grounding and component reliability were illustrated before prototype construction of the control system was begun.

9. COMPUTER/HARDWARE SIMULATIONS

Several point stability conditions were simulated in both longitudinal and lateral-direction three-degrees-of-freedom using the breadboard control system. The objective of these simulations was to thoroughly check the breadboard operation prior to its shipment to Wright-Patterson Air Force Base. Although this objective was never fully realized, it was concluded that the breadboard equipment could be used satisfactorily. Reliability and some program sequencing continued to be major problems with the very early digital logic and autopilot assemblies assigned for this use. Many problems encountered during these simulations proved to be peculiar to the equipment/power supply/computer interface at the contractor's facility.

The breadboard control system was transported to Wright-Patterson Air Force Base to be integrated into a six-degrees-of-freedom hybrid computer simulation of the vehicle developed by AFFDL and 4950 VNA personnel. The simulation was primarily intended to indicate the suitability of the system design to accomplish the 25 flight test missions proposed. Secondarily, several range performance calculations were made to check against digital calculations made by the contractor with revised aerodynamic and propulsion parameters based on wind tunnel and heavyweight motor firings. Additionally, the effects of launcher induced transients and surface and thrust misalignments were investigated.

Results and conclusions were presented to the sponsor. The system design philosophy and configuration were judged to be satisfactory, but many detail refinements and improvements were necessary. For example, grounding plans needed to be revised to minimize cross-talk between canard and aileron actuators. Reliability improvements were sought in FET controls, digital sequencing and maneuver command initiation. Performance data correlation was excellent and reasonable misalignments could be handled by the control system. Launch transients proved inconsequential. Only one major malfunction, requiring factory repair occurred in approximately 100 hours spanning about 20 days operations. Many simulations were made requiring almost continuous operation for 8 to 12 hours. Two vehicle operational limitations were discovered. In low dynamic pressure climbs insufficient energy is available to the ram air turbine to support its load. This results in an inefficient climb trajectory to cruise conditions. Also pull-ups and push-overs at high g levels can quickly extend beyond the boundaries of the performance envelope, particularly in a dive from low altitude. Both limitations can be accounted for in operational mission planning.

10. FLIGHT VEHICLE CONSTRUCTION AND TEST

As previously mentioned, simulation work pointed out many necessary design refinements which should be incorporated into the flight test vehicle. Most of the changes were incorporated during its construction, but many were left to be verified by a working system. Therefore, the first vehicle assumed the role of a test bed vehicle for a period of time.

During that same period it was also necessary to devise the acceptance test procedures and test equipment which would functionally check the many complex system performance requirements of the HAST target. The procedures evolved test of every cruise and maneuvering function of the flight control system for both programmed and commanded sequences. Test equipment developed included three electronic test consoles which contain all the read-out equipment.

11. FLIGHT CONTROL SYSTEM DESCRIPTION

A development specification for the operation and configuration of the HAST flight control system has been prepared. For the sake of simplicity, the system will be described in parts; canard control, aileron control and throttle commands. Other functions such as timing and sequencing, radio command interface, VMDI, and payload interfaces are contained in other sections of this report.

The canard control is summarized in Figures 36, 37, and 38. These schematics illustrate how the canards are used to control altitude both in climb and cruising flight, maneuver load and pitch rate. The blocks at the left of Figure 36 and 37 show interfaces with sensors, sequencing of maneuver

73

commands and the launch safety inhibit to canard actuation (two seconds). Figure 38 illustrates the canard servo system.

Interfaces with functions other than canard control shown in Figures 36, 37, and 38 are roll and roll rate gain schedule logic and recovery altitude logic.

The aileron control is summarized by Figures 39, 40, and 41. These schematics illustrate how the ailerons are used to control yaw attitude and roll attitude. The blocks at the left of Figures 39 and 40 show sensor and maneuver command sequencing interfaces. Figure 41 represents the aileron servo-system.

The throttle position command is shown schematically in Figure 42. This schematic shows how Mach number is controlled in the cruise portion of a HAST mission. Again the blocks at the left show the sensor and command interfaces while the right illustrates the oxidizer throttling valve and climb program interfaces.

Nominal design values for scaling and range which may be used in computations involving these schematics are contained in Table XIX.

TABLE XIX. HAST SENSOR RANGE & SCALING

Sensor	Parameter	Range	Units/Volt	Volts/Unit
Air Data Module	Altitude	35,000-105,000 Ft	10^4 Ft/V	10^{-4} V/Ft
	Mach Number	0.85-4.0	0.5 Mach/V	2 V/Mach
	Impact Pressure	0-1000 psf	-100 psf/V	-0.01 V/psf
Heading Reference Gyroscope	Yaw Attitude	+22.5 (R) to -22.5 (L) Deg	1.33 Deg/V	0.75 V/Deg
	Roll Attitude	+120 (L) to -120 (R) Deg	8.00 Deg/V	0.125 V/Deg
	Derived Yaw	0 to 200 Deg	-10.0 Deg/V	-0.05 V/Deg
Pitch or Roll Rate Gyroscope	Pitch Rate	+100 (DN) to -100 (UP) Deg/Sec	10 Deg/Sec/V	0.10V/Deg/Sec
	Roll Rate	+100 (L) to -100 (R) Deg/Sec	10 Deg/Sec/V	0.10 V/Deg/Sec
Normal Accelerometer	Normal Acceleration	+10 (UP) to -10 (DN) g's	1.175 g's/V	0.85 V/g

12. PITOT-STATIC PRESSURE SENSITIVITY TO ANGLE OF ATTACK

Test data from the flight of KJ-4 revealed the L-shaped pitot-static probe was highly sensitive to angle of attack. Sensed static pressure increased with increasing angle of attack, creating errors both in altitude and Mach number fed from the air data module; $dh/d\alpha < 0$ and $dM/d\alpha < 0$. Since the altitude error was destabilizing, the Δh signal was severely degraded in magnitude and direction.

Subsequent wind tunnel tests, using a 1/2 scale probe/body combination, confirmed the static pressure sensitivity at Mach numbers throughout the operational envelope of the HAST. In addition the tests provided little or no promise that the errors could be significantly reduced by modifying probe location, attach angle, or configuration. It was necessary; therefore, to obtain long period damping from a source independent of the pitot-static probe, in lieu of Δh.
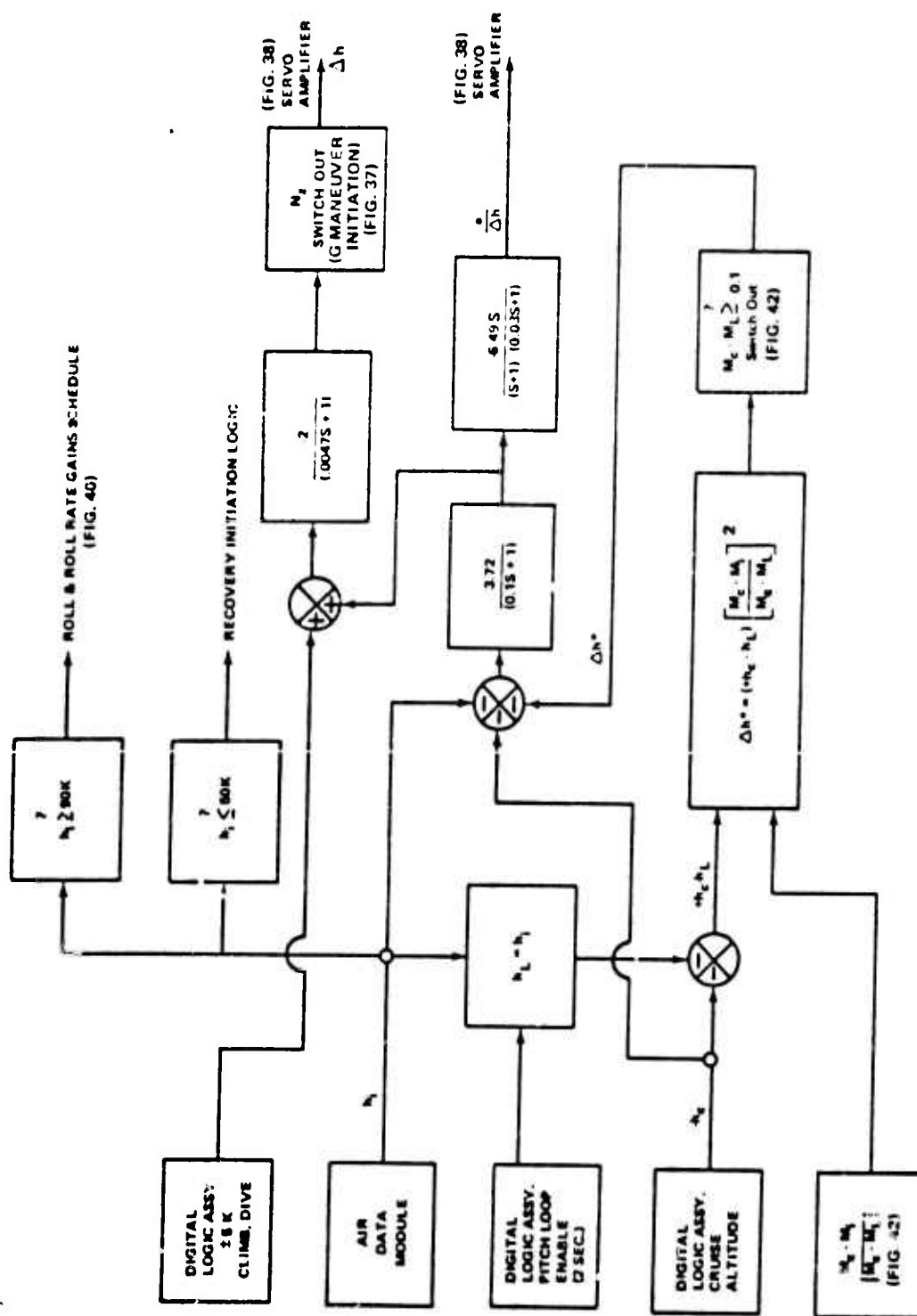
Figure 36. Altitude Control Schematic
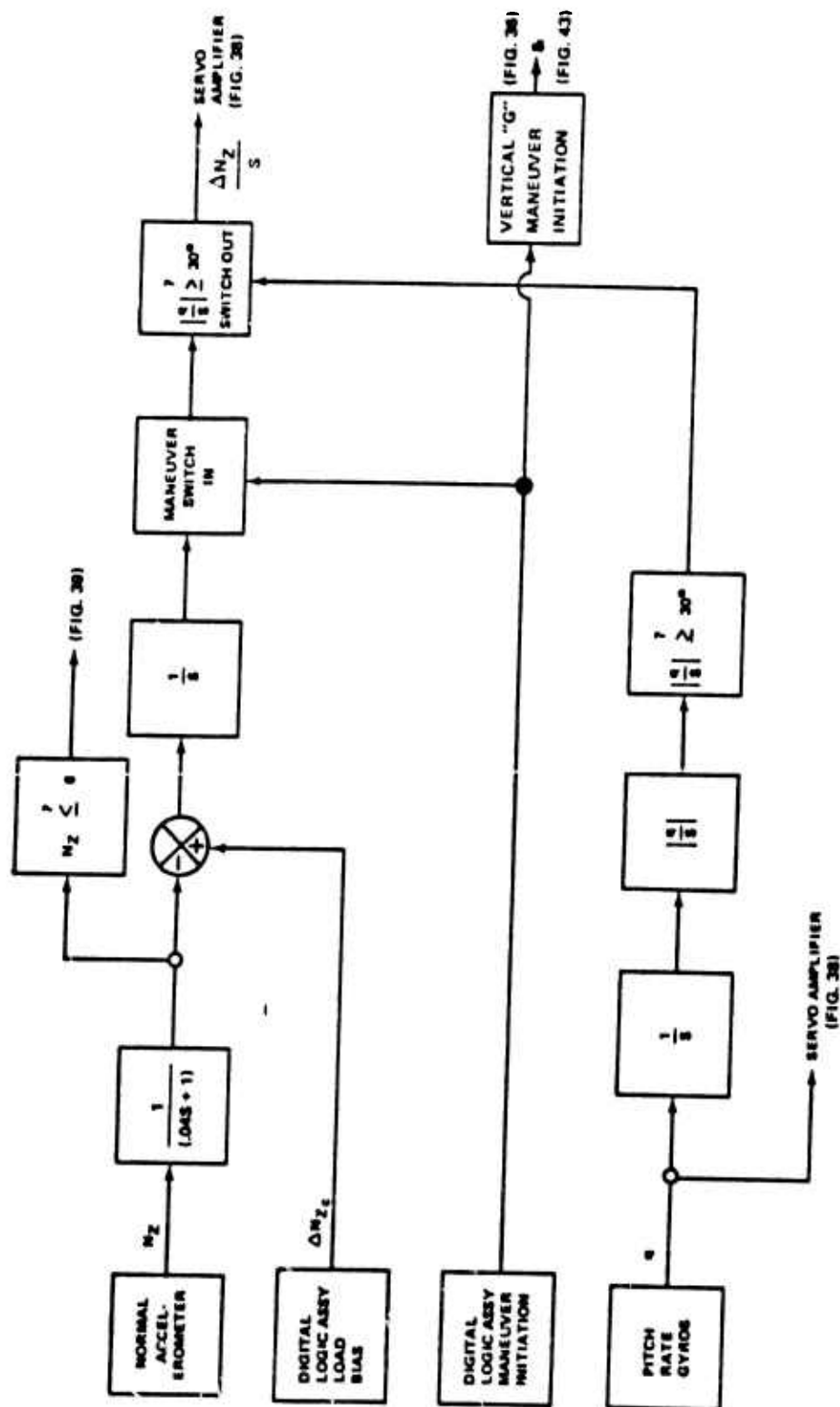
Figure 37. Maneuver Load and Pitch Rate Control Schematic
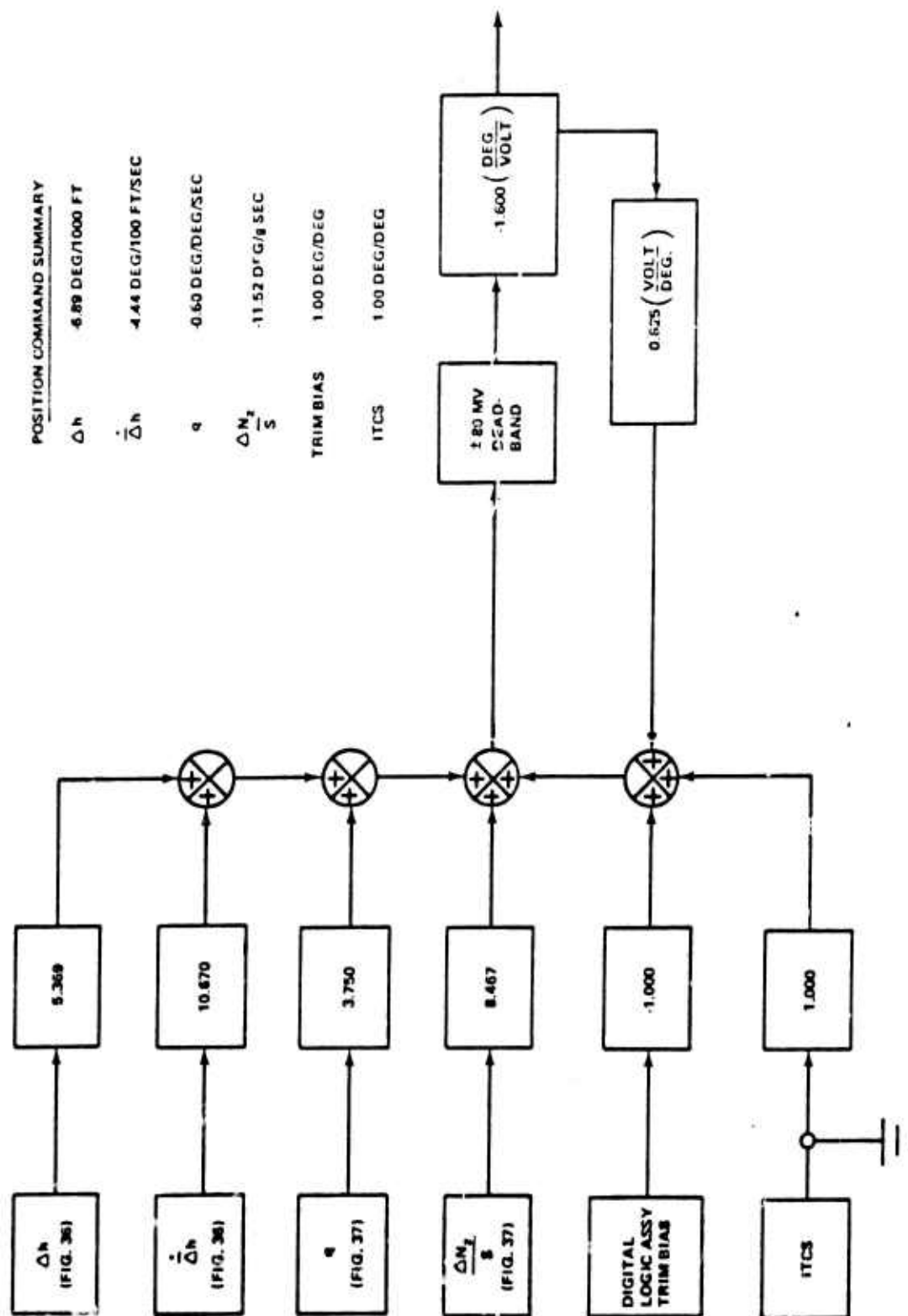
Figure 38. Canard Servo-Actuator Schematic

POSITION COMMAND SUMMARY

Δh -5.89 DEG/1000 FT

$\dot{\Delta} h$ 4.44 DEG/100 FT/SEC

q -0.60 DEG/DEG/SEC

$\dfrac{\Delta N_z}{s}$ -11.52 DEG/g SEC

TRIM BIAS   1.00 DEG/DEG

ITCS   1.00 DEG/DEG

77
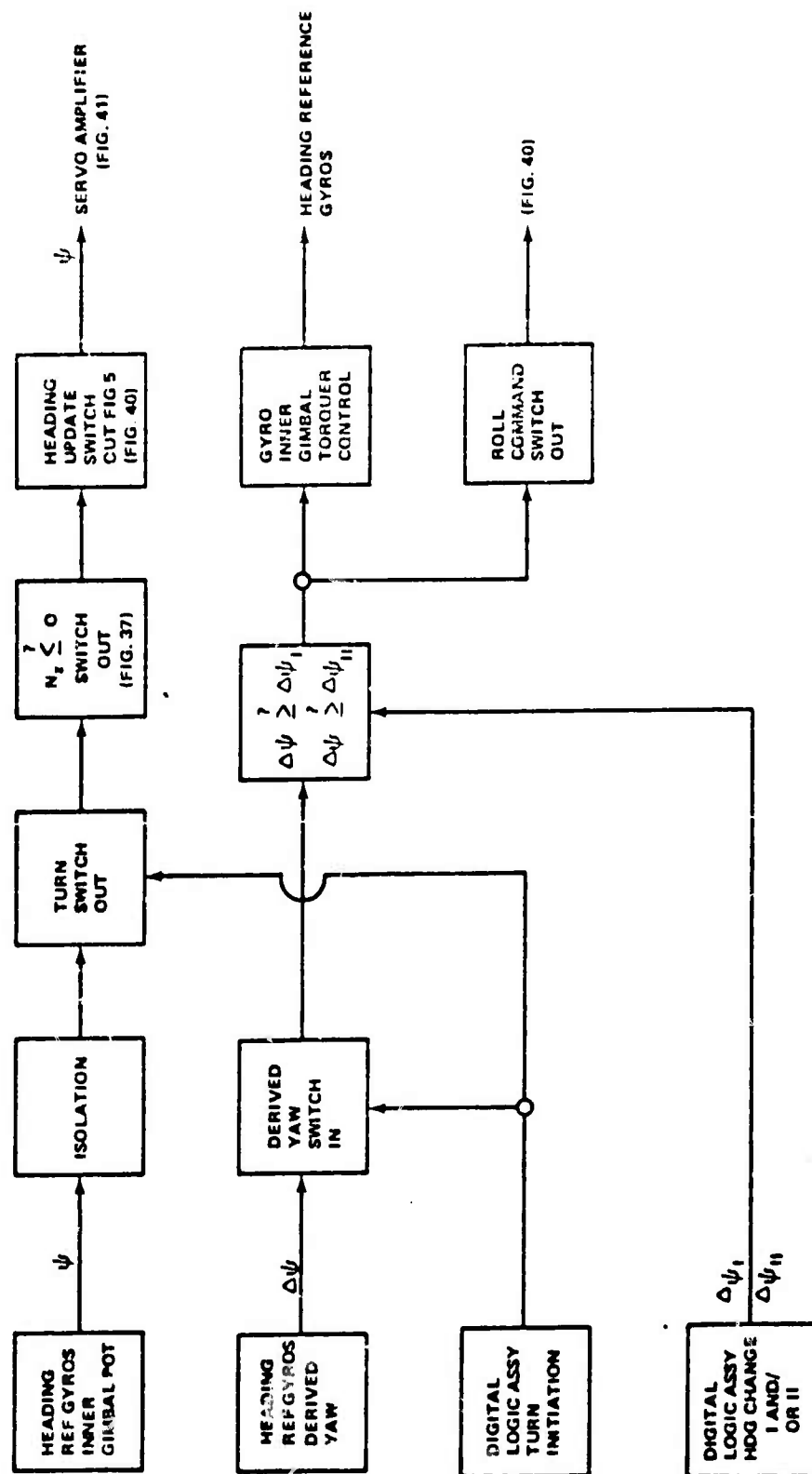
Figure 39. Yaw Attitude Control Schematic
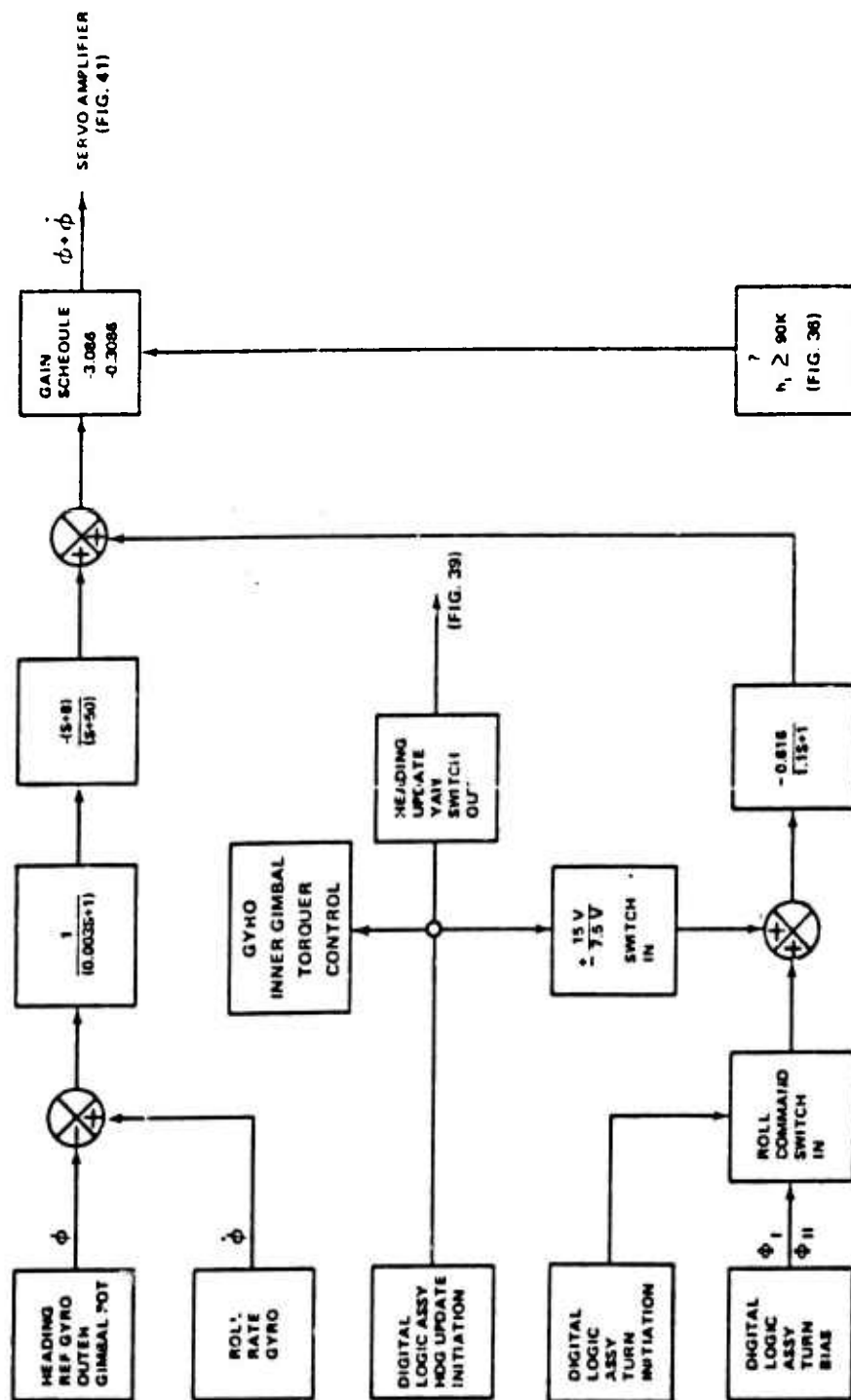
Figure 40. Roll Attitude Control Schematic
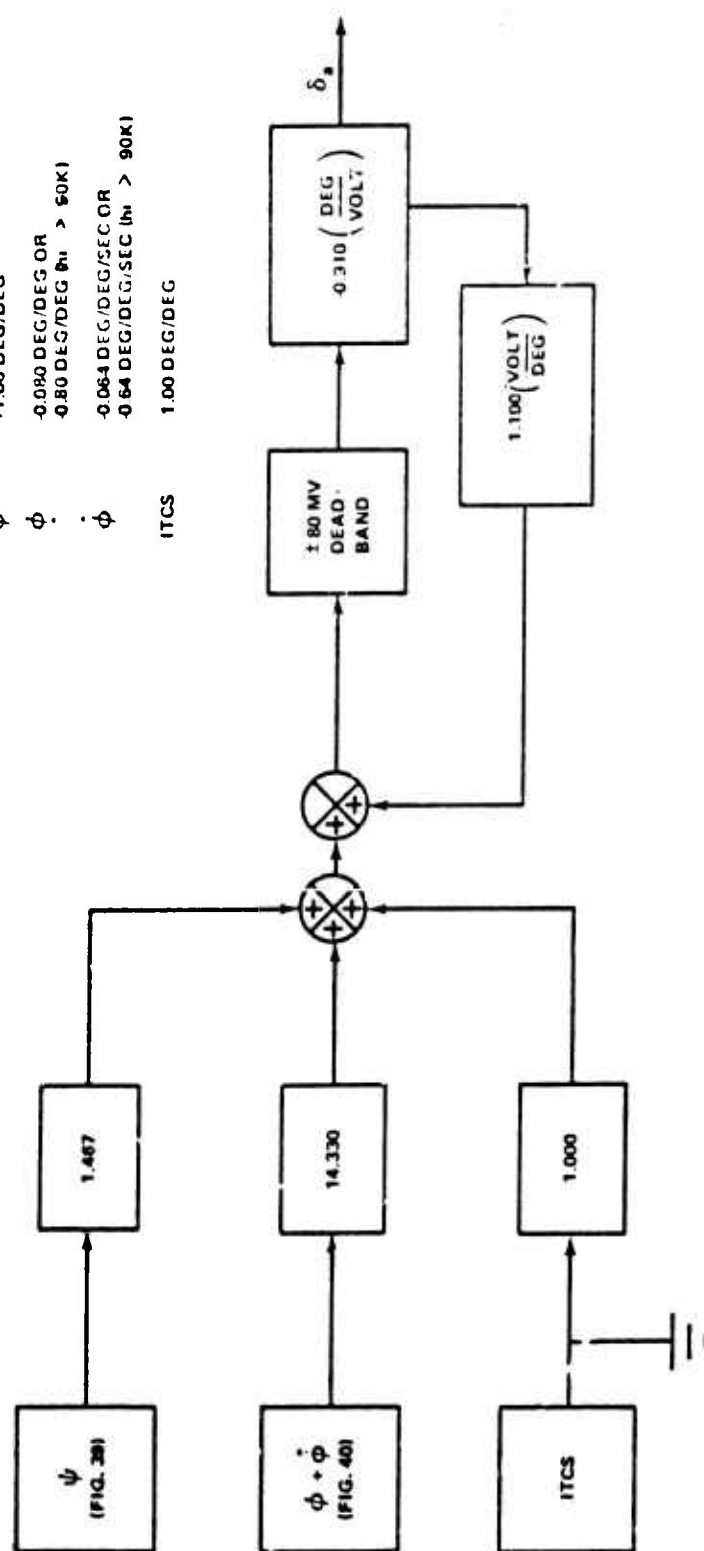
Figure 41. Aileron Servo-Actuator Schematic
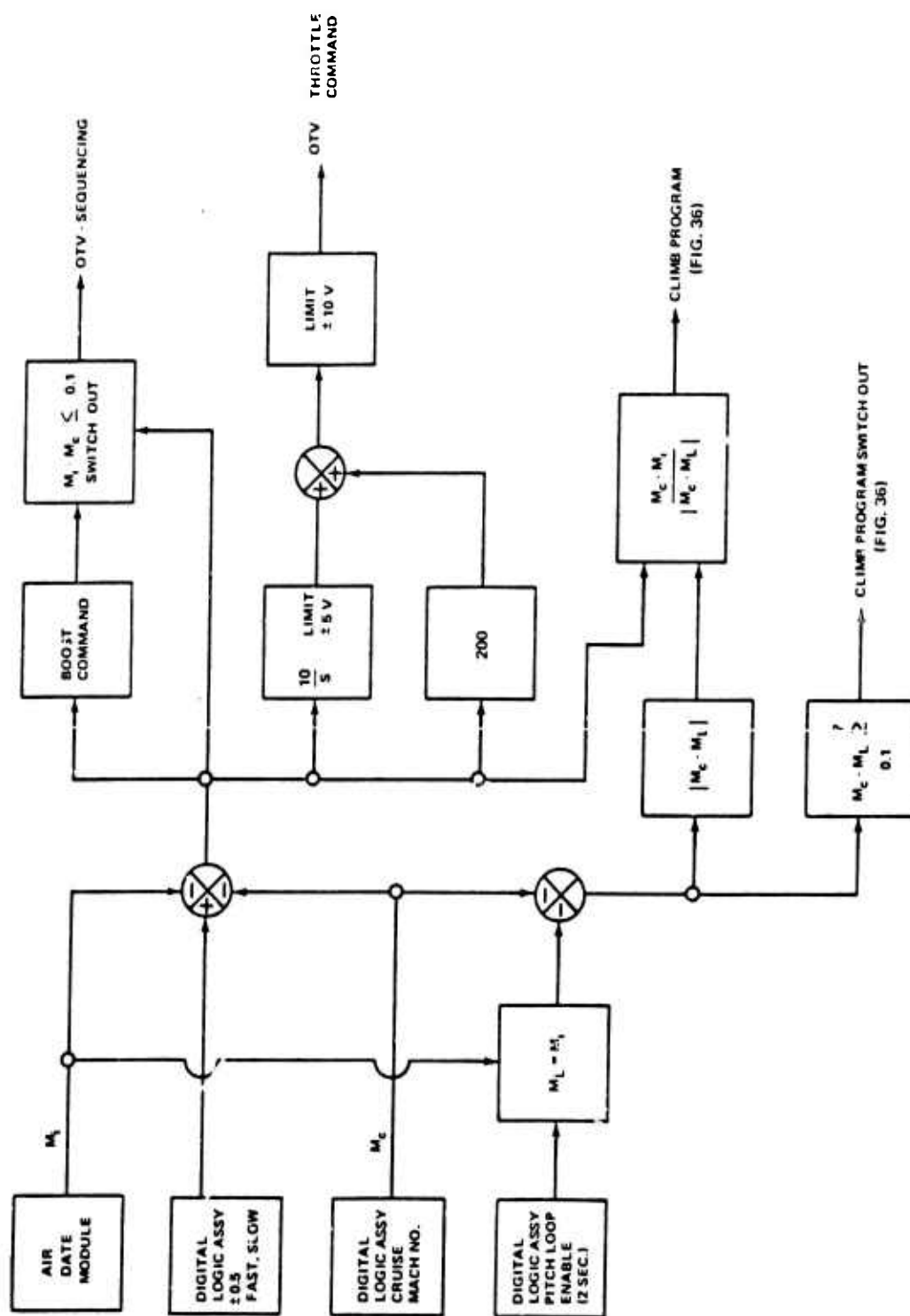
Figure 42. Mach Number Control Schematic

13. N_z AUTOPILOT

An approximation for Δh may be made using the integral of normal acceleartion. Since normal acceleration is independent from the pitot system and a normal load accelerometer already existed as part of vehicle hardware, feasibility of its usage was pursued.

The proposed longitudinal control system, using normal acceleration, has been called the "N_z Autopilot". The schematic in Figure 43 shows the signals used to generate canard command. Note that $\int (N_{zf}-1)$ and N_{zf} are used in lieu of Δh. The remaining signals are identical to those used in the KJ-4 autopilot, except a few gain changes were necessary to allow sufficiently high gain and phase margins for the N_z autopilot.

14. FEASIBILITY STUDY FOR N_z AUTOPILOT

Feasibility of the N_z autopilot was studied using a simplified, analog simulation of the HAST capable of analyzing control system stability limits and response characteristics. The simulation was simplified to essentially a point-stability problem with linear approximations allowing perturbations in altitude, pitch and speed, excited by step commands in altitude. Figures 44 and 45 show representative limits in dh/dα as a function of K_{Nz} at various flight conditions. The time axis in these figures represent time elapsed for the airframe responding to 63 percent of a step command in altitude (2,500 feet in these cases).

   a.   Significant results from this study were:

   (1) Faster response occurs when dh/dα is destabilizing (negative).

   (2) Increasing K_{Nz} allows stable flight at larger negative (destabilizing) values of dh/dα.

   (3) At a given value of dh/dα, K_{Nz} requirements for stability increase with Mach number and altitude.

   (4) Increasing K_{Nz} results in larger standoff in Mach number and altitude.

   b.   From the above, conclusions are:

   (1) Compensation required for high Mach/altitude flight conditions when pitot errors are relatively large.

   (2) Due to response characteristics, it is better to undercompensate a negative dh/dα, than to overcompensate.

   (3) K_{Nz} should be maintained at the minimum required for stability.

   (4) Ideally, K_{Nz} should be preselected appropriate to the flight conditions at cruise.

82
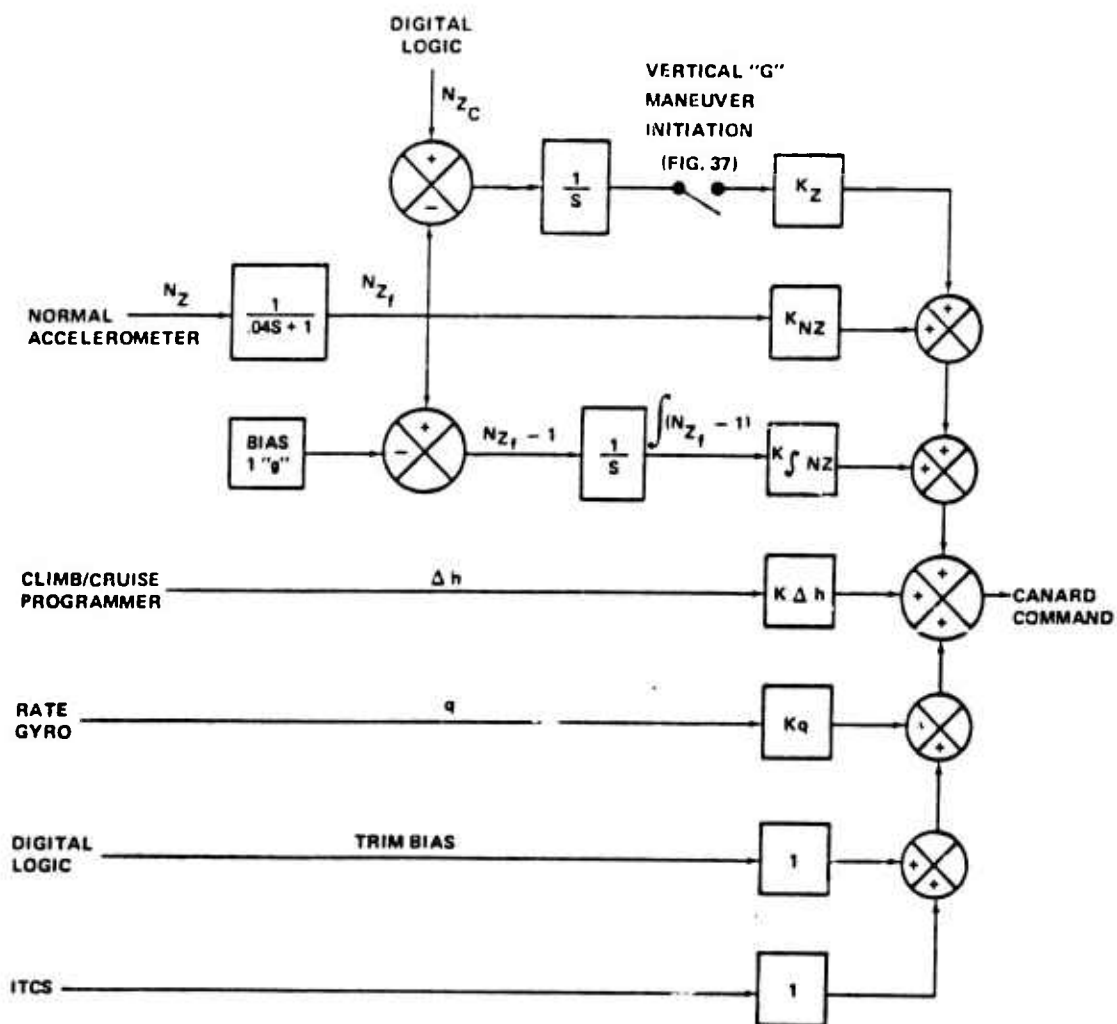
Figure 43. N_z Autopilot Control Schematic
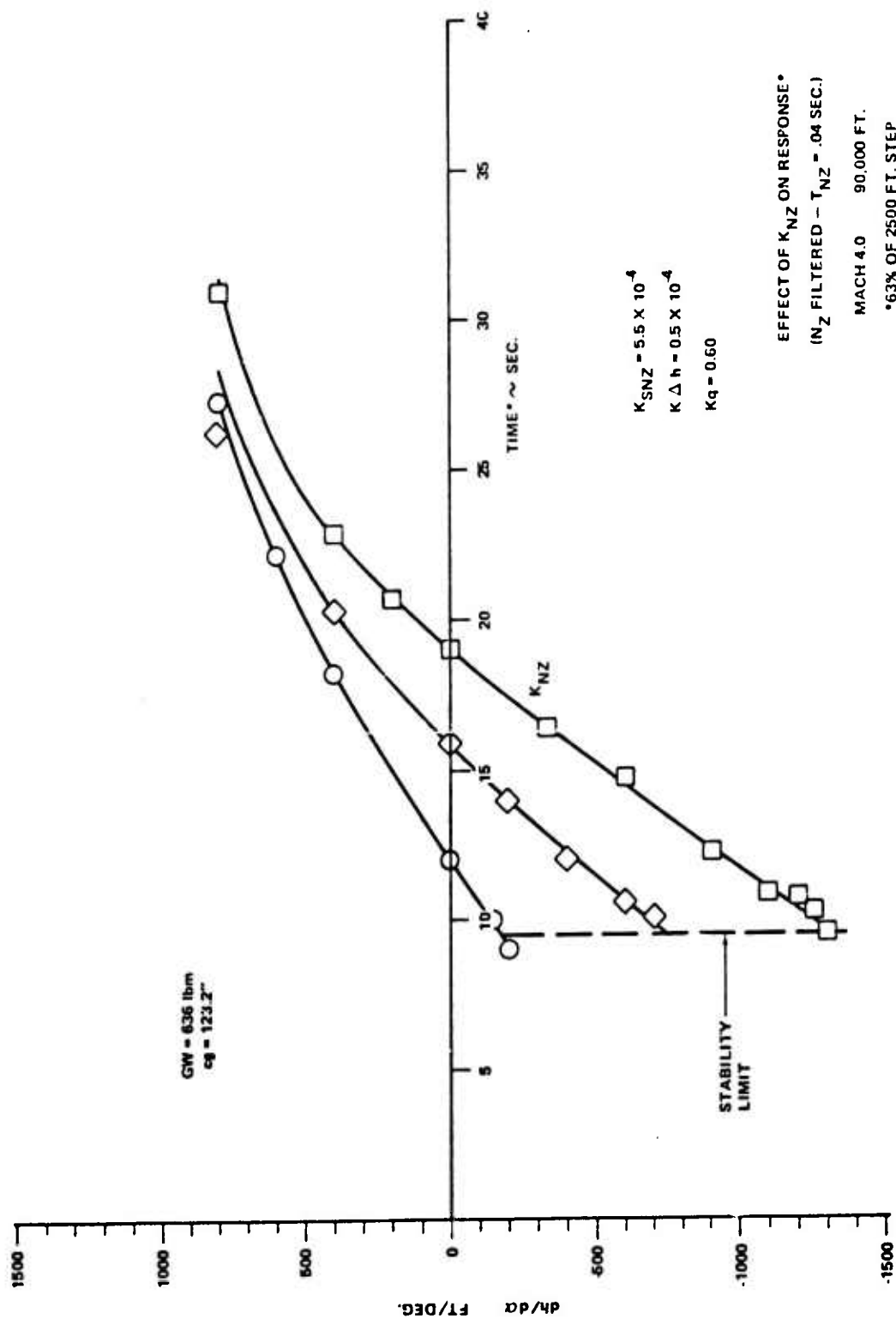
Figure 44. Effect of K_{NZ} on Response - Mach 4.0, 90,000 Feet

84
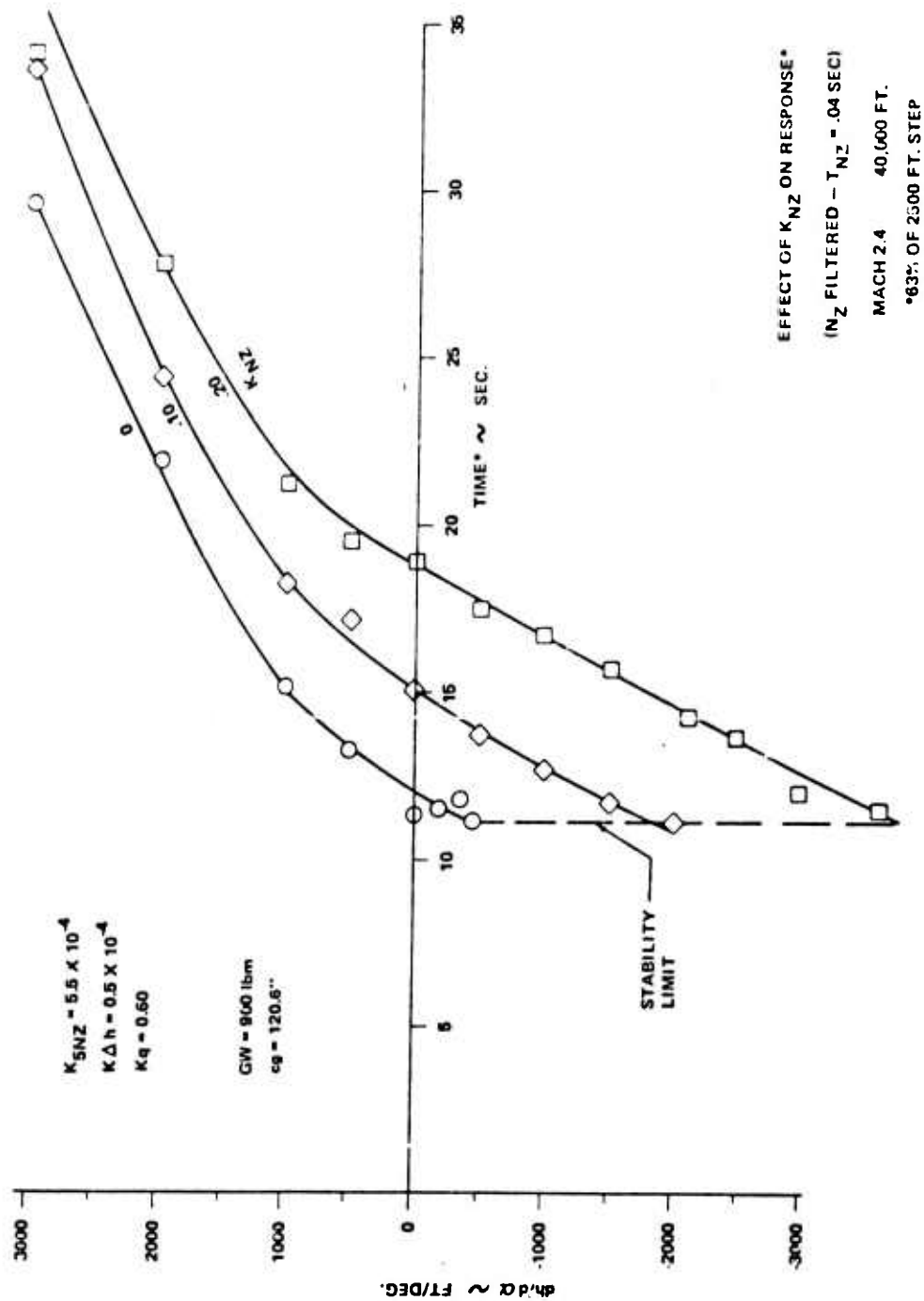
Figure 45. Effect of KNz on Response - Mach 2.4, 40,000 Feet

SECTION VII

ELECTRONICS AND ELECTRICAL SYSTEMS

The HAST electronics and electrical systems make up a considerable part of the target components. An understanding of the operation and programming of the electronics is vital to mission success. This report contains sufficient detail for flight programming after deciding upon a specific mission. A HAST sequence of events is presented first in order to get a concept of systems operation. Also it will establish a reference to be referred back to during the other discussions. A description of the aircraft launch system is included so that the entire system operation can be visualized. An abbreviated electrical load analysis is included with the aircraft and target power system sections.

Circuit descriptions are presented in block diagram form in order not to be bogged down in the specific value of, or reason for, each discrete circuit component. The reason for each circuit block is presented during the discussion of the major subassembly such as digital logic assembly, autopilot module, wire harness, and so on. Portions of circuits in some assemblies tie closely to the functions of other assemblies so that the total circuit function cannot be discussed without bringing both units into the explanation.

A physical description and the location of the subassemblies are included in the circuit descriptions. Electronic cases and assemblies have been designed to use the available space around, beside, and underneath the target structure and other major components. This was done in order to vacate the aft payload tunnel area and to prevent a major redesign of components midway through the test program. The preliminary design had utilized the aft payload tunnel area for electronic components. A redesign would have resulted in two configurations, one for flight test and one for payloads.

1. HAST SEQUENCE OF EVENTS

HAST heater power is automatically applied to the target at aircraft engine start when the engine driven generators are placed on the line. As the launch aircraft passes through 10,000-feet altitude a barometric switch, located in the launcher, closes applying power to the target pitot. The pitot heater clears any ice that may have formed in the tube during climbout.

Approximately 20 minutes prior to launch the pilot places the SELECT switch on the missile control panel to the SELECT position. This action applies power to the C-band transponder, telemetry transmitter, command receiver, target gyros and other equipment. SELECT time may be as short as three minutes or as long as one hour. Transponder, telemetry and command receiver checks are normally made during this period. SELECT is shown as the first event in the time sequence line of Figure 46.

Approximately 90 seconds before launch the pilot places the LAUNCH/READY switch on the missile control panel to the LAUNCH/READY position. This action opens a gate in the Ducted Power Unit (DPU) and allows the turbine to come up to speed. The output of the turbine alternator rises above the other power sources and powers all the vehicle systems. At this time a self-test is made by the electronics on 22 items within the vehicle. If all prelaunch parameters have been met within the vehicle, the READY lamp on the Missile Control Panel will illuminate, indicating the vehicle is ready to launch. If not, the FAULT lamp illuminates, indicating a target malfunction. Launch can take place immediately after the READY lamp illuminates. A timer in the missile control panel limits the on time of the LAUNCH/READY switch to three minutes to prevent overheating of the DPU alternator. Overheating does not occur after launch due to the cooling effect of the oxidizer flowing through the DPU oxidizer pump.

Should launch not be effected within the three-minute period and the LAUNCH/READY switch disengages, it may immediately be activated again if desired. This three-minute period also gives time for telemetry verification of target functions. LAUNCH/READY is shown as the second item in the time sequence line of Figure 46.
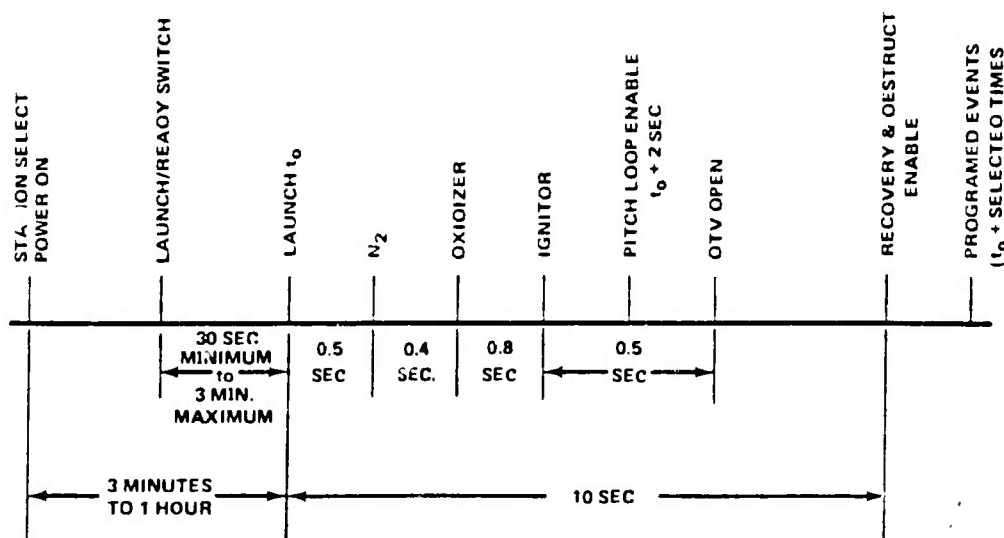
Figure 46. HAST Time Sequence of Events

After the pilot receives a READY indication and telemetry has been verified, he sets the armament switches in the aircraft to effect a centerline stores release. At T_0, as determined in the countdown, the pilot depresses the centerline stores release switch on the stickgrip. This launch signal enters the target, enables the master clock and verifies the self-test circuitry. If these parameters are met, the launch signal travels to the launcher to initiate the launch cartridge. Launch is shown as item 3 on the HAST sequence of events, Figure 46. As the launcher cartridge fires, the vehicle is ejected down and forward, pulling the target lanyard pin. Lanyard removal enables the electrical explosive device (EED) circuitry in the vehicle and removes the reset from the counters allowing timed vehicle functions to begin.

The first event to occur after the lanyard pin is removed is N_2 EED initiation. This occurs approximately 0.5 second after the lanyard pin removal, although the time may vary as much as 100 milliseconds. Variance is dependent on where in the master clock 10 Hz oscillator cycle the pin is actually removed. All other times have precise intervals. Initiation of the N_2 EED allows high pressure nitrogen to flow from the vehicle N_2 tank, through the regulator (where it is regulated down to working pressure) to the oxidizer tank.

The oxidizer valve EED is initiated 0.4 second after the N_2 EED. This allows the oxidizer to flow (under pressure) to the DPU pump which then fills the lines to the oxidizer throttle valve (OTV). The thrust chamber igniter is electrically initiated 0.8 second after the oxidizer valve EED. The interval between igniter firing and the OTV open command is 0.5 second. This interval is critical and was optimized during engine firing ground tests. The open command ramps open the OTV and allows oxidizer to flow to the thrust chamber starting ignition and thrust 2.2 seconds after target separation.

At +2 seconds after separation the target pitch loop is enabled. Until this time all pitch inputs to the autopilot have been held at zero volts with the canards held at center. At pitch loop enable, canard bias, altitude and pitch rate signals are applied. This delayed pitch loop enable allows sufficient separation between the vehicle and launch aircraft to prevent collision should some malfunction occur in the pitch portion of the autopilot.

Destruct and recovery EED relay arming occurs ten seconds after launch. The arming is delayed as a safety feature to provide sufficient aircraft/target separation in case of accidental hatch firing or destruct maneuver.

87

The last item shown in Figure 46 is programmed events. A detailed setup and explanation of these times is discussed in the section titled "Programming a Flight".

2. LAUNCH SYSTEM AND AIRCRAFT LOAD ANALYSIS

a. **Launch System Description.** The HAST launch aircraft is a modified Air Force F-4C. Modifications consist of installing an LAU-96 launcher on the aircraft centerline ejection rack, installing a missile control panel in the aircraft cockpit, and modifying aircraft electrical circuitry to provide power to the target and launcher.

The missile control panel includes all pilot operated switches and indicators to ready the target for launch. The SELECT switch controls target warm-up power and the LAUNCH/READY switch controls the power to open or close the ducted power unit (Ram Air Turbine) gate. This switch is a magnetic latching type and automatically returns to the off position should launch not be effected within three minutes after the switch is actuated. A spring guarded JETTISON switch is employed on the panel and will jettison the target and launcher when actuated. Target-only jettison is accomplished through use of the aircraft emergency stores jettison system.

Three annunciator lamps are located on the control panel and illuminate to inform the pilot of target status. The POWER lamp illuminates and blinks for three minutes when the SELECT switch is actuated. After the three-minute target warm-up period, the lamp remains illuminated. The FAULT lamp illuminates when any of the targets 22 self-test parameters have not been met within the vehicle. Target launch cannot be initiated with the FAULT lamp illuminated. The READY lamp illuminates to inform the pilot that launch parameters have been met within the vehicle and the target is ready to launch. The LAUNCH/READY switch must be in the LAUNCH/READY position for the lamp to illuminate.

Target launch is accomplished by positioning of the aircraft armament switches and depressing the store's release switch on the pilot's stick grip. These actions supply launch power from the aircraft armament bus, through the target's self-test interlocks to the launch relay in the LAU-96 launcher. When the relay closes, power is supplied to the launcher cartridge.

The LAU-96 launcher is a cartridge actuated, electrically triggered assembly that attaches to the aircraft centerline ejection rack. Large access doors on each side of the launcher provide access to all launcher components.

The launcher consists of a structural frame, a trapeze ejector mechanism, wiring harness, release hooks, cartridge powered cylinder and piston assembly and relay box. Removable mechanical and electrical pins are employed to arm and disarm the launcher. No-voltage tests are performed prior to pin removal.

An electrical signal from the aircraft armament system fires the impulse cartridge loaded in the cartridge breech block assembly.

During operation the expanding gases from the fired cartridge operate a small hook release piston which unlocks the retaining hooks through an over-center locking mechanism. As the hook release piston moves through its cylinder, a small port is exposed thereby pressurizing the large actuator cylinder. The actuator piston is connected directly to a crank arm of the trapeze mechanism.

This trapeze mechanism, through a rotational motion, cycles the launcher sled down and forward to eject the target. Continued motion of the launch mechanism retracts the sled into the launcher housing to complete the launch cycle.

b. **Load Analysis.** The following chart shows the loads placed on the aircraft electrical system by the target and launch systems. The loads are rounded off to the nearest 0.1 ampere.

TABLE XX. AIRCRAFT ELECTRICAL LOAD

Component or Function	Taxi,Takeoff & Climb	A/C Above 10,000 Ft	Station Select	Launch/ Ready	Launch
(1) Equipment Heaters	2.3	2.3	2.3	2.3	2.3
(2) Pitot Heater		3.5(8)	3.5	3.5	3.5
(3) Select Power (Target)			11.1		(20)
(4) Missile Control Panel			0.1	0.1	0.1
(5) Sta. Select Relay (Launcher)			0.1	0.1	0.1
(6) Launch/Ready Off	2.0	2.0	2.0		
(7) Launch/Ready On				0.2	0.2
(8) Total Load (Amps)	4.3	7.8 (15.8)	19.1	6.2	6.2 (26.2)

The equipment heater loads, shown on line 1 of the table , have been reduced from that shown on previous reports due to payload redesign. When the pitot heater is turned on by the barometric switch in the launcher, the initial load is approximately 8 amperes. As the pitot heats, the load is reduced to 3.5 amperes. At Station Select, the Select Power is shown to be 19.1 amperes, which includes payload warm-up power. During flight test, with the telemetry system on and the transponder being pulsed, this load will be approximately 5.5 amperes. At LAUNCH/READY, the DPU alternator comes on the line, taking over the Select Power load. Up to this point the aircraft has been furnishing power to the DPU speed control, holding the door closed. As the LAUNCH/READY switch is transferred to "ON" the aircraft momentarily furnishes the same two amperes to open the DPU door, then the alternator takes over this load. The aircraft then furnishes lamp and switch holding coil loads to the missile control panel. The same power requirement exists from LAUNCH/READY to launch separation. At launch, the launch cartridge load, which has a duration of less than 100 milliseconds, is current limited to 20 amperes. After target separation the only load on the aircraft is 0.1 ampere for the power lamp on the panel. All other power is automatic.

3. TARGET ELECTRICAL POWER SYSTEM

a.   Power Distribution System. Power requirements in the HAST electrical systems are varied in quantity and application. Power is applied to some part of the HAST electrical system from aircraft power turn-on on the ground, through takeoff, climb, loiter, prelaunch warmup. launch, normal flight and recovery. Each portion of a flight requires varying amounts of power from one or two sources. The internal power system will be discussed first, then a target load analysis and finally some details of the internal components of the system.

The internal power distribution system of the HAST is shown in Figure 47. Because the buses are diode isolated, no power switching exists in the circuit. As the voltage from one power source rises above the other, load is transferred. The diode isolated system requires less volume than power switching and eliminates switching transients that could exist as the HAST leaves the launch aircraft.

Three power sources are shown in Figure 47. These are the aircraft, the ducted power unit (DPU) alternator-diode pack and the command/recovery battery. The loads shown on the far right of Figure 47, recovery, destruct, command receiver, C-band transponder and locator beacon, are on

89
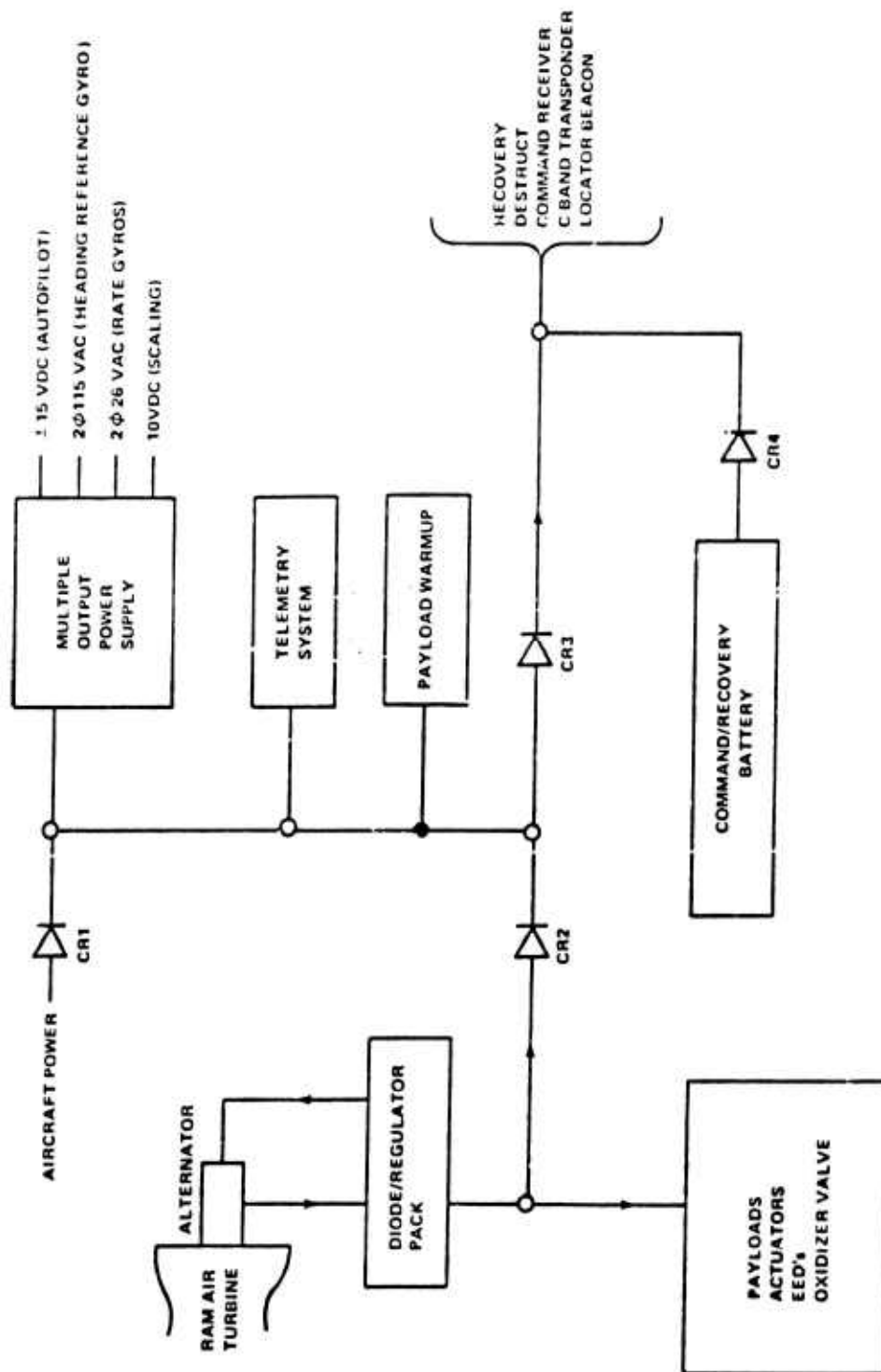
Figure 47. HAST Electrical Power Distribution System

90

the battery bus. The battery bus can be fed from any one of the power sources. The command recovery battery is not applied to the line until after the lanyard switch (not shown in Figure 47) is pulled at launch separation. A complete discussion on the sequence of events is found in paragraph 1 of this section. The loads shown in the upper center of Figure 47 are for the multiple output power supply, the telemetry system, and payload standby power. This load is referred to as the select bus. Items on this bus require long warmup or range acquisition time.

The multiple output power supply furnishes power to the heading reference gyro which requires a maximum of three minutes for the rotor to come up to speed and the torquers to erect the gyro gimbals. The telemetry system is energized to allow setup of ground monitoring of critical parameters prior to launch. The C-band transponder on the battery bus is energized from the select bus through CR3 for ground tracking acquisition. The target select bus is energized from the aircraft bus when the select switch is actuated on the cockpit missile control panel. The DPU alternator takes over the select bus load just prior to launch.

The DPU bus consists of those items shown in the box at the lower left of Figure 47. These items, which have high current requirements, are furnished power from the DPU alternator/diode pack only. The diode in the system prevents one power source from feeding back into another. The aircraft power is on a 15-ampere breaker and could not furnish the DPU bus loads without blowing the breaker. CR2 prevents this feedback. CR3 prevents feedback of the battery onto the select bus. CR1 prevents feedback of the DPU alternator onto the aircraft bus. CR4 prevents battery overcharging from the other buses. The battery furnishes 75 percent of the power to the battery bus during flight because of the diode drop of CR2 and CR3 from the DPU alternator.

b. Target Load Analysis. Loads that appear on the various power buses vary with the specific flight test being conducted. The payloads, when installed, add considerable power requirements to alternator load. In the charts that follow loads are rounded off to the next highest 0.1 ampere to simulate worse case conditions.

The select bus is energized from the aircraft. The loads shown in the table below are an analysis of the select bus between Select and Launch.

TABLE XXI. TARGET ELECTRICAL LOAD ANALYSIS DURING SELECT

	Flight Test Configuration	
Item	Start	Run
Target System	1.0 amp	1.0 amp
MOPS	2.4 amps	1.6 amps
C-Band Transponder	1.1 amps	1.1 amps
TM Transmitter	2.0 amps	2.0 amps
TM System	3.0 amps	3.0 amps
Total	9.5 amps	8.7 amps

TABLE XXI. TARGET ELECTRICAL LOAD ANALYSIS DURING SELECT (Concluded)

Item	Payload Flights	
	Start	Run
Target System	1.0 amp	1.0 amp
MOPS	2.4 amps	1.6 amps
C-Band Transponder	1.1 amps	1.1 amps
TM Transmitter	2.0 amps	2.0 amps
TM System	1.0 amp	1.0 amp
Payload Standby	3.6 amps	3.6 amps
Total	11.1 amps	10.3 amps

Note that the Telemetry System load is much less for the payload flights which make up for the increase in Payload Standby load. The difference between the Start load and Run load is caused by the gyro spin motor coming up to speed and gyro torquer shutoff after erection. Although not shown in the chart, there is an increase in load as the aircraft maneuvers and the gyro torquer re-erects to the new attitude. This is shown in the next paragraph of the Multiple Output Power Supply (MOPS) load analysis.

The MOPS loads vary as the gyro load varies. The gyro torquers remain off while the motor makes its initial high current spin-up. The Start load is shown in Column 1 of the MOPS load chart. The MOPS Run load, shown in Column 2, is MOPS turn on, plus two minutes which is after motor spin-up and plus two minutes which is after motor spin-up and gimbal erection. Maneuver loads are shown in Column 3.

TABLE XXII. MOPS INPUT/OUTPUT

	Start	Run	Maneuver
Input Voltage	2.4 amps	1.6 amps	2.3 amps
115 VAC θ_1	0.16 amp	0.05 amp	0.15 amp
115 VAC θ_2	0.15 amp	0.05 amp	0.14 amp
26 VAC θ_1	0.13 amp	0.10 amp	0.10 amp
26 VAC θ_2	0.22 amp	0.22 amp	0.22 amp
+15 VDC	0.37 amp	0.37 amp	0.37 amp
-15 VDC	0.33 amp	0.33 amp	0.33 amp
+10 VDC	3 ma	3 ma	3 ma

The maneuver load is almost that of the start load except that it exists only for short periods of time due to the torquer rate being much faster than the aircraft turn rate. The load on the +15 output is approximately 5.6 watts and has an 8-watt rating. The MOPS operates from 65 to 75 percent efficient in flight depending on the load applied.

The DPU bus load varies with the operational mode of the target. Therefore, the basic DPU bus load is shown below. As the DPU comes up to speed, the alternator/diode pack furnishes all buses.

TABLE XXIII. BASIC DPU LOAD

Item	Flight Test	Payload
Select Bus	8.7 amps	6.7 amps
Actuators	2.0 amps	2.0 amps
OTV	0.5 amp	0.5 amp
Speed Control	1.0 amp	1.0 amp
Air Data Module Heater	0.5 amp	0.5 amp
Battery Bus	1.7 amps	1.7 amps
Payload Operate		18.0 amps
Total	14.4 amps	30.4 amps

Note that the Select Bus for the payload column is not the same as in Table XXI Run column because the standby power is included in the 18 amperes shown for payload operate mode. The battery bus load is included in the total as a worse case condition because the battery level of charge will determine how much is furnished by the battery and how much by the DPU alternator. The air data module heater load is taken over from the aircraft heater bus during flight. The totals of Table XXIII therefore show a worse case straight and level flight condition for the target.

The following table lists those loads which, in addition to those shown in Table XXIII, would present a maximum power requirement to the DPU alternator.

TABLE XXIV. MAXIMUM DPU LOAD

Item	Flight Test	Payload
From Table XXIII	14.4 amps	30.4 amps
Maneuver	0.7 amp	0.7 amp
OTV Stalled	4.5 amps	4.5 amps
Aileron Actuator Stalled	5.0 amps	5.0 amps
Canard Actuator Stalled	5.0 amps	5.0 amps
Speed Control Stalled	1.0 amp	1.0 amp
Total	30.6 amps	46.6 amps

The possibility of all systems being at a stalled condition is very remote; however, the data is presented to show what each item can contribute. The alternator/diode pack-regulator power source is capable of furnishing the 46.6 amperes shown for the payload flight because the maximum specification output is 47 amperes. The alternator also furnishes the EED firing loads that are discussed in the relay board and electro-explosive device circuits paragraph.

93

For analysis of the battery loads it is assumed the battery furnisnes all of the battery bus current The battery does in actual measurement furnish approximately 75 percent of the battery bus load. Table XXV shows a breakdown of the battery bus loads. During flight and recovery the load is the same for flight test and payload configurations.

TABLE XXV. BATTERY BUS LOADS

	Prelaunch		Flight	Recovery
	Flight Test	Payload		
Target System	20 ma	2 ma	0.55 amp	0.55 amp
Command Receiver	–	–	0.05 amp	0.05 amp
C-Band Transponder	--	--	1.1 amps	1.1 amps
Locator Beacon	--	--	--	0.2 amp
	20 ma	2 ma	1.7 amps	1.9 amps

The prelaunch load is less for the payload configuration due to a reduction in TM system readout. This load exists from safety pin pull until launch. With the loads shown in Table XXV the battery will operate the system reliably for one hour from launch assuming the battery was installed in a fully charged condition.

c. Main DC Power Source. The HAST main DC power source is an alternator driven by the ram air turbine. The turbine also drives the oxidizer pump.

The alternator is a six-pole, three-phase, homopolar inductor type, driven at a nominal 30,000 RPM. The flux path of the alternator, shown in Figure 48, flows from the field winding through the stator winding and one set of pole faces, then axially along the rotor, out through the other pole faces and stator winding, then back to the field winding in one homogeneous path.

The output of the alternator is rectified to supply a nominal 28 VDC at 47 amperes, full load. In addition to the steady state load, a transient load of 30 amperes for 100 milliseconds is required to be furnished by the power system. The transient load cannot be repeated closer than 200-millisecond intervals and the voltage on the bus shall not sag to less than 22 VDC at transient load application.

Rectification is accomplished by 12 diodes forming two, three-phase, full wave bridge rectifier circuits fed into a common DC bus.

A regulator, mounted in the same package with the rectifiers, senses output voltage and compares it with a fixed reference. The error voltage controls alternator field current. Since the field winding is placed in the magnetic path of the stator output windings, as shown in Figure 48, a current of sufficient magnitude and polarity will adjust the homopolar field so that the voltage generated nulls out the error. In this manner, voltage regulation is obtained regardless of changes in load current or turbine speed. Initial field current is provided from the speed control assembly at DPU on command. The system is capable of regulating ± 0.5 VDC from the set point over any of the system specified load, temperature, and turbine speed conditions. A regulator set point was selected of 28.5 ± 0.5 VDC at a nominal load of 30 amperes for systems checkout.

The stator coils are offset by 60 degrees giving a ripple content of less than two percent when rectified by the full wave bridge circuit. Good regulation and low ripple content reduce the regulation requirements of power fed to the other systems in the target.
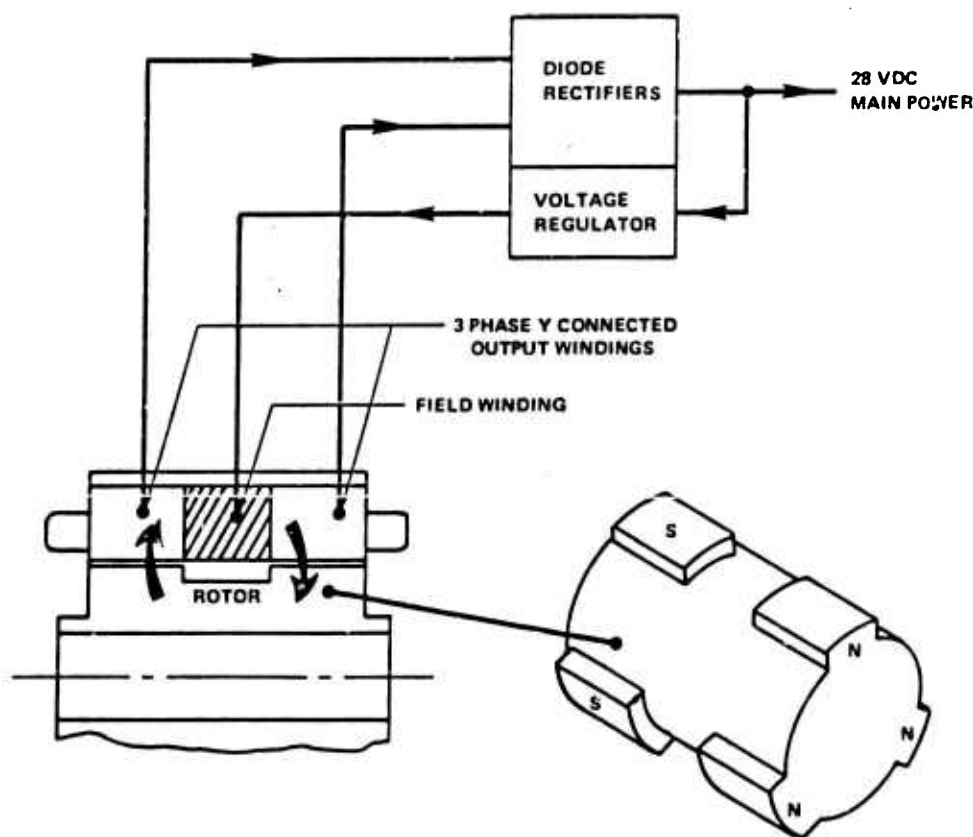
Figure 48. HAST Primary Power

Turbine RPM and therefore, pump output pressure, are controlled by a servo loop placed around the ducted power unit. A butterfly valve with associated servo motor is placed in the DPU to control the amount of air entering the turbine inlet. A block diagram of the servo loop is shown in Figure 49.

95
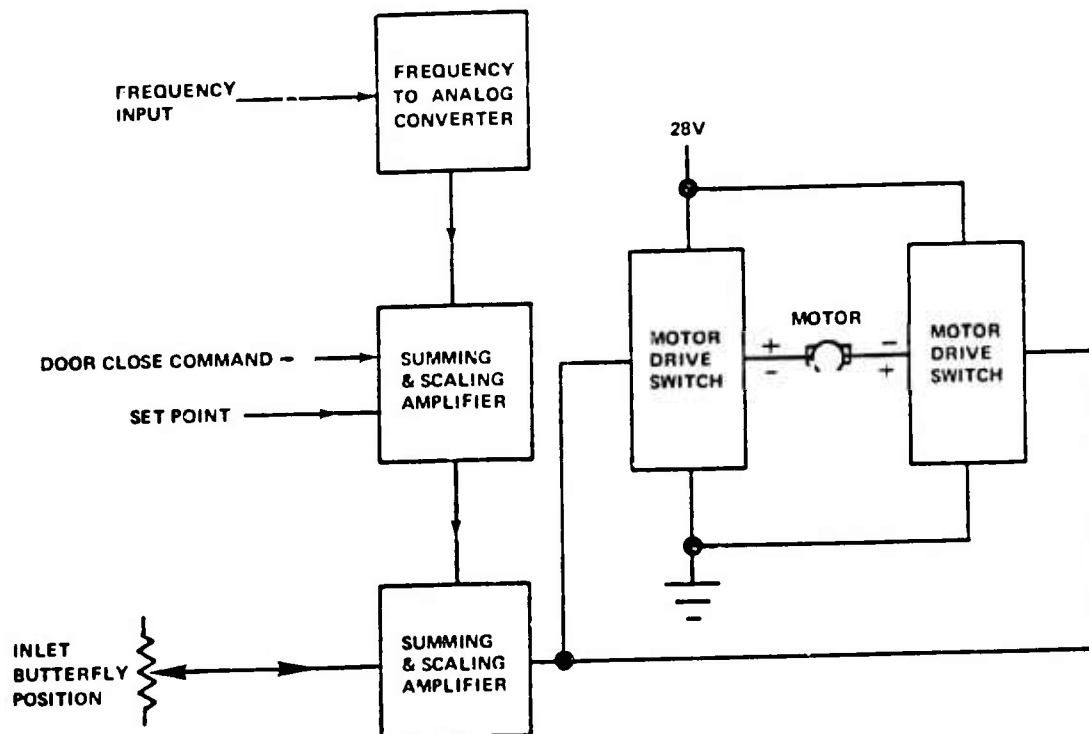
Figure 49. Turbine Speed Control

Alternator frequency is sensed from a phase to phase connection to the stator windings. This output frequency represents RPM divided by 20. A frequency to analog converter changes the frequency to a DC voltage level. Internal connections in the frequency analog converter are such that an increase in frequency (turbine speed) results in a DC voltage level decrease. The DC voltage representing turbine speed is summed with the turbine set point in the first summing and scaling amplifier shown in Figure 49. Set point is variable and must be adjusted to the individual turbine RPM requirement. Gain around this amplifier sets the correct signal level to the next summing amplifier. This amplifier is used to sum the first amplifier analog voltage output with the inlet door (butterfly) position. The inlet door position analog voltage is summed in a positive feedback manner which produces a lead network effect resulting in systems stability. The output of the second summing amplifier powers the motor drive switches. These are bilateral which alternately reverse the polarity across the motor relative to the direction the butterfly is to be driven. The motor is equipped with position limit switches that interrupt motor current in the full open or closed position.

Also shown in the first summing amplifier is the door closed command. The door closed command saturates the amplifier driving the inlet butterfly fully closed during the captive portion of the flight. This prevents the turbine from excessive free-wheeling.

Although some variation in turbine speed is seen with altitude changes, Mach number and temperature, the stability of the system is sufficient to provide adequate power and oxidizer pressure for all missions.

96

d.   Multiple Output Power Supply. The 28 VDC from the alternator to the diode pack does not provide for some of the unique power requirements of the total target system. The multiple output power supply (MOPS) has been proved to meet these requirements. MOPS outputs are +10 VDC, ±15 VDC, 26 VAC, 2 θ, and 115 VAC, 2 θ.

Scaling functions such as altitude, Mach number, roll angles, and heading changes required a highly regulated and stable source. The MOPS 10 VDC output is utilized for these scaling functions. Altitude, 0 to 100,000 feet, is scaled from 0 to 10 volts; for Mach number the scaling is 2 volts per Mach and for heading change 10 V represents 200 degrees. The 10 VDC output has a 0.5 watt capability with excellent regulation and low ripple content.

The +15 VDC output is provided for autopilot power. The autopilot system uses integrated circuits which require a +15 and a -15 volt source. The autopilot module, servo amplifiers, gyro pots, electronics, actuator pots and digital logic board components that interface with the autopilot module use these ± 15 volt outputs. The +15 VDC output is capable of 8 watts of power while the -15 VDC output is capable of 6 watts of power. The outputs have good regulation, low ripple content and are tracked to within 300 millivolts of each other.

During component selection, an off-the-shelf rate gyro was chosen which required 26 VAC, 400 Hz, two-phase power. Instead of requiring a redevelopment of the rate gyro drive motor and demodulation circuits to operate from the main DC source, a 26 VAC 2 θ output was provided from the MOPS. The 26 VAC output is capable of starting a 12 VA per phase load and a continuous load of 5 VA per phase. Frequency affects the accuracy of the rate gyro; therefore, the 400 Hz oscillator in the MOPS is controlled to ±1 percent. The second phase output is shifted 90 degrees from the first.

The heading reference gyro chosen for HAST requires 115 VAC 2 θ power to operate the gyro torquers and spin motor. The MOPS has 115 VAC 2 θ output windings capable of 78 VA per phase for start loads, 68 VA per phase maneuvering loads and 7 VA per phase continuous run load.

The MOPS operates over a narrow range of input voltage, 28 ±0.5 VDC, because of the regulation capability of the DPU alternator/regulator combination. This eliminates the need for a preregulator in the MOPS. The oscillator is highly regulated to maintain the 400 Hz accurately and then digitally phase shifted for the 90-degree phase shift for the second phase of the AC power requirements. Power transistors then drive two separate transformers. One transformer has the +15 V, 115 V θ 1 and 26 V θ 1 windings while the other transformer has the +10V, -15 V, 115 V θ 2 and 26 V θ 2 windings. The DC outputs are rectified and regulated while the AC square wave output windings are brought out direct to the gyros.

The MOPS was packaged in a special shape to fit the space available. The total assembly occupies 50 cubic inches and connects directly to the power distribution board for interfacing with other assemblies.

e.   Command/Recovery Battery. A separate power source for command destruct functions is required by specification so that the destruct system does not rely on normal HAST alternator power. When the target is descending after recovery initiate, the ram air turbine is no longer capable of furnishing sufficient power to the digital logic recovery circuitry. The recovery C-band transponder used to track the descending HAST and position the recovery helicopter must also be powered at this time. The command/recovery battery also furnishes power to fire the hatch and drogue release EED's.

A nickel cadmium cell was selected to fulfill the above requirements due to the high discharge rate capability and low internal impedance required to fire EED's. The cell, which is a 1.9 ampere hour "C" size, requires no special handling other than normal charging with equipment readily available in the Armed Forces inventory. Twenty-two such cells comprise the battery assembly.

The cells, including a heater and associated thermostat, are encased in an insulated aluminum container shaped to the inside contour of the aft boattail section. The aft boattail location provides

97

ready access to the battery assembly while enhancing the vehicle cg. The heater and thermostat holds cell temperature to a minimum of 0°F during long loiter flights at altitude. The battery assembly will furnish HAST power for approximately one hour and is rechargeable over 500 cycles.

f. Power Distribution Board. The power distribution board is a double-sided printed circuit board assembly which is mounted on the right side of the target in the radius between the parachute pack and the target skin. The power distribution board provides a power and ground distribution point for various target assemblies. Because high density connectors are used for distribution, minimum space is required for the assembly. The major bus and ground circuits are fed into the assembly through a larger terminal block module that is bonded to the board. The MOPS input and outputs are distributed in this assembly.

The MOPS, roll rate gyro and pitch rate gyro were purchased with pigtail leads instead of connectors in order to conserve space. Each has its own connector connected directly to the power distribution board. The multiple output terminations provided by the assembly reduce the number of splices required in the harness. Circuits which are not essential to a stable flight are fused within the power distribution board. These include the C-band transponder, telemetry system and payload prelaunch warm-up requirements.

As the target system developed, it was necessary to find a space for several auxiliary circuits. Blank areas on the power distribution board were utilized for these circuits. A readout of turbine speed for telemetry and prelaunch self-test was incorporated into the assembly. This circuit consists of a one-shot multivibrator that converts alternator frequency to an analog voltage which is then sent to an offset and scaling amplifier. Adjustable offset is required due to the variation in DPU set point frequencies. This requires that each power distribution board be set for the DPU with which it is used. The output of the scaling amplifier is set at 1 volt per 2,000 RPM turbine speed change. The scaling amplifier feeds the telemetry system and a dual comparator similar to that which will be discussed in the prelaunch self-test section. The dual comparator is adjusted for a window of ±2,000 RPM. If the turbine is outside of this range, a no-go is sent to the launch and fault light circuit.

The power distribution board also contains interface circuits. Two operational amplifiers perform the function of rescaling the radar augmentation and miss distance indicator payload "ok" signals from 5 VDC to the 12 VDC level required by the prelaunch self-test circuit. An additional operational amplifier interfaces the low drive capability of the normal accelerometer, N_Z, with the higher power drive required by the remainder of the N_Z circuits. A filter is incorporated with the N_Z interface amplifier to limit frequency response to the vehicle response requirements and eliminate vibration frequencies.

Logic within this board collects the radar augmentation system (RAS) "ok", vector miss distance indicator (VMDI) "ok", DPU thermal switch open and turbine speed "ok" signals. From these, one ready signal is sent to the digital logic board to be summed digitally with the other self-test inputs. Phase one of the MOPS 115 VAC is rectified, scaled and filtered, then sent to the digital board for use in the prelaunch self-test circuit. This output is also used for telemetry monitoring.

Gyro erection control is provided by circuits on the power distribution board. Gyro erection takes place by torquing the roll and yaw gimbals of the gyro so that they are repositioned to align with the roll and yaw axis of the target. At SELECT bus on, the gyro motor spins the rotor for 30 seconds before torquing power is applied to prevent unnecessary loads on the gimbals. From power on plus 30 seconds, until lanyard pin pull at launch, the gyro operates in the erection mode. Operation as a free gyro begins when erection is removed at launch. A 30-second timer integrated circuit and C/MOS logic gates provide the above controls to the gyro. Yaw gimbal torquing during turns will be discussed in the autopilot section.

g. Relay Board and Electro-Explosive Device Circuits. An electro-explosive device (EED) is defined as an electric initiator or other component in which electrical energy is used to cause initiation of explosive contained therein. With the expenditure of less than 400 milliwatt seconds of energy a force greater than 160 foot-pounds can be applied. The EED fires the explosive charge in

less than 2 milliseconds when 10 amperes or more flow in the bridgewire with the bridgewire vaporizing in 20 milliseconds or less. The HAST uses these devices for N_2 tank pressurization, oxidizer start, igniter, hatch release, drogue release, locator beacon antenna deployment, and destruct. Except for the antenna EED, all have two separate bridgewires. The cartridge firing relay board assembly provides an interface between the timed signals and the power source used to fire the EED's. This printed circuit board contains eight relays, one for the safe and arm device which is not an EED, current limiting resistors, and steering diodes.

The two-ampere rated relays receive a 100-millisecond pulse from the digital logic board. With the bridgewire vaporized at 20 milliseconds the relay does not have to open the load unless the wire fuses to the case. The short to case rarely occurs but the 100-millisecond pulse is provided to re-open the circuit, eliminating the possible short. The relays hold all four EED leads grounded until the firing pulse arrives. The EED ground leads are returned to the relay board to keep circulating current loops to a minimum. The four leads between the EED's and the relay board are twisted, shielded, and jacketed to further eliminate Hazards of Electromagnetic Radiation to Ordnance (HERO) problems and meet specification requirements.

The measured total loop resistance, which includes the EED bridgewire resistance and the one-ohm current limiting resistor in the relay board, ranges from 1.57 to 2.19 ohms. The current is limited to 12 to 18 amperes in each bridgewire, assuring positive firing without causing excessive voltage drops in other circuits. The firings are spaced at a minimum of 200-millisecond intervals to give the alternator time to recover.

h. HAST Wiring Harness. HAST vehicles require a unique and complex harness because of varying requirements and configurations for individual vehicles, i.e., captive flight, IR payload, and vector miss distance indicator payload. In addition, some vehicles must be reconfigured for a second mission. The basic vehicle wiring (excluding telemetry wiring) is defined in the Master Wiring Diagram and Harness Assembly. To simplify the problem of various configurations, separate dash numbers were assigned to fabricate wiring for the two payloads. The individual payload harnesses (dash numbers) may be added to the overall harness assembly for the equipment sections or omitted as required. Because of the wire marking problems of Teflon® coated wire, the contractor was relieved of the wire and cable marking requirement of MIL-W-5088. Cables, wires, and branches of wiring harness are not marked with reference designation numbers. Connectors, however, are identified with applicable reference designation.

The HAST wiring harness is designed with minimum voltage drop for the high power usage items with 0.5 V loop drop as the objective. An example is the payload power wiring which is a twisted 8-gage pair running from the diode pack terminal to the nose payload package. The line is fused to prevent payload electrical failure from affecting recovery of the target.

During harness design, ground loop problems were minimized. The EED ground return was terminated at the diode pack terminal to reduce the effect of the high firing current on the autopilot and other target systems. A single point grounding system is used as far as practical. Measurements were made between points in the ground wiring and ground wires were relocated to produce lowest millivolt drops. The final harness incorporates all of the changes indicated and reduces system noise to an acceptable level.

The umbilical connector, which provides the launcher interface, is the only open connector when the target is closed ready for loading, until the parachute is deployed during recovery. All wires coming to the umbilical connector are diode isolated or designed so that no voltage potential exists at the connector. The connector can be shorted without damage.

Throughout the harness, only a minimum amount of shielded wire was specified to reduce size and weight. In some areas where EMI problems might occur, the technique of special twisting of specific wires was utilized as an equivalent of shielded wire. This technique saves additional weight and space.

For ease of field maintenance, the harness was designed to permit the battery to be charged without removing the tail cone and to allow the autopilot to be slipped in and out without being disconnected. In addition, a disconnect is supplied for alternator field wires so the alternator field will not be excited during ground test procedures.

Future harness modifications are indicated for production to eliminate redundant wire runs and splices. Alternate wire types are indicated which would reduce bundle sizes, be easier to mark, and be more resistant to abrasion.

The majority of wire utilized in the harness is MIL-W-16878/4 Type E. Wiring between the digital logic assembly and the command receiver/decoder as well as the 115 VAC lines from the heading reference gyro and wiring to all the electro-explosive devices is made from twisted shielded cable. Circuitry between the power distribution panel assembly and the DPU thermal switch uses Kapton insulation due to being routed through an extremely high temperature area. In order to conserve space, splice requirements are held to a minimum. Instead, circuit interconnections are accomplished wherever possible by terminating the wires for the specific interconnection in a common connector pin or a common terminal barrel. Thermofit solder sleeves are used whenever splicing of shielded cable is required. Such solder sleeves provide a lightweight and reliable connection for grounding shielded wire and joining hook-up wire. To eliminate the possibility of shorting due to Teflon® insulation "creeping" and exposing conductors terminated at connectors, connectors in the midbody equipment section are potted. The potting, in addition to providing a suitable insulating barrier, also provides wire support. Connectors mating with electro-explosive devices were color coded to match color coding applied to cartridge installation points. Installation points are color coded as follows:

TABLE XXVI. CARTRIDGE COLOR CODE

Cartridge	Color
N$_2$	Yellow
Oxidizer Start	Green
Safe/Arm	White
Safe/Arm Test	Blue
Igniter	Red
Destruct	Black
Drogue	Grey
Locator Beacon Antenna	Orange

The overall harness is tied for support in all unprotected areas of the harness. However, the major part of the harness is protected from heat and chafing by use of two types of tape: one type (fiberglass) protects the harness in areas where chafing is possible while the aluminized tape reflects heat away from the harness when routed through high-temperature areas. In addition, wires routed in extremely high-temperature areas are protected by wraps of five layers of Fiberfrax® (ceramic paper) in addition to the insulating tape; a technique tested to withstand greater than projected temperatures during flight. To conserve space and eliminate bulkiness of the harness at high-density connectors, conductors are grouped by circuit function and spot-tied prior to termination at the connector. In cases where identical connectors are in adjacent area locations, wiring is supported by spot-ties and routed in such a manner that improper connections cannot be made. After the harness has been fabricated, the basic harness and the payload harnesses are identified by dash number and

reference designation by the installation of marker plates secured around the harness.

At the time of installation a minimum amount of hookup is required. The only connections which must be made are (1) alternator to the terminal junction, (2) wires to the diode pack, and (3) wires to the shunt. All of the above connections are in the mid-body. All wires which must be attached to the shunt are individually marked with "home" information - reference designation and mates with applicable numbered terminal of the shunt which is stamped on heat shrinkable tubing and installed on each wire. After connections are completed at the shunt, electrical terminal nipples are secured over each terminal for protection. The harness receives primary support throughout the raceway and at the multiple output power supply by use of clamps. The clamps are designed to fit the contour of the harness resulting in a snug fit without excessively compressing the wires. As the harness is installed, additional protective wraps of fiberglass tape are applied in areas where chafing is possible. Routing of the harness in the mid-body section minimizes space to provide for packing of the parachute.

4. FLIGHT PROGRAMMING

Included in this section are programming items that affect target performance during a mission. Most of these circuits are contained on the digital logic board and, therefore, its construction is discussed first. Actual switch setup is discussed in the paragraph on programming a flight. The command interface paragraph shows how the flight program may be modified during a mission by radio command uplink. Self-test circuits are discussed to show prelaunch programming. An explanation of the turn program logic circuits is left until after the other autopilot discussions for a better understanding of what is taking place during the turn programs. Recovery programming is also discussed.

a. **Digital Logic Assembly.** The digital logic assembly is mounted on the left side of the target in the radius between the parachute pack and the target skin. The assembly consists of two, ten-layer printed circuit boards tied together through a flat flexible multiconductor cable. The circuits located on this assembly perform most of the target commanded functions as opposed to the calculation functions performed by the autopilot.

The solid state digital switching logic elements that make up most of the assembly are complementary metal oxide semi-conductor (C/MOS) integrated circuits. These devices were selected because of their noise rejection and low power requirement. Also, supply voltage may range from 5 to 18 volts with excellent stability over the full military temperature range.

The C/MOS devices and most other electronics on the digital logic board, operate on 12 VDC regulated power. The 28 VDC battery bus, which is fed from either the battery or DPU, is brought into the board and preregulated to 15 volts by a zener diode. A hybrid voltage regulator further reduces and regulates the voltage to 12 VDC. The battery bus is used to power the board because some circuits must operate during prelaunch, powered flight, recovery and destruct.

The primary function of this assembly is to provide an accurate time base for engine sequencing, recovery sequencing and event time selection. A stabilized square wave 10 Hz oscillator provides digital pulses which are counted by five decade counters as shown in the block diagram in Figure 50.

The first decade counts 0.1 second, the second, 1 second, etc., until the fifth counter counts 1000's of seconds. Times out of the counter are available from 0.1 second to 9999.9 seconds in 0.1-second steps. The 10 Hz oscillator is free running from the time the cockpit switch is placed in the SELECT position; however, the pulses are not counted until launch. The C/MOS decade counters used have a count inhibit feature. Referring to Figure 50, the count inhibit connects to the launch command flip/flop. Counter inhibit is removed when launch command is received and reset with each SELECT power turn on. When launch is aborted, SELECT power should be turned off momentarily to reset the launch command flip/flop.

101
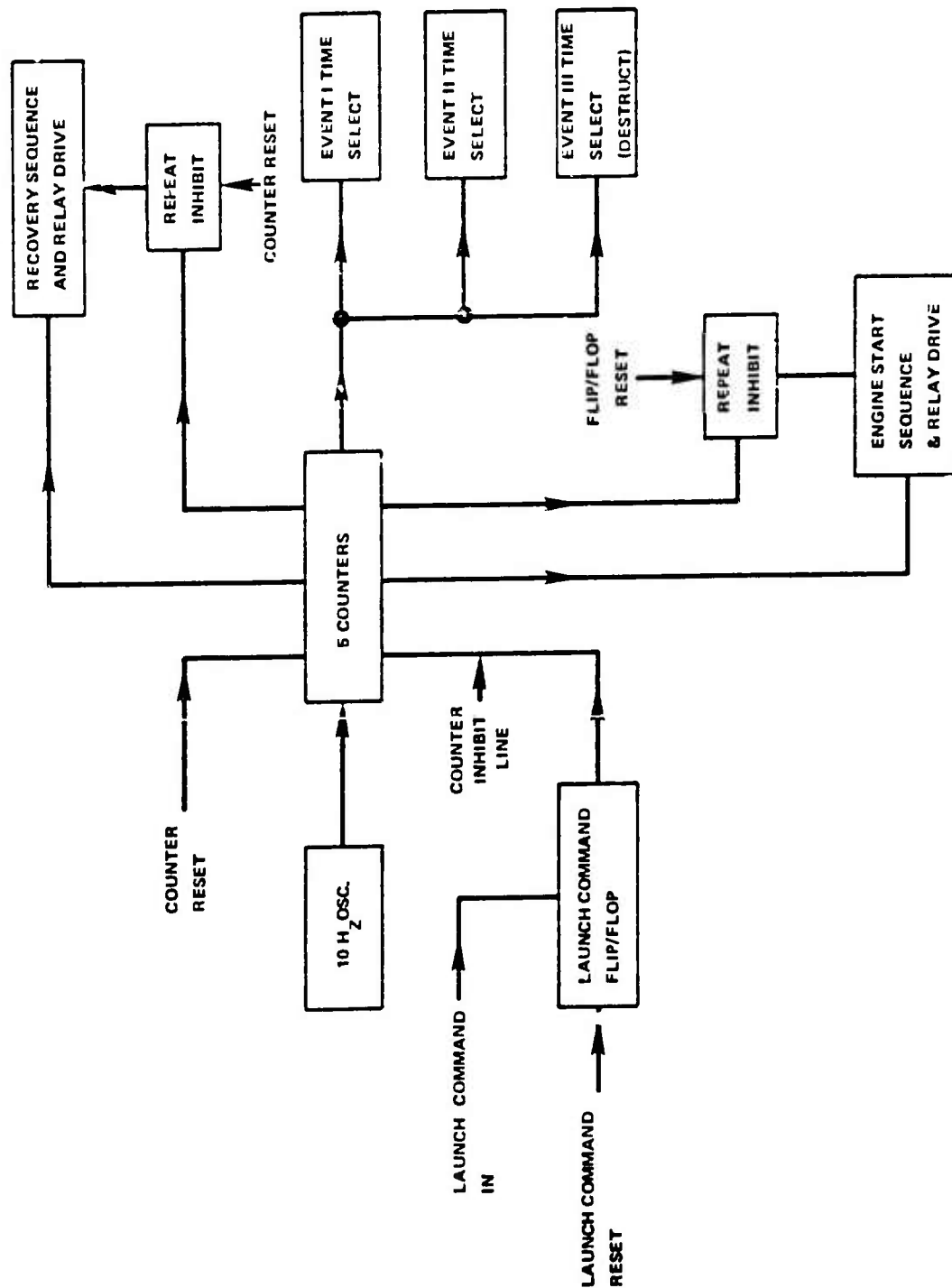
Figure 50. Block Diagram for Digital Logic Board Clock

102

Although count inhibit is removed with launch command initiate, the counters will not count because they are held to zero by the counter reset circuit. These reset circuits will be discussed later.

With the removal of the lanyard pin at launch ejection, counter reset is removed and counting begins. The engine start sequence takes place as discussed in the "Sequence of Events" section. The summed time output provides drive to a single high gain transistor which provides ground to the EED relay to be energized. The engine sequence occurs only once and is prevented from recurrence by the repeat inhibit. The inhibit prevents continued pulsing of the possibly shorted EED relays.

The counter 10-second output is used to provide destruct and recovery arming. As the counter continues to count, the selected event times occur. Setup and available times are discussed in the paragraph titled "Programming a Flight".

When recovery is initiated, the counters are reset and counting starts over. The engine sequence does not repeat because the repeat inhibit still exists for those circuits. Recovery sequencing did not take place with the original engine sequence because the absence of recovery initiate provided an inhibit. Recovery times and events will be discussed in the recovery paragraph of this section. As the recovery sequence takes place an inhibit circuit, similar to the engine sequence repeat inhibit, occurs to prevent repeat of recovery EED firings.

A block diagram of the reset circuits is shown in Figure 51. As shown, insertion of the lanyard pin resets all of the circuits except the launch command flip/flop. With the lanyard pin installed, all circuits can be reset by turning off power momentarily. Removing the lanyard pin removes ground from the counter reset circuit which in turn removes the reset signal allowing functions to begin. The flip/flop reset circuit resets all of the autopilot and digital logic board flip/flops.
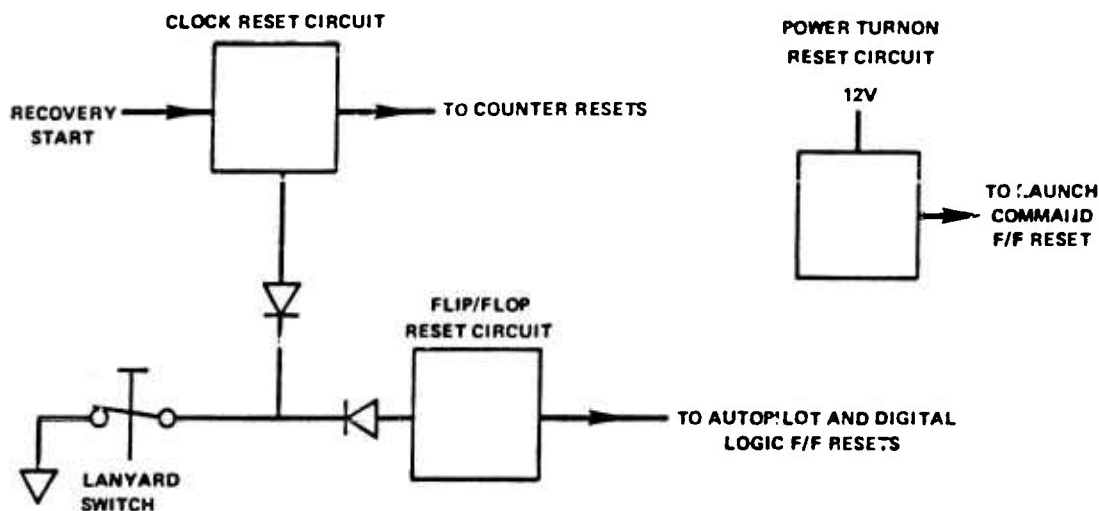
Figure 51. Block Diagram of Reset Circuits

The recovery start signal pulses the clock reset circuit to reset the counters while the diode isolation prevents operation of the flip/flop reset circuit. The reset pulse duration produces a short time delay (150 milliseconds) between the recovery start signal and the time count start for recovery.

b. Programming a Flight. The flight path of the target is preprogrammed on the ground by 19 switches. These switches are located on the lower forward edge of the digital logic board assembly. All switches have ten positions except the five-position switch, SW 19. The switch placard is duplicated in Figure 52 for reference during the following discussion.

103
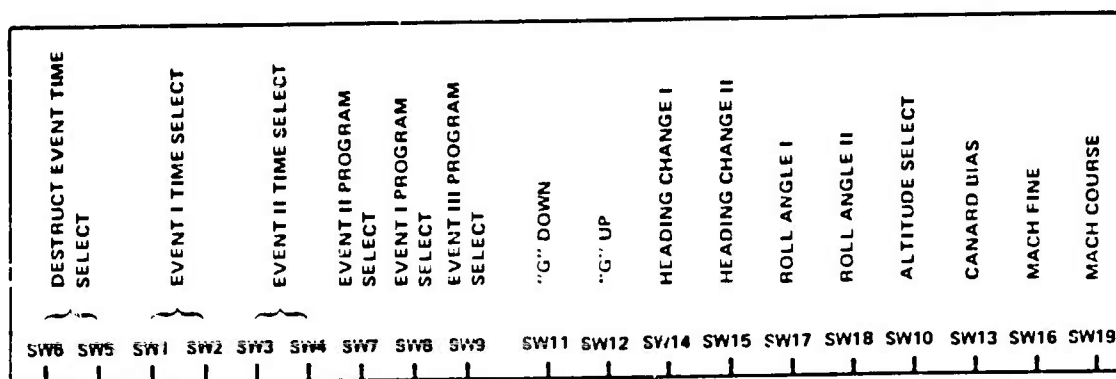
Figure 52. Flight Programming Switch Placard

The front four switches on the right program the basic flight profile. Cruise Mach number is selected by SW 19 and SW 16. Whole Mach numbers 1, 2, 3, or 4 are selected by the MACH COURSE, SW 19 and 0.1 Mach numbers are selected by the MACH FINE, SW 16. The final cruise Mach number is the summation of the MACH COURSE and MACH FINE switch settings. Switch 19 has a fifth position which is the same as position 4.

The CANARD BIAS, SW 13, is next in line. The up canard bias is selectable from 0 to 18 degrees in two-degree steps. The large range of dynamic pressures in which the HAST is flown requires the canard trim angles for straight and level flight.

The target cruise altitude is selectable in 5,000-foot steps between 35K feet and 60K feet and in 10,000-foot steps from 60K feet to 100K feet. The switch designated as SW 10 is used to select altitude.

At the left end of the board are two switches, SW 5 and SW 6, which select the DESTRUCT EVENT TIME. Times are selectable from 4 minutes to 20 minutes in 1-minute steps. Switch 5 selects time from 4 minutes to 12 minutes with time referenced from time of launch separation. When using SW 5 times, SW 6 must be in position 1. Switch 6 selects times from 13 to 20 minutes. If no destruct time is to be used, SW 6 is placed in position 10. When using the times on SW 6 the placement of SW 5 is arbitrary. Two jumpers, soldered in place on the reverse side of the printed board, can be changed to make use of switches SW 5 and SW 6 for programming a third event described in the following paragraphs.

The remaining switches on the board are used for programming the auxiliary maneuvers of the flight. Time selection of the Events I and II is made with SW 1 and SW 2, and SW 3 and SW 4, respectively. The event that is to occur at the selected times is selected by switches SW 7 and SW 8. SW 9 is a duplicate of SW 8 but is not used with the jumpers placed as discussed above. SW 6 and SW 7 times would be used with SW 9 when setup for an event instead of destruct.

Time setup for EVENT I TIME SELECT and EVENT II TIME SELECT is similar to that of the DESTRUCT EVENT TIME SELECT. These times are all counted from time of launch separation. Switches 1 and 2 select EVENT I TIME. Times may be selected from 10 seconds to 180 seconds in 10-second steps. Switch 1 selects times from 10 seconds to 100 seconds and switch SW 2 selects from 100 seconds to 180 seconds. When SW 1 times are used, SW 2 must be in position 1. If no event is desired, then SW 2 should be placed in position 10. Switches 3 and 4 select EVENT II TIME. Times may be selected from 120 seconds to 600 seconds in 30-second steps. Switch 3 selects times from 120 seconds to 360 seconds and SW 4 selects from 390 seconds to 600 seconds. When SW 3 times are used, SW 4 must be placed in position 1. If no event is desired, SW 4 should be placed in position 10.

104

After programming the time an event is to occur the next step is to select the desired event. EVENT I SELECT (SW 8) and EVENT II SELECT (SW 7) switches may be used to select the following:

TABLE XXVII. EVENT SELECTION

Position	Event
1	Auxiliary
2	Auxiliary
3	G Maneuver St
4	0.5M Slow
5	0.5M Fast
6	5K Ft Down
7	5K Ft Up
8	Turn II
9	Turn I
10	"S" Turn

When selecting positions 3, 8, 9, or 10 an additional setup is required using the remainder of the switches on the board. With position 3 selected on SW 7 or SW 8 the start of a g maneuver is sent to the autopilot module at the selected time. The g level obtained in the maneuver is determined by switch SW 11 for pushovers and by SW 12 for pull-ups. If a g UP command is selected (SW 12) then the g DOWN switch (SW 11) must be set at position 1 for 0 g's and vice versa. The g level position setting of each switch is the same with position 1 being 0 g, position 2 being 1 g, and then in 0.5 g steps until position 10 represents a 5 g maneuver.

The turn program used during a flight is selected at positions 8, 9 and 10 of SW 7 and SW 8. Turn I (position 9) and Turn II (position 8) are used when two separate turns are desired during a flight and when Turn I is to be completed some time before Turn II is to begin. Turn II is used only if there has been a Turn I programmed. When only one turn is desired during the mission Turn I must be programmed. If it is desirable to make a turn later in the flight than there is a time available on the EVENT I TIME SELECT, a Turn I must be programmed with zero heading change, then the Turn II programmed as desired. Position 10, "S" turn, is selected when the second turn is to occur immediately upon completion of the first turn. The "S" turn may be a right-left, left-right, or two turns in the same direction with different turn rates and heading changes.

The setup of the final four switches determine the roll angle and heading change of turns selected above. ROLL ANGLE I, SW 17, and ROLL ANGLE II, SW 18, are selectable as follows:

105

TABLE XXVIII. ROLL ANGLE SELECTIONS

Position	Degrees Roll
1	78.5 Left
2	75.5 Left
3	70.5 Left
4	60.0 Left
5	30.0 Left
6	30.0 Right
7	60.0 Right
8	70.5 Right
9	75.5 Right
10	78.5 Right

Left roll is indicated by the "+" or CCW roll of the vehicle when viewed from the rear and right roll is indicated by the "-" or CW roll. For any given Mach number and altitude, the turn radius will be determined by the roll angle. The heading change made for a turn is determined by the setting of SW 14, HEADING CHANGE I and SW 15, HEADING CHANGE II. These two switches are selectable from zero to 180° of heading change in 20-degree steps. Since the left or right roll selection determines the direction of turn it is not necessary to have a left or right selection of heading change, only an absolute value. The heading change command is sent to the autopilot module for comparison with the derived inner gimbal output of the heading reference gyro.

c. **Command Interfaces.** Table XXIX lists all events that can take place during a flight. Some events can be preselected that cannot be radio commanded and vice versa, as shown by the chart. The digital logic board provides circuitry for sorting and interfacing of the events that are to occur during a flight.

The radio commands come into the digital logic board from the command receiver. Two channels must be commanded for any one function to occur, thus eliminating possible interference that might exist at the 425 MHz receiver frequency. The guard tone (CH 10) must be received by the command receiver for any command, except destruct, to be possible. When CH 10 is low, indicating a signal loss, other command channels are locked out so that any noise that might exist in the receiver will not inadvertently trip one of the commanded functions.

Radio commands, in some cases, will exclude vehicle preprogrammed events. For instance, the left and right heading update commands will exclude any lateral preprogrammed events (such as turns) if the command is held on longer than three seconds. The ground control panel limits the heading update on time to 2.5 seconds unless overriaden. If the on time limit is released and the update signal held for longer than three seconds, the controller then has complete lateral control of the target. Under this condition, none of the preprogrammed turns will take place. A similar situation exists when a longitudinal maneuver is radio commanded. If the target controller sends a command for 5K up or 5K down, the onboard preprogramming for 5K up, 5K down or g command start will be excluded.

A radio command of 0.5 Mach increase or decrease will not exclude any preprogrammed event. However, these can occur only once in a flight so that the instruction occurring first (radio or

106

preprogrammed) will take precedence. A check is made by the prelaunch self-test circuit to verify the exclusion flip/flops for the lateral and longitudinal programming are reset, allowing normal, onboard control.

TABLE XXIX. EVENT MATRIX

Event	Position Selectable on Event I Switch	Position Selectable on Event II Switch	Command Receiver Chanels Required for Event	Event Latches When Commanded	Interfaces with the Autopilot Module	Automatic Onboard Command Without Preprogramming
(1) Destruct	None	None	1 & 2	Yes		X
(2) Recovery	None	None	3 & 4	Yes		X
(3) Recovery Inhibit	None	None	6 & 7	No		
(4) Drogue Release	None	None	5 & 8	No		X
(5) OTV Shutdown	None	None	5 & 6	No		X
(6) 0.5 Mach Increase	4	4	4 & 6	Yes	X	
(7) 0.5 Mach Decrease	5	5	3 & 5	Yes	X	
(8) 5000 Ft Up	7	7	5 & 7	Yes	X	
(9) 5000 Ft Down	6	6	7 & 9	Yes	X	
(10) Turn I Start	9	9	None	Yes	X	
(11) Turn II Start	8	8	None	Yes	X	
(12) "S" Turn Start	10	10	4 & 8	Yes	X	
(13) G Command Start	3	3	None	Yes	X	
(14) Heading Update Right	None	None	3 & 6	No	X	
(15) Heading Update Left	None	None	4 & 5	No	X	
(16) IR Payload Start	None	None	4 & 7	No		
(17) JEM Start	None	None	3 & 8	No		
(18) VMDI TLM CAL	None	None	3 & 7	No		
(19) AUX I	1	1	None	No		
(20) AUX II	2	2	None	Yes		

Events 6 to 15 shown in Table XXIX, interface directly with the autopilot module. These are all latched functions with the exception of the heading update commands. The autopilot module depends on the events to be latched to continue its function. For this reason, events 6, 7, 8, and 9 can be used only once during a flight. For example, if 0.5 Mach increase is activated then 0.5 Mach decrease can be activated to return the vehicle to the original cruise Mach. After this sequence is completed, however, it cannot be repeated during the flight.

Other events that are latched are the recovery and destruct functions. When they occur (either by radio command or onboard sensing) the flip/flops latch and the output remains, even though the original command signal is removed. The auxiliary events, which are not used at the present time, have one latched output and one momentary output. The chart shows the events that occur automatically during a flight without any preprogramming or radio command. These occur as a result of normal onboard sensing and sequencing.

Events 16, 17, and 18 are used in conjunction with the HAST payloads. These are jet engine modulation start for radar augmentation, telemetry calibration/VMDI for the scoring system and the initiation of the infra-red source. Drive capability and levels were coordinated with the payload manufacturers.

d. Self-Test Prelaunch Circuit. A continuous monitoring self-test feature is incorporated in the circuitry on the digital logic assembly. These self-test circuits, which monitor approximately 80 percent of critical target functions, are provided to increase the level of confidence for mission completion.

The self-test circuits are energized (and monitoring begins) when the launch pilot places the LAUNCH/READY switch on the missile control panel to the LAUNCH/READY position. Monitoring continues up through the moment the pilot depresses the weapons release switch in the cockpit. If any monitored target parameter should malfunction during this period, the FAULT lamp on the missile control panel illuminates and the launch command signal is prevented from passing through the target. Absence of the launch command signal results in a negative launch.

The critical target functions that are monitored by the self-test circuitry are listed below:

(1) Aileron Centered

(2) Canard Centered

(3) Gyro Yaw Pot Caged

(4) Gyro Roll Pot Caged

(5) Pitch Rate Gyro Centered

(6) Command Recovery Battery (greater than 24 VDC)

(7) Turbine Speed ±2,000 RPM

(8) Ram Air Turbine Thermal Switch

(9) Scoring System Okay

(10) Radar Augmentation System Okay

(11) Infra-Red Augmentation System Okay

(12) Guard Tone (CH 10) On

(13) Safe and Arm Open

108

(14) 115 VAC On

(15) Clock Oscillator On

(16) Counters Reset

(17) Oxidizer Thrust Valve Closed

(18) DPU Bus Greater than 21 VDC and Less than 31.5 VDC

(19) Recovery Not Initiated

(20) Destruct Not Initiated

(21) Lateral Commands Not Excluded

(22) Longitudinal Commands Not Excluded

Items 1 through 5 are sensed in a common operational amplifier. Input gain resistors are used to determine the tolerance requirements of each input. The roll angle and canard position inputs are buffered with follower amplifiers to prevent loading. The output of the operational amplifier is fed to a dual comparator set at a fixed + and - tolerance. The output of the dual comparator is summed digitally with the other test points. It should be noted that if an equal but opposite error exists in two items, then a launch "go" condition would be indicated. The possibility of this occurring, however, is remote and the added circuit complexity does not warrant modification at this time.

The command/recovery battery check (item 6) uses a single comparator to check for low battery voltage. The comparator output is summed digitally with the other test inputs.

Items 7 through 10 are sampled on the power distribution board and sent to the digital board as a single logic signal input. Items 9, 10, and 11 are simulated when the payloads are not installed.

The circuit used for item 18 is a dual comparator with the high tolerance point (32 VDC) on one of the comparators and the low tolerance point (22 VDC) on the other. A dual operational amplifier is used in the open loop mode to form the comparator circuit. Scaling resistors place the comparator window within the operational limits of the circuit. When the bus voltage is outside of the window, the output changes state, preventing a launch. The lower tolerance point is also used for low voltage destruct and will be discussed later. Power for the circuit is from the aircraft prior to launch and from the battery after launch to make the comparator points independent of the voltage being measured. The two power sources are diode isolated and regulated to 20 volts to operate the circuit.

Further flights in the test program will indicate if and where additional monitoring and quantitative measurements are required.

e. Recovery. The HAST parachute recovery system must be sequenced properly to assure the successful recovery of the HAST vehicle. Most of the recovery circuits are located on the digital logic board. The exceptions, $h_i < 50K$ feet and $Q_c < 150$ psf comparators, shown in Figure 53, are located in the autopilot module. With the thrust off, the target slows in speed and descends in altitude. As the target continues to slow, Q_c is reduced to less than 150 pounds per square foot. At this point the comparator output changes, sending a ready signal to the recovery logic. As target altitude decreases to below 50,000 feet, the $h_i < 50K$-foot comparator sends its ready signal to the recovery logic. When the three recovery parameters are met, a signal is sent to latch the recovery flip/flop.

The radio commanded recovery inhibit circuit, shown in the lower left of Figure 53, must be absent for onboard recovery to be initiated. The $h_i < 50K$-foot signal may occur before the $Q_c < 150$ psf signal in the target altitude is near or below 50,000 feet.
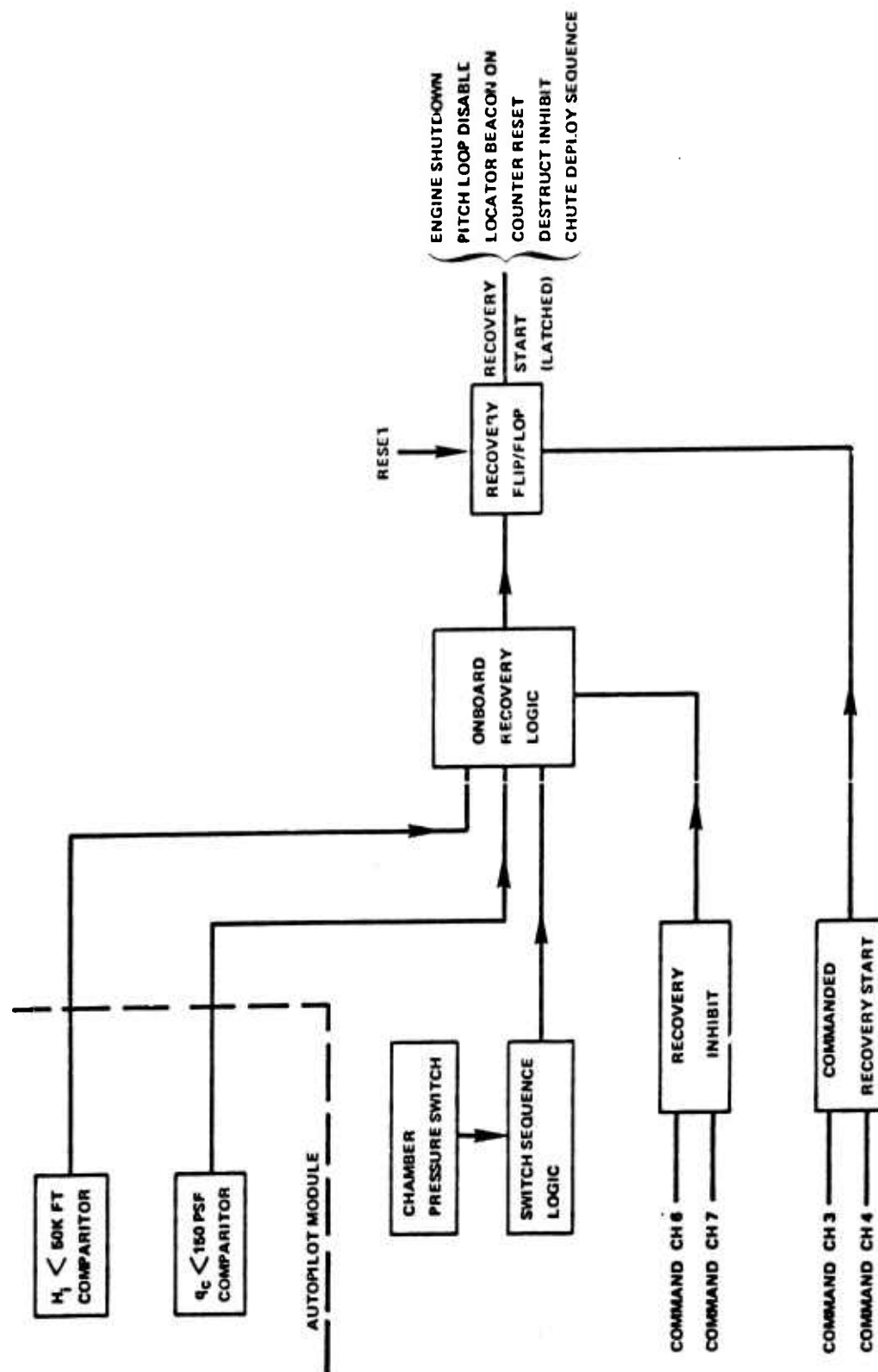
Figure 53. Recovery Logic Block Diagram

110

The radio commands, recovery inhibit and oxidizer throttle valve (OTV) shutdown, are provided to help control the point of recovery start. The OTV shutdown will permit the onboard recovery conditions to be satisfied earlier in the flight if it appears to the controller that the target will overshoot the recovery zone. If the target is short of the recovery zone, the controller can command recovery inhibit and use the target's gliding ability to extend the flight. Radio commanded recovery is provided should the normal onboard recovery function not take place. Some risk is involved, however, due to the possibility of opening the chute at a higher dynamic pressure than it is capable of withstanding. The drogue release command provides a backup to the normal timed drogue release.

After recovery start has been commanded, either by radio command or onboard logic, a sequence of events (shown on the right side of Figure 53) takes place. The recovery sequence times are shown in the time base chart of Figure 54. Engine shutdown, pitch loop disable, locator beacon, destruct inhibit and counter reset occur coincident with recovery start. The engine shutdown (OTV close) command causes the throttle valve to ramp closed in less than one second. The pitch loop disable interrupts all pitch inputs to the servo amplifier and ties them to zero signal which drives the canard to center. The canards are centered at this time while the turbine is still providing sufficient power to operate the canard actuator.
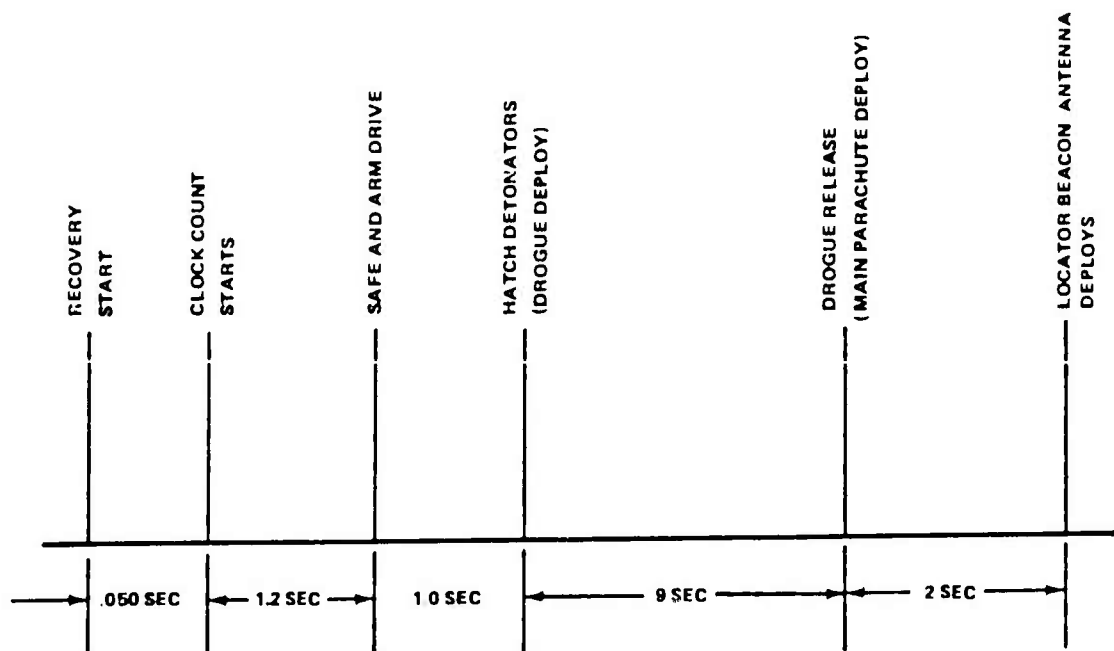
Figure 54. Recovery Time Sequence

Because end of flight, off course, and low voltage destruct mode conditions could exist during recovery the onboard destruct sensing is inhibited with the recovery start signal.

The basic counter (clock), discussed at the beginning of this section, must be reset to zero for recovery sequence timing. Reset is accomplished by the circuits shown in Figure 51, and takes approximately 50 milliseconds before the cou ters begin the recovery timing sequence.

One and two-tenths seconds after the timing begins, safe and arm solenoid drive occurs, arming the shaped charge. Up until this time the safe/arm device has been in the safe condition holding the detonators out of alignment with the transfer lines that run to the hatch removal shaped charge. The 0.2 and 1-second counter outputs are summed for this function. The 0.2 second output is on

111

for 100 milliseconds and is summed with the other recovery times to give 100-millisecond "on" time of the recovery EED's. The 0.2 second time was chosen to allow an additional time for reset transients to settle before beginning the recovery sequence

At one second after the safe/arm solenoid functions (2.2 seconds after counter restart) the S/A detonators fire, firing the shaped charge and removing the recovery parachute hatch. The hatch pulls out the drogue parachute and further reduces target speed. At nine seconds after hatch removal (11.2 seconds after counter restart) the drogue release EED fires releasing the drogue parachute. As the drogue is released the main parachute is deployed in a reefed condition. The main parachute will disreef automatically nine seconds after deployment. The locator beacon antenna EED is fired two seconds after drogue release (13.2 seconds after counter restart).

The locator beacon is least critical to mission success; therefore, beacon antenna deployment is last in the recovery sequence. This prevents a failure in this function from affecting the critical functions. The beacon was turned on at recovery start and is designed to operate continuously without damage into a shorted antenna. The beacon is provided as a means of locating the target during descent if visual sighting is not possible.

5. AUTOPILOT.

The autopilot module provides a point of interfacing for the target flight control sensors and the attitude control actuators. The autopilot module receives attitude and rate information from the gyros, altitude and speed information from the air data module, and programming from the digital logic board. Calculations and scaling operations are performed on the inputs and sent to the two servo amplifiers to drive the canard and aileron actuator. The flight control system is described schematically in the flight control section of this report. The gain and phasing of each stage is contained in that section.

The autopilot module is located in the aft tunnel directly under the OTV assembly. The module is of irregular shape to fit the space available in this area. The internal construction consists of five multilayer printed circuit boards which plug into a double-sided mother board. Interconnections are made through two high density connectors on two of the end multilayer boards. The multilayered "daughter" boards are bolted together and the total assembly encased with a metal cover. The module is structurally rugged and capable of withstanding vibration environments.

For switching and control of the operation performed, analog gate switches are used. Series or loop switching uses P channel J-FETS while grounding requirements are handled by N channel J-FETS. These field effect transistors require little or no power to operate, have low "on" resistance, occupy a small space, and increase system reliability over relay type switches.

a. Turn Programming. Commands for Turn Program Start come to the autopilot module from the digital logic assembly. The "S" turn maneuver is the most difficult and will be discussed in its entirety. Individual turns utilize the same electronics as the "S" turn. Once the turn program has started, turn completion is handled by logic in the autopilot module. A block diagram of the turn program is shown in Figure 55 and may be referred to during the following discussion. When an "S" turn command is received from the digital logic board, it goes immediately to the Turn I Logic. The Turn II Logic is not energized due to a prevent signal from the Turn Complete Logic. The Turn I Logic biases the analog gates "on" which puts the Roll Angle I from the digital board into the roll autopilot and Heading Change I into the heading change comparator. A signal is also sent to the Gyro Control Logic. The Gyro Control Logic removes the gyro yaw pot readout from the autopilot, energizes the gyro torquer on the yaw gimbal and releases the analog gate clamp on the derived yaw integrator. The integrator integrates the torquer current as the target turns and slowly sums to the point where the output is the same as the commanded Heading Change I from the digital board. The heading change comparator then switches the Turn Complete logic. The Turn Complete logic immediately excludes the Turn I Logic which returns the system to a straight and level flight on the new heading. With the gyro control released, the integrator capacitor is discharged to zero to await the next turn.

112
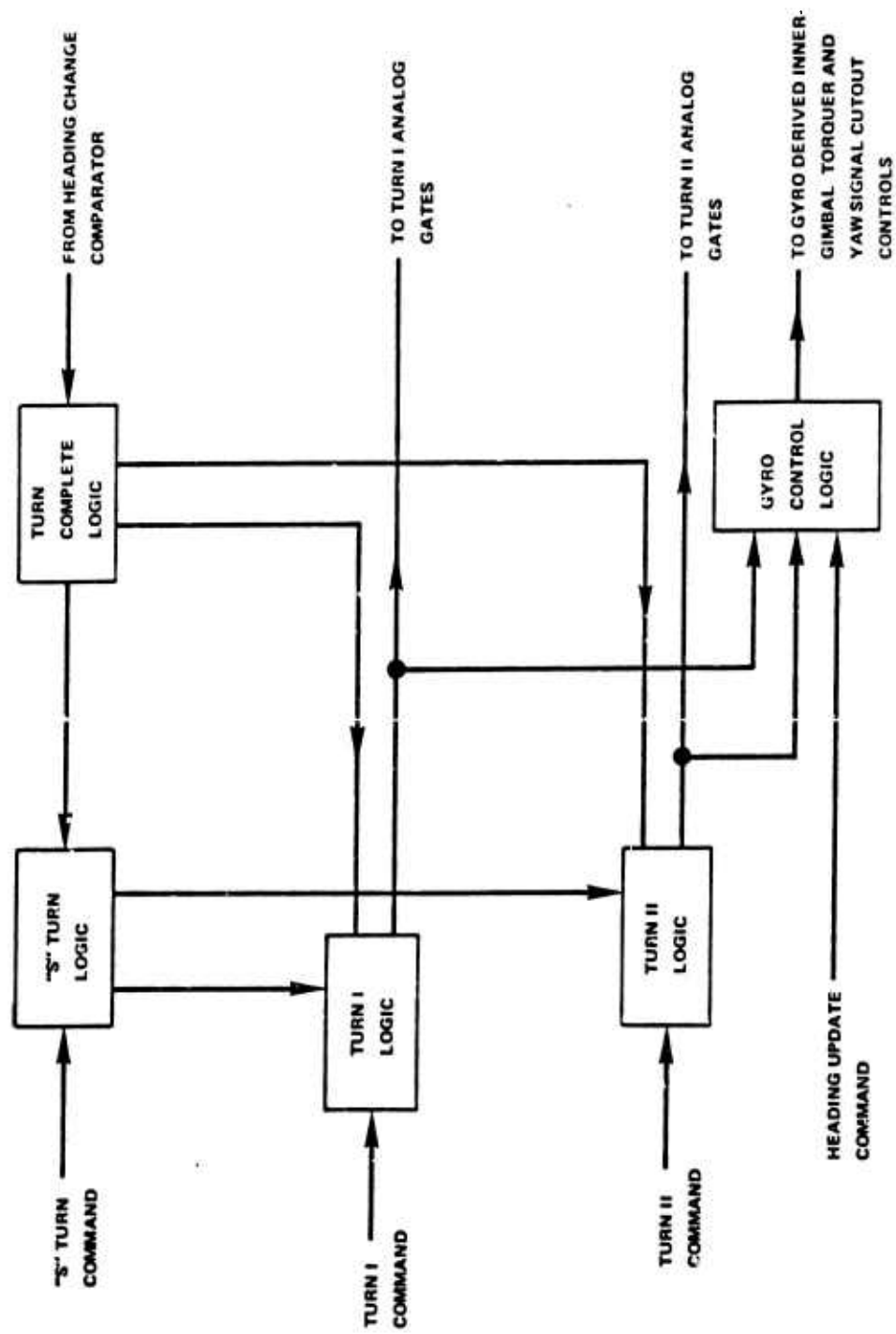
Figure 55. Turn Program Block Diagram

A timer in the Turn Complete Logic waits 100 milliseconds for the Turn I information to clear from the system, then removes the prevent signal which energizes the Turn II Logic. The Turn II Logic re-establishes gyro control as in Turn I and biases the Turn II analog gates "on". This puts the Roll Angle II from the digital board into the roll autopilot and Heading Change II into the heading change comparator. The gyro integrator again integrates the gyro torquer current to a point where the integrator output is the same as the Heading Change II command. Again, the comparator switches the Turn Complete Logic which excludes the Turn II Logic. The gyro controls are returned to the free gyro mode and the target flies straight and level on this new heading completing the "S" turn maneuver. The Turn Complete Logic now has both Turn I and Turn II inputs locked out making it impossible for any repeat of the turn maneuvers. When the turns are programmed separately, Turn II cannot occur until 100 milliseconds after Turn I is complete due to the same lockout from the Turn Complete Logic that occurred during the "S" turn. This is true even if the Turn II programmed time should occur while Turn I is in progress.

The Heading Update Command is shown in the bottom of Figure 55. This command operates the Gyro Control Logic in the same manner as the other turn commands. Again, it is not desirable to use the yaw pot of the gyro while it is being erected on a new heading and therefore the yaw is locked out during the heading update. The turn programs are not latched out by the Turn Complete Logic signals because the heading change comparator does not change state during heading updates. A logic change from a one to a zero and back to a one must take place in order to operate the Turn Complete Logic. This logic sequence takes place only when the Heading Change Commands come into the comparator through the Turn I and Turn II analog gates.

b. Heading Reference Gyro. Target programming and flight stabilization is dependent on the heading reference gyro. An understanding of the electronics incorporated in the gyro unit is essential in order to interface with the digital and autopilot assemblies.

The gyro is powered by a two-phase, 115 VAC motor. The same two-phase power is used to operate the inner and outer gimbal torquers which electrically align the gimbals with the orthogonal axis of the target. Each torquer makes up part of two servo loops within the gyro. The two loops are identical except the inner gimbal torquer is capable of 12 degrees/second and the outer gimbal torquer is capable of three degrees/second. A continuous readout is taken from the gimbal potentiometers. When these pots reflect an out of deadband condition, the electronics are switched on to torque the gimbal back into center and deadband. Control of the servo loops is external to the gyro by the caging and turn control inputs to be discussed.

A transformer coupling is made to the inner gimbal torquer current. This output is scaled, squared and filtered for control of the derived inner gimbal integrator. Since torquing rate is constant, the on time of the torquer current is directly proportional to gyro heading change. The derived inner gimbal integrator sums the on times to give a simulated yaw angle. Control of the integrator and shorting of the integrator capacitor is accomplished using an FET analog gate switch controlled externally.

c. Roll and Yaw Control. The roll and yaw pot readouts come from the heading reference and are processed in the autopilot module as shown in Figure 56. The yaw pot is input to an isolation amplifier to reduce loading and then out through the control switch to the yaw input of the servo amplifier. The control switch opens the line from the yaw pot and grounds the input to the servo amplifier. The control switch is operated from the Turn Control Logic during turns or heading updates as shown in Figure 55. Due to yaw control reversal during negative g maneuvers, the control switch is also operated by the zero or negative g comparator. The filtered normal accelerometer output (Nz) is fed to the comparator for sensing the g condition.

The heading reference gyro roll pot and the roll rate gyro pot are summed together in summing amplifier 1 of Figure 56. The output of this amplifier is passed through an active filter to summing amplifier 2. Summing amplifier 2 combines the filtered sensor signals with the commanded roll angle signal and this signal is fed to the roll servo amplifier. The roll commands for Roll Angle I, Roll Angle II or Heading Update are summed in a short time integrator with a 1.1-second time constant.
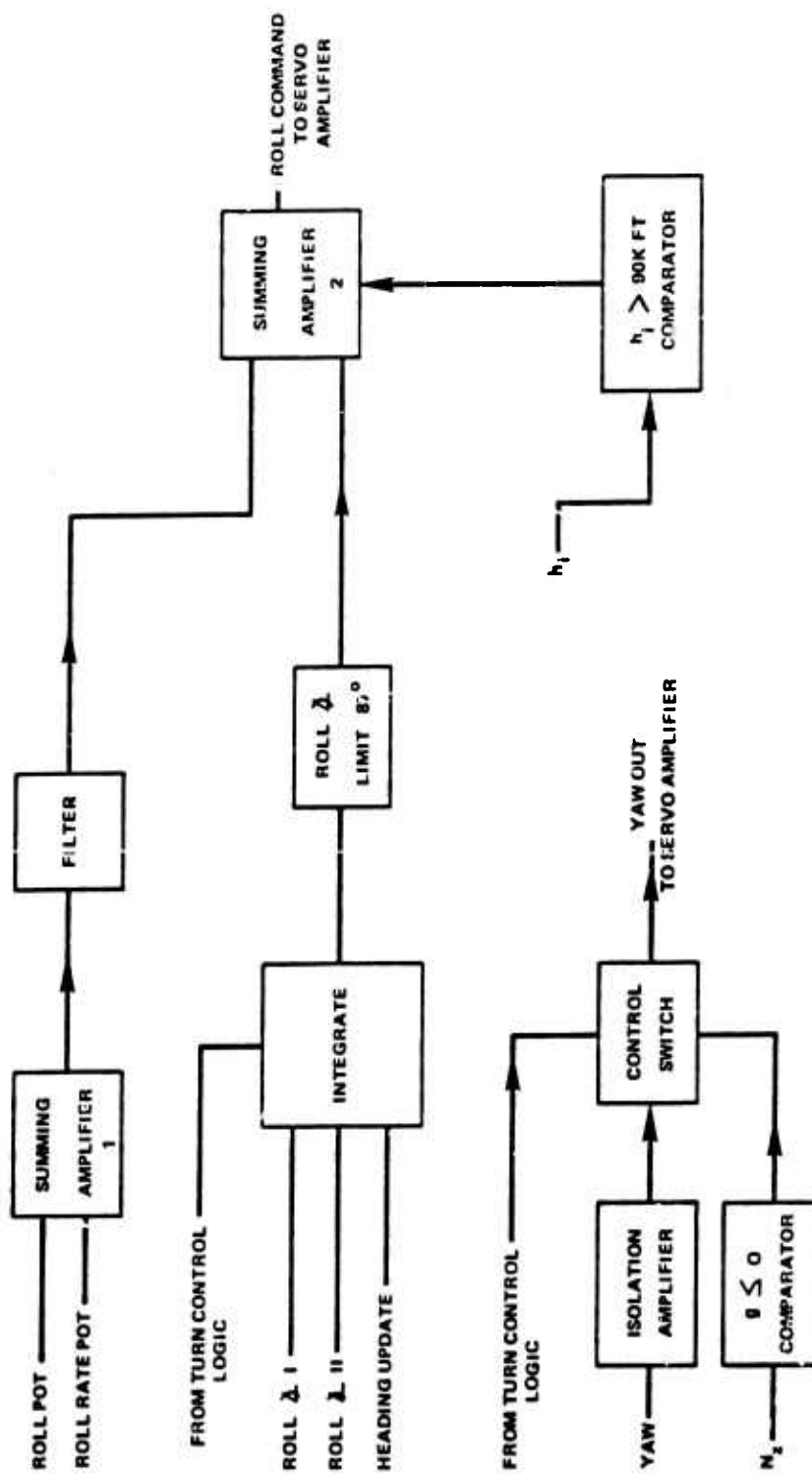
Figure 56. Roll Yaw Control Block Diagram

115

This integrating input is provided to smooth out the control changes. The integrator is shorted when not in use by the use of a FET switch which is controlled from the turn controls shown in Figure 55. The output of the command amplifier passes through the roll limit amplifier to summing amplifier 2. The commanded roll angle is limited to 87 degrees to keep the target in the active control span of the roll pot on the gyro. The roll gain must be greater for flights above 90,000 feet. Figure 56 shows h_i from the air data module fed to a comparator. The $h_i > 90K$-foot comparator switches a FET analog gate to change the gain of the summing amplifier 2.

d. Climb and Cruise Control. Climb and cruise programming and control comprise the largest portion of the autopilot module. The complexity of this part of the system is shown in Figure 57. The h_i and M_i inputs are instantaneous altitude and Mach number readouts from the Air data module. Commanded cruise altitude (h_c), commanded cruise Mach number (M_c 0.5M fast, 0.5M slow, 5K up and 5K down commands are all inputs from the digital logic assembly.

The purpose of the climb programmer is to produce the most efficient launch to cruise altitude transition. Following through Figure 57, the instantaneous altitude and Mach come into identical track and hold circuits. At two seconds after launch the track and hold circuits memorize the h_i and M_i signals and their outputs then become h_L and M_L denoting the launch condition values. The h_c and h_L signals are then summed algebraically and sent to the multiplier. The other input to the multiplier is the output of the function module.

The function module receives two inputs. One input is the algebraic sum of M_c-M_L and the other is M_c-M_i from the Mach command summing amplifier. The output of the function module to the multiplier is $10 \left(\frac{M_c - M_i}{M_c - M_L} \right)^2$. The output of the multiplier is then 1/10 of this term times (h_c·h_i) and is referred to as Δh^*. The Δh^*, h_c and h_i signals are then summed algebraically in the altitude summing amplifier and sent to the Δh input of the servo amplifier through the Δh command summing amplifier. When the difference between M_c and M_L is less than 0.1 M, the M_c-M_L comparator shown in Figure 57 removes the term (M_L·M_i) from the function module which follows through to make Δh^* zero. This makes the canard control a step function of the difference between h_c and h_i. The Δh signal also goes to a differentiator to produce altitude rate (Δh). The Δh signal feeds into a gain resistor on the input of the canard servo amplifier.

The Mach command summing amplifier (M_c-M_i) also feeds the ΔM comparator and latch circuit and the OTV throttle command circuit (T_c). When M_i comes to within 0.01 M of M_c during a climb, the ΔM comparator changes state and latches. This switches out Δh^*, removes the boost discrete signal from the OTV and removes the shunt from the ΔM integrator. With the boost discrete removed, the OTV now accepts the T_c command for control. The $\Delta M + \int \Delta M$ circuit is a dual gain type where ΔM has one gain and the integral of ΔM has another. Instead of allowing conditions where the integrator has to come out of deep saturation the integral of ΔM signal is limited so that any change of the ΔM causes an immediate change in the composite signal. This is helpful in ground checkout because a saturated condition will probably never exist in flight. The composite T_c signal is also limited to ±10 volts to protect the OTV input. With Δh^* removed from the altitude summing amplifier, the target flies on the Δh signal of (h_c·h_i) and is dampened by Δh. The Δh and Δh inputs to the canard servo amplifier are grounded until the two-second pitch loop enable signal is received. Again, at recovery initiate, all inputs to the canard servo amplifier are grounded. This ensures the target does not pull up into the launch aircraft and streamlines the canards for helicopter retrieval. The Δh signal is switched out during g maneuvers which will be discussed later.

During event programming other signals enter the cruise circuits. A 0.5M fast or 0.5M slow command is entered into the Mach command summing amplifier to bias the ΔM to a new operating point. When either signal is entered first, the other may be entered later to return the target to the original cruise Mach number. An altitude change generator is also shown in Figure 57 with the 5K-foot up and 5K-foot down commands as inputs. The output of this circuit is sent to the Δh command summing amplifier to bias the Δh signal to a new altitude operating point. When either an up or down command is received, the altitude change generator ramp biases Δh in the proper direction. The circuit is arranged so that whichever command is received first, the alternate command will return the target to the original cruise altitude.

116
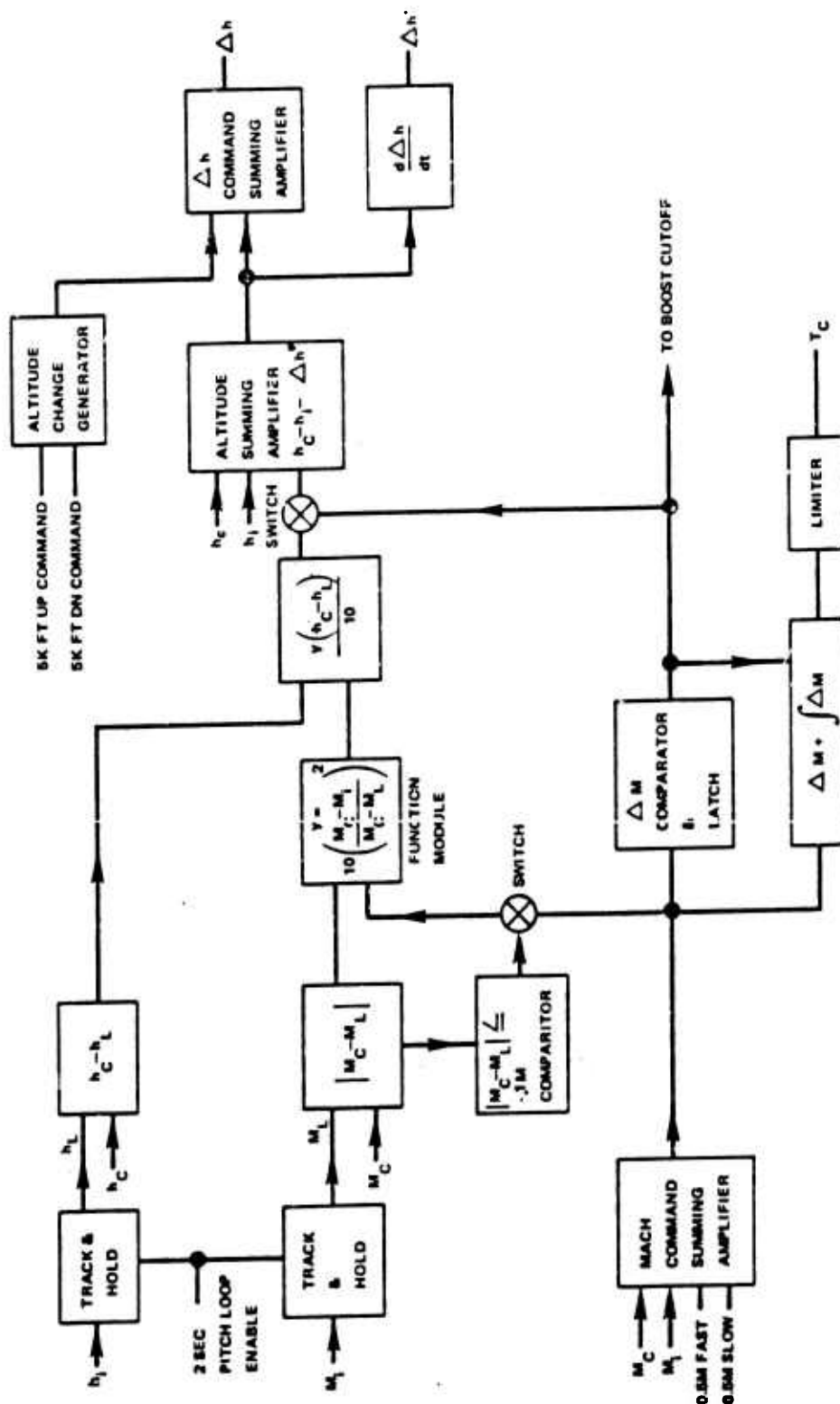
Figure 57. Climb and Cruise Control Block Diagram

117

e. **G Maneuver Control.** Another circuit designed into the pitch loop programming is for g maneuvers. The g maneuver control block diagram is shown in Figure 58. A g up or g down level is selected by rotating switches SW 12 or SW 11 on the digital logic board. The g command start is selected by moving SW 8 (Event I) or SW 7 (Event II) program select switches.

Until event selected time occurs, a FET gate clamp is placed on the capacitor of the integrator and bleed-off amplifier as shown in Figure 58. When G Command Start occurs, the clamp on the amplifier is removed along with the clamp on the pitch rate integrator. The Δh signal to the servo amplifier is also opened. The difference between the g level command and the normal accelerometer (N_z), summed in the command summing amplifier, passes onto the canard servo amplifier at the one-second time constant rate of the integrator. The canard angle ramps with the integrator to start a pull-up or push-over attitude change. As the target attitude changes, the pitch rate integrator sums the pitch rate gyro output. The output of the pitch rate integrator feeds an absolute value circuit whose output is always positive regardless of angle change polarity. This circuit provides the input to a comparator which is set to switch at a 30-degree pitch angle change. The comparator output opens the switch from the command summing amplifier and also operates a FET switch. When energized, this switch bleeds off the charge on the integrator comparator over a 5.1-second period. The target then returns to straight and level flight. The Δh signal stays out of the circuit after maneuver completion because the altitude change that takes place can be large and variable.

6. DESTRUCT SYSTEM

The purpose of the destruct system is to render the vehicle aerodynamically unstable should any deviation from the desired flight path occur or vehicle condition that might render the vehicle uncontrollable. Destruct system circuits are contained on the digital logic board which collects information from various destruct sources and sends it to the destruct EED relay. The EED relay energizes, sending the firing voltage to the destruct EED. The firing of the destruct EED removes a pin from the spring loaded aileron bellcrank. The spring action forces the ailerons to a hard roll condition. The vehicle then goes unstable and spins to impact.

Destruct can be initiated either by radio command or by several target internal and external conditions. These conditions are jettison from the launch aircraft, end of flight timer, low main bus voltage, loss of command receiver guard tone and target off-course by more than 10 degrees for 30 seconds.

a. **Destruct Arming.** Destruct arming must take place before any of the destruct functions can occur. The destruct arming block diagram is shown in Figure 59. Vehicle separation at launch removes the target lanyard pin which starts the auxiliary 10-second timer. The 10-second timer is typical of some of the timers used on the digital logic board. It consists of a transistor which holds a capacitor shorted until the timing function is to occur. The transistor opens and the capacitor begins to charge. This voltage is fed into an operational amplifier used in an open loop mode as a comparator. The other input of the operational amplifier is the comparator point. As the capacitor charges up to the comparator point, the output of the operational amplifier changes state, showing that the timing function has taken place. Either the output of the 10-second auxiliary timer, or the 10-second count from the decade counters on the main clock, will latch the arming flip/flop.

After latch, whatever happens to the input is of no consequence. Latching the flip/flop provides a signal to turn on the switch powering EED relays for destruct and recovery systems. The 10-second delay allows a safe separation between the launch aircraft and the target. The main timer and destruct back-up timer are provided in a redundant system to assure destruct arming takes place. The arming latch is reset by the flip/flop reset circuit shown in Figure 59.

b. **Radio Command Destruct.** The radio command destruct circuit is shown as part of the destruct command circuits in Figure 60. The radio command is the most simple and direct route to initiate target destruct. Two channels (CH 1 and CH 2) are reserved for the command destruct function. In order to guard against operation from spurious signals, the two channels are not common to any other function. If vehicle destruct becomes necessary, the two channels are sent simultaneously and summed in the radio command circuit as shown in Figure 60. Output of the
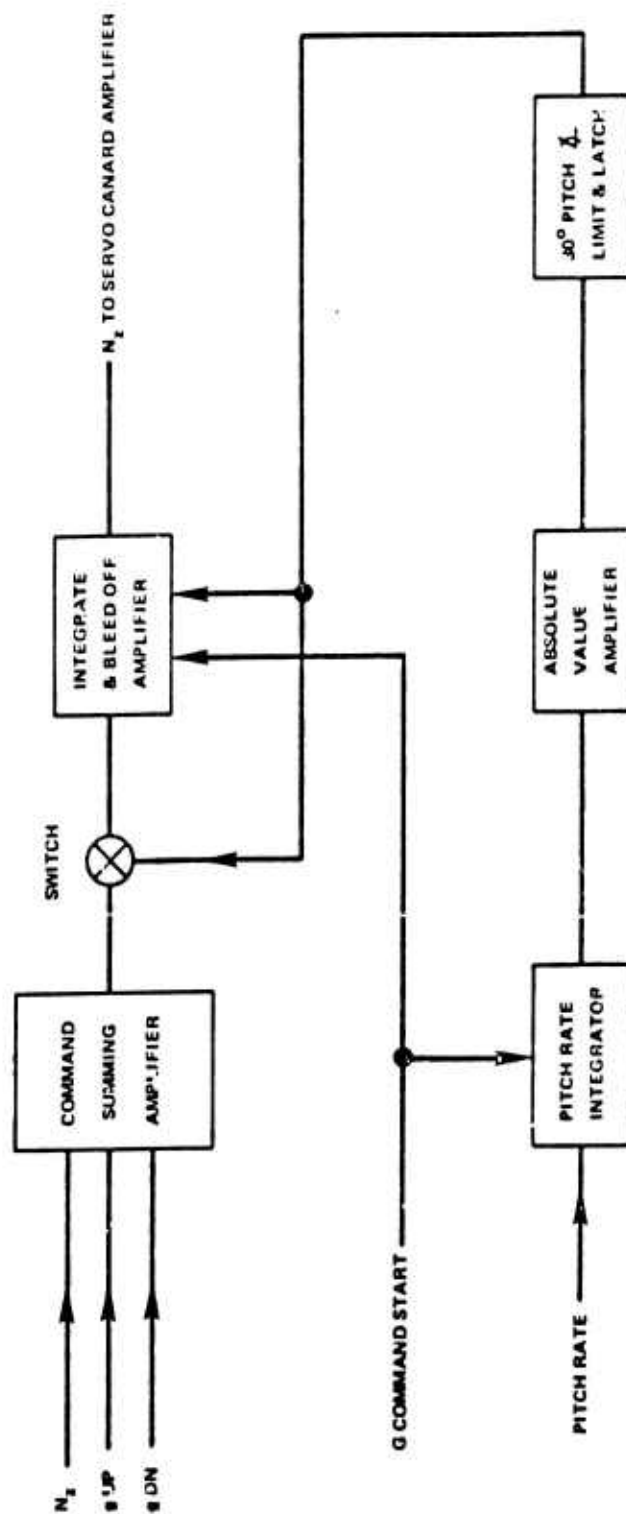
Figure 58. G Maneuver Control Block Diagram

119
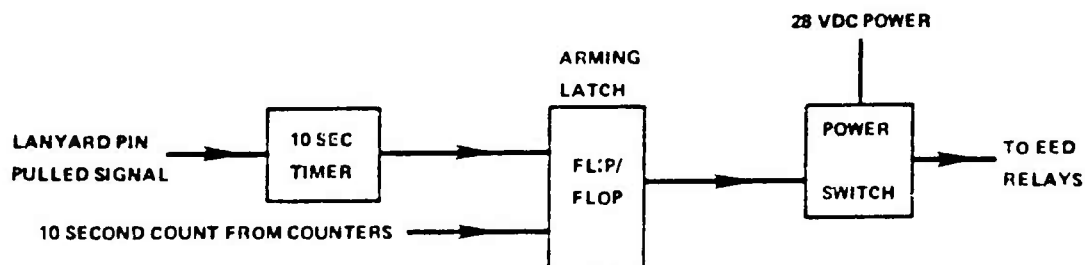
Figure 59. Destruct/Recovery Arming

radio command circuit is used to latch the destruct flip/flop. The output of the latched flip/flop drives the power switch which grounds the destruct relay and fires the destruct EED.
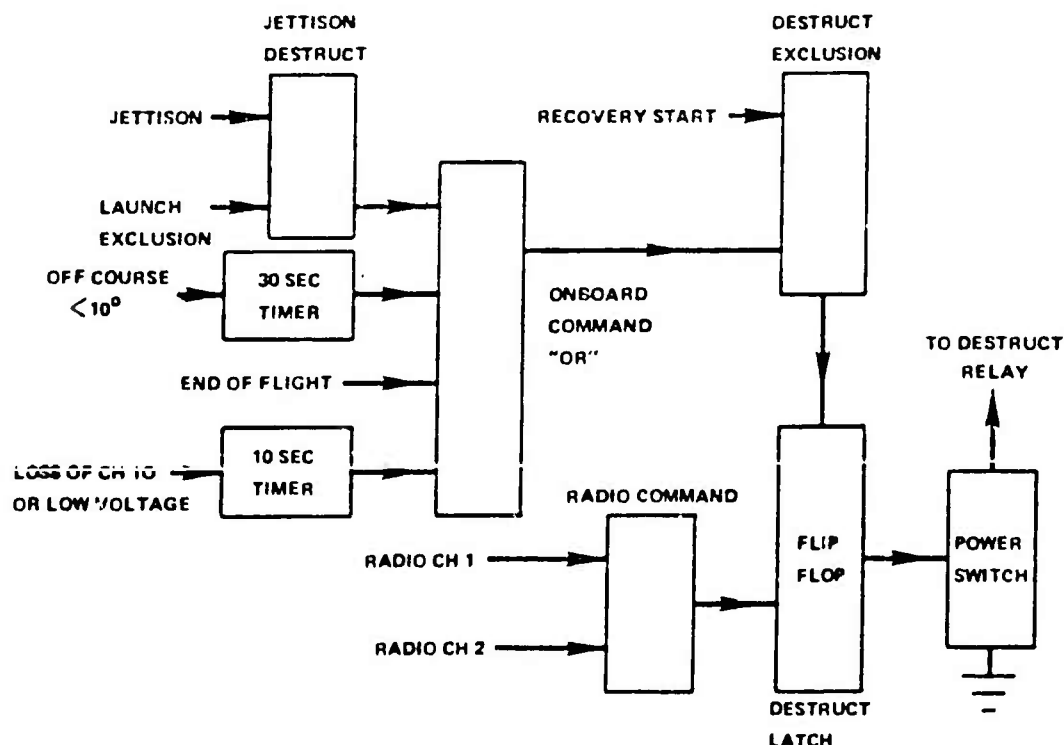
Figure 60. Destruct Circuit Block Diagram

c. Jettison Destruct. In case of a launch aircraft emergency it may become necessary to jettison the target. Since a fully fueled target cannot be recovered, and jettison could occur on an unknown heading, destruct must be initiated. Figure 60 shows the path of the jettison signal to cause destruct. The jettison signal is always present if launch command has not been initiated. Launch command will exclude the jettison signal from passing through to the onboard destruct command "OR" circuit. In a jettison situation the jettison signal passes through the "OR" and destruct exclusion circuits to set and latch the destruct flip/flop.

The destruct flip/flop is held in reset by the flip/flop reset circuit of Figure 51 until launch separation which occurs after launch command. The SELECT switch on the missile control panel

120

should be placed in the SELECT position prior to jettison to assure proper time out of the 10-second arming delay.

    d.   Loss of Command Receiver Guard Tone. Channel 10 of the command receiver is monitored to show the receiver is receiving the ground transmitter carrier. The channel is used instead of monitoring receiver AGC because AGC voltage can be at a minimum and still have sufficient signal strength to provide command control. As long as the CH 10 tone is locked in, the communication link is adequate for control. Destruct takes place if there is a CH 10 loss or the receiver becomes inoperative for greater than 10 seconds.

    The 10-second timer used to time CH 10 loss is shared with the low bus voltage input as shown in Figure 60. The figure also shows the output of the 10-second timer inputs to the onboard command "OR" circuit. From there it takes the same path as described in the jettison destruct paragraph. The timer is the same type as discussed in the destruct arming paragraph.

    e.   Low Voltage Destruct. Failure of the DPU alternator, regulator, diode pack or a short in the system would result in a power loss and possibly an unstable flight outside the range boundary.

    Main bus voltage is monitored as described in the prelaunch self-test circuit. The low level sensing side of the dual comparator circuit is used for the low voltage sensing. Output of the comparator feeds the same 10-second timer as the loss of guard tone circuit which is shown in Figure 60. If either the guard tone loss or low voltage lasts for 10 seconds (or any combination thereof) destruct will be initiated through the same path as described in the jettison destruct paragraph. Intermittent or permanent return to the 21 VDC level will reset the timer requiring another full 10-second off period for destruct to occur.

    f.   Off-Course Destruct. The off-course destruct circuit monitors the deviation from the desired flight path. A preset limit of ±10 degrees is set into the monitor. Any deviation outside of the ±10-degree corridor will start a 30-second time delay as shown in Figure 60. At the end of 30 seconds the timer will enable the destruct circuit as described in the jettison destruct paragraph. Automatic reset takes place when the off-course error is reduced to less than 10 degrees. When the gyro torquers are called in during a preprogrammed or a radio commanded (heading update) turn, the off-course timing does not start. This is because the torquing rate is always faster than the turn rate of the target so that the maximum off-course signal is two degrees.

    The circuit used in the off-course sensing is a dual operational amplifier used as a comparator. One operational amplifier is used for the left off-course comparator point and the other for the right off-course comparator point. The comparator is powered by the ±15 VDC MOPS output. Comparator outputs are fed to a common gate which starts a 30-second time delay. This time delay is similar to that described in the discussion on destruct arming.

    g.   End of Flight Destruct. The end of flight destruct function is a selectable elapsed time counted from launch. The time is selectable by setting up switches SW 5 and SW 6 as described in Flight Programming, paragraph 1, the end of flight destruct may be omitted by selecting the no event position on the switches. The path taken by the end of flight destruct signal is similar to those already discussed and is shown as part of Figure 60.

    All of the onboard commanded destruct functions (jettison, loss of guard tone, low voltage, off-course and end of flight time) pass through the destruct exclusion circuit as shown in Figure 60. Recovery initiation prevents these onboard destruct functions from latching the destruct flip/flop. The radio command destruct remains at all times in case of parachute destruct or other system malfunctions.

7. RANGE COMPATIBILITY EQUIPMENT

    Communication with the target during powered flight and recovery is essential for a successful flight test. The range compatibility equipment provides the communication. Originally, the Integrated Target Control System (ICTS) was to perform this function, but it has been delayed pending the availability of a compatible configuration. In the absence of the ITCS, equipment is

provided to be compatible with existing range ground equipment. A diagram of the target/ground interface links is shown in Figure 61; the telemetry system is discussed later in this section of the report.

The FPS-16 range radar and the FRW-2 command transmitter are presently installed on the test range. The FPS-16 radar is used to track the target during flight and to direct the MARS equipped helicopter to the target after recovery. Parameters which can be obtained from the radar are speed, altitude, position and climb or descent rates.

a. Transponder. A Vega 302C-2 C-band transponder is installed in the target to increase the tracking ability of the FPS-16 radar. The transponder provides a minimum pulsed power of 400 watts. The double pulse input spacing is adjustable to the specific range requirements and the transmitter and receiver are tunable between 5400 and 5900 MHz.

b. Command Receiver. The FRW-2 command transmitter is used to transmit control commands for destruct, heading update, recovery and flight programming. A command receiver/decoder is installed in the vehicle to receive and process these signals. The receiver/decoder receives and decodes IRIG Channels 1 through 10. The individual channel assignments are shown in Table XXIX. Receiver sensitivity is 2 u V minimum for active control operation. The receiver is squelched to reduce interference.

Antenna isolation was studied to minimize interference between all radio frequency (RF) emitting devices (including payloads) and to ensure an RF compatible system. Bandwidths of separation and power indicated the telemetry transmitter should be moved as high in S-band as practical. A telemetry frequency assignment was obtained as recommended. The specific frequency assignments for the command receiver/decoder and C-band transponder were obtained from the Air Force.

8. HAST ANTENNA SYSTEMS

Antenna systems on the HAST vehicle consist of the C-band transponder antenna system, the telemetry antenna system, the command receiver antenna system, and the locator beacon antenna system. These antennas are designed and manufactured by the contractor with the exception of the locator beacon antenna. All of the vehicle antennas are either flush mounted or low silhouette types with the exception of the locator beacon antenna which is extended when in use. Antenna placement and description for the payload are delineated in the augmentation and scoring section of this report.

a. Transponder. The transponder antenna consists of a half-circular cavity backed, slot decoupled, center fed half-wave dipole radiator and a curved dome radome which protrudes through the skin of the vehicle. Four of these antennas equally phased and connected through a four-way power divider are used in this antenna system to provide nearly spherical coverage. The antennas are mounted at station 37.35 and as near equally spaced as internally mounted components will allow.

b. Telemetry. The telemetry antenna consists of a curved cavity backed T-bar fed slot radiator and a curved radome which is mounted flush with the skin of the vehicle. Four of these antennas equally phased and connected through a four-way power divider are used in this antenna system to provide nearly spherical coverage. The antennas are mounted at station 39.10 and as near equally spaced as internally mounted components will allow.

c. Command Receiver. The command receiver antenna is a scaled version of the AT-134/ARN flush mounted marker beacon antenna. The radiator is thicker to provide more heat sink for the hot flights. It consists of a curved rectangular cavity, a curved radiator that runs almost the full length of the cavity, a temperature compensated trimmer capacitor and a curved radome which mounts flush with the skin of the vehicle. Three of these antennas arranged as follows are used in this system:

TM READOUT

MISSLE PARAMETERS
TEMPEI ATURES
PRESSURES
ATTITUDE
COMMAND VERIFICATION

TELEMETRY
RECEIVING &
RECORDING

COMMAND
FUNCTIONS

FRW 2

COMMAND TRANSMITTER

TRACKING
& RANGING

FPS 16

RANGE RADAR
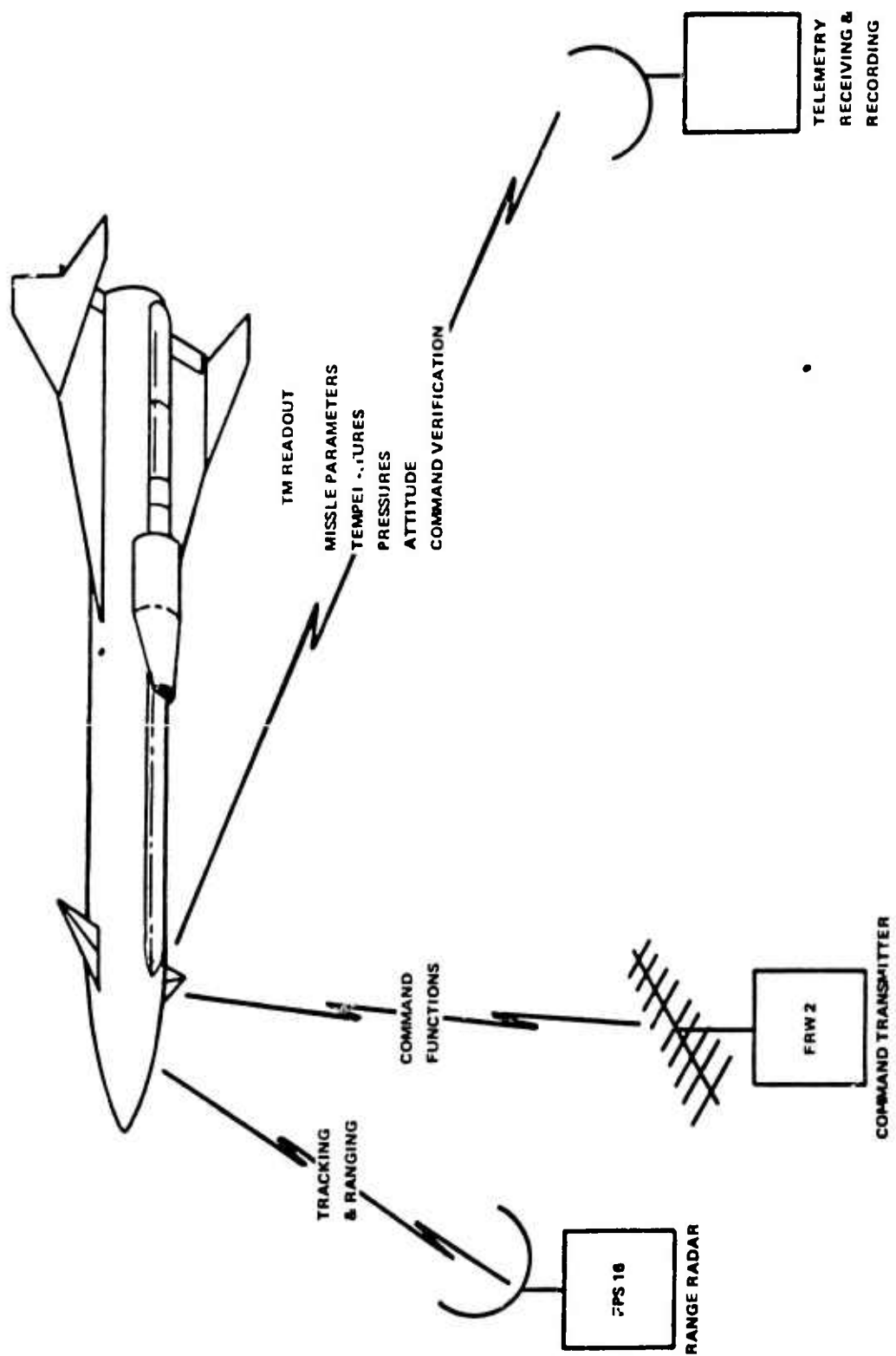
Figure 61. Range Compatability Equipment

(1) One mounted on the tunnel at station 38.50.

(2) One mounted on the right top approximately 122° from the tunnel antenna at station 37.35.

(3) One mounted on the left top approximately 122° from the tunnel antenna at station 37.35.

These antennas are connected to a three-way resistive power divider with the left antenna 180° out of phase with the other two antennas. Initial testing on this system indicated that it provided adequate angular coverage. However, later tests indicated that there was as much as 20 to 30 degrees differential phase shift through the power divider. Therefore, a new hybrid power divider which provides less loss and one degree phase balance was chosen. Initial testing on a prototype system using the new power divider was accomplished. These tests showed that if the flight profile is such that the vehicle is never pointed at the ground station, the prototype system provides adequate coverage. However, a firm flight profile for the long flights has not been established; therefore, this system has not been incorporated into the HAST vehicle. The new system uses the same antennas and cables as the old system except that the location of the top left and right antennas are exchanged with their feeds oriented toward the horizontal centerline of the vehicle and the top right antenna is 180 degrees out of phase with the other two antennas.

d. Locator Beacon. The locator beacon antenna assembly consists of a purchased part and an aluminum cover for this part which also provides mounting for an RF connector. The purchased part consists of a machined polycarbonate block, a helical wound spring and tip piece, a shear pin, a knife and an explosive actuator. The outside coil of the spring is mounted to the inside of the machined block. When the spring is compressed and the shear pin inserted, the antenna can be extended by applying an electrical signal to the explosive actuator. The antenna is mounted at station 41.00 with the tip piece flush with the skin.

9. HAST TELEMETRY

The purpose of the HAST telemetry system is to sample, encode, and transmit to a remote receiving station, the data relevant to the performance of the test vehicle. It will also accept and transmit scoring data from the vector miss distance indicator scoring system.

The type of telemetry system used is a combination of continuous channels on separate subcarrier frequencies and a pulse amplitude modulated (PAM) return to zero (RZ) format for multiplexed information. Data frequency modulates a 5-watt, S-band transmitter at a base frequency of 2267.5 MHz. The telemetry system is divided into the following components:

- Antennas
- Transmitter
- Multiplexers

- Voltage Controlled Oscillators
- Signal Conditioning Circuits
- Sensing Devices

  (1) Temperature

  (2) Pressure

  (3) Strain

  (4) Acceleration

  (5) Vibration

The telemetry system for flight test vehicles is in two basic configurations: (1) For those vehicles whose primary purpose is flight dynamics and vehicle performance, and (2) for those vehicles which contain scoring systems.

124

Configuration (1) is a modularized package which permits changing or deletion of test parameters depending on the flight schedule or program progress and has a capability of up to 186 channels of data. A maximum of 149 channels is now planned to be used on any one flight based on the present flight schedule. The signal conditioning components are mounted on small single or double sided printed circuits which plug into an 8-layer master circuit board. Required changes can, therefore, be made on the small boards without affecting the master circuitry. Additions or deletions of parameters can be accomplished by the addition or deletion of the small signal conditioning boards. The design utilizes two multiplexers, one with high level inputs (0-5 VDC) and one with a combination of high level and low level inputs (0-50 MVDC). Low level signals are primarily for thermocouple measurements.

Due to space limitations imposed by addition of the VMDI scoring system, the telemetry of configuration (2) is greatly reduced. It is composed of one 45 x 20 multiplexer and microminiature voltage controlled oscillators. Scoring data is presented on a 450 KHz subcarrier frequency. This subcarrier frequency was necessary to process the 50 KHz bit rate data from the scoring encoder.

The telemetry antennas used on HAST are a flush mounted 4-antenna array with two antennas mounted on the upper half and two mounted on the lower half of the forward section of the vehicle to provide uninterrupted transmission in all vehicle attitudes.

Block diagrams of the systems are shown in Figures 62 and 63.
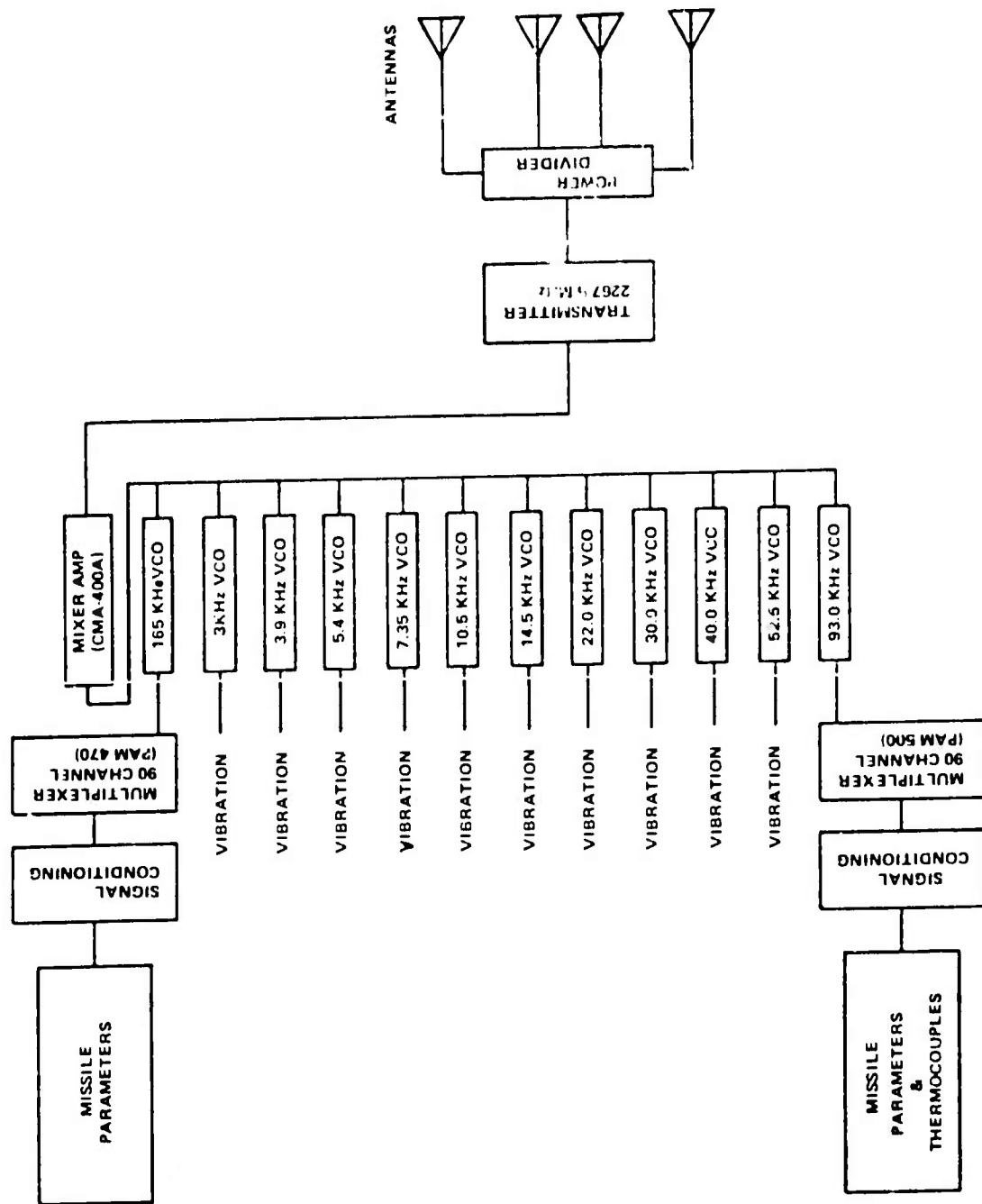
Figure 62. HAST Telemetry System, Configuration 1

126
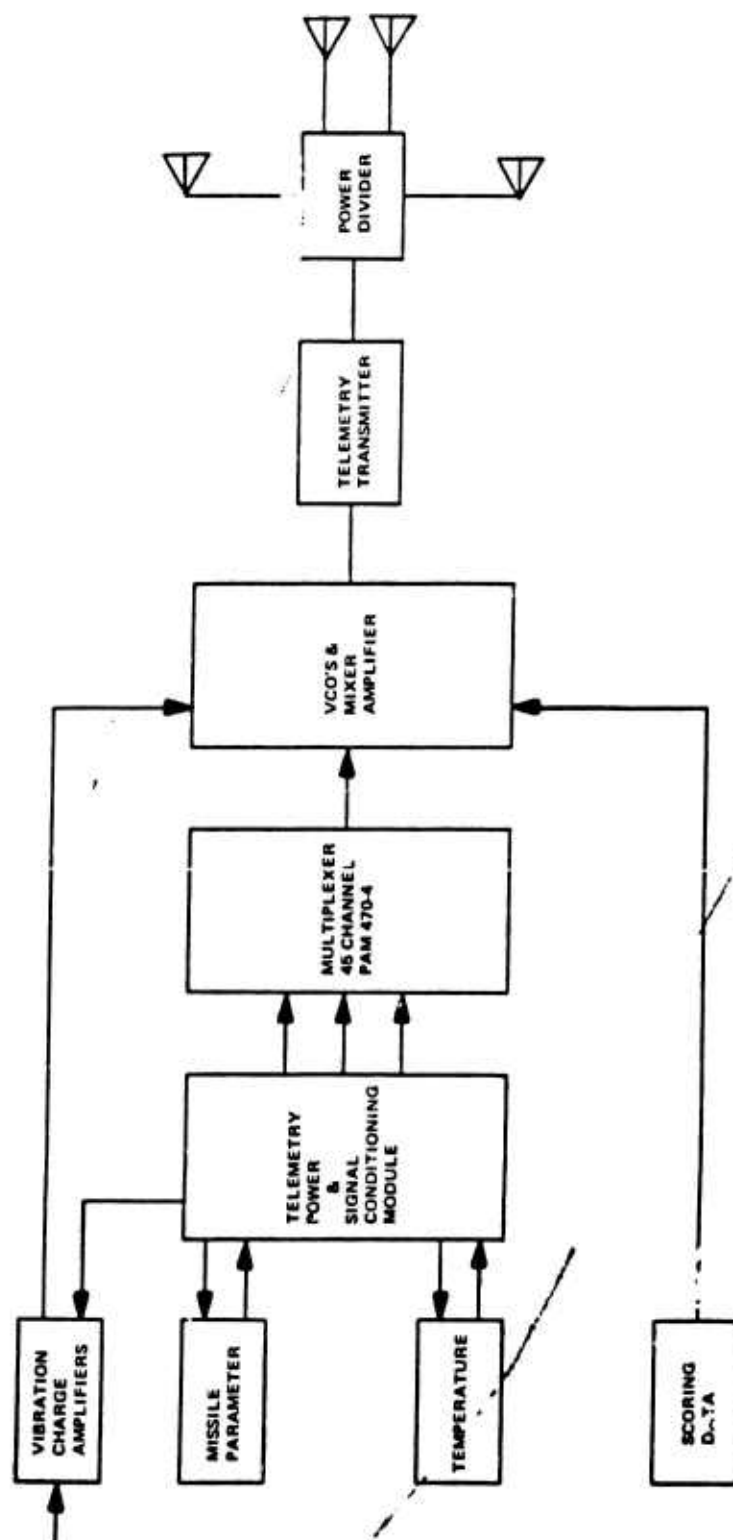
Figure 63. HAST Telemetry System, Configuration 2

127

SECTION VIII

AUGMENTATION AND SCORING SYSTEM INTEGRATION

The development of the radar augmentation system (RAS) and the vector miss distance indicator scoring system (VMDI) has been contracted to the Government Electronics Division of Motorola, Ind., and the infrared system to Ordnance Research Incorporated of Ft. Walton Beach, Florida. These are prime contracts and the technical work performed under those contracts is not covered in this technical report. It is the responsibility of Beech Aircraft Corporation, however, tc integrate these systems into the HAST vehicle and this effort is covered herein. The contractors have maintained coordination through a series of monthly meetings and formal exchange of data during the development phase. Coordination with respect to electrical and mechanical interfaces and acceptance test procedures has been accomplished. These augmentation and scoring systems have been referred to as payload since their function is not essential to target flight operation.

The payload has been developed in a modular configuration which will allow minimal time required for installation and removal. The main electronic package for both the RAS and VMDI systems is housed in a modular package forward of station 35.0. The remaining subsystem items such as antennas, inter-connecting components and cabling are mechanically installed aft of station 35.0 throughout the HAST vehicle. The total package has been designed to facilitate installation and removal so that field configuration can be maintained.

General arrangement of RAS/VMDI systems is illustrated in Figure 64. The payload systems are listed below in three phases of installation and test:

- Radar Augmentation System (RAS)

- Scoring System (VMDI)

- Checkout and Analysis

1. RADAR AUGMENTATION

The radar return augmentation system, an active system, is designed to fulfill reflectivity requirements and to be compatible and integrate electrically and mechanically into the HAST vehicle. Three basic subsystems make up the total RAS system:

- Electronic Module, Forward Package

- Antenna System

- Interconnecting Components and Cables System

a. The main electronic package located in the nose cone of the HAST vehicle is designed on a modular basis, which will allow rapid installation or removal for field configuration. Two integral parts of the payload module forward of vehicle station 35.0 combine to form this total electronic package. This module consists of the following:

- Electronic Chassis Assembly

- Radome

(1) The electronic chassis, a brazed aluminum frame, houses the electronic components and also interfaces with the HAST vehicle at station 35.0. It becomes an integral part of the fuselage structure. The chassis is cantilevered at station 35.0 with four mounting lugs which are a part of the HAST forward fuselage. All components pertinent to RAS/VMDI systems are mounted directly to th chassis. Figure 65 illustrates this configuration.

128
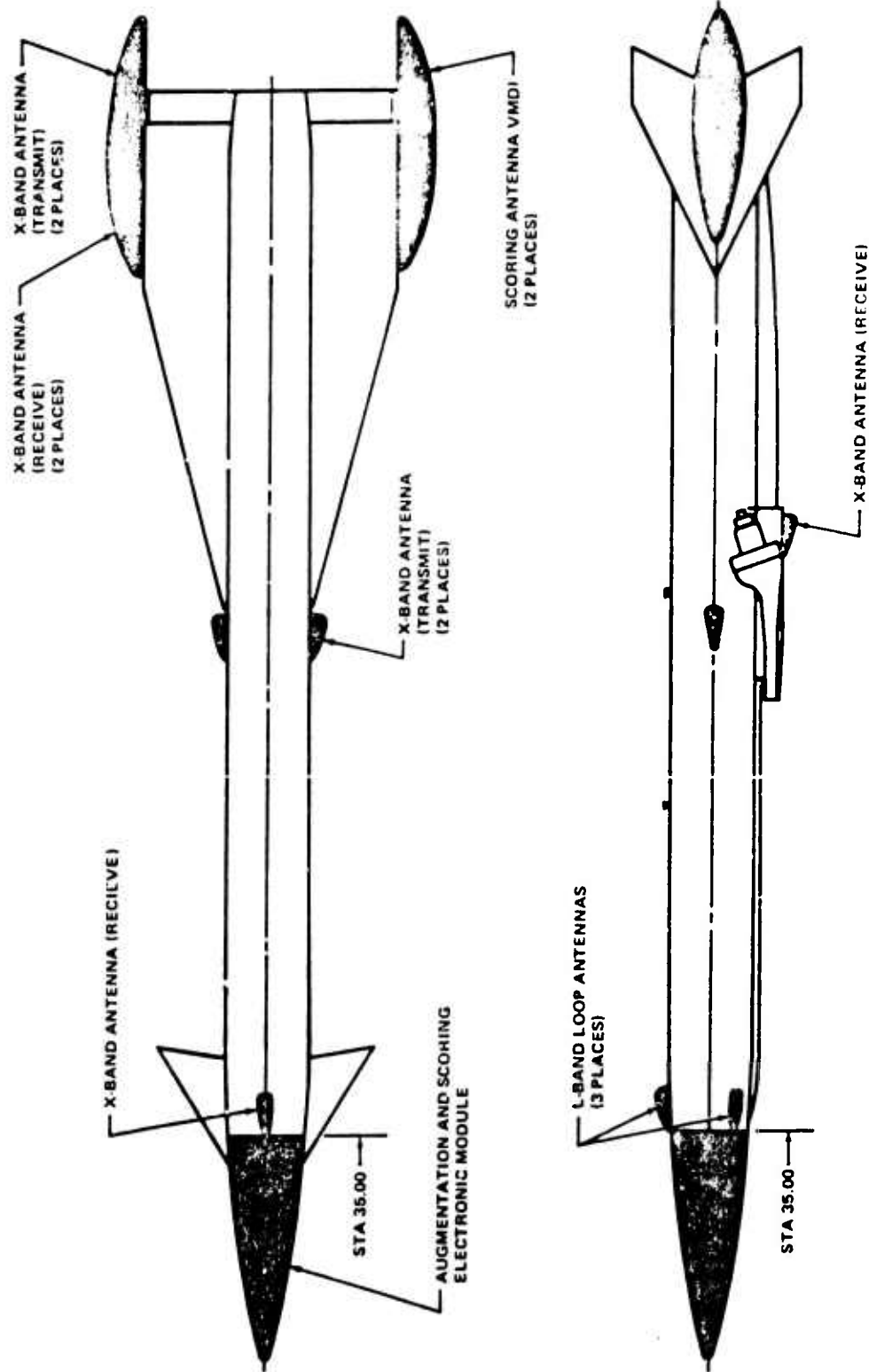
Figure 64. General Arrangement RAS and VMDI Systems

X-BAND ANTENNA (RECEIVE) (2 PLACES)

X-BAND ANTENNA (TRANSMIT) (2 PLACES)

SCORING ANTENNA (VMDI) (2 PLACES)

X-BAND ANTENNA (TRANSMIT) (2 PLACES)

X-BAND ANTENNA (RECEIVE)

AUGMENTATION AND SCORING ELECTRONIC MODULE

STA 35.00

X-BAND ANTENNA (RECEIVE)

L-BAND LOOP ANTENNAS (3 PLACES)

STA 35.00

129
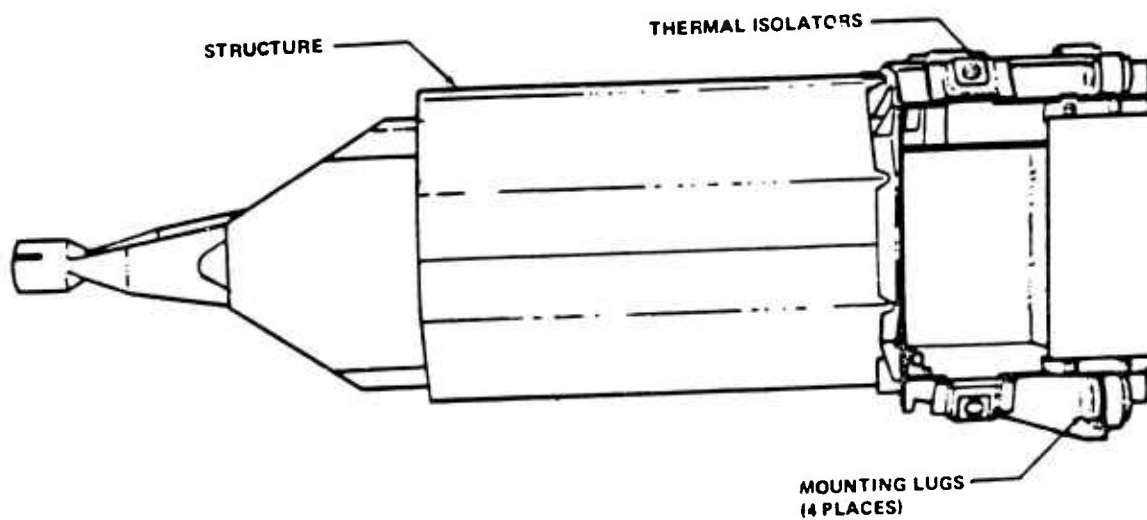
Figure 65. Payload Forward Chassis
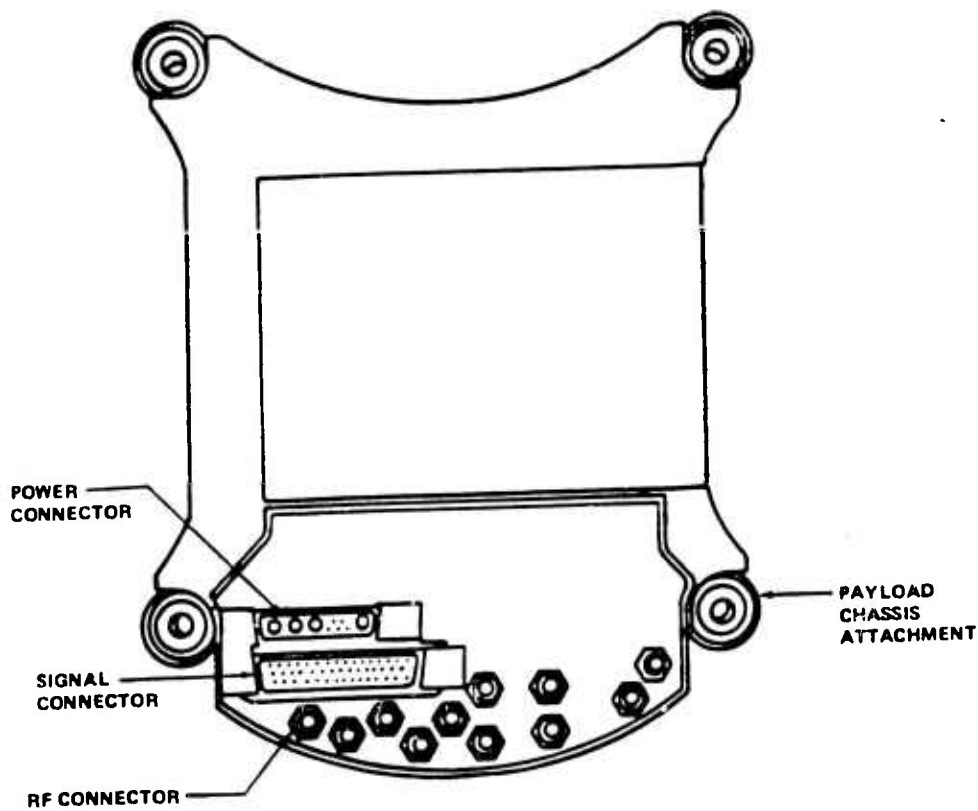
Figure 66. Payload Chassis Attachment and Electrical Disconnect

130

(2) To interconnect the payload electronics with the HAST vehicle electrical system a common disconnect plate is utilized. The payload contractor electronic chassis has incorporated connections for electrical interface as shown in Figure 66. The HAST vehicle duplicates this connector interface with a compatible connector arrangement at vehicle station 35.0. This design incorporates the modular concept that was originally conceived, and mating takes place at mechanical interface with the forward payload chassis.

(3) The radome and its mounting ring encompasses the forward electronic chassis and its components. The radome fabricated from aluminum phosphate matrix (ALPO$_4$) and quartz reinforcement is attached to a structural mounting ring which in turn is secured to the HAST forward fuselage section. A four-point attachment is made with the radome mounting ring and the electronic chassis to provide a completed structural path. The modular application is again achieved by this method of attachment.

(4) Thermal isolation is necessary for the payload module due to the extreme heat encountered in this forward location. To insulate the electronic chassis from the structural frame, isolation washers are employed at the attachment points of contact with the metal structure. Additional insulating blankets are installed around the metal radome attach ring to further reduction and transfer of heat to the electronic payload package. Figure 65 denotes the thermal isolation for the metal chassis.

b.   Antennas for the payload are installed in the HAST vehicle as shown in Figure 67. These locations and installation were established to obtain the optimum system function and mechanical interface with the HAST vehicle. This figure illustrates the total system of antennas required for both RAS and VMDI.
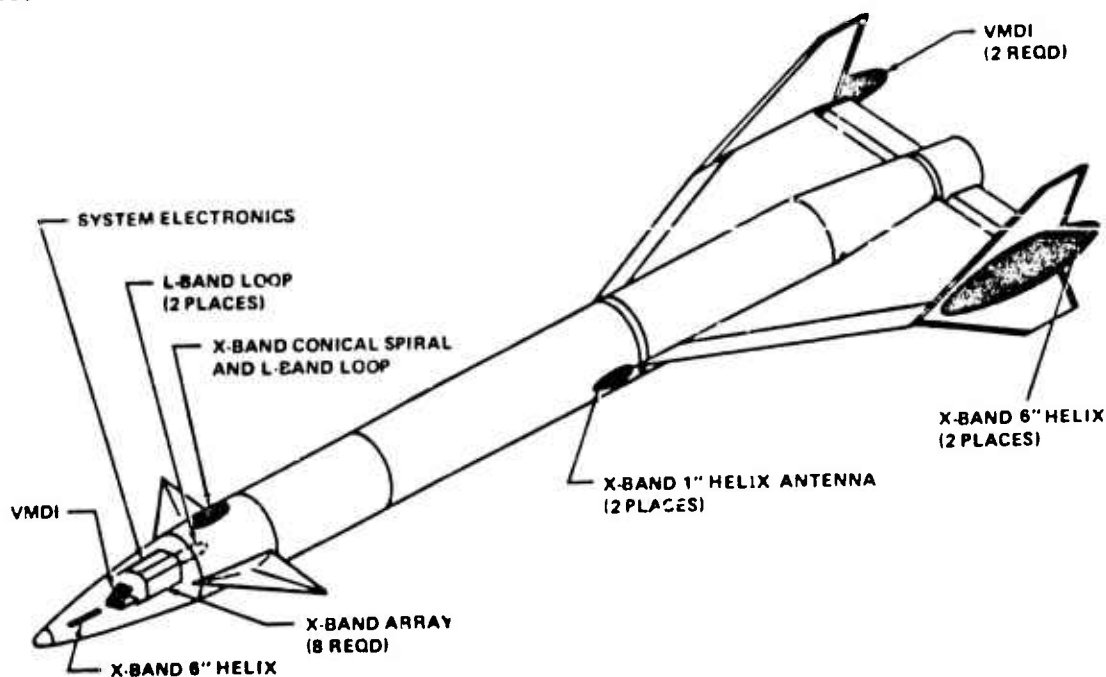
Figure 67. Payload Antenna Locations

(1) The X-band transmit antennas system installed in the vehicle is noted in Figure 67. A six-inch Helix is mounted on the payload chassis in the nose cone. Along with this is another antenna group packaged in an octagonal shape with eight arrays. Both items are a part of the nose

131

module and are forward of station 35.0. Installation and removal is modular and access can be obtained by removal of the nose cone.

Two 1-inch Helix antennas are located forward of wing fuselage intersection at approximate station 122.25. This antenna is typical for both right- and left-hand sides of the HAST fuselage.

The two remaining six-inch Helix antennas which complete the transmit antenna system are located in the aft section of the HAST vehicle mounted on the vertical stabilizers on both the right- and left-hand sides of the vehicle. All antennas within this transmit system are externally mounted for rapid installation and removal.

(2) The X-band receive antenna system is a conical log spiral located in four key locations aft of station 35.0. These antennas are externally mounted with radomes configured with low drag efficiency. Figure 68 depicts their location. The receive system encompasses the entire vehicle with a forward antenna in the canard section fuselage top centerline and one antenna mounted on the bottom centerline of the ram air turbine. Two addition antennas complete the receive system with installation in the aft section on both right- and left-hand sides of the vertical stabilizer. Again, all antennas are accessible external to the vehicle.
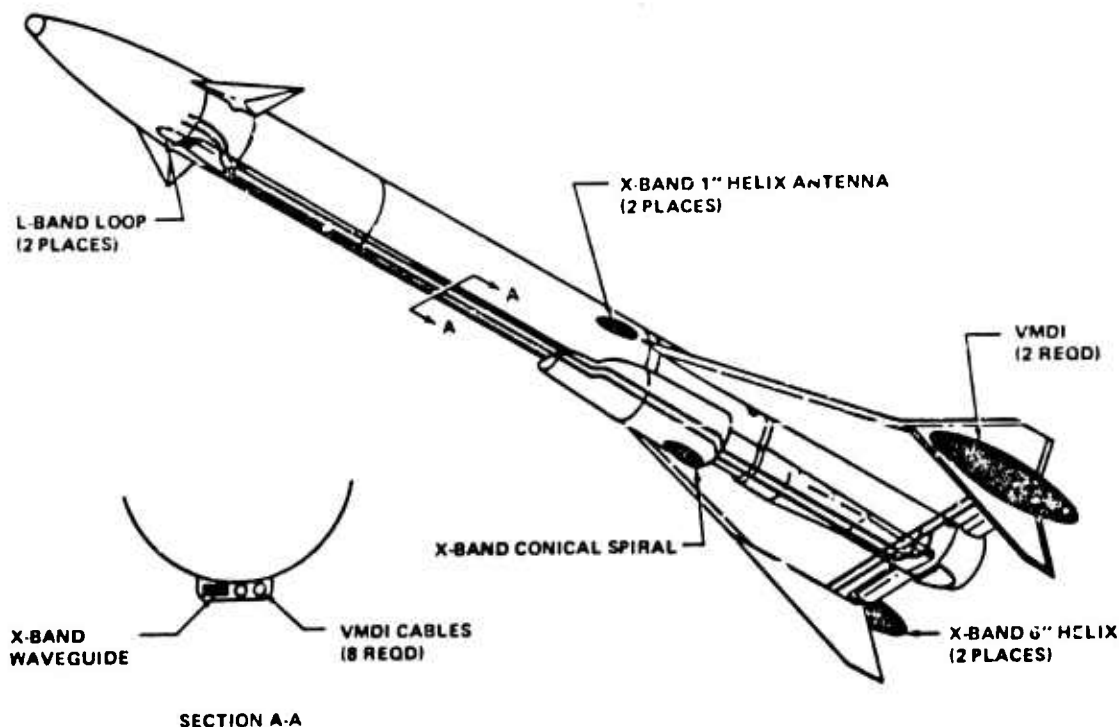
Figure 68. Cable and Wave Guide Routing

(3) The L-band augmentation antenna completes the system with installation of the antenna in the forward canard fuselage section shown in Figure 68. The L-band antenna is used for both receiving and transmitting.

(4) Radomes of aluminum phosphate (ALPO4) are designed for low drag considerations cover all external mounted antennas.

132

(5) Antennas are individually wrapped with form fitting MIN-K® for insulation from extreme heat. Radomes ar internally lined with the same material. The choice of insulation depends on location and severity of temperature expected.

c. Transmission lines and interconnecting components are packaged aft of station 35.0. Location and routing is noted in Figure 68. This figure shows that routing of the lines from station 35.0 aft is through the raceway tunnel section of the vehicle. A combination of coax cables and wave guides is used.

(1) Routing for the RAS system begins at the station 35.0 disconnect plate. From the disconnect plate coax cables are routed through the forward canard fuselage section to appropriate hybrid couplers and aft through the forward raceway with a waveguide to another hybrid coupler in the electronic section. A waveguide again picks up the transmission and carries it to the aft tail cone area where cabling is again employed to transfer signals.

Transmission lines for the L-band system are all contained in the forward command fuselage section utilizing 0.141 diameter semi-riged cable for interconnection between components.

2. SCORING SYSTEM

The electronics of the scoring system developed by the Government Electronics Division of Motorola is packaged in the forward nose section of the HAST. Antennas are positioned at key locations and interconnected with the electronics by coaxial cables through the HAST vehicle.

a. Antennas for the VMDI scoring system are mounted in the extreme forward and aft sections of the HAST vehicle. Two antenna groups are mounted in the forward end of the payload chassis and are a part of the payload module. These antennas are positioned on the vertical and horizontal centerline of the vehicle. Two other VMDI antenna groups are mounted on the horizontal centerline of the vertical fin on both right- and left-hand sides of the vehicle and externally mounted. Location of these units with reference to the HAST vehicle is noted in Figure 67.

(1) Radomes that cover the VMDI antenna also cover X-band Helix and X-band conical spiral. This one unit radome is of heat resistant $ALPO_4$ and designed to low drag configuration.

b. Each fin antenna is fed by four 0.250 inch diameter semi-rigid coax cables. These cables run from the station 35.0 disconnect plate through the raceway to the vertical left-hand stabilizers of the vehicle as shown in Figure 68. To protect these cables from the extreme heat encountered due to the routing, insulation is utilized throughout at key locations within HAST vehicle.

3. INSTALLATION VERIFICATION

Acceptance test procedures have been prepared to verify the installation of the antennas, interconnecting components, and the cables. These tests are conducted to verify installation conformance with respect to payload and vehicle. The checkout verifies discrete payload-antenna interconnecting cables including the variable standing wave ratio (VSWR) and the radio frequency (RF) loss. Block diagrams of the antenna and interconnecting lines are shown in Figures 69, 70 and 71.

4. IR AUGMENTATION SYSTEM

The infrared (IR) augmentation system consists of a pressurant tank, electromechanical controls, a slurry tank, and a flame holder. When loaded it weighs 40.6 pounds. The outside diameter is four and one-half inches and the length is 58 inches. It is covered by a sheet metal fairing when attached to the HAST vehicle.

133
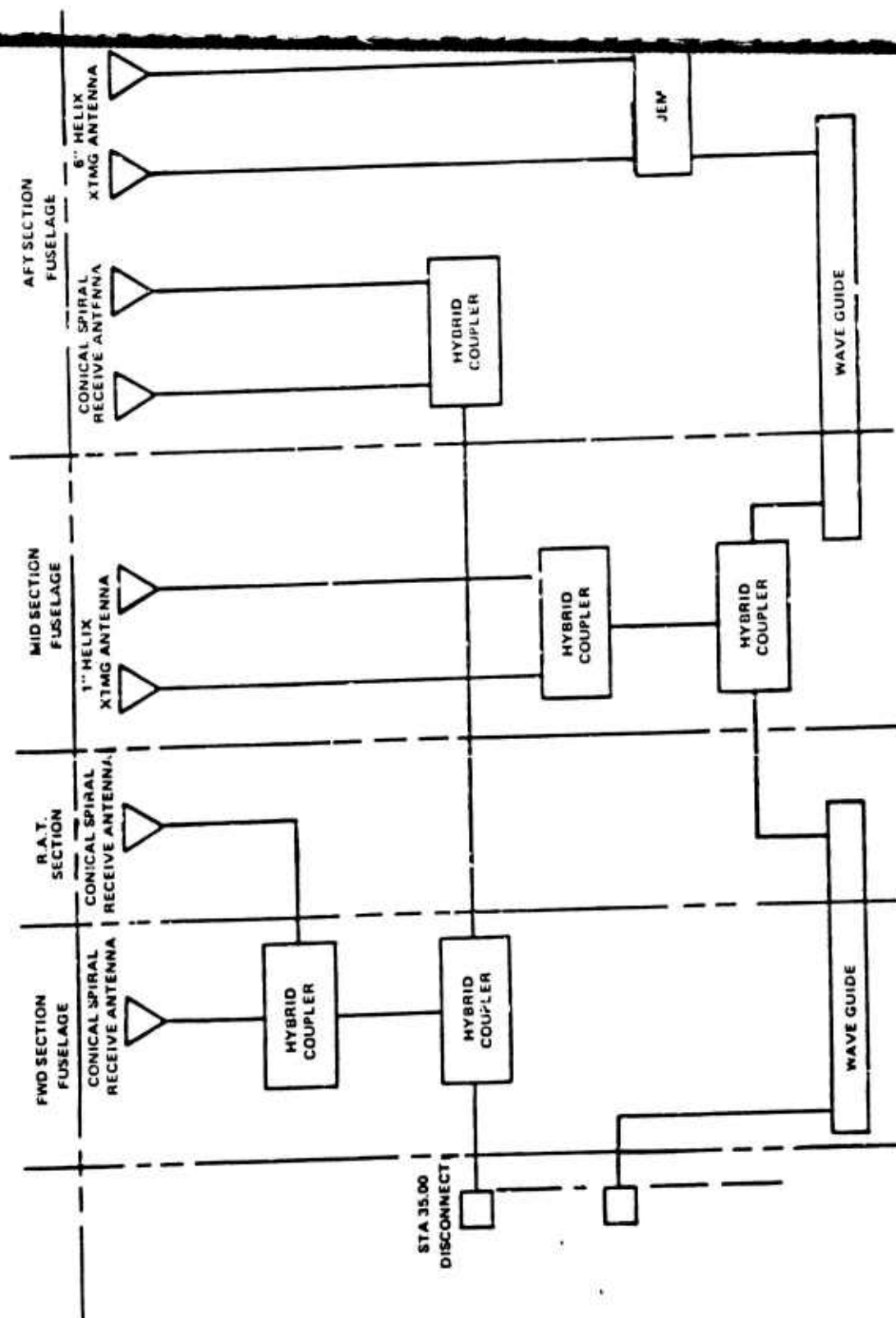
Figure 69. Block Diagram X-Band System
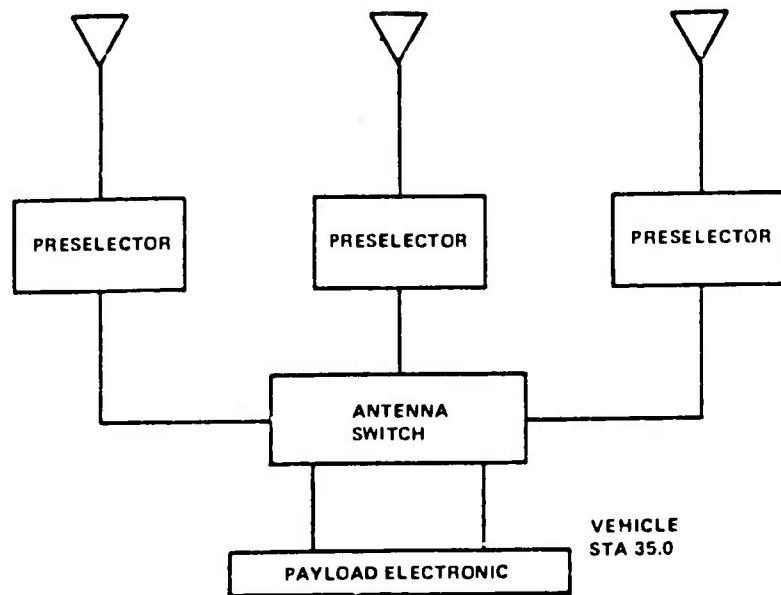
Figure 70. Block Diagram, L-Band Loop Antennas
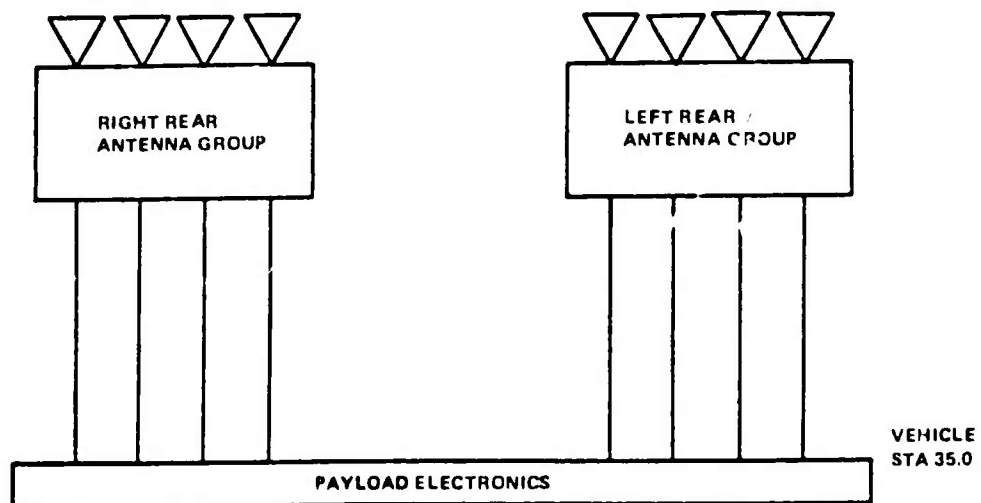
Figure 71. Block Diagram, VMDI Antennas

135

replacing the fairing support bracket. The IR system is positioned under the HAST and the electrical connection made into a receptacle at station 149. The IR payload is then attached to the HAST vehicle by three bolts at station 149 and two bolts at station 192. The IR fairing is installed using the same attachments and fasteners as the aft raceway cover.

SECTION IX

PROPULSION

The propulsion system chosen for the HAST is a hybrid rocket motor consisting of a liquid oxidizer and a solid fuel. Because of the extreme Mach number and altitude performance envelope required, a pure rocket motor was chosen for this application rather than an air breathing system. Auxiliary boosters were not employed because of the variety of system boost requirements presented by the various missions to be flown. A nonhypergolic hybrid system was chosen to provide the safest possible system. The hybrid system also provides the necessary throttle ratio (as high as 10:1) at minimum cost since the thrust level can be controlled by adjusting the oxidizer flowrate. The prepackaged system consists of four major components: (1) a hermetically sealed oxidizer storage tank equipped with a propellant acquisition device; (2) an oxidizer prepressurization subsystem; (3) an oxidizer throttle valve (OTV); and (4) a thrust chamber, assembly (TCA) containing the solid fuel. The first two have been combined into an oxidizer management assembly (OMA), while the last two have been combined into a controlled thrust assembly (CTA). The function of the OMA is to supply oxidizer at a given flowrate potential and pressure under all flight conditions while the function of the CTA is to provide a thrust level prescribed by the HAST automatic flight control system (AFCS). The engine ignition and ramp to maximum boost thrust level is controlled by electronics associated with the oxidizer flow control valve while the AFCS controls the engine sustain thrust level during cruise.

The operation of the propulsion system can best be described in conjunction with the system schematic shown in Figure 72. During vehicle readiness operations prior to loading onto the carrier aircraft, the nitrogen prepressurization storage tank is filled with cold gas. After launch, the nitrogen is expanded through a regulator into the oxidizer tankage to provide a positive oxidizer pressure at the tank outlet. The oxidizer outlet valve opens and oxidizer is allowed to flow to the oxidizer pump where its pressure is boosted. The igniter is initiated producing hot fuel rich gases. The oxidizer throttle valve then opens admitting oxidizer flow to the injector manifold arriving at the proper time to combine with the hot fuel rich gases of the igniter to initiate combustion of the fuel in the thrust chamber. The oxidizer flow control valve then opens progressively to the full open position allowing the engine thrust to ramp to the maximum boost level. The oxidizer aeration system provides nitrogen to the injector manifold to promote oxidizer dispersion during low sustain thrust levels. The aeration gas is provided at a constant pressure above the motor chamber pressure to provide automatically compensated aeration flowrates.

Uninterrupted oxidizer flow is provided by a free siphon located in the aft end of the oxidizer tank. Constant oxidizer pressure is provided by a ducted power unit driven pump controlled to a constant speed by an air inlet control valve. The oxidizer throttle valve is used to provide the variable thrust level.

As the vehicle approaches the desired cruise condition, the thrust level is gradually decreased to the expected cruise condition. The cruise thrust level is adjusted on command from the AFCS to provide the desired cruise Mach number. As the vehicle speed changes due to maneuvers and weight changes, the AFCS commands the oxidizer throttle valve to change flow rate providing constant Mach number. Upon depletion of the usable oxidizer the prepressurization nitrogen is allowed to blow down through the open throttle valve.

The propellant combination chosen as a result of a trade study was inhibited red fuming nitric acid (IRFNA) as the oxidizer and a mixture of 80 percent polybutadiene and 20 percent polymethylmethacrylate as the fuel.

1. OXIDIZER MANAGEMENT ASSEMBLY

The basic function of the OMA portion of the propulsion system is to supply IRFNA to the CTA oxidizer throttle valve at a nominal pressure of 700 psig and flow capability of 3.6 pounds/second to supply gaseous nitrogen (GN_2) to the CTA aeration.

137
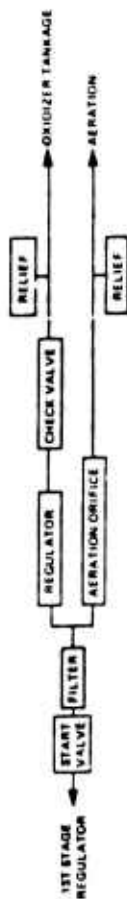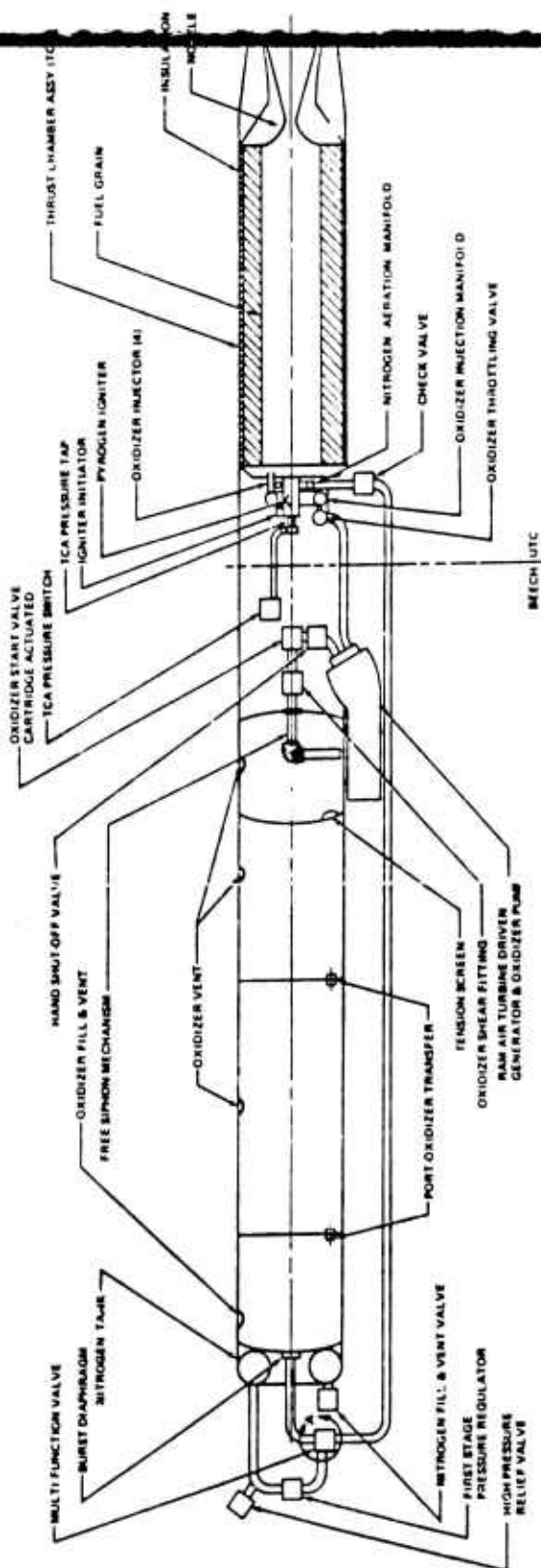
Figure 72. Propulsion System Schematic

2. GN2 SUBSYSTEM

The GN2 (gaseous nitrogen) subsystem is used for two functions on the HAST vehicle, these being prepressurization of the oxidizer and aeration to the TCA injectors. Prepressurization of the oxidizer is required to prevent cavitation of the centrifugal pump. The pressure must be maintained at a level slightly higher than the vapor pressure of IRFNA at maximum temperature conditions. Aeration is required to the TCA injectors during low IRFNA flow rates to assure acceptable oxidizer spray patterns on the fuel grain surface.

The GN2 is stored in a 318 in^3 toroidal tank located forward of the oxidizer tank. The tank contains 3.27 pounds of GN2 at a nominal pressure of 3500 psig at 70°F. One pound of the GN2 is used for aeration and the remainder used for oxidizer tank pressurization. The GN2 tank is pressurized prior to launch from standard GN2 carts or from a standard GN2 "T" size bottle with a pressure intensifier. A fill and vent valve compatible with these items is mounted on the toroidal tank. Also incorporated into the GN2 tank is a high pressure relief valve set at 4200 psig for protection against overpressure.

Directly downstream of the GN2 tank is a first stage regulator, shown on Figure 73, that reduces the pressure to 260-380 psig. A multifunction valve, shown in Figure 74, is coupled to the first stage regulator. This valve consists of a start valve, pressure regulator, check valve, flow control orifice and two relief valves. The start valve consists of a sealed replaceable shear cap that is sheared by a squib actuated pressure cartridge initiating flow to the regulator and flow control orifice. The pressure regulator is a standard spring loaded type maintaining the oxidizer tank pressure at 53 to 73 psig. The flow control orifice for aeration is 0.0225 inch diameter and utilizes the first stage pressure regulator output as the upstream pressure.
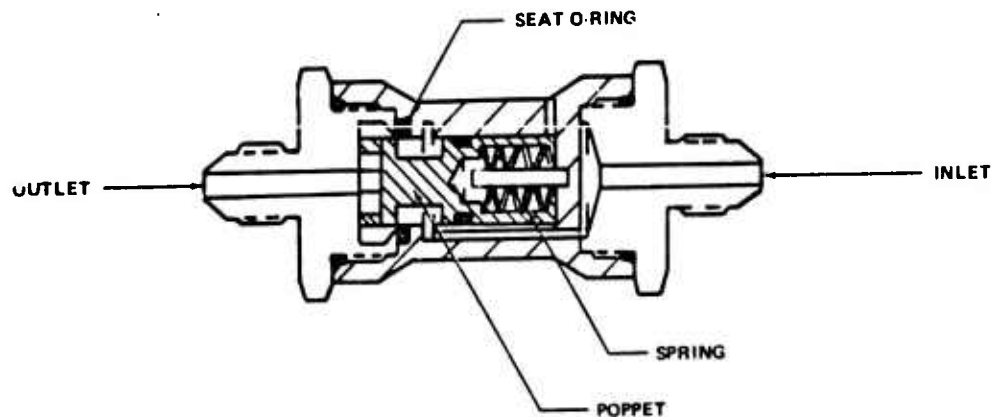
Figure 73. First Stage Regulator

Each regulator has a relief valve on the downstream side as a safety feature protecting each system against overpressurization in the event of a regulator failure. The oxidizer relief valve is set at 250 psig and the aeration relief set at 700 psig. A check valve is located between the oxidizer pressure regulator outlet and relief valve to prevent IRFNA fumes from entering the regulator portion of the multifunction valve after completion of a mission. The check valve is set to crack at 2 psig and reseat at 1 psig.

3. OXIDIZER TANK

The oxidizer tank shown in Figure 75 is a nominal 9465 in^3 17-7 PH stainless steel tank providing for 496 pounds of IRFNA, 488 pounds of which are usable. The IRFNA is sealed in the tank at the fill and vent ports with seals previously qualified for the AQM-37A and with a long and

139
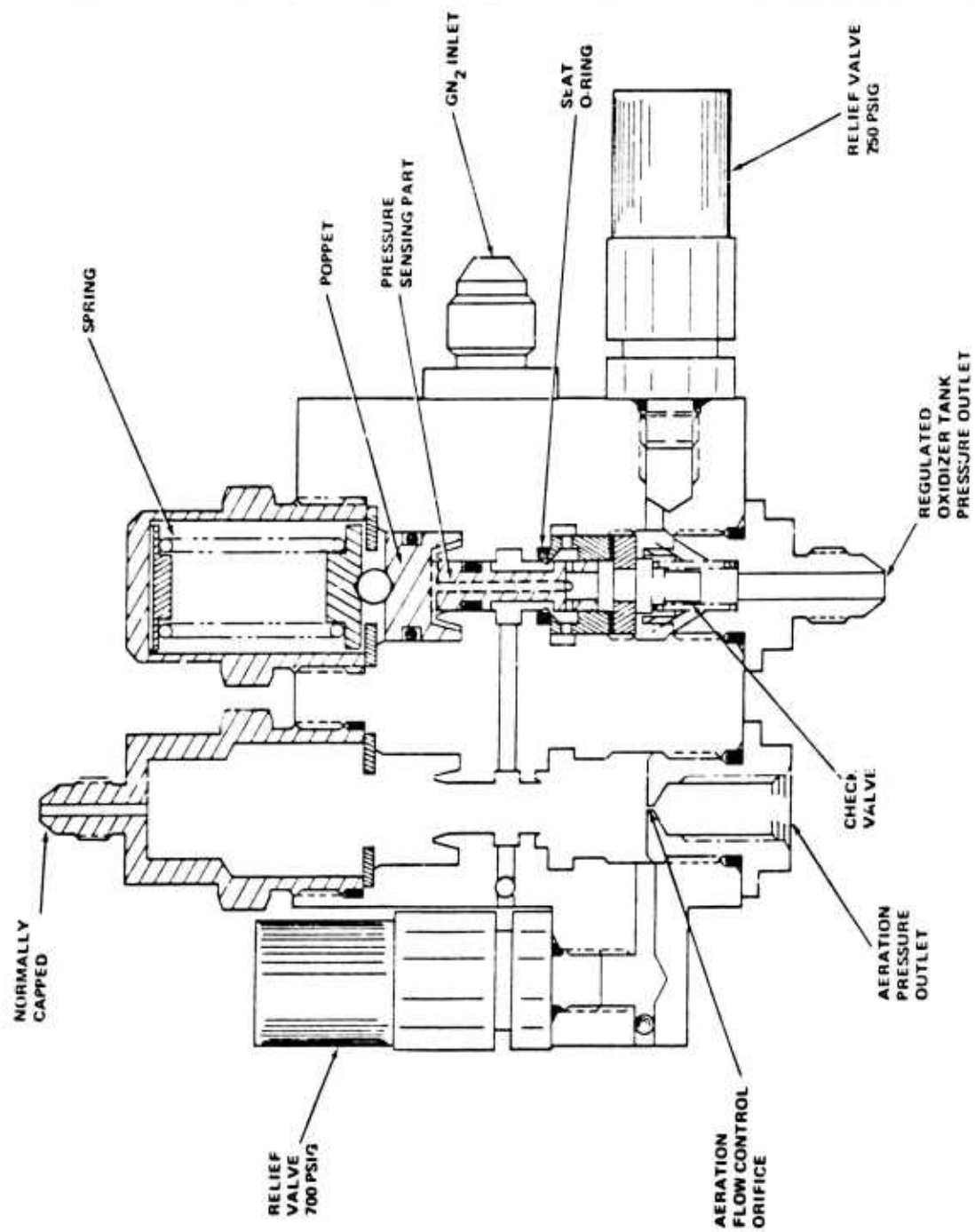
Figure 74. Multifunction Valve
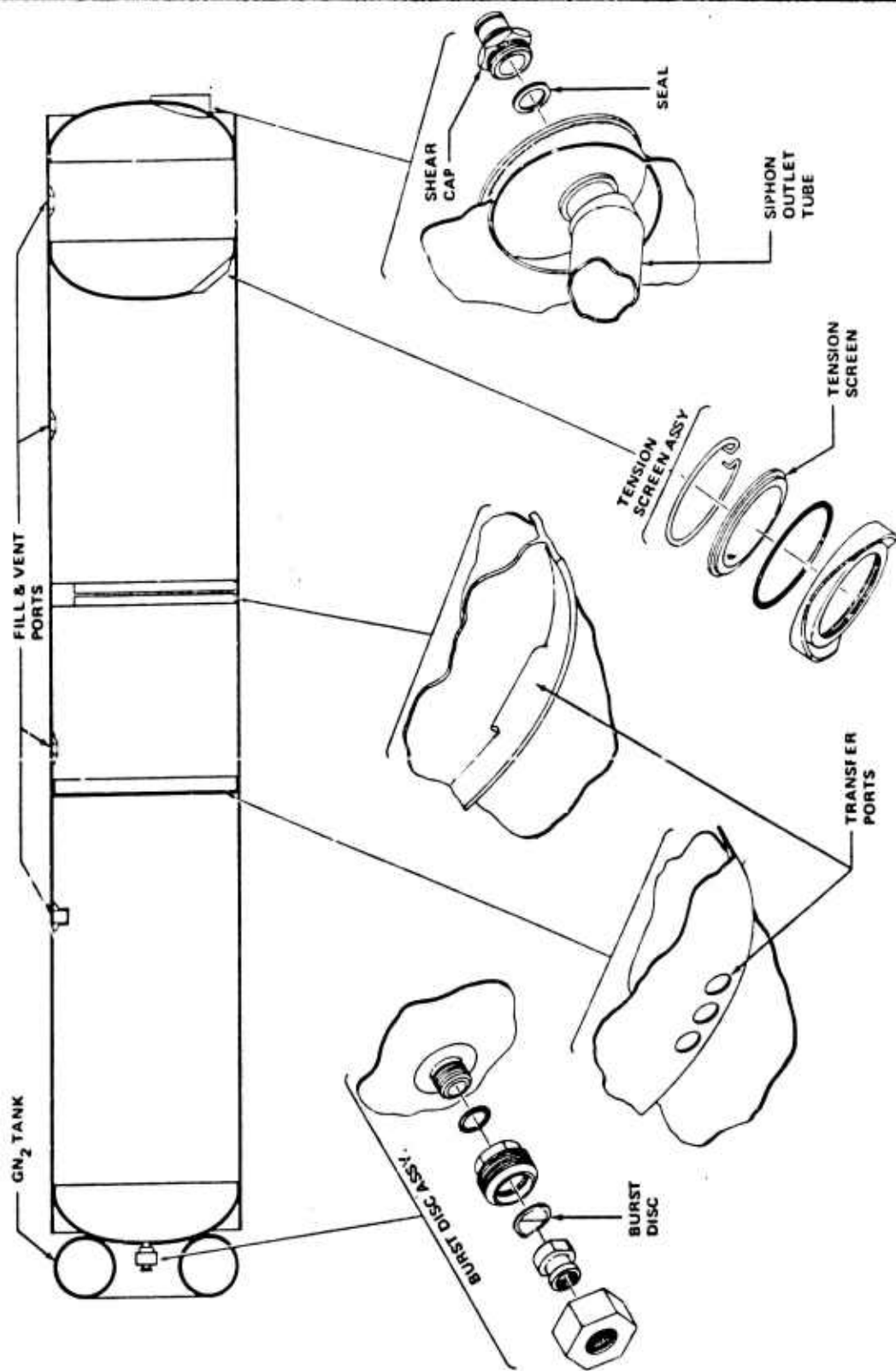
Figure 75. Oxidizer Tank

SHEAR CAP

SEAL

SIPHON OUTLET TUBE

TENSION SCREEN ASSY

TENSION SCREEN

FILL & VENT PORTS

TRANSFER PORTS

GN₂ TANK

BURST DISC ASSY

BURST DISC

141

satisfactory production history. An 1100 aluminum burst disc isolates IRFNA from the GN_2 subsystem and a shear cap installed with a seal similar to those used in the fill and vent ports seals the outlet port. The burst disc will rupture with a pressure differential of 20-0 psia from the GN_2 subsystem and by means of a backup plate will hold tank pressures up to 150 psig. This allows the burst disc to be compatible with normal operation but maintain sealing under excessive pressures associated with fires and with the normal storage pressure required on the ullage for temperature compensation. Teflon® coated 1100 aluminum washers are being investigated as potential replacements for the seals in the fill and vent ports and the outlet port.

The forward compartment contains approximately 35 percent of the total oxidizer and all of the ullage. The aft compartment where the siphon device is located holds IRFNA to be expended during negative g maneuvers and is the last oxidizer section to be depleted. This internal compartment arrangement gives optimum center of gravity travel for better maneuverability.

The front three compartments are connected with ports on the lower portion of each bulkhead. The aft compartment contains a 75-micron tension screen on the lower portion of the aft bulkhead. The tension screen, when wet, will readily pass a liquid but will not pass GN_2 gas. This is a positive method of assuring the IRFNA contained in the aft compartment will continue to flow to the thrust chamber during negative g maneuvers and will not flow forward into the next compartment during normal operation.

4. OXIDIZER START VALVE

The shear cap on the oxidizer tank outlet is sheared with a pressure cartridge actuated piston housed in an oxidizer start valve shown in Figure 76.

Sealing after the shear cap has been sheared is accomplished with an O-ring on the shear cap that mates with the cylindrical inlet to the start valve. The start valve also has a hand operated shutoff valve that is closed as soon as practical after recovery. This hand operated valve, in conjunction with the GN_2 subsystem check valve, will allow the oxidizer tank to become a sealed system and eliminate IRFNA fume leakage from the target after initial recovery operations.

5. FREE SIPHON

A free siphon device was selected for the positive expulsion system and is shown in Figure 77. The selection was based on its simplicity of design; it also allows maximum oxidizer storage. The siphon is a welded assembly with a thin (0.005 to 0.007 inch) heat shrinkable Teflon® tube over the coil forming the bellows. The coil has a major diameter of 2.90 inches and the coil wire has a 0.078 inch diameter. The short tube on the inlet is heavy walled for weight purposes, assuring the siphon inlet stays on the bottom during fill. All metallic parts are constructed of 17-7 PH stainless steel with heat treat identical to that of the tank. The siphon assembly is welded into the aft dome of the oxidizer tank. A chain attached to two bails control the position of the inlet tube allowing sufficient clearance from the tank wall at all positions.

6. DUCTED POWER UNIT

The ducted power unit (DPU) shown on Figure 78 consists of a ram air turbine providing shaft horsepower to an alternator for electrical power and a centrifugal pump for raising the oxidizer pressure from the 30 to 70 psia supplied by the GN_2 subsystem (63 ± 10 psig minus flow losses) to 685 to 755 psig required at the throttle valve inlet.

A fixed geometry normal shock inlet with an air flow control (butterfly) valve supplies ram air to the turbine. The air is accelerated through the stator and directed to the rotor. The rotor converts the air kinetic energy into torque which is transmitted to the load by the drive shaft.

Both the electrical generator and the oxidizer pump are mounted directly on the turbine drive shaft. The resulting design is a simple, lightweight energy converter which utilizes ram air as the energy source and whose driving and driven members are all on a common shaft.
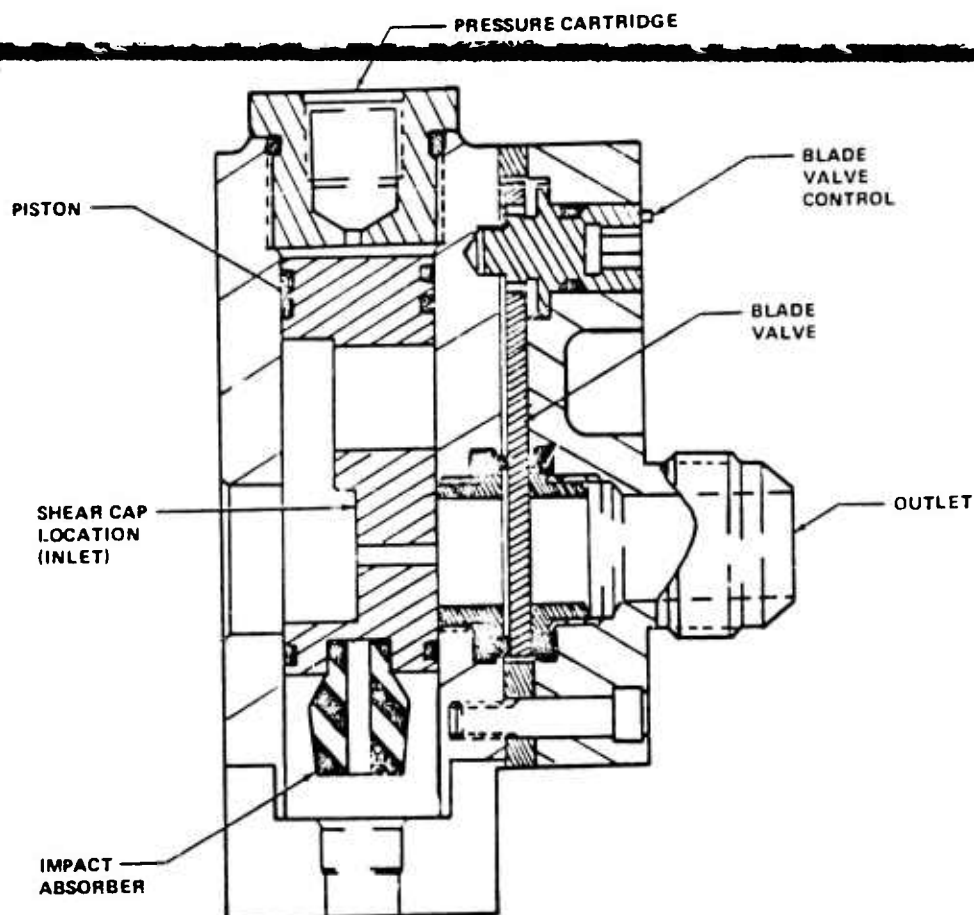
Figure 76. Oxidizer Start Valve

The horsepower requirements of the DPU, Model No. AD26A, has been defined through IRFNA pumping tests and experience on similar alternator designs. The horsepower requirements assume a full load of 45 amperes on the alternator and the maximum boost flow rate of 3.6 pounds/second. Horsepower is also defined for the launch conditions since oxidizer flow rate during that period will be reduced to 2.2 pounds/second and then increased linearly to 3.6 pounds/second during the ramp time interval. The horsepower budget is as follows:

TABLE XXX. DPU HORSEPOWER BUDGET

	Horsepower at Launch 2.2 lb/sec	Horsepower at Boost 3.6 lb/sec
Alternator (70% eff) 45 amps at 28 volts	2.52	2.52
Pump	12.53	16.88
Bearings	0.25	0.25
Total Horsepower	15.30	19.65
Total Horsepower + 5% Margin	16.10	20.60

143

TEFLON O-RINGS

OUTLET
TUBE

COIL

ADAPTER,
MATES WITH
TANK OUTLET

HEAT SHRINKABLE
TEFLON

CHAIN

BAIL

TEFLON CLAMP

HEAVY WALLED
INLET
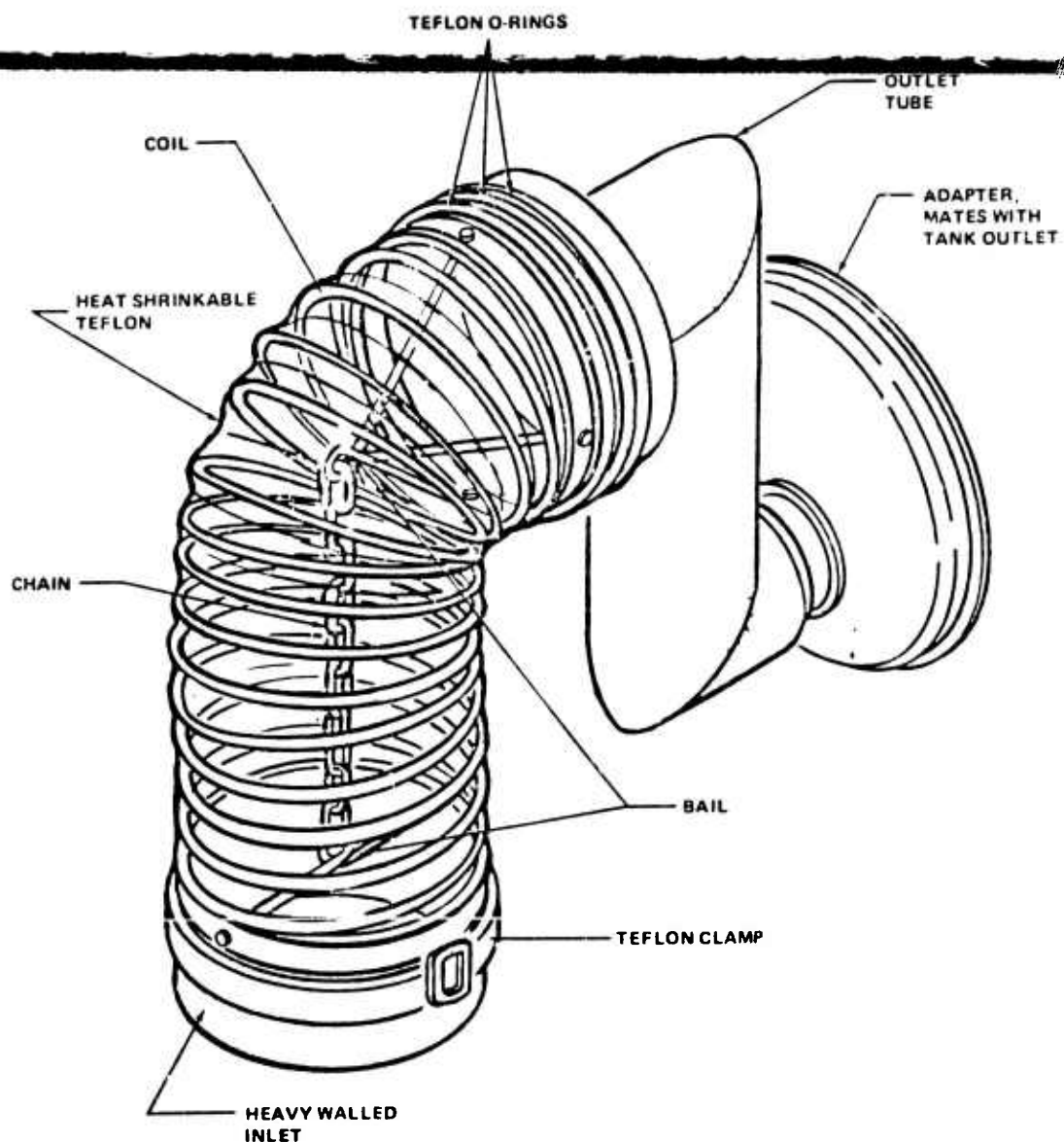
Figure 77. Free Siphon Device

The pump horsepower includes that required for disc friction and the pump seal.

The alternator is a brushless AC type with a rectified output for conversion to DC power. The alternator output voltage is 28 ± 2.8 VDC. Full alternator load is 45 amperes at 28 VDC. The alternator is capable of providing transient loads of an additional 30 amperes at 28 VDC for 100 milliseconds. A 100-millisecond time period will elapse from the completion of one transient load to the initiation of the second.

The oxidizer pump is a radial vane centrifugal pump capable of raising the oxidizer pressure 685 psid under nominal operating conditions. A nonrubbing seal assembly has been included in the pump design to accommodate periods of dry pump operation. The seal, identified as "VISCOSEAL" consists of a sleeve with 0.003 inch deep parallel grooves set at a 15° helix angle.

144
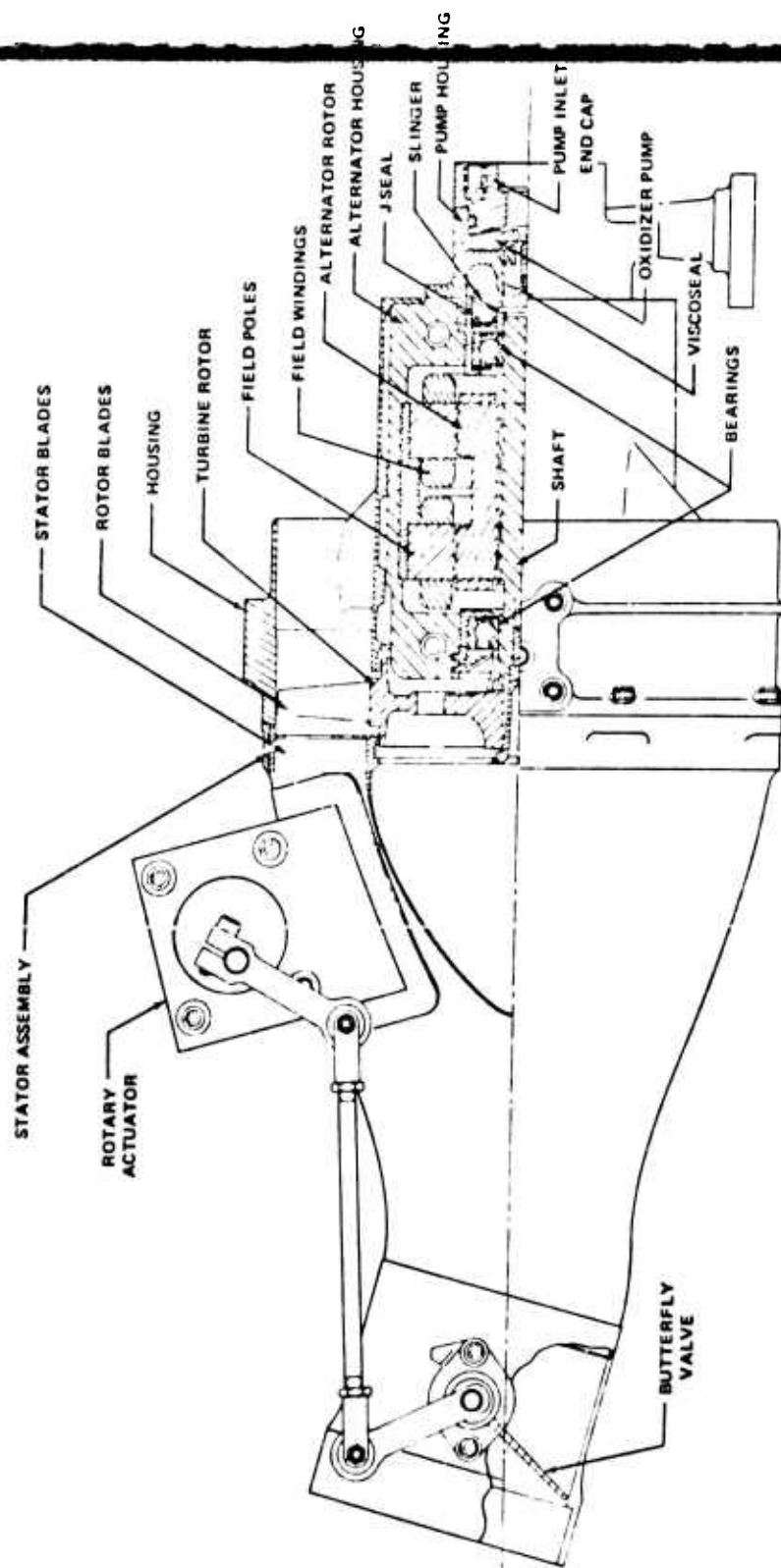
Figure 78. Ducted Power Unit

145

A speed control is used to maintain the turbine at a constant speed required by the pump and alternator. The speed is set by operating the system and obtaining the speed at which the pump Δp is 685 psid. The nominal set point is 31,500 rpm. The speed control generates a signal to the actuator motor which positions the butterfly valve to vary the airflow to the turbine, thus controlling speed.

An analytical approach was used to determine the best combination of inlet area, turbine diameter, and exhaust area to achieve maximum performance with the minimum component size system. The rationale used in sizing the system was to select a combination which delivered the required launch horsepower (16.1) at $M = 0.9$ and 40,000 feet, and which delivered maximum boost horsepower (20.6) over the majority of the flight envelope. The selected combination consists of a 10 in^2 inlet area, 6.0-inch mean turbine blade diameter, and a 25-in^2 exhaust area.

7. PLUMBING

All IRFNA plumbing lines are 6061 aluminum 3/4 inch in diameter with Wiggins connectors for relief of structural loads. Kel-F$^®$ elastomer O-rings are used for sealing. The GN$_2$ subsystem has stainless steel lines upstream of the start valve with aluminum lines in the low pressure areas.

8. CONTROLLED THRUST ASSEMBLY (CTA)

The basic function of the CTA portion of the propulsion system is to provide thrust from a hybrid rocket motor in response to command voltage signals to the oxidizer throttle valve (OTV).

9. FUEL GRAIN

The fuel grain consists of 20 two-inch thick molded billets composed of 80 percent polybutadiene (PBB) and 20 percent polymethylmethacrylate (PMM) which are stacked into the TCA as shown on Figure 79.

Because of injector effects on the fuel grain, the axial fuel regression rate is not constant (i.e., increased local heat transfer resulting in higher regression rate). A fuel grain with increased web thickness is therefore required in the region where the injector effects are the greatest. In addition to these two configurations, the first fuel billet has an increased port area in order to aid in ignition of the fuel grain. The two most aft fuel billets have two-inch diameter cylindrical ports. This restriction in the nozzle area increases the combustion efficiency and aids in reducing the nozzle throat erosion. The total fuel grain is composed of a grouping of these various configurations in order to maximize the fuel utilization and minimize case heating. The average volumetric loading is 0.90 based on an exterior fuel grain diameter of 12.6 inches.

10. NOZZLE AND AFT CLOSURE

The nozzle is shown in Figure 80. The assembly is composed of a number of insulative and structural components bonded into a 4130 steel shell. These components are: the entrance section, throat insert (pyrolytic graphite), exit cone (phenolic), retaining ring exist cone, heat sink/throat support (high density graphite), entrance support ring, and entrance and exit insulative components.

The nozzle is a heat sink design having a re-entrant (submerged entrance section (25° half-angle) and full nozzle exit. The nozzle has a throat diameter of 1.47 inches and an overall expansion ratio of 15:1. Significant design features are a sliding entrance cap to allow for axial pyrolyte graphite expansion, positive component retention (no dependence on bonds), sliding pyrolyte graphite throat insert, and circumferential lockwire attachment to the case.

WEB DISTANCE = 2.6

12.6

WEB DISTANCE = 3.0

NOTE: LOADED WEIGHT = 152 LBS
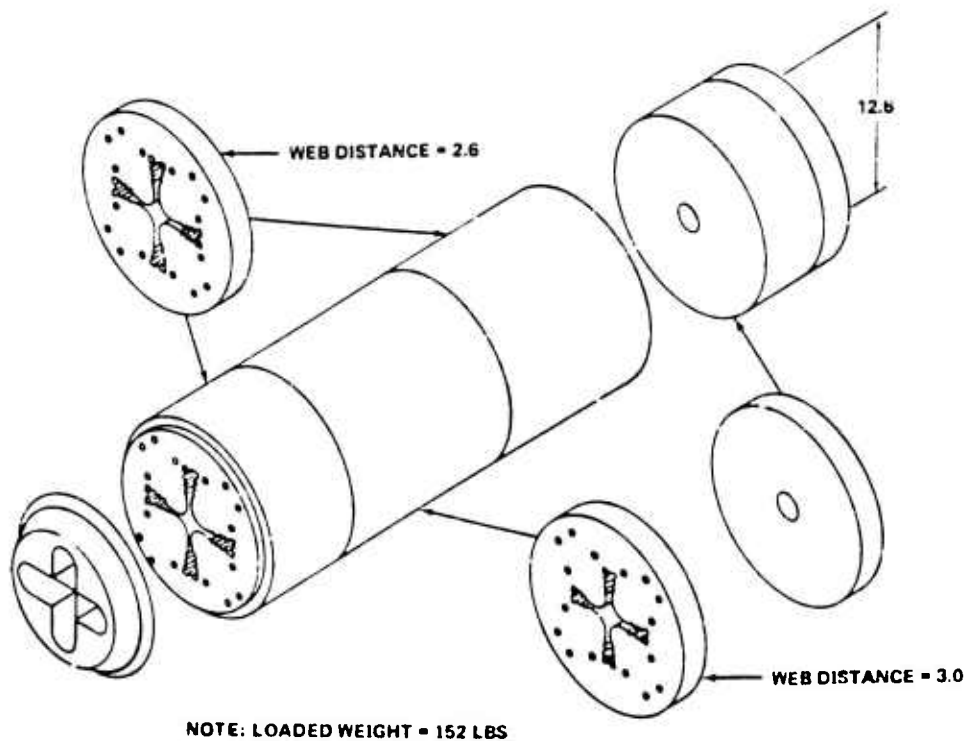
Figure 79. Fuel Billets

11. OXIDIZER INJECTOR AND MANIFOLD

The basic function of the injector-manifold assembly shown on Figure 81 is to deliver the oxidizer into the combustion chamber in a manner which ensures optimum motor performance throughout the required throttling range. To accomplish this, the manifold must distribute the oxidizer to the injectors with minimum pressure loss. The injectors must then atomize and disperse the oxidizer such that the proper distribution over the entire exposed surface of the fuel grain is assured. At the low flow rates, where the pressure potential and injection velocity of the oxidizer is inadequate, aeration provides the necessary injection velocity for proper atomization and dispersion of the oxidizer. Aeration as used herein defines a process in which gaseous fluid is mixed with a liquid to decrease its bulk density and increase the atomization and dispersion of oxidizer particles.

The injector is designed to produce a solid cone spray and is comprised of a spinner and a properly shaped nozzle. The function of the spinners is to impart the tangential velocity component to the passing fluid; however, the spinner must maintain a proper balance between the tangential and axial velocities. The velocity distribution, therefore, determines the resulting spray pattern.

This velocity distribution must be developed with a minimum pressure loss as the remaining pressure differential determines the injection velocity. The function of the nozzle is to efficiently convert the pressure potential into kinetic energy. This is accomplished by providing smooth transitions during the acceleration processes.

At low flow rates the available pressure differentials are inadequate to maintain the injection velocities necessary to properly atomize and disperse the oxidizer. With a design pressure differential of 150 psi and a throttling range of 8.9:1 (ratio of boost thrust to minimum sustain thrust) the pressure differential is reduced to less than 3.0 psi at the minimum flow rate. This is not

147

PYROLYTIC GRAPHITE WASHERS

SILICA PHENOLIC TAPE

HIGH DENSITY GRAPHITE

SILICA PHENOLIC MOLDING COMPOUND
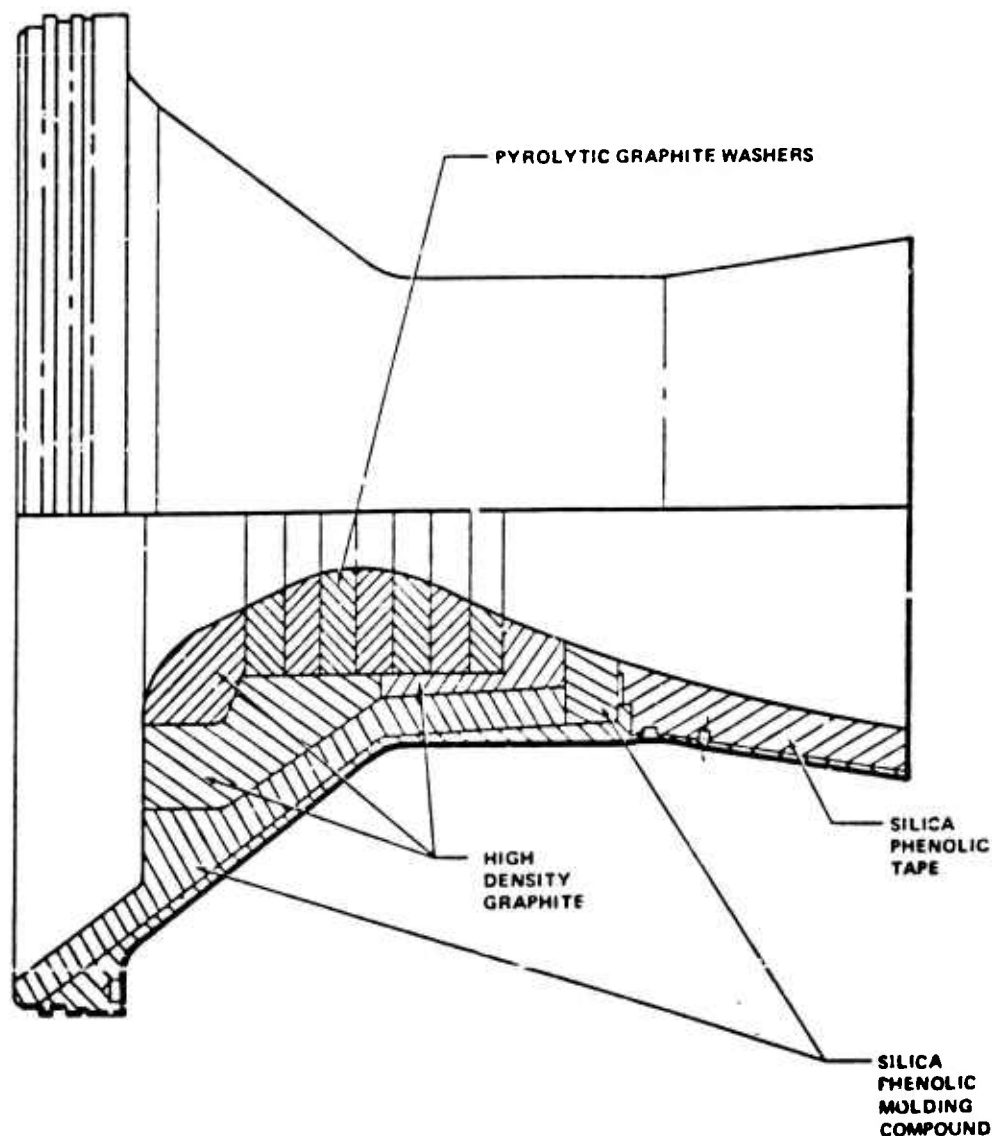
Figure 80. HAST TCA Nozzle

sufficient to atomize rnd disperse the oxidizer as desired. Therefore, nitrogen gas from the toroidal 'tank is used to atomize and disperse the oxidizer.

Test results indicate that efficient mixing of the gas and liquid can be achieved by injecting gas in the center of the liquid stream immediately downstream from the spinner. This is accomplished by inserting the aeration tube in place as shown in Figure 81. Proper aeration is obtained by controlling the pressure at the aeration inlet by a sonic flow control orifice 0.0225 inch in diameter located in the GN_2 subsystem which ensures that a minimum flow of 0.0024 pound/second GN_2 is obtained under choked flow conditions. A check valve between the sonic orifice and injector is required to

148

isolate the GN2 subsystem during periods that the injector pressure is higher than the regulated pressure upstream from the sonic orifice.
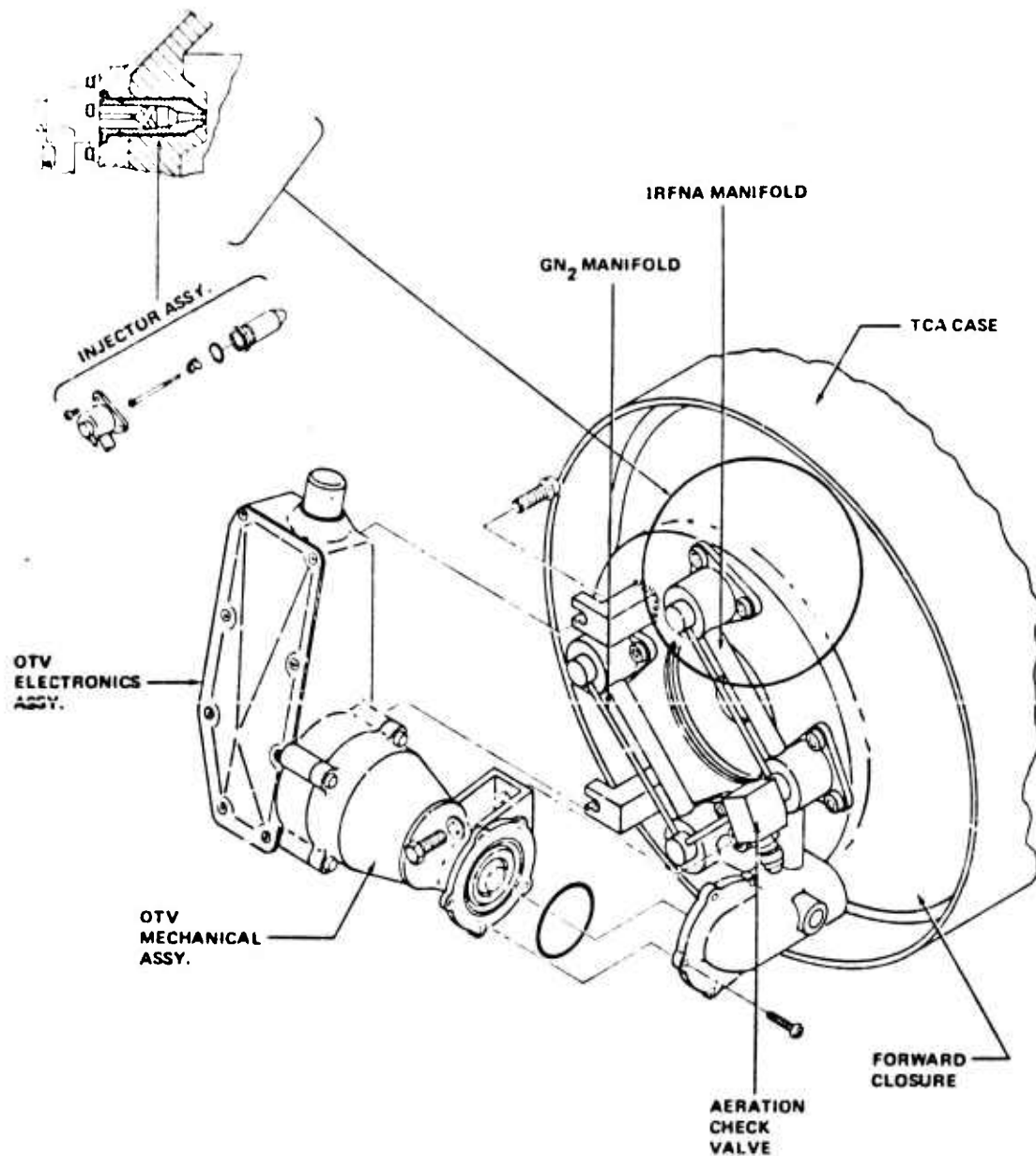
Figure 81. Oxidizer Injector and Manifold

The primary function of the manifold is to distribute the oxidizer and nitrogen to each injector with minimum pressure loss. The manifold assembly is presented in Figure 81. An oxidizer distribution block interfaces with the outlet of the oxidizer throttle valve. This block diverts the oxidizer into two feeder tubes, each of which leads to two series connected injectors. Aeration gases are apportioned through a distribution block located on top of one of the injectors. The components of the manifold are fabricated from aluminum.

149

12. IGNITER

The igniter assembly for the HAST motor is shown in Figure 82. It consists of an insulated igniter case, end cap or closure housing, a dual bridgewire initiator and a solid propellant grain.

The igniter case is a cylindrical shell with an integral aft closure and nozzle shell. A lip is provided at the aft end for snap ring retention of the igniter case in the motor forward closure. The case forward end is threaded and includes provisions for an O-ring. The case material is 4130 steel with an OD of 2.185 inches and a wall thickness of 0.100 inch.

The igniter closure is a forged cylindrical cap of 4130 steel with provision for an initiator to be installed at 90 degrees to the closure centerline.

The igniter throat insert is fabricated from carbon fiber reinforced phenolic resin. The insert has a throat diameter of 0.140 inch and is bonded on a 30-degree ramp with epoxy adhesive to the steel igniter shell. This ramp supports the insert when the igniter is pressurized and prevents it from being ejected into the case. Silica Buna-N rubber is used to insulate the igniter chamber. The igniter propellant grain is cast into a 0.010-inch thick paper phenolic cartridge. A liner is applied between the propellant and internal surfaces of the cartridge to ensure propellant adhesion. The grain design of the progressive burning pyrogen igniter is a simple cylindrical configuration weighing 0.45 pound. The igniter is expended in 2.4 seconds.

13. MOTOR CASE

The case, shown in Figure 83, is fabricated from AISI 4130 steel heat treated to 180,000 to 200,000 psi minimum ultimate tensile strength. The case consists of a 13.000 inch outside diameter cylindrical shell, 41.945 inches in length, with a 0.060 inch minimum wall thickness. At the forward end, a shear lip and sealing surface are provided for the forward closure. The forward closure is inserted into the aft end of the motor case and translated forward until it contacts the shear lip. The closure is retained by three threaded dowel pins. At the aft end, the aft closure/nozzle shell is retained by a circumferential lockwire joint. The lockwire joint uses square keystock installed through an exterior slot to fill matching circumferential grooves in mating parts. With the key installed, the parts are locked together and able to withstand extremely high ejection loads. The aft circumferential lockwire joint provides a full opening diameter for insertion of the grain cartridge.

Case fabrication is accomplished by shear forming a forged preform over an internal mandrel. Acceptance of each delivered motor case is based on successful completion of a hydrostatic proof test to 1.2 times operating pressure followed by radiographic inspection of all welds and a thorough inspection of all case surfaces using a magnetic particle process.

14. INSULATION

The CTA has two key insulation components other than the nozzle insulation. These are the forward closure and the case insulations (shown in Figure 83). Each insulation has somewhat different operating requirements. The forward closure must not only direct the igniter gases into the thrust chamber, but it must also resist burn through tendencies created by both the igniter gases and the combustion gases in the TCA. The fuel provides the primary case insulation; however, once the fuel is consumed in any one location, the case insulation prevents localized heating and subsequent burnthroughs in the case. Silica phenolic is the material used for insulation.

15. FORWARD CLOSURE

The forward closure shown in Figure 82 is machined from a one-piece forging of 4130 steel heat treated to 180,000 to 200,000 psi ultimate tensile strength. Openings and attachment provisions are provided for the igniter, four injector ports, and a pressure tap. Sealing surfaces are provided for the igniter and injector interfaces.

150

Figure 82. HAST Igniter

CASE

CARBON/PHENOLIC NOZZLE INSERT

SILICA/Bu7aN RUBBER INSULATION DISC

PAPER/PHENOLIC INSULATION SLEEVE

PROPELLANT GRAIN

LINER

RUBBER INSULATION

INITIATOR

FORWARD CLOSURE

O-RING

IGNITER ASSY

SNAP RING

PRESSURE PORT

151
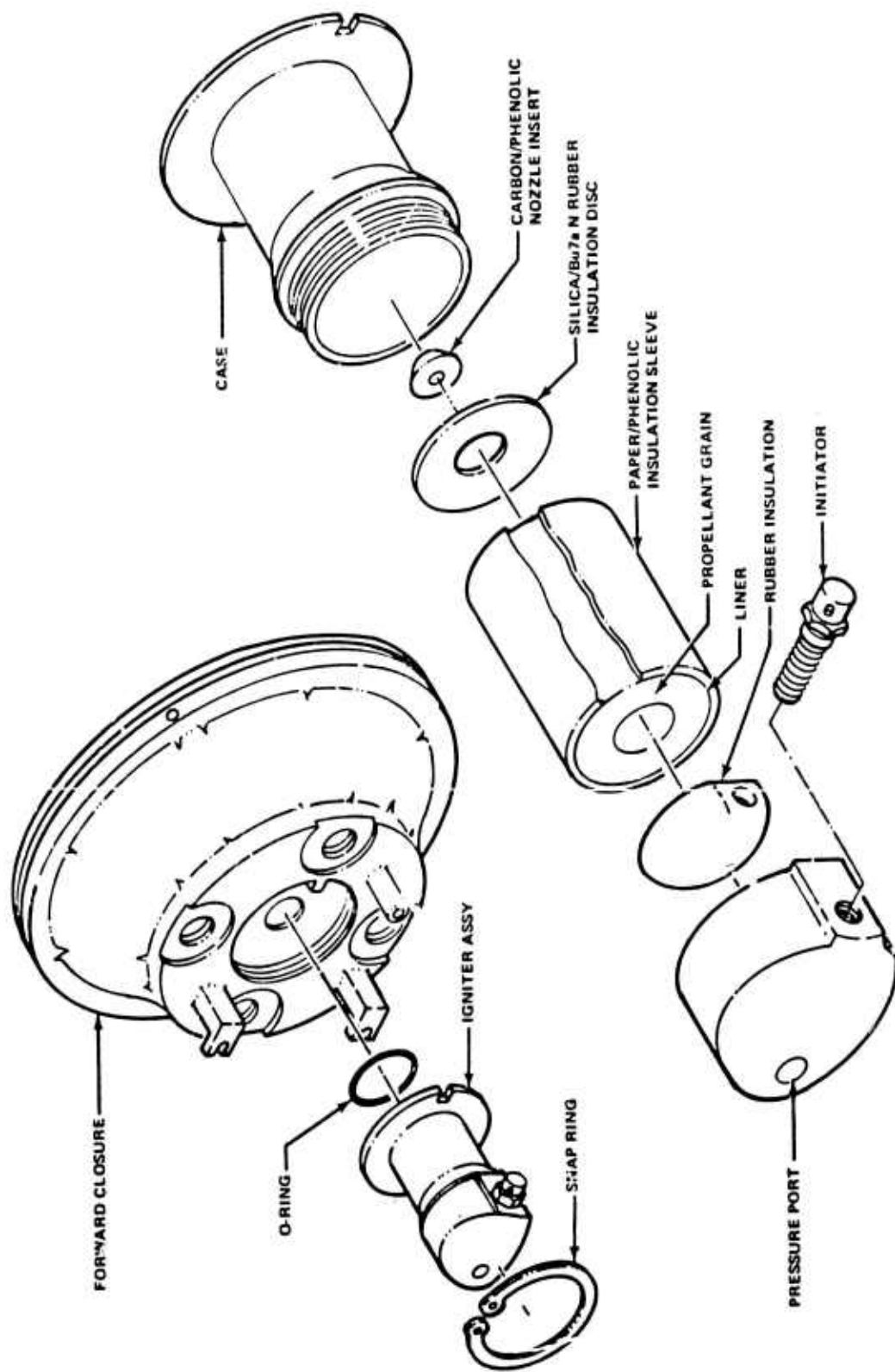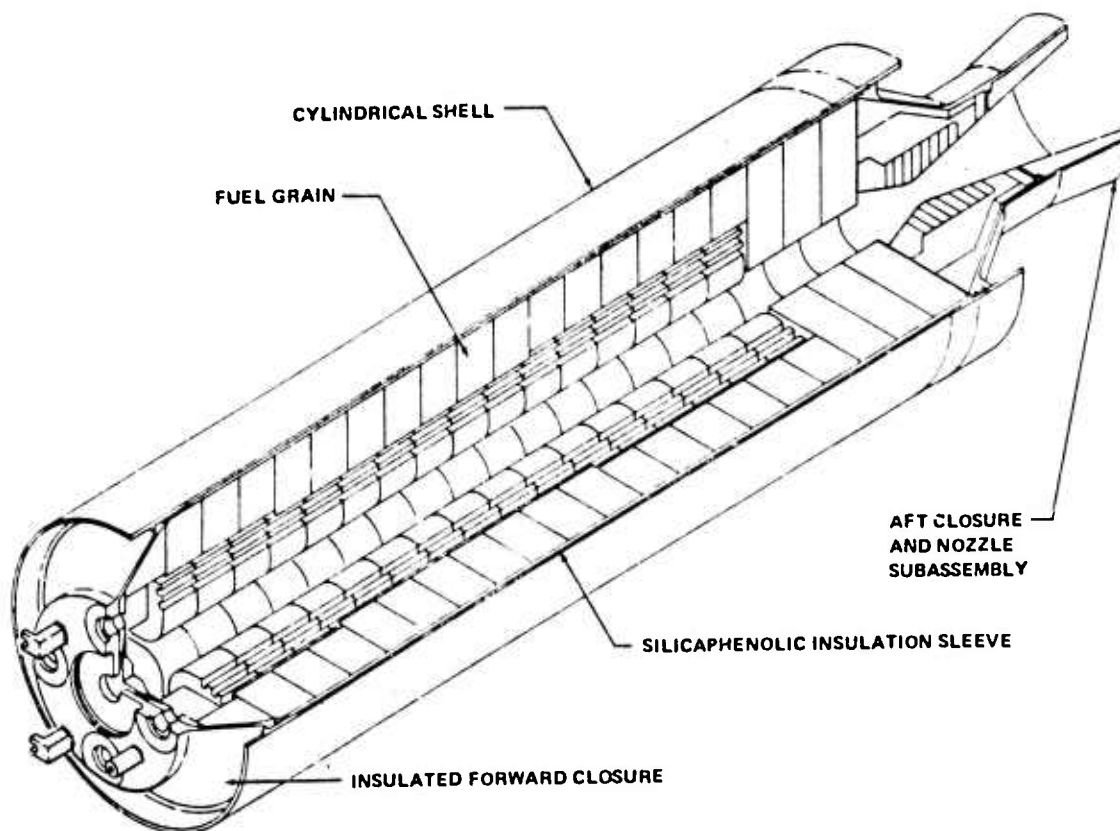
Figure 83. HAST Motor Case

The truncated cone configuration provides maximum volume within envelope restrictions. The forward closure slides into the aft end of the motor case and is retained at the forward end of the motor case by a shear lip and three set screws. A 3.5-inch diameter igniter case snap ring fits into a snap ring groove provided in the forward closure.

16. OXIDIZER THROTTLE VALVE

The OTV shown in Figure 81 is rigidly mounted by three support posts to the forward closure of the TCA. The valve contains all the electromechanical, mechanical, and electronic components required to control the flow of oxidizer (from the supply of IRFNA at the inlet to the CTA) in response to analog and discrete commands provided by the automatic flight control system (AFCS). In addition, signal shaping, dynamic compensation, and variable limits are incorporated in the OTV to provide protection from an inadvertent quenching (excessive oxidizer flow rate) or starvation (insufficient oxidizer flow rate) throughout the mission duty cycle. The OTV has five basic operating modes, as described below:

a. **Prelaunch.** As vehicle power is initially applied to the valve, the valve is closed automatically by internally generated commands. The valve remains closed independently of any other command until an ignition command is received.

b. **Start.** Within one second from receipt of the discrete OTV start command from the vehicle flight control system, the valve provides oxidizer flow to the TCA corresponding to the boost or analog commands present and the density (temperature) of the oxidizer liquid.

c. **Booster.** Subsequent to ignition, prior to shutdown and upon receipt of the discrete boost signal, the valve will increase the oxidizer flow rate to the maximum allowed, independently of the

152

analog input command. The maximum allowed flow rate is controlled as a time integral of flow by the valve in order to avoid quenching of the TCA during the initial seconds of the mission.

d. Sustain. Subsequent to ignition, prior to shutdown and in the absence of a boost command, the valve proportionally controls oxidizer flow rate in response to the analog command from the AFCS. Also in this mode, command limiting networks prevent TCA quenching throughout the burn. Oxidizer flow is controlled by the analog sustain command until a discrete shutdown command is received.

e. Shutdown. Upon receipt of a discrete shutdown signal from the AFCS, the valve will automatically close independently of any boost or analog command present. The valve will remain closed until another ignition command is received.

The function of the mechanical assembly is to convert the applied electrical energy to mechanical energy and position the flow metering pintle with respect to the seat. The electrical energy is converted into rotational mechanical energy by a torque motor. The rotational motion is then translated into rectilinear motion through a ballscrew and nut assembly. As the flow metering pintle is attached to the ballscrew shaft, any motion of the shaft is imparted to the pintle. Precise positioning of the pintle is achieved by a feedback potentiometer which provides a positioning error signal to the electronic assembly.

The electronic assembly of the OTV provides electrical drive to the torque motor in proportion to an error signal derived from comparison of command and feedback voltages. Additionally, the electronics provide the dynamic compensation required for valve damping and stability margins. The assembly also provides the control logic and sequencing required prior to ignition, during boost, during sustain and during engine shutdown.

The electronics are contained in a housing constructed of stainless steel and designed to interface with the mechanical assembly and mounting interfaces.

17. COMPONENT TESTS

Development testing was conducted on each of the major components in the propulsion system prior to system testing. The test program was minimal in nature, consisting of only tests deemed absolutely necessary to initiate system testing. Qualification of components is not planned until after the flight test program.

a. Multifunction Valve and First Stage Regulator. Extensive testing has been completed on the multifunction leading to several design modifications required to maintain the proper regulation band. A summary of the basic tests is shown in Table XXXI. The multifunction valve was not able to pass qualification tests at -65°F. The low temperature requirements were relieved to 35°F for the flight test program.

All multifunction valves and first stage regulator sets are acceptance tested by installing the sets on a GN$_2$ prepressurization subsystem and simulating a flight duty cycle with regulated pressures and flows recorded. Acceptance test results were excellent once the final design was established.

b. Oxidizer Tank. The oxidizer tank testing consisted of IRFNA ullage and flow tests as shown on Table XXXII. The primary item resulting from these tests was that the tank cannot be used after storing with residual IRFNA. When tanks were used more than once during system tests, they were filled upon completion of the test.

c. Tension Screen. Initially the tension screen was tested individually as shown on Table XXXIII. These tests were found to be invalid due to air exposure not representative of the environment in which they would be used. Subsequent testing consisted of that described in oxidizer tanks in the preceding paragraph.

d. Start Valve. The start valve required a minimum amount of development tests as shown on Table XXXIV. Basic pressure tests showed no leakage problems and pressure loss during flow was negligible.

153

e. **Free Siphon.** The original free siphon design was similar to the final design previously described except the bellows diameter was 1.60 inches and the suspended angle was 135°. This design resulted from numerous preliminary tests involving bearing type siphons which encountered severe leakage problems, especially over a nominal temperature range.

TABLE XXXI. MULTIFUNCTION VALVE TESTS

Tests	Results	Comments
Functional	Start valve portion operated satisfactorily using a Mark 44 pressure cartridge.	
Pressure Regulation	Regulation was 50±5 psig at 12.0 SCFM.	Per specification at this time period. Would not maintain this pressure level at low flow rates as discussed under OMA tests.
Pressure Regulation Band	Regulating band over the flow range of 1.0 to 8.0 SCFM was extremely wide.	Add first stage regulator to eliminate effects of inlet pressure on regulation band.
Pressure Regulation Band with First Stage	Regulation band of 53-73 psig over flow range of 1.0 to 8.0 SCFM. First stage band was 260 to 380 psig over flow range of 2.0 to 10.0 SCFM.	Per specification. All testing conducted at ambient temperature.

TABLE XXXII. OXIDIZER TANK TESTS

Test	Results	Comments
Ullage	Extreme increase in ullage pressure at ambient temp after cycle of ambient, -65°F, +165°F, return to ambient.	Disassociation of IRFNA at high temp.
Ullage	No increase in ullage pressure at ambient after cycle of ambient, -20°F, return to ambient.	Reduce temperature extreme limits.
Flow after exposure to temperature cycles of Tests 1 and 2.	Tension screen pressure drop four times that predicted.	Corrosion severe at +165°F. Repeat tests.

154

TABLE XXXII. OXIDIZER TANK TESTS (Concluded)

Test	Results	Comments
Flow test at ambient	Tension screen pressure drop of 10 psid at 3.6 lb/sec.	Acceptable.
Flow test, soak 72 hrs. at +125°F.	Tension screen pressure drop of 10 psid at 3.6 lb/sec.	Acceptable.
Flow test at ambient	Tension screen pressure drop of 8 psid at 3.6 lb/sec.	Acceptable. Repeated 5 times.
Flow test after residual storage for one week.	Tension screen pressure drop doubled.	Sto... nks only when ... or properly cleaned.
Flow test after residual storage and cleaning.	Tension screen pressure drop of 8 psid at 3.6 lb/sec.	Documented flush procedure is acceptable.

TABLE XXXIII. TENSION SCREEN TESTS

Test	Results	Comments
Storage	No increase in pressure drop after one week in IFRNA at 125°F.	
Storage	13% increase in pressure drop after two weeks in IRFNA at 125°F.	
Storage	Extreme increase in pressure drop after one month in IRFNA at 125°F.	Screen was exposed to air between storage and pressure drop testing, allowing any buildup on screen to dry and harden. All subsequent screen tests are to be in the oxidizer tank under proper environment.

Manufacturing was the primary problem initially, but once tooling was developed the siphon could be made according to schedule. The testing summarized on Table XXXV indicated the design was adequate. System tests defined later in this report will define the problems later encountered with this design which eventually led to the configuration defined in Section III.

TABLE XXXIV. START VALVE TESTS

Test	Results	Comments
Functional	Shear piston forced thru valve housing.	Change from Mark 45 pressure cartridge
Functional	Shear piston forced thru valve housing with Mark 44 cartridge	Install impact absorber
Functional	Valve operated properly using an impact absorber (nylon tapered plug).	

TABLE XXXV. FREE SIPHON ORIGINAL DESIGN TESTS

Test	Results	Comments
Pressure Drop	Less than 0.5 psid through bellows	
Flexibility	No measurable effect at -65°F and +140°F	
Vibration	Vibrated to MIL-STD-810B, Fig. 514.1-4, Curve C without damage.	
Storage	Stored in IRFNA one week at ambient temp. and two weeks at +125°F with no degradation.	
Start transient using solenoid valve to initiate flow.	Siphon floated during fill but sank upon pressurization of tank, only minor movement observed during start transient.	Siphon design is satisfactory.

f. **Ducted Power Unit.** A series of development tests was conducted on the DPU at the vendor (The Marquardt Company). These tests are summarized in Table XXXVI. The major objective of these tests was to document the turbine, alternator and pump performance and to finalize the speed control design.

A preflight rating test (PFRT) program was conducted on one PFRT DPU to demonstrate endurance, cold start-up, ambient start-up and simulated duty cycle operation. Fifteen hundred start-up cycles were accomplished at ambient conditions. These tests simulated the launch sequence that will be used during flight test. Total run time for these tests was seven hours. Two hot air runs at sea level and one at altitude conditions were conducted with the same unit to check out the altitude and heating facility which totaled four hours of run time. The test condition runs are considered to be more severe in terms of total heat input than those which the unit will encounter at the Mach 4.0, 90,000 feet flight condition. The sea level runs were made at 425°F and 690°F.

156

The altitude run was conducted at 63,000 feet and 650°F. Total heat input during each of these tests was approximately 4 times that expected during the Mach 4.0 mission. The combined tests above gave a total endurance time of 11 hours and in addition the unit was acceptance tested a total of one hour.

The PFRT unit was then cold soaked at sea level pressure conditions for 24 hours at -50°F. The DPU altitude facility was set at Mach 1.5 at 50,000 conditions and a launch signal input was given. Alternator voltage rose to 27.9 VDC and the speed control started regulation. Within a 5-second period, output voltage dropped to zero and the test terminated. The unit had failed and was severely damaged. This resulted in a full failure analysis including a full review of the basic design. Failure was attributed to ice buildup on the turbine wheel from the facility causing an unbalanced condition which resulted in a wobble of the turbine wheel. This resulted in excessive loading of the turbine wheel attach bolt which failed in tension. The design modifications resulting from this test were minor and the balancing procedure was changed to one whereby the rotating assembly is never touched once balancing is complete to assure proper balance is maintained in the final assembly.

The PFRT unit was rebuilt and subjected to a more realistic cold test procedure which consisted of running after a two-hour stabilized condition at -50°F. The test installation was identical to that previously used; however, provisions were made in the setup to blow down facility air trapped upstream of the butterfly valve eliminating the possibility of introducing wet air into the unit at the start of the test. The unit was soaked for an additional two hours and 15 minutes at which time start-up was initiated. At the start-up condition, cell ambient and bearing temperatures were -55°F. The test consisted of a 30-ampere load only, a five-minute run, to simulate altitude cruise operation followed by a high power run with full pump load for an additional six minutes. No problems were encountered and normal operation was observed during the test. Start-up was smooth with no evidence of drag or hesitation. Control response to the start-up transient was normal with a minimum of speed overshoot evident.

TABLE XXXVI. DUCTED POWER UNIT DEVELOPMENT TESTS

Test	Results	Comments
Performance mapping of pump, alternator, and turbine	Pump performance as predicted, alternator output 28.0 ±0.5 volts at 45 amps, no leakage through viscoseal.	Tests conducted with S/N 0001.
Speed control development	Forward alternator rotor magnet for start-up failed in fatigue. DPU had operated 9 hours prior to failure.	Eliminate magnets and use external power for excitation during start-up.
Speed control at sea Level and 65,000 feet	Satisfactory speed control operation control band of ± 1.6 percent.	
Speed control at -65°F to + 160°F	Greater than 10 percent drift.	Compensation added and drift reduced to 0.15 percent.
High temperature	Unit performed satisfactorily at bearing temperatures higher than predicted.	Three simulated duty cycles were run.

Following completion of the cold test, the test facility installation was modified for hot running. All electrical lines were insulated and protected from the high temperature environment. Three typical duty cycles at elevated temperature were successfully accomplished. The altitude during this testing was 63,000 feet which is the limit of the facility used and temperatures observed were 670°F, 600°F and 690°F. The duration of each test was again extended such that total heat input during each test was approximately 4 times that expected during the Mach 4.0 mission.

157

During the fourth run, a rapid rise in turbine end bearing temperature was noted, and the test terminated. Examination disclosed a turbine tip and generator rotor rub, and the onset of incipient bearing failure due to a loss of lubrication.

Problems were encountered during propulsion system proof testing and propulsion system PFRT with the rotating assembly building up with contamination subsequent to each test. Several cleaning methods were tried during the test program to establish a suitable procedure and eliminate expensive refurbishment costs.

The last three propulsion system PFRT were conducted with the same DPU without any damage demonstrating a successful shutdown procedure. This was accomplished by letting the GN$_2$ prepressurization subsystem bleed down to 10 psia or less with the DPU still running and the cell at altitude conditions. The cell is brought to sea level conditions with the DPU running. Once at sea level the DPU no longer has sufficient air to operate. This same sequence of events will occur during a normal flight and refurbishment of flight DPU's should be at a minimum.

g. Oxidizer Throttle Valve (OTV). A series of tests were conducted on the OTV electrical and mechanical portions of the valve by the United Technology Center (UTC). The objectives of the OTV electronic components assembly breadboard testing were to:

- Verify circuit continuity

- Determine noise levels at assembly interfaces

- Determine sensitivity of individual circuits

- Demonstrate input/output relationships

- Demonstrate operation of command/control logic

- Demonstrate voltage and current levels at primary points

- Verify math model parameters.

With the exception on the analog buffer amplifier and the error compensation network, no significant problems were encountered. Design changes to the analog buffer amplifier were made and verified to correct a DC shift due to common inputs. Design changes were made to the error compensation network and verified to correct a transfer function.

The OTV was flow tested with Freon 113 to determine its flow characteristics. Tests were also conducted to define the frequency response, transient response to step command, hysteresis and resolution. The results were used to derive the flow equation as functions of command voltage and pressure differential and update the math model. The flow rate was, by necessity, described by two equations. This was found necessary because the fluid cavitates at low flow rates and does not cavitate at high flow rates. The frequency response characteristics of the valve were generally predicted.

The next series of testing was conducted with the preprototype and prototype OTVs consisting of the combined electrical and mechanical components. The objective of these tests was to verify the performance characteristics. Testing was successfully completed with resolutions of all observed problems. Significant problem areas were as follows:

- Failures of power amplifier and regulator microcircuits due to improper bonding to mounting brackets.

- Slow OTV dynamic response at low temperature due to type of bearing lubricant.

- Abnormal motor voltage waveform and power consumption at low temperature.

158

- Excessive feedback potentiometer noise during exposure to vibration.

Design and/or procedural corrections were taken in all cases to assure proper operations of flight hardware.

Temperature extremes during this program were -65°F to +165°F. Vibration was per MIL-STD-810B, Figure 514-1-4, Curves Q and AH.

h.   **Thrust Chamber Assembly (TCA).** A series of 30 heavyweight thrust chamber assemblies were tested by the United Technology Center to demonstrate the propulsion system performance, test component materials and evaluate component configurations. The heavyweight configuration consisted of the case, forward closure and nozzle assembly each using heavy wall construction. These were used to minimize the hardware requirement, each being used for several refurbishments. Oxidizer flow was controlled by external solenoid valves and metering orifices until Test No. 23 when the OTV was added to the system. A summary of these tests is contained in Table XXXVII.

i.   **Igniter.** A series of igniter tests was conducted. These tests are summarized in Table XXXVIII.

j.   **Injector.** The testing conducted for the selection of the injector configuration is summarized in Table XXXIX.

TABLE XXXVII. HEAVYWEIGHT TCA TEST SUMMARY

Test Number	Test Objectives	Test Results
1	Obtain data on ignition characteristics, nozzle erosion, injector flow patterns, fuel regression and internal ballistics.	Nozzle development was required to decrease erosion.
2	Obtain data on ignition characteristics, nozzle erosion, injector flow patterns, fuel regression and internal ballistics.	Further nozzle evaluation indicated.
3	Obtain data on ignition characteristics, nozzle erosion, injector flow patterns, fuel regression and internal ballistics.	Tungsten was ruled out as a throat material.
4	Case insulation material, nozzle, and injector evaluation.	The case insulation being evaluated burned through causing early termination of the test. Further nozzle development was also indicated to reduce throat erosion.

TABLE XXXVII. HEAVYWEIGHT TCA TEST SUMMARY (Continued)

Number	Test Objectives	Test Results
5	Case insulation material, nozzle, and injector evaluation.	A case insulation material being evaluated burned through. The Mod II injector eliminated due to impingement in the nozzle area. The Mod I injector to be used on remaining tests with grain configuration and insulation changes made to compensate for injector effects. Further nozzle development was also indicated to reduce throat erosion.
6	Obtain data on nozzle erosion, nozzle, efficiency, injector flow patterns, fuel regression and internal ballistics.	Improved nozzle entrance section and material using 8882 graphite indicated improvement in nozzle design. Low entrance half angle increased overall erosion.
7	Obtain data on nozzle erosion nozzle, efficiency, injector flow patterns, fuel regression and internal ballistics.	Improved nozzle entrance section indicated improvement in nozzle design over previous tests.
8	Obtain data on nozzle erosion, nozzle efficiency, injector flow regression and internal ballistics.	Improved nozzle entrance section indicated improvement in nozzle design.
9	Case insulation material evaluation. Obtain data on nozzle erosion, nozzle efficiency, fuel regression and internal ballistics. Demonstrate the effect of a fuel rich boundry layer at the nozzle throat.	Results indicated a different grain configuration was needed to increase propellant consumption and also combat injector effects. Silicon case insulation appeared to withstand burn-through better than glass insulation. The nozzle erosion was less than previous tests indicating an improvement in design.
10	Case insulation material evaluation. Obtain data on nozzle erosion, nozzle efficiency, fuel regression and internal ballistics. Demonstrate the effect of a fuel rich boundry layer at the nozzle throat.	The asbestos case insulation did not restrict burn-through as well as the silica which had a more severe duty cycle. A decision was made to use silica phenolic case insulation on remaining tests. Placement of fuel to provide a fuel rich boundry layer appeared to reduce nozzle erosion.

160

TABLE XXXVII. HEAVYWEIGHT TCA TEST SUMMARY (Continued)

Test Number	Test Objectives	Test Results
11	Obtain data on nozzle erosion and efficiency, TCA performance, axial fuel regression and internal ballistics for a nominal boost duration of 112.5 seconds.	The fuel rich boundry layer significantly increased nozzle efficiency. Further development was indicated to reach an optimum grain configuration to increase combustion efficiency while maintaining nozzle efficiency, and case protection.
12	Obtain data on case insulation, nozzle erosion and efficiency, axial regression and internal ballistics.	The fuel rich boundry layer significantly increased nozzle efficiency.
13	Obtain data on case insulation, nozzle erosion and efficiency, axial regression and internal ballistics.	Nozzle results were similar in No's. 11 and 12. Injector Δp was lower than previous tests and performance was down below that on test No. 12.
14	Obtain data on nozzle erosion and efficiency, TCA performance, axial fuel regression and internal ballistics for a nominal boost duration of 75 seconds.	Large stacks of pyrolytic graphite washers in the throat proved satisfactory. The grain configuration still requires change to increase the combustion efficiency. Forward end flooding was believed to have occurred.
15	Obtain data on case insulation, nozzle erosion and efficiency, axial fuel regression and internal ballistics.	The fuel and case insulation sleeve provided full protection to the case. Forward end flooding was believed to have occurred.
16	Obtain data on case insulation, nozzle erosion and efficiency, axial fuel regression and internal ballistics.	The unbonded nozzle throat washers used in test No. 15 proved to be better than the bonded washers from test No. 16. A composite forward closure proved to be better than the unitary graphite phenolic design. Forward end flooding was believed to have occurred.
17	Obtain data on case insulation, nozzle erosion and efficiency, axial fuel regression, combustion efficiency and internal ballistics.	The flight type igniter successfully ignited the TCA and the nozzle, also a flight type, was near optimum. Injector Δp was slightly lower than normal.
18	Obtain data on case insulation, nozzle erosion and efficiency, axial fuel regression, combustion efficiency and internal ballistics.	Thermal data indicated the composite forward insulation performed as predicted.

TABLE XXXVII. HEAVYWEIGHT TCA TEST SUMMARY (Continued)

Test Number	Test Objectives	Test Results
19	Obtain data on case insulation, nozzle erosion and efficiency, axial fuel regression, combustion efficiency and internal ballistics.	Improved combustion efficiency and acceptable nozzle erosion indicated the TCA configuration is near optimum.
20	Obtain data on case insulation, nozzle erosion and efficiency, axial fuel regression, combustion efficiency and internal ballistics.	The duty cycle and nozzle were the same as test No. 17. The combustion efficiency was better on No. 20 than No. 17. Injector Δp was higher. The fuel at the nozzle entrance did not protect the nozzle as well as the configuration used on No. 17.
21	Obtain data on case insulation, flight-weight design forward closure insulation, nozzle erosion and efficiency, axial fuel regression, combustion efficiency and internal ballistics.	Ignition flooding and a performance drop-off at 34 seconds into the firing was observed. The least risk approach to correct the performance problem was to change the forward fuel billet to increase ignition and combustion recirculation in the forward end of the TCA. The injector Δp was lower than normal during this test.
21-R1 (Test 22)	Obtain data on case insulation, flight-weight design forward closure insulation, nozzle erosion and efficiency, axial fuel.	The change made on the forward fuel billet corrected the ignition flooding problem, but did not have any effect on the performance drop off. Performance drop off occurred at 42 seconds into the test, followed by a recovery approximately 20 seconds later. The injector Δp was again much lower than normal.
23	Demonstrate CTA thrust control by varying OTV commands and therefore oxidizer flow rate. Obtain data on case insulation, nozzle erosion and efficiency, axial fuel regression, combustion efficiency, internal ballistics and OTV performance.	The feasibility of the CTA concept was established. The OTV and TCA performed together to give smooth ignition and a variable thrust duty cycle conforming to all valve commands. Nozzle results were excellent.
21 R2	Terminate test 45 seconds to investigate fuel grain geometry injector, and forward closure insulation effects in the TCA.	The test was completely successful - no performance drop off occurred. The test results and an examination of the interior of the TCA substantiated the theory that combustion degradation is related to both the injector Δp and the forward closure geometry.

TABLE XXXVII. HEAVYWEIGHT TCA TEST SUMMARY (Concluded)

Test Number	Test Objectives	Test Results
25	Same as Test No. 23.	Thrust was an exact duplicate of CTV commands. Injector Δp appeared lower than normal. Nozzle results were excellent.
26	Obtain data on case insulation, nozzle erosion and efficiency, axial fuel regression, combustion efficiency and internal ballistics.	Higher pressure drop across the injectors (220 vs 150 psi) produced good atomization of the oxidizer and resulted in good combustion efficiency in the TCA. A modified forward closure with extended injectors increased the fuel utilization. Nozzle erosion was 0.3 mils/second.
27	Duplicate the results achieved on test No. 26.	This test established the repeatability of performance by duplicating the performance of test No. 26. Nozzle erosion was 0.2 mils/second.
28	Demonstrate an all boost capability for a total duration of 145 seconds.	This was a successful test which demonstrated the full boost capability of the CTA. Delivered total impulse was 154,690 lbs/sec which was one percent higher than predicted. Nozzle erosion was 1.3 mils/sec.
29	Demonstrate a boost duty cycle consisting of a nominal boost thrust of 1200 lbs (vac) and an average sustain thrust of 250 lbs (vac) for a total duration of 370 seconds after being conditioned to -55[F.	This was a successful test which demonstrated CTA capability and operation at -55°F. Nozzle erosion was 0.6 mils/sec.
30	Demonstrate the duty cycle of Test No. 29.	This was a successful test which demonstrated CTA capability and operation at +165°F. Nozzle erosion was 0.1 mils/second.

TABLE XXXVIII. IGNITER TEST SUMMARY

TEST OBJECTIVES	TEST RESULTS
1. Design and perfect an igniter capable of igniting a HAST Controlled Thrust Assembly (CTA) while physically not exceeding the interface envelope stipulated by Beech Aircraft Corporation.	A successful series of ten igniter tests culminated the developemnt of an igniter suitable for use in the temperature range of -55°F to +165°F.
2. Develop an igniter which would ignite the CTA at extreme temperatures (-65°F to +165°F).	

TABLE XXXIX. INJECTOR TEST SUMMARY

TEST OBJECTIVES	TEST RESULTS
1. Select by cold flow testing, two injector configurations from various injector candidates. The two selected configurations will be tested in heavyweight TCA's to determine the preferred configuration.	A successful series of tests led to the the selection of a modified FULL JET injector and a UTC designed aeration orifice. The initial design was modified for use in the final series of tests to increase the pressure across the injector. (Reduction in orifice diameter.)
2. Test and perfect an aeration system compatible with the selected injectors that is suitable for TCA operation at sustain oxidizer flow rates.	

18. OXIDIZER MANAGEMENT ASSEMBLY TESTS

Oxidizer management assembly testing at the Marquardt Company used an assembly consisting of the OMA hardware described earlier in this section plus a HAST mid-section for DPU mounting. A total of six tests were run. Freon 113 was used as the test fluid on Tests 1 thru 5 and water on Test 6. Development problems on the initial burst disc design resulted in its elimination from the test hardware. The burst disc coin thickness was extremely thin for the low pressure burst, and cracking occurred during coining, installation, or application of tank ullage pressure. The size of the burst disc was increased which allowed a thicker and stronger coin.

All the OMA components operated properly with the exception of the multi-function valve regulator. The regulator was acceptable at the boost flow conditions but raised to unacceptable pressures during sustain flow conditions. A design study was conducted and several design modifications made to correct the regulated pressure.

The turbine, pump, and alternator operated normally with proper air supply. OMA air supply difficulties alerted the contractor to make a careful study of the air supplies to be used during propulsion proof and PFRT.

It was determined the piston in the oxidizer start valve will need to be added to the refurbishment kit. Repeated firings of the same piston tended to deform it and make removal impossible without damage to the valve housing.

The tankage compartment concept to control cg travel during flight functioned properly and Δp across the tension screen was as predicted. Free siphon operated properly during all tests.

19. PROPULSION PROOF TESTS

A propulsion proof test series was conducted at United Technology Center using five flightweight hybrid propulsion systems. The tests conducted were to demonstrate integrated propulsion system performance using the OMA and CTA. Testing involved evaluations of IRFNA filling, GN2 filling, DPU performance and control, OTV performance, and TCA operation and performance.

a. **Proof Test No. 1.** The first hybrid propulsion system proof test was successfully completed on 20 July 1972. The test article consisted of the flight configuration OMA and digital logic circuitry used in the HAST vehicle mated to the flight configuration CTA. Turbine operation was accomplished with the direct connect facility compressed air supply.

A complete launch sequence was initiated with the digital electronics including select, launch ready, launch command, GN2 start, oxidizer start, CTA ignition, and OTV ignition. The first flight

164

test duty cycle was simulated by preprogramming boost cutoff to occur at approximately 38 seconds from ignition and controlling the OTV directly during sustain. The OTV shutdown discrete was initiated from the facility control room at approximately 220 seconds.

Turbine RPM was between 5 and 10 percent low during boost and sustain due to a speed control and facility air supply matching problem. Pump discharge pressure, chamber pressure, and oxidizer flow rate were consistent with predicted values for the observed turbine speeds.

A successful demonstration of the multifunction valve regulator was performed prior to testing. However, due to inadvertent exposure to IRFNA fumes during filling the multifunction valve was replaced by a facility regulator during the proof test. Contamination of the multifunction valve was caused by the premature rupturing of the burst disc. Development of a new burst disc was near completion and incorporated into subsequent proof tests. Post-test inspection of the multifunction valve indicated no visible degradation due to the IRFNA exposure.

b. Proof Test No. 2. The second propulsion system proof test was completed on 4 August 1972. A complete launch sequence was successfully initiated with the digital electronics. Boost cutoff occurred at 87 seconds. The test was terminated at approximately 290 seconds.

The multifunction valve (all functions), burst disc, oxidizer start valve, pump, DPU, CTA, and digital electronics all performed satisfactorily.

The following problems occurred during the test:

      (1) Speed control did not regulate properly

      (2) Sharp drop in pump discharge pressure occurred at 209 seconds.

      (3) Poor TCA performance was observed during sustain.

The cause of the low TCA performance during the second proof test was due to insufficient aeration resulting in incomplete combustion during sustain. Since the aeration system used in the heavyweight test program consisted of a choked orifice supplied by a constant upstream pressure, a similar system was selected for use on the flight propulsion system. This change was incorporated by replacing an aeration regulator with the first stage regulator and multifunction valve defined in paragraph 2 of this propulsion section.

An oxidizer tank with windows in the aft and next to aft compartments was constructed to fully evaluate the flow phenomenon associated with the free siphon and determine the drop in pump discharge pressure at 209 seconds. These tests indicated the free siphon was affected by GN_2 bubbles when the last tank compartment is being emptied causing the siphon to float to the top of the tank. A weight was added to the siphon and expulsion was normal.

Checkout of the speed control disclosed that the position feedback potentiometer orientation was displaced and as a result feedback voltage went to zero as the potentiometer rotated through an open segment of the resistance winding. This was reset and normal feedback voltage was noted although the unit was found to be controlling below 30,000 RPM.

c. Proof Test No. 3. Prior to proof test No. 3, an OMA cold flow test was successfully completed. The test duration was 440 seconds with a 73 second boost. The test digital electronics system was used to sequence the GN_2 start and oxidizer start events. Oxidizer flow was controlled with facility venturi. The GN_2 aeration system was isolated during boost allowed to exhaust to ambient during sustain.

All portions of the OMA functioned properly during the test. System pressures and turbine speed were consistent with component acceptance test data. The butterfly valve and speed control maintained the proper turbine speed after a slight adjustment of the facility air supply during boost. Approximately 6 pounds of IRFNA remained in the oxidizer tank at the completion of the test.

The third propulsion system proof test was conducted on 23 September 1972. A DPU failure occurred at approximately 150 seconds after ignition. The first indication of malfunction was a drop in pump discharge pressure and RPM. This was followed by erratic RPM and a sharp drop in alternator voltage. Initial post test visual inspection revealed that one turbine blade was missing and several other blades were slightly damaged. The butterfly valve actuator linkage could be moved freely by hand from open to close. Prior to the failure, all system parameters appeared normal.

Examination of the DPU disclosed that the turbine end generator rotor balance ring had loosened from the rotor proper. The turbine end bearing had failed, and the generator rotor laminate stack, at the turbine end, had severe physical damage in the area of its contact with the generator stator. Evidence of severe heat was present on only the rotor laminate stack and generator stator assembly.

The loose balance ring, held in place by epoxy only, had caused an unbalanced condition equal to 0.1 ounce-inch in the DPU balance assembly. This condition resulted in radial loads far in excess of the capability of the turbine end bearing, and caused the bearing to fail. The DPU is normally balanced to 0.005 ounch-inch. The DPU balance ring and laminate stack was changed to an all welded assembly.

d. Proof Test No. 4. Proof Test No. 4 was successfully conducted on 30 November 1972. The duty cycle was a simulated Mach 3 at 80,000 feet mission. The boost phase ran for a total of 82 seconds with an oxidizer flow rate of 3.55 lb/sec and average chamber pressure of 395 psia, both nominal. The sustain phase at an average oxidizer flow rate of 1.25 lb/sec and average chamber pressure of 85 psia. The total duration was 253 seconds, slightly less than was predicted and is attributed to higher than predicted nozzle erosion.

Total oxidizer loaded was 492 pounds. All data indicates a highly successful test. Inspection of the hardware indicated it to be in excellent condition.

e. Proof Test No. 5. Proof Test No. 5 was successfully conducted on 1 December 1972. The duty cycle simulated the first flight mission. The boost phase duration was 34.5 seconds at an oxidizer flow rate of 3.51 lb/sec. The total duration was 234 seconds, slightly higher than predicted. The sustained flow rate was an average of 1.55 lb/sec. All performance parameters indicated normal operation. Inspection of the hardware indicated it to be in excellent condition.

f. OMA Testing at AFRPL. Also a series of tests was conducted at Air Force Rocket Propulsion Laboratory (AFRPL) to assure the system would perform properly at altitude conditions.

A free siphon failure occurred on the first test during the boost flow portion. The failure was attributed to excessive pressure drop across the siphon due to improper clearance between the entrance of the siphon and the bottom of the oxidizer tank. This siphon was not a current configuration and did not receive an inspection of the siphon clearance during manufacture. The second and third OMA tests were performed with the latest configuration siphon and no further siphon problems occurred.

Excessive pump cavitation was observed at high oxidizer flow rates on the next two tests. Subsequent bench tests revealed that a facility hand valve located between the multifunction valve and the oxidizer tank was restricting the normal flow of GN_2 into the oxidizer tank.

The fourth altitude OMA was conducted at AFRPL and excessive pump cavitation was observed. This problem was attributed primarily to an excessive pressure drop through the tension screen due to extended IRFNA exposure. A thorough investigation was conducted to better define all pressure drops ahead of the pump. The following action was taken as a result of this investigation: (1) Oxidizer tanks will be thoroughly cleaned or stored in the full condition before each use to insure a clean tension screen; (2) The burst disc adapter was redesigned to reduce the burst disc pressure drop; (3) The multifunction valve 2nd stage regulator was reset to increase the regulated pressure by 10 psia establishing the final band of 53 - 73 psig.

166

The fifth altitude OMA conducted at AFRPL had all modifications incorporated and the test was successful. The results of this test indicated the OMA and test facility were ready for PFRT initiation.

20. PROPULSION PFRT

A series of nine propulsion PFRTs were conducted at the AFRPL to demonstrate the performance of the HAST propulsion system. A summary of the test results is shown in Table XI, followed by a description of each test and discussion of questionable data.

a. PFRT No. 1. PFRT No. 1 was successfully fired on 10 February 1973. The performance of the propulsion system was as predicted. All hardware was in excellent condition with the exception of the GN_2 first stage regulator. Examination of the regulator indicated an excessive hard seat which appeared to have been caused by IRFNA exposure. The data shows the output of the regulator was significantly higher than normal; however, it did not affect motor performance. All O-rings in GN_2 system regulators were changed as part of the refurbishment procedure in further tests. Total oxidizer loaded was 420 pounds. The thrust measurement exhibited a large zero shift at the beginning of the test and did not return to the same level at burnout. There was no certainty of the zero during the test making thrust questionable. This is further indicated by nominal chamber pressure associated with the low thrust value.

b. PFRT No. 2. The second altitude PFRT was performed on 10 March 1973. A free siphon failure occurred at approximately 19 seconds after launch. All system parameters were nominal prior to the failure. The oxidizer flowrate dropped from 3.44 lbs/sec due to the collapse of the siphon and remained there for approximately 200 seconds. At approximately 219 seconds the flowrate abruptly increased as the Teflon© ripped, thereby reducing the blockage of the tank outlet.

Tests were conducted by the contractor to establish the failure mode of the free siphon during PFRT No. 2. These tests utilized the HAST oxidizer tank with plexiglas windows to observe the free siphon. The tank was filled similar to the method used with the IRFNA fill rig. A ball valve was used at the tank outlet to simulate the oxidizer start valve.

The tests were initiated using a new free siphon. An ullage pressure was placed on the tank and the ball valve opened, simulating a normal flight start. Flow was set at a rate simulating pressure drops that would be evident during a normal boost. No effect on the free siphon was observed during several flow tests. To further simulate flight starts, the line downstream of the start valve was evacuated, which is the flight condition. Flow tests were repeated and no effect on the free siphon was observed. The siphon could be made to collapse at extremely high flow rates which was not the case when failure occurred during PFRT No. 2.

A series of free siphon tests using all components of the flight system was conducted at AFRPL. A HAST oxidizer tank with plexiglas windows was utilized to obtain movies and videotape data on the free siphon. The major objective of these tests was to determine if a physical deformation is required for a free siphon failure or if altitude start-up transients could cause the failure.

The test results indicated that the free siphon was deformed during the start-up transient coincident with oxidizer start valve initiation. The deformation was caused by the fluid forces associated with the high velocity of the fluid during the start-up transient. The free siphon did not fail during every start-up; however, during those tests where failure did not occur, the tendency toward failure was evident. Based on these tests, the following action was taken:

(1) A solid tube type siphon was installed in the OMA in order to continue propulsion PFRT at AFRPL.

167

TABLE XL. PROPULSION PFRT SUMMARY

ITEM	PFRT NO.	NOMINAL	1	2	3	4	5	6	7	8	9
Duration (Sec)	Boost		38	80	83	65	125	62	88	83	83
	Total		263	290	277	270	168	264	276	260	268
First Stage Pressure, (psig)	Boost	260-380	500	290	265	285	318	140	171	290	215
	Sustain		300-148	265	335-360	260-275	306-316	200	167-258	230-420	260-270
Pump Inlet Press. (psig)	Boost	30	30.4	49.0	34.2	24.2	40.0	42.0	40.8	39.0	43.0
	Sustain	30	40.8-57.0	2.5-70.0	56-73.8	39-59	50-64	54-68.7	48-76.4	58-74.5	58.8-70.4
Pump Outlet Press. (psia)	Boost	685	764	820	720	675	685-740	750	730	750	690
	Sustain	685	776	65	790	750	740	775	760	800	735
Tension Screen ΔP (psid)	Boost	11	7.1	8.8	15.4	25.5	5.0	4.4	5.4	9.8	10.8
	Sustain	11	1.4-2.1	--	2.0-4.6	4.0-24.0	0.2	0.1	0.7	2.1	2.0-7.5
Thrust (lbs)	Boost	1200	1170	1280	1250	1170	1140-1260	1240	1240	1280	1190
	Sustain	--	320-550	180	270-290	290-390	250-280	210-300	200-250	270-340	305
Chamber Pressure (psia)	Boost	400	432	320	395	410	288-436	430	424	430	375
	Sustain	--	100-190	58	82-90	108-148	67-78	68-110	56-68	77-100	80
Oxidizer Flow Rate (lb/sec)	Boost	3.6	3.6	3.4	3.7	3.4	4.1	3.6	3.6	3.8	3.7
	Sustain		1.4-1.6	3.5	0.8-1.4	0.8-1.6	0.9	0.8-0.9	0.6-1.45	0.8-1.6	0.9-1.6
Fuel (lb)	Used	147	135.8		149.1	145.9	142.4	147.3	147.3	150.5	153.0
Oxidizer (lb)	Used	488	407	400	476	448	479	468	500	468	484

(2) A quick fix for flight vehicles already cc was inspected per existing tank was used to determine the feasibility of removing the Teflon® from an installed free siphon. The removal was successful and was to be used as a quick fix for vehicles with compatible recovery weights.

(3) Two new siphon designs were investigated. One design (Design B) is similar to the former free siphon except the bellows diameter was increased from 1.20 to 2.90 inches and the suspended angle changed from 135° tc 90°. Changes in the number of coils and free length also resulted from the increased diameter. The second design (Design A) is a one-degree-of-freedom solid tube type with a Teflon® face seal at the swivel joint connecting the stationary and movable tubes.

(4) Test programs were initiated to duplicate the test results at AFRPL with the former free siphon in order to evaluate the new designs without the elaborate setup used at AFRPL. The free siphon testing conducted at AFRPL showing the free siphon deforming during the start transient was duplicated by using two air operated ball valves to replace the start valve and throttle valve and evacuating the volume between the two for altitude simulation.

Design A proved satisfactory during static expulsion tests and as then flight tested to determine its ability to follow a resultant g vector. The siphon placed in the plexiglass window tank which together with a pressurization source and orifice were mounted in a light aircraft. A movie camera was used to record the ment and a g meter was used to record the negative g environment. The siphon followed the resultant g vector only during the no-flow condition. The siphon remained on the bottom of the tank during flow periods of 5, 10, 15 and 21 gpm with negative g values of 0.2 to 0.3. Design A was thus eliminated from the test program.

Design B with a 0.078 inch diameter coil wire operated satisfactorily during ten start transients. There was no deformation to the coils and flow was unrestricted at boost flow rates. The siphon was then vibrated according to MIL-STD-810B, Figure 514.1-4, Curve C in each of three axes and did not encounter leakage. Earlier vibration testing had indicated wear through the heat sinkable Teflon® which was initially 0.003 to 0.005 inch thick. Increasing the thickness to the 0.005 to 0.007 inch eliminated this problem. It was then cooled to -65°F to determine cold performance and no change was evident in the flexibility characteristics when compared to these at ambient conditions.

Design B was then flight tested to determine its ability to follow the resultant g vector. The siphon followed the resultant g vector under all flow conditions including no flow. The flow rates were 5, 10, 15 and 21 gpm with negative g values ranging from 0.2 to 0.3. Design B was selected as the final configuration with the first unit being used for PFRT No. 8.

c. PFRT No. 3. PFRT No. 3 was successfully completed on 3 May 1973. The duty cycle was that of the Mach 3 at 80,000 feet mission. All system components functioned properly. Total oxidizer loaded for this and the remaining tests was 496 pounds. When examining the total oxidizer used during each test, it should be pointed out that the best accuracy that can be attained on this measurement is ±3 percent. Visual examination of IRFNA remaining after each test indicated at least 488 pounds were used during PFRT No. 3 thru PFRT No. 9.

d. PFRT No. 4. PFRT No. 4 was successfully completed on 24 May 1973. A zero shift in the facility load cell during the test prevented the predicted thrust time history from being followed during sustain. Excessive tension screen pressure drops were observed, causing a slight reduction in maximum boost flow rates. Post test inspection revealed severe corrosion inside each compartment of the oxidizer tank and on the forward surface of the tension screen. The IFRNA temperature was lost during this test making flow rate corrections invalid. Total oxidizer used, assuming the IFRNA at 70° during the entire test resulted in 162 pounds.

The AFRPL conducted an inhibitor analysis on IFRNA used and determined the inhibitor content to be sufficient. Inhibitor content was originally believed the cause of the pressure drop.

The history of each tank used at AFRPL was studied indicating that the pressure drop could be correlated with the number of cleanings the tank had gone through and that the acid baths were

probably etching the tank surface making it more susceptible to corrosion. PFRT was continued using tanks that had been through only the original acid cleaning and water flushing.

A test program was initiated at Beech to verify the correlation between cleaning and corrosion. This consisted basically of exposing tank material samples to a various number of IRFNA storage and cleaning cycles and an analysis of the samples and of the IRFNA.

The results of these tests indicated the tank corrosion problem encountered during PFRT was not associated with the number of tank cleanings. Subsequent PFRT's were conducted with a tank that had only one cleaning and corrosion was at a minimum; however, the IRFNA used for PFRT was changed from AFRPL supplied to contractor supplied at this time period. This indicated the problem was probably associated with the IRFNA used rather than the number of cleanings completed on each tank.

e. PFRT No. 5. PFRT No. 5 was successfully completed on 28 June 1973. The duty cycle was a Mach 4 at 90,000 feet mission. The data indicates all system components functioned properly. The total oxidizer data was marred during this test by bad time increments caused by instrumentation overheating. An attempt to correct the data resulted in a total flow measurement of 480 pounds. The high flow during boost gives an indication of the nozzle erosion associated with the long boost.

f. PFRT No. 6. PFRT No. 6 was successfully completed on 3 July 1973. The duty cycle consisted of a 62-second boost, with a simulated 180° turn maneuver during sustain. The sustain data does not exhibit the thrust increase required during the maneuver. Total flow was again in question. All components functioned properly with the exception of the first stage regulator which was low. This did not appear to hinder the performance of the propulsion system because periods of sustain flow were in the range where first stage regulator was high enough to provide sufficient aeration.

g. PFRT No. 7. PFRT No. 7 was successfully completed on 12 July 1973. The duty cycle consisted of an 83-second boost with a scheduled decrease in flow occurring at approximately 50 seconds to simulate a turbine RPM limit condition. First stage regulated pressures were low during sustain. Post test disassembly revealed black carbon like particles in the area of the seat. The origin of these particles is uncertain; however, special precautions in keeping all GN$_2$ lines sealed were taken and the problem did not recur.

h. PFRT No. 8. PFRT No. 8 was successfully completed on 28 August 1973. The propulsion system was soaked at -40°F for 25 hours prior to the test. Approximately 1.75 hours elapsed between cold soak and ignition and the IRFNA temperature had warmed to -5°F. The duty cycle consisted of an 83-second boost and total duration of 260 seconds. This was a duplication of the Mach 3.0 at 80,000 foot mission which was earlier conducted on PFRT No. 3 at ambient temperature. The duration was approximately 17 seconds shorter than at ambient which was expected.

The first stage regulator was operating below the minimum pressure during the early sustain phase followed by a step increase. The multifunction valve regulator outlet pressure started a steady decrease at this time and the first stage dropped to an acceptable value. The multifunction valve regulator data can be duplicated by assuming there was no flow through it and the tank was depleted by blowdown of the nitrogen in the ullage volume at that time. Post test flow checks of the multifunction valve indicated normal operation and disassembly revealed no anomalies.

The flow stoppage in the valve was attributed to icing in the regulator or check valve. Moist, ambient air could have entered the GN$_2$ prepressurization subsystem during fill as several leaks were encountered requiring the disconnection of all lines and heating and cooling of the GN$_2$ bottle from pressurization and depressurization.

i. PFRT No. 9. PFRT No. 9 was successfully completed on 13 September 1973. The propulsion system was heat soaked at +125°F for approximately eight hours on 11 September 1973, returned to ambient on 12 September 1973, and soaked at +125°F for approximately 10

170

hours prior to the test on 13 September 1973. The duty cycle again was a duplication of the Mach 3 at 80,000 feet mission conducted on PFRT No. 3. All system components functioned satisfactorily during the test.

j. **Conclusion.** The propulsion system completed nine PFRTs and with the modifications incorporated during the test program is considered acceptable for the flight test program.

SECTION X

RECOVERY SYSTEM

Design, development, and testing of the HAST Recovery System was completed during Phase II of the HAST development program. During Phase I a three-stage design consisting of a drogue, reefed main, and fully developed main was selected based on total system requirements. Subcontractors, Irvin Industries, Inc., and Quantic Industries developed the parachute system and safe-and-arm device, respectively, while Beech Aircraft performed systems integration and developed the parachute container which includes the pyrotechnic deployment hatch.

A series of seven flight tests at the El Centro parachute test facility resulted in the selection of a 6.9-foot ribbon chute for the drogue and a 43.0-foot ringsail for the main canopy. The use of a structural cover to deploy the drogue parachute and helicopter retrieval were also proven feasible during this test program.

1. INITIAL HAST RECOVERY SYSTEM FLIGHT TESTS

Subsequent to providing the parachute system integrity and feasibility of helicopter retrieval of a parachute of this size, the recovery system was tested in a vehicle aerodynamically similar to HAST so the performance of the parachute and vehicle could be evaluated. Two Sandpiper target vehicles were modified to provide a HAST Recovery System Test Vehicle (HRSTV) consisting of adding a HAST recovery system and an auxiliary recovery capability. The HAST recovery system modular design was incomplete at this time period and an interim design was used to contain the parachute system.

The basic operation of the recovery system is shown in Figure 84. An electrical signal is sent to the detonators firing the linear shaped charge and thereby removing the hatch cover. The hatch cover removes the drogue bag through a cable arrangement and pulls the bag from the 6.9-foot diameter ribbon drogue chute upon line stretch. The drogue remains inflated for 8 seconds to decelerate the vehicle after which the drogue release mechanism is initiated. The drogue chute then pulls the main bag from the main chute at line stretch. The 43-foot diameter ring sail main is initially reefed. The reefing cutters are activated 10 seconds after main deployment for further vehicle deceleration, completing the recovery system cycle. The target vehicle is thus ready for aerial retrieval with land or sea retrieval as back-up.

The initial flight tests were conducted at Point Mugu and Edwards Air Force Base. A summary of these tests is contained in Table XLI.

2. DESIGN

This section defines the initial baseline design of the recovery system module utilizing the results of Phase I testing. Modifications made to this design as a result of Phase II testing are specified throughout the remainder of this section.

a. **Parachute.** As a result of the Phase I flights the fundamental parachute design was considered to be sound. However, as test flights were being conducted, the recovered weight of the HAST vehicle gradually increased. This increase was approximately 40 pounds. In order to keep the descent rate of the vehicle at a maximum of 25 ft/sec, the drag area of the main canopy had to increase and the diameter of the main canopy was increased from 43 feet to 45.5 feet. It was deemed desirable not to increase the weight of the parachute assembly if possible. To trade off this increased diameter with weight it was necessary to decrease the strength of some of the elements, specifically, the engagement network, suspension lines, and radial tapes. Data from Phase I testing indicated the structural loads to these items were lower than predicted.
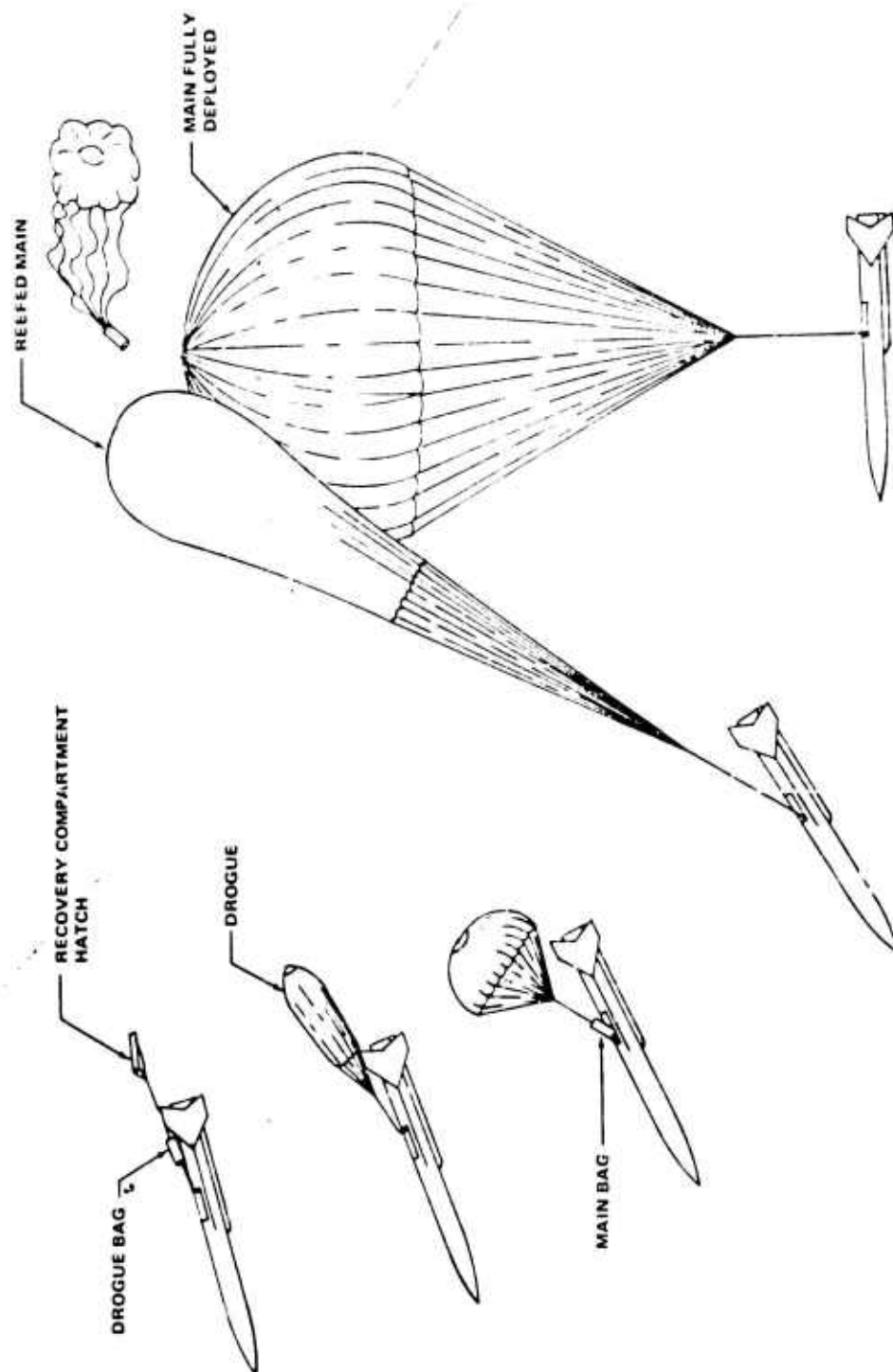
Figure 84. Recovery System Deployment Sequence

173

The basic design consists of two parachutes comprising a three-stage deceleration system as shown on Figure 85. The drogue and main parachutes are packed as a module with the drogue pack retained in flaps attached to the rear upper section of the main deployment bag. It is held to the main pack with retention flaps. An inter-connecting cover bridle is attached to a break cord closure on the retention flaps and this break cord is separated immediately prior to drogue pack extraction. The drogue riser is attached to a pin puller disconnect and is attached to the main pack extraction straps.

TABLE XLI. RECOVERY SYSTEM
FLIGHT TEST RESULTS AT PT MUGU AND EDWARDS AFB

TEST NUMBER	INITIATION ALTITUDE (FT)	INITIATION SPEED (MACH)	REMARKS
1	- -	- -	Autopilot Malfunction, Vehicle Lost
2	20,200	0.40	Recovered on Third Pass at 4,940 Feet
3	19,800	0.41	Recovered on First Pass at 10,200 Feet
4	36,300	0.63	Recovered on Second Pass at 8,400 Feet
5	46,000	0.72	Main Chute did not Deploy, Vehicle Lost, Insufficient Data for Analysis
6	19,200	0.40	Recovered on First Pass at 9,200 Feet
7	48,500	0.80	Recovered on First Pass at 9,800 Feet
8	48,500	0.80	Premature Main Deployment, Vehicle Lost, Drogue Released with Shaped Charge Initiation, Contributed to Relay Shock

At drogue release the drogue extracts the main parachute bag from the compartment and pulls the bag away from the main at line stretch.

174
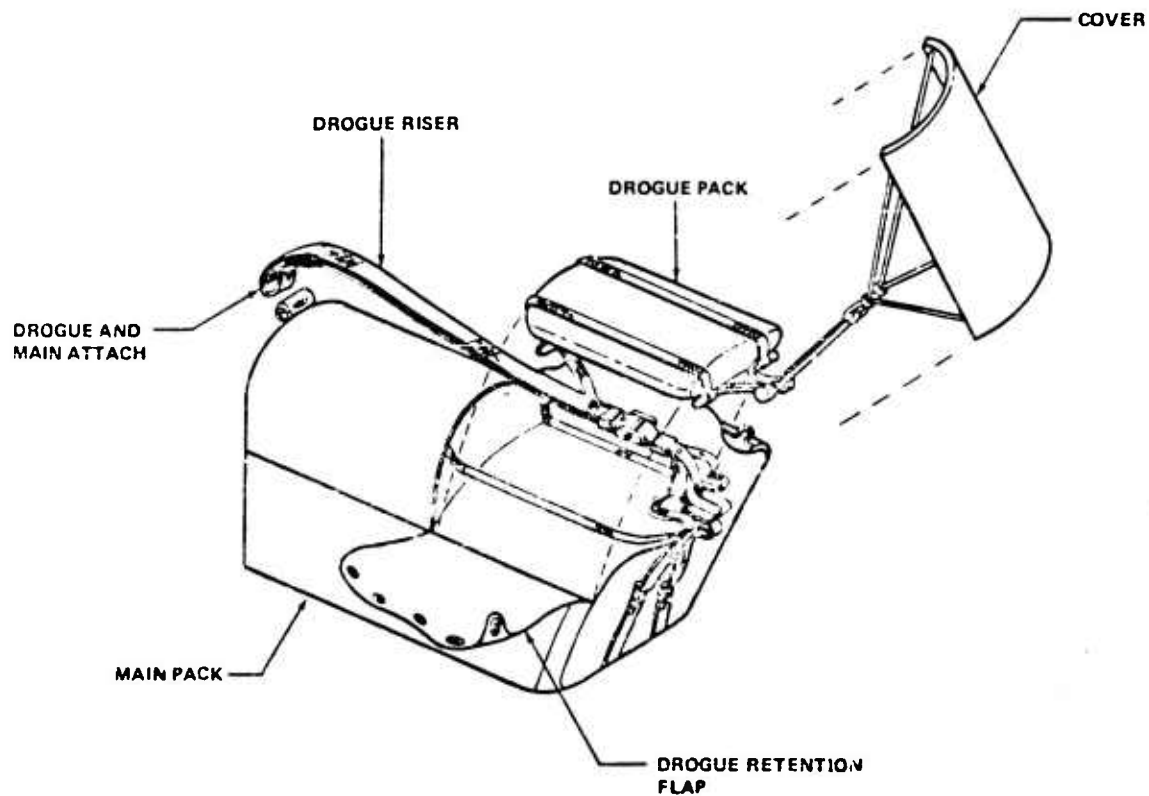
Figure 85. Parachute System

The main parachute is a conventional ringsail design with a cross-over network of pickup straps for aerial retrieval. These pickup straps are formed as two loops crossing the vent and are routed along diametrically opposite radials and suspension lines to final attachment at the riser. The design characteristics of the parachute are as follows:

Nominal Diameter, D_o	=	45.5 ft
Nominal Area, S_o	=	1593 ft^2
Drag Coefficient, C_{D_o}	=	0.70
Suspension Line Length/ Diameter Ratio, $1_S/D_o$	=	1.1
Ringsail Fullness	=	5.5%
Reefing Ratio, $(C_DS)_R/ (C_DS)_o$	=	0.165
Reefing Time Delay	=	10 seconds
Number of Gores, Z	=	36

The main parachute is illustrated in Figure 86.

175
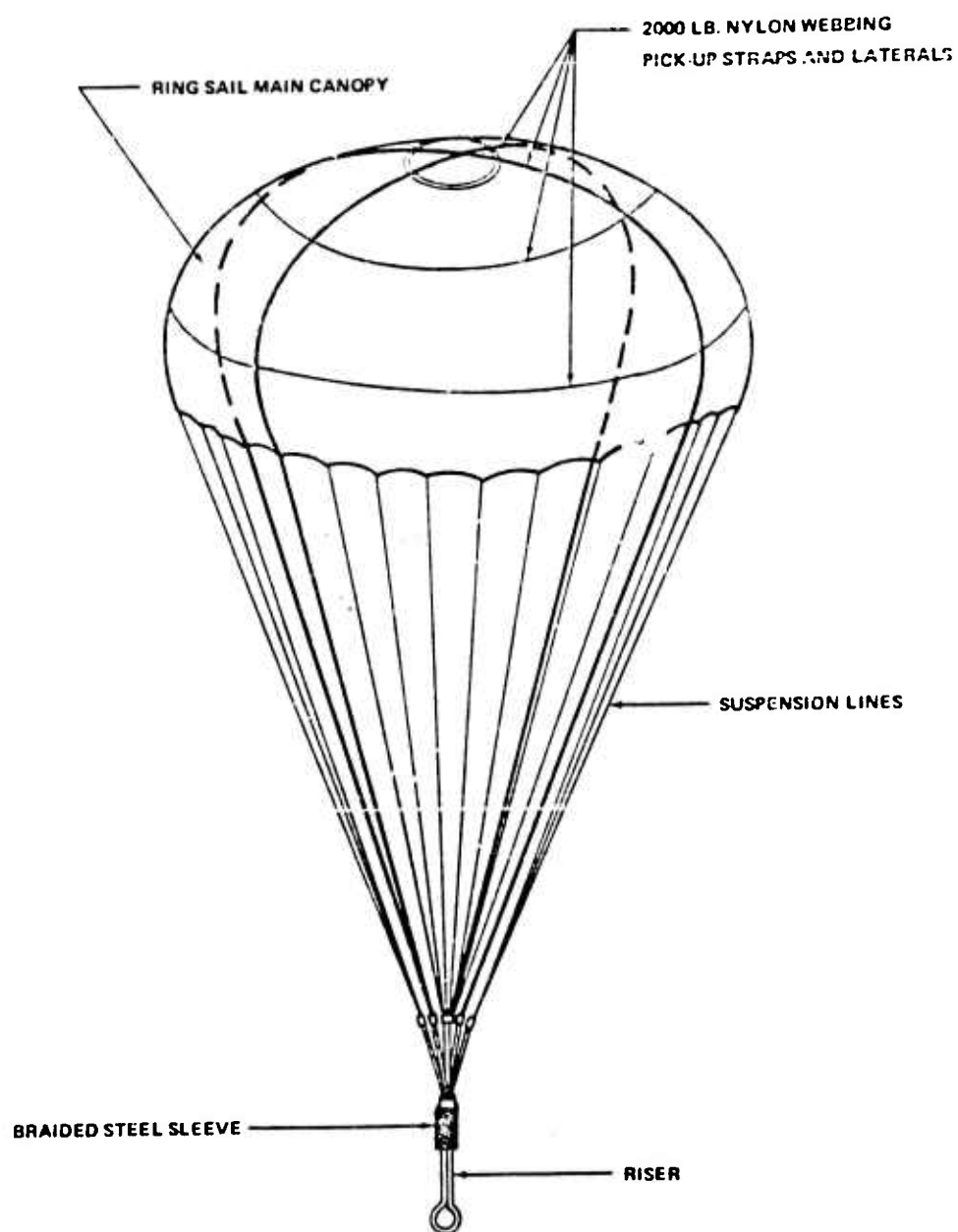
Figure 86. HAST Main Parachute

176

The design characteristics of the drogue are as follows:

Type		Conical Ribbon
Nominal Diameter, D_o	=	6.9 ft
Nominal Area, S_o	=	36.8 ft^2
Drag Coefficient, C_D	=	0.55
Number of Gores, Z	=	8
Cone Angle	=	20°
Suspension Line Length/ Diameter Ratio, l_S/D_o	=	1.0

The component weights of the recovery system are summarized as follows:

Drogue Parachute	2.12
Drogue Deployment Bag	0.31
Deployment Bridle	0.18
Main Parachute	29.76
Main Parachute Riser	0.90
Main Deployment Bag	2.00
Reefing Line	0.12
Reefing Cutters	0.06
Total Parachute System Weight	35.45 pounds

The system is packed into a 1527-in^3 envelope which is nominally one-eighth inch smaller than the compartment. This is done to account for "growth" of the pack during transfer to the compartment. The packing density required is 40.1 pounds per cubic foot.

b. Recovery System Module. The recovery system module consists of the components shown cn Figure 87.

(1) Pan and Cover. The parachute pan is required to be lightweight and sufficiently stiff for storage for long periods of time without excessive deformation or bulging. These requirements were basically met by constructing the pan of rigidized aluminum (sheets with raised diamond pattern) bonding two sheets together with the diamond patterns oriented to maximize bending stiffness. Three brackets are attached to each side of the pan for attachment to the structural cover. The sides have a 3° slope and the back is 14° slope to allow the parachute to be easily extracted during operation.

The cover is a rolled piece of 0.125 inch 17-4 PH stainless steel sheet which is chem-milled to a nominal 0.040 inch thickness in the center area leaving an inch wide flange along the perimeter. The flange is required for structural loads and fastening the cover to the vehicle. The nominal 0.040 inch thickness is a critical number in that the minimum allowable for the loads carried is 0.035 inch and the maximum of safe cutting with the shaped charge used is 0.050 inch. The practical tolerance in

177
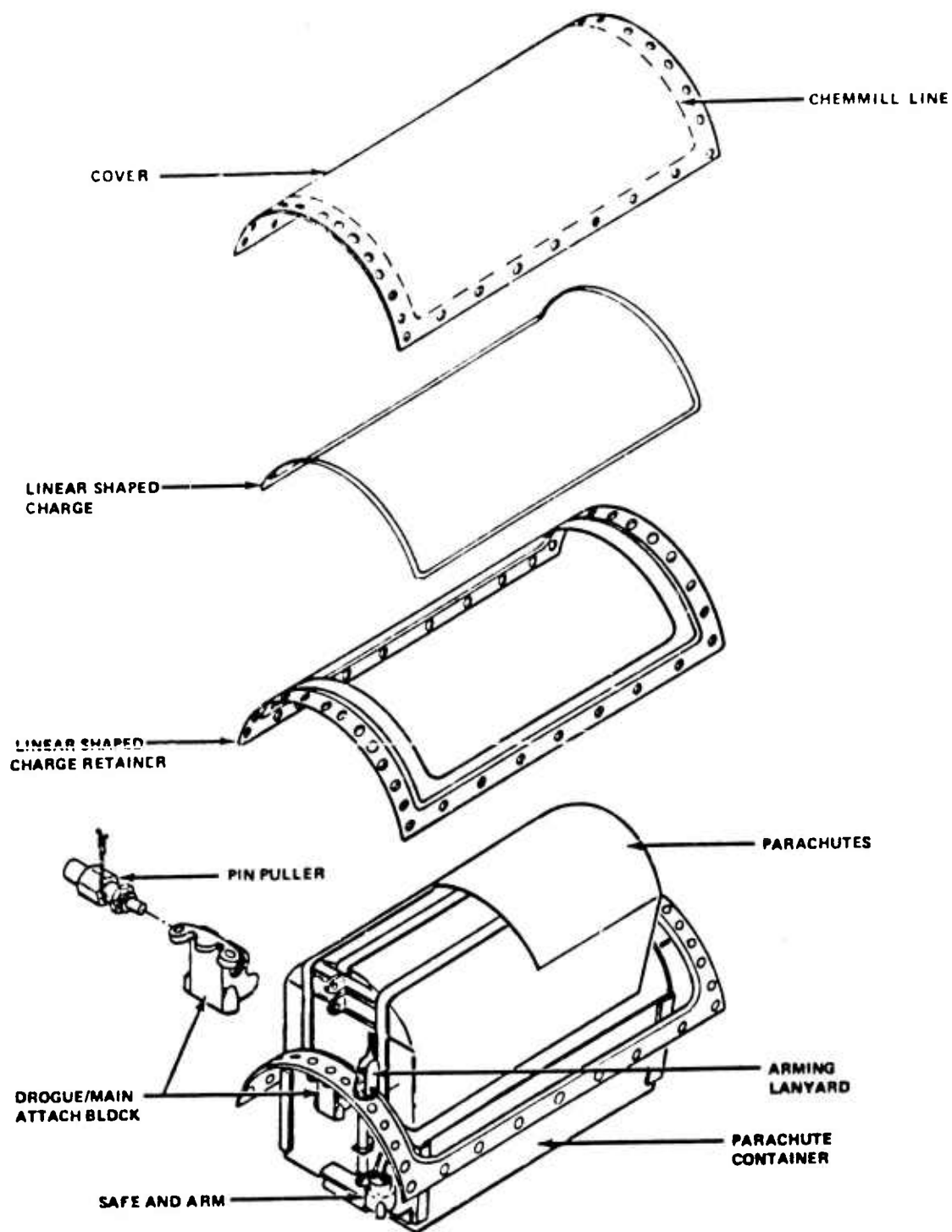
Figure 87. Recovery Module

the cover chem-mill operation is ± 0.005 inch. Considering these factors the cover thickness was set at 0.040 inch ± 0.005 inch to keep the thickness as small as possible.

The cover is heat treated to a very close tolerance, 180,000 to 190,000 psi ultimate. The lower figure is the minimum allowable from structural considerations. The upper figure represents an attempt to keep the brittleness of the cover to a minimum. If the cover is too brittle, there is an opportunity for it to break up when the shaped charge initiates and not properly deploy the drogue parachute. Attached to the cover around the perimeter of the chem-milled area is a stamped stainless steel channel, or retainer, into which an explosive linear shaped charge and its holder are fitted. The retainer positions the shaped charge with respect to the cover to define the path of the cut and to ensure the charge is spaced for effective cutting.

Upon initiation of the shaped charge, sufficient momentum is imparted to the cover for it to clear the vehicle by several feet. The air flow past the vehicle catches the cover as it comes off and forces it further up and back. Four cables are attached to the cover and to the drogue parachute bag. As the cover comes off, it generates sufficient forces to break ties which hold the drogue bag in and to pull the drogue bag out of the pan. The bag is stripped from the drogue parachute at line stretch deploying the drogue.

(2) Linear Shaped Charge. As was mentioned above, the cover is removed by cutting with a linear shaped charge. The charge consists of a "V" shaped aluminum sheath into which is packed 15 grains/foot of HNS-II high explosive. This sheath is then installed in a square Teflon© holder which, when held against the cover, sets the stand-off distance from the charge to the cover. For this particular charge and cover material the proper stand-off distance for optimum cutting performance is between 0.032 inch and 0.050 inch. This particular explosive was chosen for its safety in handling, being a relatively insensitive charge, and its stability at temperature, having no auto-ignition characteristics.

(3) Flexible Contained Detonating Cords (FCDC). The shaped charge is initiated by a pair of one-watt, one-ampere no-fire detonators which fire into a pair of flexible contained detonating cords (FCDC) commonly called transfer lines. The core load in the FCDC is also HNS, chosen for its safety and high temperature stability. Each end of the FCDC has a threaded fitting which permits it to be mechanically connected to its initiator and to the device it is initiating. Each end has a cylindrical tip which has about 1-1/2 grains of HNS packed in it. One tip functions as a receptor, receiving the detonation impulse and passing it on to the explosive train, which in turn, passes it on to the other tip, the donor. The donor then fires into the shaped charge, initiating it.

(4) Safe and Arm. For safety considerations, the detonators are encased in a safe and arm (S&A) device. The FCDCs, of course, are in the system to connect the S&A to the shaped charge explosively. The S&A device shown on Figure 88 is designed with multiple mechanical and electrical interlocks so that events must occur in a definite sequence for the detonators to fire and initiate the FCDCs. First, the rotor in which the detonators are installed is locked in the safe position with a two-position safety pin. The rotor is also secured internally with a solenoid operated pin. In this locked position, the detonator circuits are isolated from their connector and are shunted internally. In addition, the solenoid circuit is open in this position. When the safety pin is pulled out, the rotor is unlocked and is allowed to rotate 13°, where the solenoid pin holds it. At this point the solenoid circuit is established. The solenoid requires 28 VDC at 1.5 amperes to operate. When this current is applied the solenoid pulls its pin and releases the rotor. The rotor may then move to an intermediate test position or all the way to the arm position, depending on whether the safety pin is pulled to its first notch or its second notch. In the first notch, the rotor can move only to the test position. In the second notch the rotor can move all the way to the arm position. When the rotor is in the test position the detonator circuits are established, allowing these circuits to be checked and the detonator bridgewire resistance to be measured. The detonator circuit is established in this test position and the detonators could be initiated. However, in this position the detonators are 45° out of alignment with the output ports, and detonator initiation will not set off the FCDCs.

(5) Load Attach Block. Attachment of the parachute risers to the airframe must be made within the constraints of the modular design philosophy. The load block has loading from two different points, the drogue attach points and main attach point. To do this two pins are secured in

179

FLEXIBLE CONTAINED DETONATING CORDS

SAFE and ARM

POSITION INDICATOR
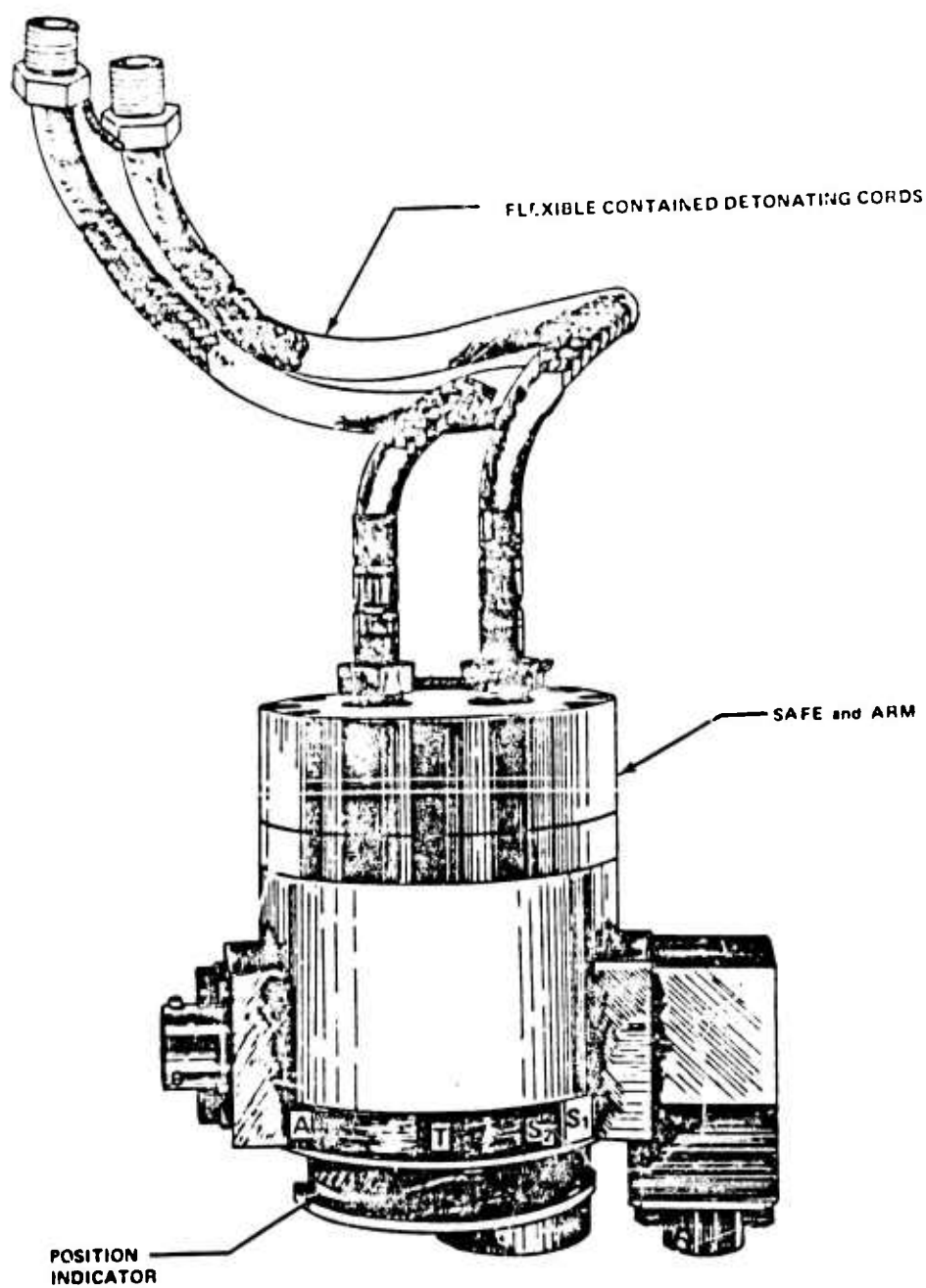
Figure 8-8 Safe and Arm Device

180

the bottom of the block and two matching holes are drilled in the structural frame. ese pins will then carry load compo ents in the axial direction. Then, to carry the vertical loads nd some axial loads, three holes are drilled in the top part of the fixture and the corresponding poi : in the frame so when the block is slipped into place it is secured to the frame with three screw In addition to these features, the block must incorporate a means by which the drogue riser may be released. This is accomplished by securing the drogue riser attachment with a single pin housed in a pin puller. The pin puller is a hollow threaded fitting in which a pin and piston are encased. A Mark 44 cartridge is installed in the case to provide the impulse for pushing the piston, i.e., the pin back into the case, releasing the drogue riser.

3. DEVELOPMENT TESTING

Development testing was conducted on all major components of the recovery system module. This testing was completed before a second series of vehicle drop tests were to be conducted at Eglin Air Force Base using the final system module design. A summary of these tests is shown in Table XLII.

The components requiring the most development were the cover and linear shaped charge. Several tests were required to determine the proper combination of cover thickness, heat treat, gap and energy from the linear shaped charge. Once the proper combination was established, testing of these components was consistent and repeatable. All other components functioned properly during the development test program.

At this point in the recovery development program an inert recovery system vehicle to be used for drop tests at Eglin AFB was available for a full system ground test. This all-up system test employed a safe-and-arm device within the recovery module which was installed in the airframe.

TABLE XLII. RECOVERY SYSTEM COMPONENT DEVELOPMENT TEST SUMMARY

Cover + Linear Shaped Charge	Cutting Characteristics at Ambient, -65°F and +165°F
Linear Shaped Charge, Transfer Lines and Detonators	Explosive Train Characteristics at Ambient, -65°F and +165°F Gap Testing at Maximum and Minimum Tolerance
Safe and Arm	Operation Using Complete Explosive Train at Ambient, -65°F, +165°F and Altitude Demonstrate No Detonation Transfer in Safe and Test Positions
Drogue Release	Structural Tests Operation Under Various Load Conditions
Pressure Cartridge	Fully Qualified Mark 44 Cartridge
Main Chute Attach	Structural Tests

The vehicles' electrical power system was used to sequence and fire all pyrotechnic devices including simulated electrical loads for the back-up recovery system.

This test was sequenced simulating an actual launch mission, i.e., S&A safety pin was pulled, vehicle launch pin was pulled (which powered and initiated the clock), in two seconds the S&A

armed, one second later it fired and the cover cut completely. The drogue release cartridge was to fire ten seconds later and the clock was set to then go into the auxiliary recovery mode. However, after the S&A initiated the linear shaped charge, the clock stopped, terminating the rest of the sequence. There was no apparent damage to the system or the printed circuit boards from the charge detonation. It was thought that transient voltages associated with the S&A solenoid had feedback into the timer circuitry causing a reset of the clock. This circuit was isolated from the rest of the system and the test repeated. The results were the same, with the S&A performing properly, the cover cutting completely, and the timer stopping after the cover detonated. In investigating this problem further, it was determined that the momentary power spike required by the detonators dropped the power supply voltage enough to stop the timer. The external power supply used was a substitute for the recovery battery. This was replaced with a battery equivalent in power output to the recovery battery.

The performance of the two safe and arm devices had been satisfactory. Therefore, the safe and arm device was simulated in further testing. A third test was set up using a safe and arm device placed in the recovery section and its solenoid circuit connected. The detonator command circuits were wired to a pair of externally mounted detonators instead of the S&A. The provided total simulation of the device. The drogue release cartridge and the fuzes simulating the auxiliary recovery system's electrical loads were wired in as before. Thus, electrically, the primary recovery system was identical to the two previous tests even though the ordnance features were not complete. This test was successful. The safe and arm armed at the proper time and the detonators, drogue release cartridge, auxiliary detonator fuzes, and auxiliary drogue release fuzes all functioned at the proper time. Thus the recovery system was ready for flight testing.

4. INERT DROP TESTS AT EGLIN AFB

The next task was to flight test the system with a vehicle similar to HAST. The vehicle, designated R-3, was basically a modified AQM-37A. A HAST midsection, complete with end frames was used to hold the recovery system. It was placed such that the parachute attach fitting would be positioned relative to the vehicle cg in the same way as it would be installed in the HAST vehicle. The recovery system developed in the previous flight test phase of the program was included in the design to be used as the auxiliary recovery system. The auxiliary system was equipped with the same drogue parachute as the primary system. The main, however was a 43.0-foot ringsail, identical to the main in the primary system except for the diameter (45.5 feet). The auxiliary section was attached to the aft of the midsection with the cover oriented downwards so the auxiliary system could function if the primary system was deployed.

The flight test plan was to fly four recovery missions with two R-3 vehicles to prove out the system. All of these tests were to be flown at the recovery design condition, launch at 50,000 feet at a dynamic pressure of 150 psf, approximately Mach 0.9. Problems encountered during the test program increased the number of tests to seven. A summary of these tests is shown on Table XLIII.

Five modifications were made to the recovery system as a result of this seven-test series to demonstrate the readiness state of the recovery system design. The electrical system which interfaces with the lanyard switch was modified to prevent relay contact bounce from interfering with timer operation. The drogue riser was strengthened to make it less susceptible to shock loading. The safe-and-arm device was modified for more reliable operation at altitude and to minimize the effects of corrosion of contacts during storage. A lateral engagement line was added to the main parachute canopy to increase the probability of successful engagement when the parachute is hit off-center. An abrasion shield was added to the main parachute riser to minimize the possibility of cutting the main riser on the compartment edge. At the conclusion of the seven flight tests, the recovery system design incorporating the five modifications was considered sound and acceptable for the HAST flight test program.

TABLE XLIII. RECOVERY TESTS, INERT VEHICLE

Test Results	Corrective Action
Drogue Not Released, Recovered on Auxiliary	Timing Circuit Changed
Drogue Separated from Vehicle Prematurely, Vehicle Lost	Drogue Riser Designed
No Cover Separation, Retrieval on Auxiliary Failed, Recovered from Water	Safe and Arm Designed Lateral Added to Main Chute
Nominal Flight	None Required
Two Main Chute Risers Cut, Recovered From Water	Braided Steel Sleeve Added to Riser
Nominal Flight, Braided Sleeve was Mislocated	Braided Sleeve Relocated
Nominal Flight	None Required

SECTION XI.

AEROSPACE SUPPORT EQUIPMENT

HAST Aerospace Support Equipment consists of all support equipment necessary to complete a successful mission but not carried on the HAST vehicle during flight. Support equipment required to accomplish the various tasks are divided into five categories as follows:

- Airborne Support Equipment
- Ground System Checkout
- Auxiliary Systems Test Sets
- Line Service Equipment
- Ground Handling Equipment

The description and function of the support equipment are discussed in the following paragraphs.

1. AIRBORNE SUPPORT EQUIPMENT

Airborne support equipment consists of a LAU-96/A launcher, launcher adapter, aircraft electrical harnesses and a target control panel in the aircraft cockpit.

a. The LAU-96/A launcher, manufactured by the Breeze Corporation, is the ejection launcher used to mount, carry, and air-launch the HAST target from a launch aircraft. The launcher consists of a structural frame housing, a trapeze mechanism, harness assembly, release hooks, and a cartridge powered cylinder actuator. Modifications to the LAU-96/A launcher to adapt it to the HAST vehicle included relocation of the umbilical connector and lanyard pull mechanisms.

b. The target control panel operates in conjunction with the launcher to apply power to the target and give a visual indication of target launch status. The control panel assembly is housed in an aluminum box with an edge lighted front panel. The panel consists of a power READY and FAULT lamp, a SELECT switch which applies warm-up power, a LAUNCH READY switch that opens the ram air turbine gate to put the target on internal power, and a guarded JETTISON switch. The LAUNCH READY switch is a magnetic type that returns to the off position should launch not be initiated within three minutes after switch actuation. The FAULT lamp illuminates to inform the pilot that the target has a malfunction. Launch cannot be initiated with this lamp illuminated. The READY lamp illuminates to inform the pilot that target launch parameters have been met within the vehicle and launch may be initiated. Launch is accomplished using the existing weapons release provisions in the launch aircraft.

2. GROUND SYSTEM CHECKOUT EQUIPMENT

The ground system checkout equipment is that equipment required to assure that all basic systems in the target are functioning within specified tolerances required to assure a successful mission. The ground system checkout equipment used in the development program (Figure 89) consists of a set of multifunction test and checkout consoles, a target tilt fixture, a set of control surface protractors and a ram air turbine test set.

a. The test and checkout console set consists of three upright rack and panel consoles interconnected by wire harness assemblies. The equipment is functionally grouped as follows:
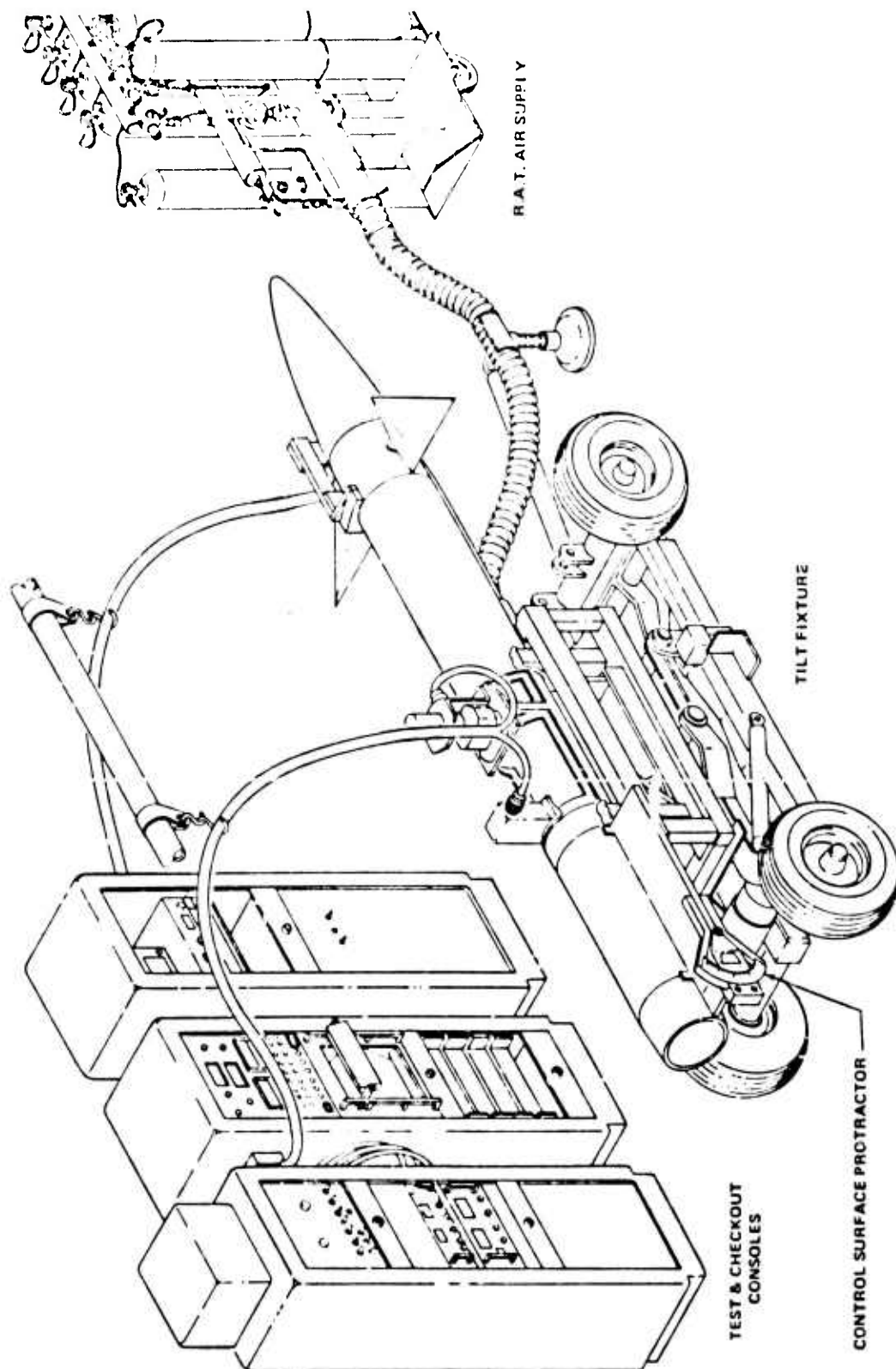
184

Figure 89. HAST Checkout Equipment for the Development Program

R.A.T. AIR SUPPLY

TILT FIXTURE

TEST & CHECKOUT CONSOLES

CONTROL SURFACE PROTRACTOR

185

- Power Supply Console

- Control and Monitor Console

- Air Data Console

The power supply console contains a 50-ampere, 28-volt dc power supply to simulate the output power of the ram air turbine and the power required by the electrical systems of the test consoles, a 10-ampere, 28-volt dc power supply to simulate recovery battery power and two vacuum pumps for the air data simulator. Controls for checking vehicle cartridge wiring are also on this console.

The control and monitor console contains a digital multimeter, a frequency counter, two digital clock timers and a strip recorder. The digital read-outs of all vehicle inputs, outputs, and mission parameters eliminate any reading errors. The strip recorder gives a permanent record of each checkout.

The air data console contains a pressure source and a quartz manometer/controller air data test instrument for controlling the static and pitot pressures required to simulate the flight altitude and vehicle Mach number.

The target tilt fixture, shown in Figure 89, is required to test and check the autopilot system position and rate components. The tilt fixture is a GFE MDE 3458 hydraulic trailer modified by the contractor.

The control surface protractors are required to accurately measure canard and aileron movement and position, also, to correlate control surface attitudes with the electrical output of the actuator potentiometers. The control surface protractors, of aluminum construction, incorporate a vernier scale capable of reading one-tenth of a degree. To assure consistency from target to target, these protractors are mounted on a vehicle using only jig bored tool coordinated holes.

The ram air turbine test set is required to supply air to run-up and check out the ram air turbine, turbine alternator, and power transfer circuits. The turbine air supply consists of sixteen high pressure bottles and three manifolds with pressure regulators to provide the proper mass air flow required to operate the turbine. The test set may be operated remotely with a control that connects to the test set.

3. AUXILIARY SYSTEMS TEST SETS

Auxiliary systems test sets check those systems not essential to vehicle flight. These test sets consist of the telemetry ground station, the beacon test set, the payload test sets and the command receiver test set. The telemetry, beacon and command receiver test sets are necessary to check out the interim systems prior to incorporation of the production ITCS. Power and flight simulation is provided to the target from the test and checkout console during the usage of these auxiliary systems test sets. This equipment must be compatible with the ground stations at the test site and is GFE. Therefore, no detailed description is given in this document.

4. LINE SERVICE EQUIPMENT

Line service equipment is used to provide additional tests and to service the target and launcher after system checkout and prior to uploading on the launch aircraft. The line service equipment consists of the following items:

- Bridgewire Test Set

- No Voltage Test Set

- Launch System Test Set

186

- Nitrogen Fill Coupling

- Battery Charger

- Command Control Box

- Oxidizer Fill Equipment

a.   The bridgewire test set is required to test all ordnance items for proper resistance and continuity prior to installation in the HAST vehicle or launcher. An MB Electronics Model 101-5CFG or equivalent bridgewire test set will be used for the HAST program.

b.   The no-voltage test set provides a method of performing a no-voltage check on the IR augmentation, engine, destruct, recovery, and launcher cartridge connectors prior to installation of the ordnance items. The set consists of a voltmeter selector switch, sensitivity switch, self-test panel and electrical wire harness packaged in a metal suitcase type cabinet.

c.   The launch system test set is used to check the electrical circuitry and operating controls of the launching system prior to uploading the target. The launcher test set is installed in a metal suitcase type cabinet. An electrical wire harness interconnects between the test set and the launcher umbilical connector. The test set provides a go or no-go indication by illuminated placards indicating target or launch aircraft functions. Electrical power required for operating this test set is furnished by the launch aircraft electrical system through the launcher umbilical connector.

d.   The nitrogen fill coupling is a manually connected and disconnected fitting that provides a convenient means of interfacing between the nitrogen source regulator and the target nitrogen inlet fitting for filling and bleeding the target nitrogen tank.

e.   A battery charger is required to charge the command/recovery battery prior to uploading the target.

f.   The mission control panel is a table mounted console with an inclined front panel. The command switches are functionally grouped and placarded to correspond with the target functions which include recovery, engine, payloads, vehicle functions (maneuvers) and heading control. These functions are discussed below:

- **Recovery.** The recovery portion of the panel contains the RECOVERY, START, DROGUE RELEASE and RECOVERY INHIBIT switches. The RECOVERY START switch will initiate recovery regardless of vehicle speed or altitude. The DROGUE RELEASE switch is a backup for the automatic drogue release function. When activated, the RECOVERY INHIBIT switch excludes any recovery.

- **Engine.** The ENGINE SHUTDOWN switch closes the target OTV which shuts off oxidizer to the engine.

- **Payloads.** Payloads include IR, VMDI and RF. The Vector Miss Distance Indicator (VMDI) is calibrated by placing the VMDI switch to the TLM CAL position. The VMDI is started by placing the VMDI switch to ON. Jet Engine Modulation (JEM) is simulated by placing the RF switch ON. Infrared (IR) augmentation is started by placing the IR switch ON.

- **Vehicle Functions.** The vehicle functions portion of the panel contains the TURN START, SPEED CHNG and ALT CHNG switches. When actuated, the TURN START switch starts whatever turn has been programmed into the target. All other turn start times are excluded. When actuated, the SPEED CHNG switch will cause the target to increase to decrease speed by 0.5 Mach. This function will not exclude programmed target speed changes. It may only be used once, however; and then from fast to slow or slow to fast. The target may be made to climb or descend by 5,000 feet by actuating the ALT CHNG switch. Use of this switch excludes any programmed altitude changes. Like the speed function, it may only be used once and from down to up or up to down.

187

- Heading Control. The HEADING CONTROL portion of the control panel consists of the UPDATE switch and lamp and the guarded DELAY switch. The DELAY switch limits the heading update command to 2.5 seconds. With the switch OFF, the command will be held in as long as the update switch is held either LEFT or RIGHT. Any command held in longer than three seconds will exclude target programming.

- Power On. The power on (PWR ON) switch controls power to the mission control panel.

g.   Special oxidizer handling equipment is required to accurately measure and safely transfer the oxidizer from its storage containers to the target oxidizer tanks. The equipment required consists of an upright flow control console, a target fill and vent manifold, a set of stainless steel wrenches and a set of interconnecting flex lines. Personnel must be dressed in protective clothing while handling the oxidizer.

5.   GROUND HANDLING EQUIPMENT

Ground handling equipment is the equipment used in lifting, transporting, or loading the HAST vehicle. The HAST ground equipment consists of the following items:

- Transporter

- Shop Stand

- Parachute Module Lifting Handle

- Strongback Hoist Beam

- Balance Beam

- Shipping Container

- Parachute Module Cover

a.   The transporter is the vehicle provided to move the target from the storage or preparation area to the launch aircraft area. A second function is to provide the necessary position adjustments required to upload and download the target. One transporter is an A/M 32K weapons carrier modified by the contractor to accept a cradle assembly for mounting the HAST vehicle. The MHU-12 bomb trailer is also used to transport the target, with the MJ-4 loader to load.

b.   The shop stand provides a means of handling the target during assembly, preparations for flight, and disassembly. The stand assembly consists of a padded cradle assembly and a tubular steel stand with lockable swivel casters on the front wheels.

c.   The recovery module lifting handle is required to install and remove a complete parachute module in the vehicle. The lifting handle is a padded aluminum strap with handles on each side for lifting. The complete assembly attaches to the recovery module with two captive fasteners.

d.   The strongback hoist beam is required to provide a safe and convenient means of removing the target from its shipping container or storage area and placing it on the shop stand or transporter. The beam is a welded aluminum component which attaches to the launch fittings of the target and has multiple attach provisions for various combinations of target sections and configurations.

e.   The balance beam is a tool required to accurately weigh and locate the vehicle center of gravity. The beam is a sheet steel and machined part assembly that attaches to the strongback beam described above. The balance beam has a variable poist hoint with a scale to accurately measure the fuselage station of the hoist point.

f.   The shipping container is required to protect the target during transportation and storage. The complete fuselage assembly with wings, stabilizers and canards removed is packaged in one crate. The reusable shipping container is of wood construction with bracing located at the HAST hard areas. Vehicle attach points are shock mounted to prevent damage during transportation.

SECTION XII

PRODUCT ASSURANCE

A Product Assurance program was conducted during Phase II. Under this program those reliability and safety activities started earlier in the development program were refined and expanded as more design and test data became available. Other activities such as Quality Assurance were initiated and functioned actively during the phase as components and vehicles were subjected to acceptance procedures.

1. RELIABILITY

The estimate of reliability was refined during Phase II to include selected vendor's hardware. Both the contractor and major component vendors analyzed their hardware using standard failure rates and methods in MIL-HDBK-217A. When detail parts lists are available, and end use environment is known, an accurate estimate of reliability for electronic items will be possible.

Reliability goals required for the HAST are 95 percent for preflight checkout and 90 percent for overall flight reliability. The overall flight reliability includes warm-up while aboard the launch aircraft, automatic launch-ready checkout, launch, flight and recovery parachute deployment.

Failure probability of two years storage is tabulated in Table XLIV together with the percentage of these failures discovered by the preflight checkout. The preflight checkout discovers 62 percent of the total storage failure potential. Some failures such as the engine, igniters and cartridges are not testable. When the failure probability of nontestable items is removed from the total, the failures discovered by the preflight checkout is then 92.6 percent.

Warm-up of the target components starts when the control panel select switch is initiated. This furnishes power to spin-up ~ os and warm-up electronics and all the other components except the ram air turbine (RAT) oxic _er pump and generator.

Prelaunch checkout is a continuous self-check which is initiated when the launch ready switch is operated. The RAT spins up and the target is then on its own power. The self-check monitors 59 percent of possible failures and prevents launch when an out of tolerance condition develops. All failures discovered by this checkout are still counted against overall flight reliability. But, this checkout does allow failed targets to be returned to base rather than lost early in the free flight phase.

Flight failure potential for the 4-minute minimum and the 15-minute maximum flight is also shown in Figure 90. These flight times include system operation while gliding down to 50,000-foot altitude for parachute recovery. Overall reliability includes the flight failure potential and 100 percent of the prelaunch failure potential. These flight reliabilities are 96.6 and 95.9 percent for minimum and maximum flight after no storage, and 96.1 and 95.3 percent after a maximum of two years storage. These reliabilities plus the area of expected usage are shown pictorially in Figure 90.

Reliability to launch when considered separately is 99.2 percent. Thus, reliability for flight given that launch separation has occurred is approximately 0.8 percent higher than the overall reliability values stated above.

TABLE XLIV. PREDICTED FAILURE RATES

SYSTEM AND COMPONENT	FAILURE RATE/HR (FLT)	STORAGE FAILURE POTENTIAL (2 YEARS) 17,520 HR	STOR. FAILURES DISCOVERED BY PREFLIGHT CHECKOUT AFTER 2 YEARS	PRELAUNCH FAILURE POTENTIAL 20 MIN.	PRELAUNCH FAILURES DISCOVERED BY PRELAUNCH CHECKOUT	FLIGHT FAILURE POTENTIAL 15 MIN.
PROPULSION: CTA						
OX THROTTLE VALVE	0.005000	0.001314	0.001314	0.001667	0.000167	0.001250
TC INSULATED CASE	CY0.000020	0.000002	0.0	0.0	0.0	0.000020
NOZZLE	CY0.004255	0.000426	0.0	0.0	0.0	0.004255
IGNTR & DUAL INIT	CY0.000010	0.000001	0.000001	0.0	0.0	0.000010
AERATION CHECK VALVE	CYC.001000	0.000100	0.0	0.0	0.0	0.001000
AERATION ORIFICE	0.003364	0.000884	0.0	0.0	0.0	0.000841
OXIDIZER INJECTOR	0.004164	0.001094	0.0	0.0	0.0	0.001041
GRAIN	CY0.001712	0.000171	0.0	0.0	0.0	0.001712
SUBTOTAL		0.003992	0.001315	0.001667	0.000167	0.010129
PROPULSION: OMA						
N2 PRESSURE TANK	CY0.000100	0.000010	0.0	0.0	0.0	0.000100
N2 FILL & VENT V	CY0.000100	0.000010	0.000010	0.0	0.0	0.000100
N2 MULTIFUNCTION V	CY0.000500	0.000050	0.0	0.0	0.0	0.000500
FREE SIPHON MECH	CY0.001500	0.000526	0.0	0.0	0.0	0.001500
OXIDIZER TANKS	0.003000	0.001051	0.0	0.0	0.0	0.000750
OXIDIZER START V	CY0.000500	0.000050	0.0	0.0	0.0	0.000500
TENSION SCREEN	CY0.000100	0.000010	0.0	0.0	0.0	0.000100
DPU GEN & PUMP	CY0.001000	0.000100	0.000100	0.001000	0.001000	0.001000
SUBTOTAL		0.001807	0.000110	0.001000	0.001000	0.004550
LAUNCHER: MISSILE CONT PANEL:	CY0.001000	0.000100	0.000100	0.000333	0.000167	0.001000
STRUCTURE:	CY0.000500	0.000050	0.000050	0.000167	0.000167	0.000500
AIRFRAME	CY0.000200	0.000020	0.0	0.0	0.0	0.000200
CONTROL SURFACES	CY0.000200	0.000020	0.000018	0.0	0.0	0.000200
SUBTOTAL		0.000040	0.000018	0.0	0.0	0.000400

TABLE XLIV. PREDICTED FAILURE RATES (Continued)

SYSTEM AND COMPONENT	FAILURE RATE/HR (FLT)	STORAGE FAILURE POTENTIAL (2 YEARS) 17,520 HR	STOR. FAILURES DISCOVERED BY PREFLIGHT CHECKOUT AFTER 2 YEARS	PRELAUNCH FAILURE POTENTIAL 20 MIN.	PRELAUNCH FAILURES DISCOVERED BY PRELAUNCH CHECKOUT	FLIGHT FAILURE POTENTIAL 15 MIN.
AFCS:						
PWR DISTR PNL ASSY	0.000113	0.000030	0.000027	0.000038	0.000019	0.000026
HEADING REF GYRO	0.001333	0.000350	0.000350	0.000444	0.000444	0.000333
ANLR RATE GYRO-PITCH	0.000333	0.000088	0.000088	0.000111	0.000105	0.000083
DIGITAL LOGIC MODULE	0.001000	0.000350	0.000315	0.000333	0.000033	0.000250
AUTOPILOT CONT ASSY	0.002500	0.000876	0.000876	0.000833	0.000250	0.000625
AIL ACTR & AMPL	0.001228	0.000427	0.000427	0.000407	0.000183	0.000305
CANARD ACTR & AMPL	0.001220	0.000427	0.000427	0.000407	0.000183	0.000305
PITOT TUBE	0.000333	0.000088	0.000088	0.000111	0.000111	0.000083
AIR DATA MODULE	0.000666	0.000175	0.000175	0.000222	0.000111	0.000167
NORMAL ACCLRM	0.000067	0.000023	0.000023	0.000022	0.000022	0.000017
SUBTOTAL		0.002834	0.002797	0.002928	0.001461	0.002194
PLD, ITCSLCRTG:(GFE)						
DROGUE CHUTE REL	CY0.001000	0.000100	0.000050	0.0	0.0	0.001000
AILERON CESTR	CY0.001000	0.000100	0.000050	0.0	0.0	0.001000
UX START VALVE CRTG	CY0.001000	0.000100	0.000050	0.0	0.0	0.001000
N2 START VALVE CRTG	CY0.001000	0.000100	0.000050	0.0	0.0	0.001000
RADAR TWT & POWER SP	0.002000	0.000525	0.000525	0.000666	0.000666	0.000500
SCORING SYSTEM	0.002000	0.000525	0.000525	0.000666	0.000666	0.000500
ITCS	0.000500	0.000131	0.000131	0.000167	0.000167	0.000125
FLR-CHAFF OR IR POD	0.002000	0.000525	0.000315	0.0	0.0	0.000500
SUBTOTAL		0.002106	0.001696	0.001499	0.001499	0.005625
RECOVERY SYSTEM:						
LINEAR SHAPED CHG	CY0.001210	0.000121	0.0	0.0	0.0	0.001210
DROGUE CHUTE & LNS	CY0.000500	0.000050	0.0	0.0	0.0	0.000500
MAIN CHUTE & LINES	CY0.000500	0.000050	0.0	0.0	0.0	0.000500
MN RFR SQUIBS IOF2	CY0.000001	0.0	0.0	0.0	0.0	0.000001
RECOVERY BEACON XMTR	0.000143	0.000033	0.000038	0.0	0.0	0.000036
SAFE & ARM DEVICE	CY0.000100	0.000010	0.000005	0.0	0.0	0.000105
SUBTOTAL		0.000269	0.000043	0.0	0.0	0.002352

TABLE XLIV. PREDICTED FAILURE RATES (Concluded)

SYSTEM AND COMPONENT	FAILURE RATE/HR (FLT)	STORAGE FAILURE POTENTIAL (2 YEARS) 17,520 HR	STOR. FAILURES DISCOVERED BY PREFLIGHT CHECKOUT AFTER 2 YEARS	PRELAUNCH FAILURE POTENTIAL 20 MIN.	PRELAUNCH FAILURES DISCOVERED BY PRELAUNCH CHECKOUT	FLIGHT FAILURE POTENTIAL 15 MIN.
ELECTRICAL:						
MULT OUT PWR SPLY	0.001333	0.000316	0.000316	0.000444	0.000222	0.000333
RECOVERY BATTERY	CY0.001000	0.000100	0.000100	0.0	0.0	0.001000
CONNECTORS & WIRING	.005000	0.001752	0.001401	0.001667	0.001000	0.001250
SUBTOTAL		0.002166	0.001817	0.002111	0.001222	0.002583
MISC HARDWARE:	0.005000	0.001314	0.001183	0.001667	0.001000	0.001250
TOTAL		0.014680	0.009128	0.011372	0.006683	0.030583
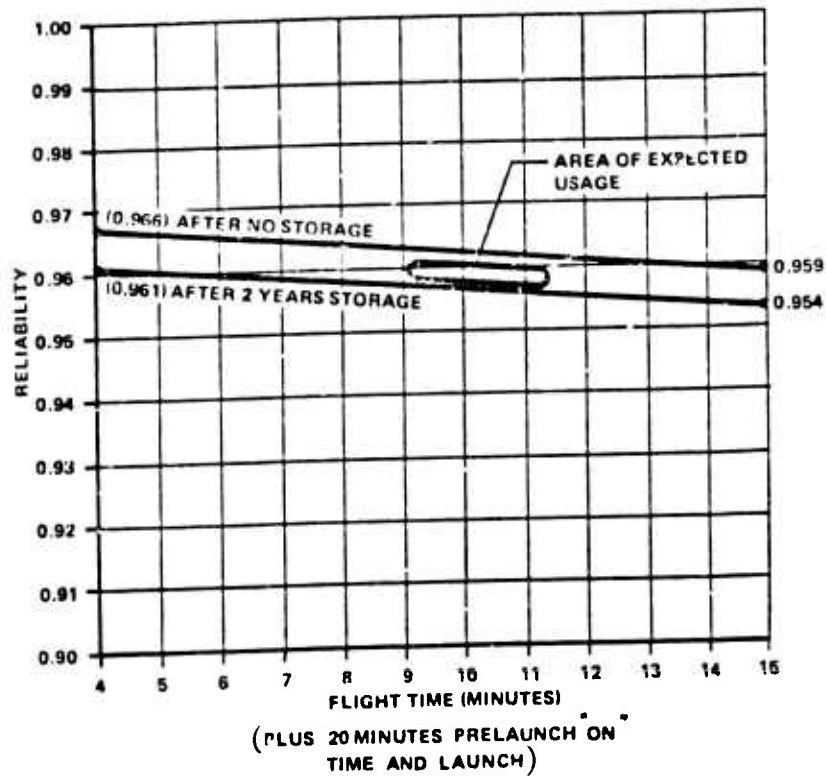
Figure 90. HAST Overall Flight Reliability Rate

Criticality of each of the components and subsystems was calculated. This shows what percent of the total failure probability the component or system is responsible for. System criticality considering maximum storage and length of flight is as follows:

TABLE XLV. CRITICALITY OF COMPONENTS AND SUBSYSTEMS

	Percent
Automatic Flight Control System	10.8
GFE (RF & IR Augmentation, Scoring, and Cartridges)	15.9
Recovery System	5.4
Oxidizer Management Assembly and Tanks	15.3
Controlled Thrust Assembly	30.5
Launcher	2.8
Missile Control Panel	1.4
Structure	0.9
Electrical Power	10.6
Miscellaneous Hardware	6.4
Total	100.0

2. SAFETY

Safety activities were conducted in accordance with MIL-STD-882 and with established safety design and test criteria. The program was monitored to detect and eliminate any hazard or safety problem during design and development in order to prevent costly design changes or need for safety devices later in the program.

a. Safety data was collected and filed using a closed loop data flow system. This system kept engineering and management personnel informed on all safety problems as well as the corrective action taken. It also generated an adequate safety file which supplied most of the information to develop four required documents. These documents are:

- System Safety Program Plan

- Explosive Technical Data Sheet

- Explosive Ordnance Disposal Procedure

- Hazard Analysis

A preliminary System Safety Program Plan was prepared outlining the basic criteria for the safety effort, safety management structure and safety milestones. In addition, the plan includes milestones for the completion of hazard analyses, design reviews, data reporting and safety testing.

The Explosive Technical Data Sheet was prepared and submitted to the sponsor on DD Form 1664. The document contains a consolidation of studies performed on all explosive devices in the HAST vehicle. The explosive devices are first considered individually and then collectively within the HAST system. This data sheet was generated to assist in the assignment of an overall explosive classification to the HAST vehicle. It was also used in establishing a quantity distance table for both storage and target maintenance.

The Explosive Ordnance Disposal Procedure was prepared and published outlining the necessary steps to follow to render the target safe in case it is involved in an incident or accident.

A preliminary Hazard Analysis was performed as the initial analysis task of performing a gross hazard analysis. It was accomplished early in the program to detect weak or unsafe conditions and initiate corrective action before the design became firm. The information from this analysis was also used in further development of the safety design criteria published in a revision of the System Safety Program Plan. The analysis was then expanded to include both a subsystem and system hazard analysis and published as the HAST Hazard Analysis. The document indicates the target does not contain any unacceptable safety problems, and, that it is compatible and safe to use with a launch aircraft during the flight test phase.

b. The primary safety goal for HAST was for safety to be inherent. Every effort was made to design safety into each subsystem rather than rely on a safety device to reduce a potential hazard to an acceptable level. Safety features of the HAST include a hybrid propulsion system, two sources of electrical power, and a destruct system. A safe-and-arm device is used in the recovery system.

The hybrid propulsion system consists of a solid fuel grain and liquid oxidizer. The fuel grain consists of 80 percent butylrubber and 20 percent plexiglass, while the oxidizer is Inhibited Red Fuming Nitric Acid (IRFNA). The fuel grain and oxidizer are not hypergolic and the fuel grain will not burn without an oxidizer. This makes the propulsion system inherently safe.

Other safety features designed into the propulsion system are pressure relief valves, burst diaphragms, a manual shut-off valve and the throttle valve in the oxidizer system. The IRFNA is pressurized from 3500 psig nitrogen (N_2) tank which is regulated to 6 ± 10 psig. The nitrogen system is equipped with a high pressure relief valve to prevent over-pressurizing the nitrogen tank. It

also contains a lower pressure relief valve to prevent over-pressurizing the oxidizer tank. In case the target is involved in a fire, the oxidizer tank is designed with a burst diaphragm which will rupture prior to reaching burst pressure of the oxidizer tank. This provides a controlled release of IRFNA rather than a mechanical explosion of the oxidizer tank. When the oxidizer tank is pressurized by N_2 after launch a start valve is opened and oxidizer is supplied to the oxidizer pump of the DPU at approximately 60 psig. During flight the DPU, powered by external air flow, boosts the oxidizer from 60 to 700 psig to the throttle valve. The throttle valve is normally closed and does not open until the motor igniter is initiated. During engine shutdown the throttle valve is again closed to prevent any unused oxidizer from entering the motor during recovery. An added safety feature is a shutoff valve located on the start valve. This valve is closed manually after the target is recovered to provide safe handling prior to purging the oxidizer system.

Electrical power is supplied to the target from two sources. An alternator is attached to the RAT which functions only during captive or free flight. Should the alternator fail, an emergency nickel cadmium battery will automatically supply power to the command receiver, recovery and destruct systems. This assures that the target is always under ground command and can be recovered or destructed as necessary under any circumstances.

The aero destruct system is another safety feature of HAST. Target destruct is accomplished by firing a pressure cartridge in a pin puller which completely contains the total explosive force. The pin puller extracts a lock pin from the spring loaded bellcrank system and the ailerons are forced hard over in opposite directions. This puts the target in a high speed roll and it follows a ballistic trajectory to impact.

The automatic flight control system will sense any of the following malfunctions and initiate the target destruct sequence:

- Heading deviation of ± 10 degrees for 30 seconds

- Loss of target electrical power for a preselected delay

- Loss of command carrier tone for a preselected delay

- Jettison from the launch aircraft.

The target is equipped with a recovery system which is initiated by the AFCS when the flight is completed. The recovery system is a complete removable module which requires only external arming and firing signals from the target to function.

The first step in the recovery sequence takes place when an arming lanyard is extracted from the recovery safe-and-arm device (S&A) as the target is launched. This allows the S&A detonator rotor to move 13 degrees to a pre-arm position, but still held in a safe condition by an electrically operated solenoid stop pin. The target performs the entire mission in the pre-armed condition and must sense all of the following conditions before the S&A will fully arm.

- Time must be greater than ten seconds from launch.

- The motor must ignite and reach operating pressure.

- The motor must return to ambient pressure.

- Target must descend below 50,000-foot altitude.

- Target must be at a subsonic velocity.

When all these conditions have been met, the AFCS will generate a signal that will operate the S&A solenoid and the detonator rotor will fully arm One second later the AFCS will generate a fire signal which will initiate two contained explosive transfer lines which in turn initiate a shaped charge. The shaped charge, a 78-inch long closed loop, cuts out the stainless steel parachute cover which pulls out the drogue chute. Nine seconds later a pressure cartridge releases the drogue and the main parachute is deployed in a reefed condition. Two reefing line cutters function 10 seconds after main chute deployment and allow the main to fully open. The target is then retrieved by a helicopter with an aerial pickup or recovered after water or land impact.

During the hazard analysis, target launch conditions were studied to determine if a possible hazard might exist to the launch aircraft. A computer study indicated that if the target is launched with the canards 13 degrees up or greater, a possible hazard could exist. To assure safe separation from the aircraft, the canard setting must be at 0 degrees on the target or it cannot be launched. In addition, the AFCS is blocked from the canard actuators for two seconds after launch, which assures a safe distance is reached before system activation.

c. The HAST safety program has met or exceeded all requirements of the Statement of Work and MIL-STD-882 during Phase II. All engineering and testing functions have been adequately monitored for safety and required safety reports prepared and submitted. Inherent safety has been designed into the target and only one safety device is required to reduce a potential hazard to an acceptable level.

At the end of this phase it has been determined that the HAST system is safe to handle, store, and fly. It is compatible with handling equipment, military storage facilities, and launch aircraft.

SECTION XIII

STRUCTURAL FABRICATION TECHNIQUES

Operational requirements for the HAST system restricted the materials which could be used in the vehicle structure. Fabrication techniques which could be employed were dependent, in turn, upon the materials selected. These materials were not common to aircraft airframe construction, but the basic philosophy used for fabrication of the structure for the HAST was to adhere to state-of-the-art manufacturing processes for the development and test vehicles. In addition to the requirement of meeting close tolerances of a high performance vehicle was the contradictory need to provide a low cost vehicle for target use. For the development vehicles the techniques employed have provided a balance between costs and the rigid requirements of the vehicle system. Major structural sections of the vehicle are shown in Figure 23.

1. FORWARD FUSELAGE SECTION

This section is hot spun from a rolled and welded 17-7 PH sheet 0.160 thick. The material thickness is to accommodate good spinning practices and to insure adequate material for subsequent fabrication operations. Design criteria was based on past experience obtained by the contractor during fabrication of the AQM-37A target vehicle. Even with a good background of chem-milling 17-7 PH material, some difficulties were encountered obtaining the desired wall thickness. Uneven wall thickness developed during the chem-mill process. The inconsistency of etch rate was traced to metal working during the spinning operation, and was not completely removed with an annealing operation.

Some difficulties also arose during fabrication of this assembly when calculated growth rates for heat treat did not meet expectations. This variation from predicted growth has been traced to two sources. Different furnaces used during heat treat produce different growth patterns and different melts of material have different growth rate. To insure predetermined size, assemblies were assigned to the same furnaces, and the raw stock is monitored in an effort to keep all assemblies on a shop order manufactured from the same melt of material produced by the vendor.

2. OXIDIZER TANK SECTION

Past experience in dealing with pressure vessels for IRFNA permitted orderly and economical development of this section. Existing tooling was used for fabrication of tank ends and fill parts, and chem-milling of the internal surface of cylinders. Weld techniques, both TIG (Tungsten Inert Gas) and electron beam, were used for pressure vessels. With the experience of heat treating of 17-7PH material tankage, size could be predetermined eliminating any extensive fabrication development programs.

3. NITROGEN TANK

To take advantage of current state-of-the-art in metal forming, the two sections of the nitrogen tank were originally designed to be formed from a sheet of 0.187 thickness 17-7 PH material on a Cincinnati Hydroform. With this method subsequent machining operations would be eliminated. Because of lack of machine capacity in tonage for hydroforming and thinning of material in a critical area it was necessary to use available methods of hot spinning and machining. This method of fabrication increased the material gage up to 0.250 and added additional machining operations. Techniques developed by the contractor of electron beam welding both the inner and outer closure weld simultaneously resulted in improved quality and reduced costs of the welding operation.

4. MID-SECTION ASSEMBLY

The material selected for this assembly is 17-4 PH. This selection offered some manufacturing advantages not available in other materials. Advantages included established casting procedures and full strength of the material after welding with a simple heat treating operation. The two bulkheads, which close both ends of this assembly, are investment castings machined only on critical surfaces

to insure interface with mating components. Considerable effort was expended in working with various casting vendors to develop adequate casting and straightening techniques.

Four skins, which make up the lower half of the fuselage between the casting and the ram air turbine cover, are formed from 17-4 PH 0.060 sheet. Preliminary tests conducted indicated 17-4 PH material could not be stretch formed using conventional tooling and methods. Because of these tests, the skins were designed to be fabricated utilizing power brake and rolls. The castings and skins are joined by two methods of welding -- electron beam welding and TIG.

The upper part of this section contains the parachute module assembly. The cover of this assembly is the upper outer structure. It is rolled from 0.125 sheet of 17-4 PH and chem-milled to extremely close tolerances in order to meet the material gage required for proper function of the shaped charge. Modification of chem-milling techniques and chemical solutions were required to meet the extremely close tolerances.

Attached to the cover is a ring which retains the shaped charge against the cover. A series of dies were built which permitted fabrication of the retainer ring in one piece, alleviating the alternative requirement of welding four pieces and straightening. This one piece assembly gives greater assurance that the shaped charge will be held properly in place.

5. WING AND VERTICAL STABILIZERS

A study of industry production facilities revealed few methods available that meet the rigid requirements for the HAST wing. Fabrication processes such as metal bonding and composites were included in the study, but present state-of-the-art techniques would not meet the environmental requirements. Two methods stood out as acceptable fabrication processes:

a.   Brazed stainless steel sandwich construction.

b.   Fabrication from resistance welded honeycomb stainless steel panel material.

The second alternative was chosen because of cost. It also offered some major advantages:

a.   Tooling costs were lower. Tooling could be held to soft hardware permitting economical development changes to be incorporated as the program developed.

b.   Detail part tolerance could be established permitting use of conventional fabrication equipment reducing detail part costs.

c.   Cost estimations indicated a more economical wing could be developed with basic fabrication methods. Techniques of forming and welding closures and structure attachments to honeycomb panels of the HAST wing and vertical stabilizer were unknown. Before full committment was made, a research and development program was established to define fabrication processes. Samples of panel were secured and a crush tool was fabricated that simulated a ten-inch section of the leading edge.

When desirable results were obtained from the crushing operation the effort was expanded to include cleaning and welding. Information obtained from this program was used as guidelines for final design, fabrication of tooling, and establishment of weld parameters.

Warpage during heat treat operation could not be predicted without flight-weight hardware to fully define the tooling. Development of tooling to hold and align the wing occurred over the period. To further improve the alignment of the wing, a straightening process using glass peening was employed.

6. AIRFRAME TESTS

The airframe structure designed and fabricated as described has been subjected to the structural testing covered in Section V. All testing requirements have been met.

199

REFERENCES

1. Carman, J. B.; Static Stability and Inlet Characteristics of the HAST Missile at Transonic Mach Numbers. AEDC-TR-71-178 (AFATL-TR-71-115), September 1971.

2. Jones, J. H.; Aerodynamic Characteristics of the HAST Missile at Mach Numbers 2.25, 3, and 4, AEDC-TR-72-6 (AFATL-TR-72-5), January 1972.

3. NASA Report 1307, Lift and Center of Pressure of Wing, Body, and Tail Combinations at Subsonic, Transonic and Supersonic and Supersonic Speeds, 1959.

4. NACA TN 1662, Aerodynamic Properties of Slender Wing Body Combinations at Subsonic, Transonic and Supersonic Speeds, by Spreiter, John R. Ames Aeronautical Laboratory, July 1948.

5. Francis, J. G. F., "The QR Transformation - A Unitary Analog to the L. R. Transformation," The Computer Journal 4, pp 265-271, 332-345.

6. Investment Casting Handbook, Investment Casting Institute, 2535 Peterson Road, Chicago, Illinois.

7. Spicer, John A., "HAST Digital Program", FGD-TM-71-3 September 1971, AFFDL-Wright-Patterson AFB, Dayton, Ohio.

8. Laflamne, Herbert A., Capt. USAF, "HAST Linear Analysis", FGD-TM-71-R September 1971, AFFDL-Wright-Patterson AFB, Dayton, Ohio.

9. Pietrzak, Paul E., "HAST Hybrid Simulation", EGD-TM-71-5 September 1971 AFFDL-Wright-Patterson AFB, Dayton, Ohio.

10. UTC Report, HAST Phast IIA Design and Analysis Report, 7 October 1971.

11. TMC Report S-1229, HAST AD26A Power supply, Final Technical Report, December 1972.

12. TMC Report S-1021, HAST AD26A Power Supply, Final Design Analysis Report, January 1972.

13. Irvin Industries Report GIR85-176, Design Analysis Report, HAST Missile Parachute Recovery System, 6 April 1971.

14. Irvin Industries Report GIR77-128, HAST Recovery System Subsystem Development Tests (El Centro), 17 August 1970.

15. UTC Report, Heavyweight TCA Test Summary, 9 June 1972.

USAF (RDPNJ)	1	6585TH TEST GP (GD)	1
USAF (RPPA)	2	AUL (AUL-LSE-70-239)	1
USAF (RDQRM)	2	ATC (XPOS)	1
USAF (XOOFA)	2	NASC (AIR-5323)	1
AFSC (INN)	2	NASC (AIR-5324)	1
AFSC (SDAS)	1	NWL (Code FGR Hoye)	1
AFSC (SDHA)	1	ODDR&E (T&E)	2
AFSC (DLCAW)	2	DARPA (TIO)	1
AFSC (DLC)	1	NASC (AIR 360)	1
AFSC (DLZ)	1	VX-5 Code 9020	1
AFSC (SDW)	1	NWC (Code 143)	1
AFSC (DLOX)	1	NWC (Code 456)	2
AFSC (DPSL)	1	NWC (Code 603)	1
AFSC (YR)	2	NWC (Code 753 Tech Lib)	2
AFSC (SDWM)	1	NWC (Code 4063)	1
TAC (DRA)	1	NWC (Code 50)	2
TAC (OA)	1	Redstone Sci Info Ctr	2
AFAL (TE)	3	DDC	2
AFAL (AA)	1	TAWC (TRADOCLO)	1
AFAL (TEM)	1	AFATL (DLOSL)	2
AFAL (NVA)	1	AFATL (DL)	1
AFAL (NV)	1	ADC (DOV)	2
ASD (YN/EV)	2	ADWC (TE)	2
ASD (XR)	1	ADWC (4750th Test Sq)	2
ASD (YFM)	2	USAF TAWC (TE)	2
ASD (ENO)	1	WSMR (STEWS-TE-MF)	2
ASD (ENYS)	3	Robins ALC (MM)	2
ASD (ENV)	2	Ogden ALC (MMEEA)	1
ASD (YP)	1	The Marquardt Co (Ed Wecker)	2
ASD (RWD)	2	AFFDL (PTR)	2
ASD (RWR)	2	AFAPL (RJA)	1
ASD (SD)	2	AFAPL (POP-1)	1
ASD (SD7)	2	AFRPL (LK)	1
ASD (SD5)	2	AFRPL)LKCG)	1
ASD (SD4)	2	NASC (PMA-247)	1
AFFDL (FE)	1	NMC (Code 5160)	1
AFFDL (FG)	1	NOS (C. L. Adams)	1
AFFDL (FX)	1	USAMICOM (AMSMI-TM)	2
AFFDL (FY)	1	United Tech Ctr (R. A. Jones)	3
AFML (LA)	1	Beech Aircraft Corp (D. Wells)	10
AFML (LL)	1	AFTEC (TET/Maj Potter)	1
AFML (LN)	1	USAF (SAMI)	1
AFML (LP)	1	Ogden ALC (MMNOP)	1
AFLC (MMWM)	1	ASD (ENYEHM)	1
Ogden ALC (MMNO)	1	AFWL (LR)	1
RADC (IRA)	1	Commander VX-4	1
6585th TEST GP (TD)	1	TAC (DRR)	1

201

INITIAL DISTRIBUTION (Concluded)

ADTC (SDQ)	2
AFATL (DLMQ)	6
AFATL (DLMH)	15

DOCUMENT CONTROL DATA - R & D

(Security classification of title, body of abstract and indexing annotation must be entered when the overall report is classified)

1. ORIGINATING ACTIVITY (Corporate author)	2a. REPORT SECURITY CLASSIFICATION
Beech Aircraft Corporation	Unclassified
Wichita, Kansas 67201	2b. GROUP

3. REPORT TITLE

High Altitude Supersonic Target (HAST) - Phase II

4. DESCRIPTIVE NOTES (Type of report and inclusive dates)

Final Report - January 1971 to June 1974

5. AUTHOR(S) (First name, middle initial, last name)

John A. Engelland
William M. Byrne, Jr.

6. REPORT DATE	7a. TOTAL NO OF PAGES	7b. NO OF REFS
August 1974	216	15

8a. CONTRACT OR GRANT NO	9a. ORIGINATOR'S REPORT NUMBER(S)
FO8635 70 C 0100	
b. PROJECT NO	1070E411 MER
c.	9b. OTHER REPORT NO(S) (Any other numbers that may be assigned this report)
d.	AFATL-TR-74-129

10. DISTRIBUTION STATEMENT

Distribution limited to U. S. Government agencies only; this report documents test and evaluation; distribution limitation applied August 1974. Other requests for this document must be referred to the Air Force Armament Laboratory (DLMO, Eglin Air Force Base, Florida 32542.

11. SUPPLEMENTARY NOTES	12. SPONSORING MILITARY ACTIVITY
Available in DDC	Air Force Armament Laboratory
	Air Force Systems Command
	Eglin Air Force Base, Florida 32542

13. ABSTRACT

A High Altitude Supersonic Target (HAST) is under development by the Air Force Armament Laboratory to provide a high performance, air launched, advanced aerial target system for tri-service use. This technical report covers the second phase of the multiphased development program. Final design of the target vehicle and supporting equipment was completed and flight test vehicles and supporting equipment were fabricated in this phase. Ground test programs were conducted on subsystems and components. Acceptance tests were conducted on components and the complete vehicle. Analyses confirmed that the canard-clipped delta wing configuration could meet required maneuvers. Materials for the airframe were selected which provide a fair compromise of both manufacturing costs and efficient and reliable thermo-structural performance capability. A hybrid rocket propulsion system was specified and test firings have confirmed the ignition and boost thrust capability and that a variable thrust can be obtained by use of an oxidizer throttle valve. To meet maneuvering requirements a free siphon device has been developed to provide positive expulsion of the oxidizer under all vehicle flight conditions. Maneuvers can be preprogrammed or initiated by radio command and hardware computer tie-in simulations have confirmed the effectiveness of the automatic flight control system to control the vehicle throughout the required flight regime.

DD FORM 1473 (NOV)

14	KEY WORDS	LINK A		LINK B		LINK C	
		ROLE	WT	ROLE	WT	ROLE	WT
	High Altitude Supersonic Target						
	HAST						
	Mach-Altitude Flight Envelope						